The University of Nottingham
UNITED KINGDOM · CHINA · MALAYSIA

Eshtaya, Majd (2016) TOWARDS SUSTAINABLE PRODUCTION OF RENEWABLE CHEMICALS FROM LIGNIN. PhD thesis, University of Nottingham.

Access from the University of Nottingham repository:
http://eprints.nottingham.ac.uk/38392/1/Majd%20Eshtaya_ID%204194525.pdf

Copyright and reuse:

The Nottingham ePrints service makes this work by researchers of the University of Nottingham available open access under the following conditions.

This article is made available under the University of Nottingham End User licence and may be reused according to the conditions of the licence. For more details see: http://eprints.nottingham.ac.uk/end_user_agreement.pdf

For more information, please contact eprints@nottingham.ac.uk



TOWARDS SUSTAINABLE PRODUCTION OF RENEWABLE CHEMICALS FROM LIGNIN

MAJD ESHTAYA

Thesis submitted to the University of Nottingham for the degree of Doctor of Philosophy in the Faculty of Engineering

November 2016

Department of Chemical and Environmental Engineering
University of Nottingham
Nottingham
NG7 2RD
United Kingdom

ABSTRACT

Environmental concerns have brought attention to the requirement for more efficient and renewable processes for chemicals production. Lignin is the second most abundant natural polymer, and might serve as a sustainable resource for manufacturing fuels and aromatic derivatives for the chemicals industry after being depolymerised. In this work, two main approaches were investigated with the aim of treatment of lignin with a mediator, 2,2'-azinobis(3-ethylbenthiazoline-6-sulfonic acid) diammonium salt (ABTS), in 1-ethyl-3-methylimidazolium ethyl sulfate, ($[C_2mim][C_2SO_4]$). In the first approach, laccase from *Trametes versicolor* (LTV) was used to treat organosolv lignin, using $[C_2mim][C_2SO_4]$ as a co-solvent in the presence of ABTS. LTV was shown to possess catalytic activity for the degradation of organolsov lignin in systems containing ionic liquid and syringaldehyde was found to be a major product obtained from the process.

ABTS alone has been evaluated for its reaction with lignin by means of cyclic voltammetry (CV). Here, the non-phenolic lignin model compound veratryl alcohol and three types of lignin (organosolv, Kraft and lignosulfonate) were specifically examined. The presence of either veratryl alcohol or organosolv lignin increased the second oxidation peak of ABTS under select conditions, indicating the ABTS-mediated oxidation of these molecules at high potentials in $[C_2mim][C_2SO_4]$. Furthermore, CV was applied as a quick and efficient way to explore the impact of water in the ABTS-mediated oxidation of both organosolv and lignosulfonate lignin. Higher catalytic efficiencies of ABTS were observed for lignosulfonate solutions either in sodium acetate buffer, or when $[C_2mim][C_2SO_4]$ (15% v/v) was present in an aqueous solution, whilst there was no change found in the catalytic efficiency of ABTS in neat $[C_2mim][C_2SO_4]$-lignosulfonate mixtures relative to ABTS alone. In contrast, organosolv showed an initial increase in oxidation, followed by a significant decrease on increasing the water content of a $[C_2mim][C_2SO_4]$ solution.

Despite enhanced lignin solubility in ionic liquids, the yields of small molecules attributed to depolymerisation in ionic liquids are often quite low. Since depolymerisation approaches examined herein are thought to proceed *via* free-radical mediated mechanisms, two different stable radicals 2,2-diphenyl-1-picrylhydrazyl

(DPPH) and ABTS were assessed for the rapid monitoring of radical activity of lignin-related compounds in ionic liquid systems. While these assays are successful in aqueous and organic solvent systems, the presence of the ionic liquids complicates the assay procedure, requiring further developmental work.

LIST OF PUBLICATIONS

Eshtaya, M., Ejigu, A., Stephens, G., Walsh, D. A., Chen, G. Z. & Croft, A. K. 2016. Developing energy efficient lignin biomass processing - towards understanding mediator behaviour in ionic liquids. *Faraday Discussions,* 190**,** 127-45.

Note: Chapter 4 (Section 4.1-Section 4.3) summarises material from the above paper, which is appended at the end of the thesis (Appendix 23).

ACKNOWLEDGEMENTS

In the name of Allah, the most gracious and most merciful

First and foremost, I wish to express my sincere gratitude to my supervisor, Dr Anna Croft, for her constant support, direction, suggestions and encouragement throughout this project. I would also like to thank my second supervisor Prof. Gill Stephens for the knowledge she has shared. I am also very grateful to Prof. George Chen for the help that he gave me.

My gratitude and thanks to Dr Stephen Hall, Dr Angela Tether and my research group, especially Dr Ayixiamuguli Nueraimaiti and Alison Woodward for their valuable discussion, help, and cooperation in this project.

I would also like to thank Dr Yu Linpo, Dr Darren Walsh, and Dr Aynalem Andinet for their help with the electrochemical oxidation experiments and a lot of helpful discussions.

I gratefully acknowledge the financial support by Islamic Development Bank (IDB) and the University of Nottingham. I would like to thank An-Najah National University for providing the opportunity to do the doctoral research.

I would also like to thank my entire family and all of my friends for their love, endless support, and encouragement.

Lastly, and most importantly, I am sincerely grateful to my parents, Khalid Eshtaya and Amira Eshtaya who raised me, supported me, taught me, and loved me.

DECLARATIONS

No portion of work referred to in the thesis has been submitted in support of an application for another degree or qualification of this or any other university or another institute of learning.

Majd Eshtaya

This thesis is dedicated to my beloved parents, sisters and brothers

TABLE OF CONTENTS

ABSTRACT I
LIST OF PUBLICATIONS III
ACKNOWLEDGEMENTs IV
DECLARATIONS V
TABLE OF CONTENTS VII
LIST OF FIGURES XI
LISTS OF SCHEMES XIV
LISTS OF TABLES XV
LIST OF ABBREVIATIONS XVI
IONIC LIQUIDS ABBREVIATIONS XIX
CHAPTER ONE 1
OBJECTIVES AND THESIS OUTLINE 1
CHAPTER TWO 3
LITERATURE REVIEW 3
2.1 Lignin 3
2.2 Methods for Isolating Lignin 3
2.2.1 Kraft Lignin Process 5
2.2.2 Sulfite (Lignosulfonate) Process 5
2.2.3 Organosolv Process 5
2.3 Lignin Applications 6
2.4 Lignin Depolymerisation 6
2.5 Ionic Liquids (ILs) 7
2.5.1 Properties of ILs 7
2.5.2 Uses and Applications of ILs 7
2.6 Ionic Liquids as Solvents for Lignin 8
2.6.1 Lignin Dissolution and Isolation Using ILs 8
2.6.2 Lignin Depolymerisation and Degradation Using ILs 10
2.7 Laccase 17
2.7.1 The Laccase-Mediator System (LMS) 18
2.7.2 Applications of Laccase 19
2.8 Ionic Liquids as Solvents for Laccase 20
2.8.1 Effect of IL Types and Concentration on Laccase Activity and Stability 20
2.9 Electrochemical Oxidation of Lignin 24
2.10 Antioxidant Reaction Mechanisms and Evaluation Methods 31
2.10.1: 2, 2-Diphenyl-1-picrylhydrazyl 1 (DPPH) Assay 32
2.10.2: 2, 2'-Azino-bis(3-ethylbenthiazoline-6-sulfonic acid) Diammonium Salt (ABTS) Assay. 33
2.10.3: Ferric Ion Reducing Antioxidant Power (FRAP) Assay 34
2.10.4 Radicals Reactions in Ionic Liquids 35
CHAPTER THREE 38
ENZYMATIC TREATMENT OF ORGANOSOLV LIGNIN IN [C_2mim][C_2SO_4] 38

3.1 Introduction 38
3.2 Materials and Methods 39
3.2.1 Chemicals 39
3.2.2 Sodium Acetate Buffer Preparation 39
3.2.3 Laccase from *Trametes versicolor* (LTV) 39
3.2.4 Activity of LTV 39
3.2.5 Treatment of Organosolv Lignin in Sodium Acetate Buffer with LTV 40
3.2.6 The Activity of LTV at Different Concentrations of [C_2mim][C_2SO_4] 40
3.2.7 Treatment of Organosolv Lignin in 100% (v/v) [C_2mim][C_2SO_4] 41
3.2.8 Treatment of Organosolv Lignin in 30% (v/v) [C_2mim][C_2SO_4]/buffer mixtures with LTV 41
3.2.9 Extraction of Non-Polar Lignin Breakdown Products by Benzene 42
3.2.10 Extraction of Non-Polar Lignin Breakdown Products Using Different Solvents 43
3.3 Analytical Methods 45
3.3.1 Gas Chromatography–Mass Spectrometry (GC-MS) 45
3.4 Quantification 47
3.4.1 Calculation of Product Yield after Benzene Extraction by Using Single-Point Internal Standard Method 47
3.4.2 Amount of Syringaldehyde after Solvent Extraction Using the Calibration Curve 48
3.4.3 Determination of Michaelis-Menten Parameters 48
3.5 Results and Discussion 50
3.5.1 LTV Kinetics using the Michaelis-Menten Relationship 50
3.5.2 Effect of LTV on Organosolv Lignin Treatment in Sodium Acetate Buffer Solution 51
3.5.3 The Activity of LTV at Different Concentrations of [C_2mim][C_2SO_4] 52
3.5.4 Effect of LTV on Organosolv Lignin in a [C_2mim][C_2SO_4]/Buffer Mixture 53
3.5.5 Effect of ABTS on Organosolv Lignin in [C_2mim][C_2SO_4]/Buffer Mixture 55
3.5.6 Effect of Laccase-Mediator System (LMS) on Organosolv Lignin in [C_2mim][C_2SO_4]/Buffer Mixture 56
3.5.7 Influence of Temperature on Organosolv Lignin in [C_2mim][C_2SO_4] 57
3.5.8 Effect of [C_2mim][C_2SO_4] Concentration on Dissolution of Organosolv Lignin 60
3.6 Lignin Product Identification - Extraction Process 64
3.7 Summary and Conclusions 68
CHAPTER FOUR 71
TOWARDS UNDERSTANDING MEDIATOR BEHAVIOUR IN [C_2mim][C_2SO_4] 71
4.1 Introduction 71
4.2 Materials and Methods 73
4.2.1 Chemicals 73
4.2.2 Buffer Preparation 73
4.2.3 Viscosity and Water Content Measurements 74
4.2.4 Cyclic Voltammetry (CV) Measurements 74
4.2.5 Bulk Electrolysis 75
4.2.6 Gas Chromatography–Mass Spectrometry (GC-MS) 78
4.2.7 Lignosulfonate Pretreatment 79
4.3 Results and Discussion 80

4.3.1 Electrochemical Behaviour of ABTS in $[C_2mim][C_2SO_4]$ 80
4.3.2 Cyclic Voltammetry of Veratryl Alcohol (VA) 83
4.3.3 Cyclic Voltammetry of Different Lignins in $[C_2mim][C_2SO_4]$ 86
4.3.4 Cyclic Voltammetry of Lignosulfonate (LS) 90
4.3.5 Cyclic Voltammograms of Organosolv Lignin in Alkaline Aqueous Solution/$[C_2mim][C_2SO_4]$ at Different Concentrations 94
4.4 Bulk Electrolysis 95
4.4.1 Bulk Electrolysis of Organosolv Lignin 95
4.4.2 Bulk Electrolysis of Lignosulfonate without Pretreatment 98
4.4.3 Bulk Electrolysis of Lignosulfonate after Pretreatment 102
4.5 Conclusions 105
CHAPTER FIVE 108
UNDERSTANDING THE RADICAL BEHAVIOUR OF LIGNIN RELATED COMPOUNDS IN IONIC LIQUIDS 108
5.1 Introduction 108
5.1.2 Objective 108
5.2 Materials and Methods 109
5.2.1 Chemicals 109
5.2.2 DPPH Assay Using 96 Well Plate Reader 110
5.2.3 DPPH Assay Using UV-Vis Spectrophotometer 111
5.2.4 ABTS Assay Using UV-Vis Spectrophotometer 111
5.2.5 FRAP Assay Using 96 Well Plate Reader 112
5.2.6 Preparation of *N*,*N*-dimethyl ethanol ammonium Formate ([DMEA][HCOO]) 112
5.2.7 Water Content Measurements 113
5.2.8 Viscosity Measurements 113
5.2.9 Generation of ABTS Radical Cation in Ionic Liquid 114
5.3 Results and Discussion 114
5.3.1 FRAP Assay 114
5.3.2 Radical Activity Scavenging of Lignin-Related Monomers by DPPH in Methanol Using 96 Well Plate Reader 117
5.3.3 Comparison between the UV-Vis Spectrophotometer and Microplate Reader for Determination the Antiradical Efficiencies Using DPPH Assay 128
5.3.4 Radical Scavenging Activity of Lignin Monomers in Ionic Liquids 130
5.3.5 Radical Scavenging Activity of Trolox and Syringol in Methanol-Ionic Liquid Mixture 137
5.3.6 Influence of Solvent Type on the Quenching of the DPPH Radical by Lignin Monomers and Standards 140
5.3.7 Absorption Spectra of DPPH• in Different Solvents 144
5.3.8 ABTS Radical Scavenging Activity of Lignin-Related Compounds and Standards 150
5.4 Conclusions 155
CHAPTER SIX 158
GENERAL DISCUSSION, CONCLUSIONS AND SUGGESTIONS FOR FUTURE WORK 158
6.1 Summary and Conclusions 158
6.2 Suggestions for Future Work 163
REFERENCES 166

APPENDICES 180
Appendix A.1: Names, abbreviation and chemical structure of Ionic liquids mention in this study ..180
Appendix A.2: Names, abbreviation and chemical structure of the mediators mention in this study .184
Appendix A.3: Names, abbreviation and chemical structure of the compounds mention in this study 187
Appendix A.4: Laccase (EC 1.10.3.2) Enzyme Assay with ABTS as a Substrate 189
Appendix A.5: DC Protein assay (20 µL sample scale) 190
Appendix A.6: GC-MS Syringaldehyde Standard Calibration Curve 191
Appendix A.7: Enzyme kinetics by Eadie-Hofstee plot 191
Appendix A.8: GC-MS Analysis of Organosolv Lignin Treatment Products after dissolution with 30% (v/v) IL/buffer at 30 °C for 6 h. 192
Appendix A.9: GC-MS Analysis of Organosolv Lignin Treatment Products in [C_2mim][C_2SO_4] 194
Appendix A.10: GC-MS Analysis of products obtained by extraction with different solvents after organosolv dissolution in [C_2mim][C_2SO_4] at 30 °C for 6 h. 200
Appendix A.11: GC-MS Syringaldehyde Standard Calibration Curve 201
Appendix A.12: Standards for Lignosulfonates-Bulk Electrolysis Experiment 201
Appendix A.13: Cyclic voltammograms of 1 mM ABTS in 0.1 M sodium acetate buffer (pH 4.5) recorded at a scan rate of 400 mV/s 204
Appendix A.14: GC-MS analysis of products obtained from electrochemical oxidation of organosolv Lignin after 6 h in [C_2mim][C_2SO_4]. 205
Appendix A.15: GC-MS analysis of products obtained from electrochemical oxidation of as-received lignosulfonate after 8 h in sodium acetate buffer. 205
Appendix A.16: GC-MS analysis of products obtained from electrochemical oxidation of lignosulfonate after MeOH washing after 8 h in sodium acetate buffer. 206
Appendix A.17: ^{1}H NMR and ^{13}C NMR spectra of the [DMEA][HCOO] 206
Appendix A.18: FRAP assay 207
Appendix A.19: Rate of increase in absorbance at 593 nm of vitamin C and gallic acid in [C_2mim][C_2SO_4], water and isopropanol. 208
Appendix A.20: Reaction kinetics behaviour and DPPH radical scavenging activities by standards and lignin monomers. 209
Appendix A.21: Time course (8 h) of scavenging of DPPH free radical by lignin monomers dissolved in ILs ([C_2mim][C_2SO_4] and [DMEA][HCOO]) 214
Appendix A.22: UV spectra of DPPH (60.86 µM) in acetonitrile and toluene at different time and different storage conditions. 215
Appendix A.23: Published Paper 216

LIST OF FIGURES

Figure 2.1: The three building blocks of lignin: (1) *p*-coumaryl alcohol (2), coniferyl alcohol and (3) sinapyl alcohol. 4
Figure 2.2: Schematic representation of a hardwood lignin structure highlighting the major linkage types. 4
Figure 2.3: Batch process for the production of aromatic aldehydes from lignin coupled with the extraction process 14
Figure 2.4: Proposed mechanism of the oxidative cleavage of the lignin Cα–Cβ bond in protic ionic liquids. Adapted from 15
Figure 2.5: Structure of laccase from *Trametes versicolor (LTV)*. The four copper active sites are shown as blue spheres. 17
Figure 2.6: Schematic representation of lignin degradation by laccase and mediator system. 18
Figure 2.7: Chemical structure of ABTS mediator and formation of the cation radical and the dication by removal of one and two electrons, respectively, from ABTS. 19
Figure 2.8: a) Laccase-mediator system (LMS) and b) electrolytic mediator system (EMS) 24
Figure 3.1: Schematic diagram for organosolv lignin treatment in the IL experiment set up. 42
Figure 3.2: Flowchart of extraction process after organosolv lignin treatment with IL as a solvent or co-solvent. 43
Figure 3.3: Flowchart for extracting lignin degradation products from lignin/IL mixtures. 45
Figure 3.4: Effect of ABTS concentration on the reaction rate by LTV. ABTS was added to start the reaction containing sodium acetate buffer (0.1 mM, pH 5) and LTV (0.1 mg/mL). The change in absorbance at 420 nm was recorded at 30 °C. 51
Figure 3.5: The GC-MS chromatograms of products that have been extracted in benzene. The samples were incubated in sodium acetate buffer under identical conditions (at 30 °C for 6 h, shaken at 200 rpm). Benzene extract fraction of organosolv lignin after treatment with (A) LTV and ABTS (B) LTV only (C) ABTS only and (D) benzene extract fraction of organosolv lignin only. 52
Figure 3.6: Time courses for ABTS oxidation in sodium acetate buffer (pH 5.0) containing various amounts of $[C_2mim][C_2SO_4]$ (0-50% (v/v)) at 30 °C. The reaction was started by adding ABTS after 22 min. 53
Figure 3.7: Major and minor lignin breakdown products from lignin after dissolution with 30% (v/v) of $[C_2mim][C_2SO_4]$ with LTV and without LTV at 30 °C for 6 h. Identification of products was based on the NIST library data. 54
Figure 3.8: Lignin breakdown products (vanillin and syringaldehyde) after dissolution with 30% (v/v) IL/buffer at 30 °C for 6 h. Identification of products was based on the NIST library data and single-point internal standard method 54
Figure 3.9: Major and minor lignin breakdown products from organosolv lignin after dissolution with $[C_2mim][C_2SO_4]$ at 30 °C and 160 °C for 6 h. Identification of the compounds were based on the NIST library. 58
Figure 3.10: Organosolv lignin products (vanillin and syringaldehyde) after dissolution with $[C_2mim][C_2SO_4]$ at 30 °C and 160 °C for 6 h. 58
Figure 3.11: Chemical structures of products produced from organosolv lignin degradation in $[C_2mim][C_2SO_4]$ at 30 °C and 160 °C. 59
Figure 3.12: Major and minor lignin breakdown products from organosolv lignin after dissolution with 100%, 30% and 0% (v/v) $[C_2mim][C_2SO_4]$ at 30 °C for 6 h without presence of LTV 61
Figure 3.13: Lignin breakdown products (vanillin and syringaldehyde) after dissolution with 100%, 30% and 0% (v/v) $[C_2mim][C_2SO_4]$/sodium acetate buffer at 30 °C for 6 h without presence of LTV. 61
Figure 3.14: The effect of incubation time on product formation during lignin dissolution process in the IL at different concentration, 100% $[C_2mim][C_2SO_4]$ and 30% (v/v) $[C_2mim][C_2SO_4]$/buffer. 63
Figure 3.15: Major and minor lignin products obtained by extraction with different solvents after the dissolution of organosolv lignin in $[C_2mim][C_2SO_4]$ at 30 °C for 6 h. 67

Figure 3.16: Chemical structures of products obtained from organosolv lignin dissolution in [C_2mim][C_2SO_4] after extraction with different solvents. 68
Figure 4.1: Chemical structure of ABTS mediator and formation of the cation radical and the dication by removal of one and two electrons from ABTS, respectively. 72
Figure 4.2: Schematic diagram of the electrochemical cell: (1) graphite rod working electrode (2) Ag/Ag^+ reference electrode (3) graphite rod counter electrode (4) glass frit. 76
Figure 4.3: Flowchart of electrochemical oxidation experiments-bulk electrolysis of organosolv lignin in the IL with the presence of ABTS. 76
Figure 4.4: Flowchart for extracting lignin degradation products from lignin/IL mixtures. 77
Figure 4.5: Flowchart of electrochemical oxidation experiments-bulk electrolysis of lignosulfonate in sodium acetate buffer (pH 4.5). 78
Figure 4.6: Cyclic voltammogram of 10 mM ABTS in [C_2mim][C_2SO_4] recorded at a scan rate of 200 mV/s. The inset shows the cyclic voltammogram of 10 mM ABTS in [C_2mim][C_2SO_4] with varying scan rates (from inside to outside (mV/s): 50, 100, 200, 400, 600, 800 and 1000). 81
Figure 4.7: Cyclic voltammograms of 50 M ABTS in [C_2mim][C_2SO_4] recorded at scan rates of 50 mV/s and 200 mV/s 82
Figure 4.8: (A) Potential step chronoamperogram obtained at a 3 mm diameter glassy carbon disk electrode in 10.0 mM ABTS in [C_2mim][C_2SO_4]. The potential was stepped from 0.3 V to 0.6 V *vs.* ABTS /$ABTS^{\cdot+}$ and held for 10 s. (B) Cottrell plot of $i\,(t)$ *vs.* $t^{-0.5}$ for the oxidation process 83
Figure 4.9: Cyclic voltammograms of 1 mM ABTS, 13.8 mM veratryl alcohol 4, 13.8 mM veratryl alcohol 4 mixed with 1 mM ABTS in 15% (v/v) [C_2mim][C_2SO_4] in 0.1 M sodium acetate buffer (pH 4.5) recorded at a scan rate of 10 mV/s. The inset shows the portion of the CVs with current above 25 μA between 0.9 and 1.1 V 84
Figure 4.10: Cyclic voltammograms of 1 mM ABTS, 13.8 mM veratryl alcohol, 13.8 mM veratryl alcohol mixed with 1 mM ABTS in [C_2mim][C_2SO_4] recorded at a scan rate of 10 mV/s. The inset shows the portion of the CVs with current abo ve 2.0 μA between 0.9 and 1.1 V 86
Figure 4.11: Representative structure of a fragment of lignin 87
Figure 4.12: Cyclic voltammograms of organosolv, Kraft and lignosulfonate lignin (5 wt %) in [C_2mim][C_2SO_4] recorded at a scan rate of 50 mV/s. 87
Figure 4.13: Cyclic voltammograms of ABTS (10 mM), organosolv lignin (5 wt %) and organosolv lignin (5 wt %) mixed with 10 mM ABTS in [C_2mim][C_2SO_4] recorded at scan rate of 50 mV/s. 88
Figure 4.14: Cyclic voltammograms of ABTS (10 mM), lignosulfonate (5 wt %) and lignosulfonate (5 wt %) mixed with 10 mM ABTS in [C_2mim][C_2SO_4], recorded at a scan rate of 50 mV/s 88
Figure 4.15: Cyclic voltammograms of ABTS (10 mM), Kraft lignin (5 wt %) and Kraft lignin (5 wt %) mixed with 10 mM ABTS in [C_2mim][C_2SO_4] recorded at a scan rate of 50 mV/s 89
Figure 4.16: Cyclic voltammograms of 1 mM ABTS, 1 wt % lignosulfonate, 1 wt % lignosulfonate mixed with 1 mM ABTS in 15% (v/v) [C_2mim][C_2SO_4] in 0.1 M sodium acetate buffer (pH 4.5) recorded at a scan rate of 10 mV/s 91
Figure 4.17: Cyclic voltammograms of 1 mM ABTS, 1 wt % lignosulfonate, 1 wt % lignosulfonate mixed with 1 mM ABTS in 0.1 M sodium acetate buffer (pH 4.5) recorded at a scan rate of 10 mV/s 93
Figure 4.18: Cyclic voltammograms of organosolv lignin (OSL) (5 wt %) mixed with 10 mM ABTS in pure [C_2mim][C_2SO_4], 5% (v/v) alkaline solution/[C_2mim][C_2SO_4], 7% (v/v) alkaline solution/[C_2mim][C_2SO_4], 10% (v/v) alkaline solution/[C_2mim][C_2SO_4], 15% (v/v) alkaline solution/[C_2mim][C_2SO_4] and 20% (v/v) alkaline solution/[C_2mim][C_2SO_4] recorded at a scan rate of 50 mV/s 94
Figure 4.19: Major and minor lignin breakdown products from organosolv lignin after electrochemical oxidation in [C_2mim][C_2SO_4] for 6 h. 96
Figure 4.20: Chemical structures of products produced from organosolv lignin chemical oxidation in [C_2mim][C_2SO_4]. 98
Figure 4.21: Major and minor lignin breakdown products from the electrochemical oxidation of as-received lignosulfonate in sodium acetate buffer pH 4.5 for 8 h. 99
Figure 4.22: Major and minor lignin breakdown products by concentration, from electrochemical oxidation of as-received lignosulfonate in sodium acetate buffer pH 4.5 for 8 h.. 101

Figure 4.23: Chemical structures of products obtained from lignosulfonate electrochemical oxidation in sodium acetate buffer (pH 4.5). 102
Figure 4.24: Major and minor lignin breakdown products from the electrochemical oxidation of washed-lignosulfonate in sodium acetate buffer pH 4.5 for 8 h. 103
Figure 4.25: Major and minor lignin breakdown products concentration from washed-lignosulfonate and as-received lignosulfonate after electrochemical oxidation in sodium acetate buffer pH 4.5 for 8 h. 104
Figure 5.1: Schematic diagram of electrochemical cell (1) graphite rod working electrode (2) Ag/Ag^{+} reference electrode (3) graphite rod counter electrode (4) glass frit. 114
Figure 5.2: Example of a calibration curve for FRAP assay using ferrous sulfate as standard. 115
Figure 5.3**:** The relative activity of gallic acid and vitamin C (expressed as Ferrous sulfate (μM) equivalents) using different concentration dissolved in three solvents in FRAP assay after 60 min of reaction. 116
Figure 5.4: Example of the calibration curve of DPPH• 118
Figure 5.5: Examples of three reaction kinetics behaviour (A): Vitamin C (rapid) (B): Syringol (intermediate), and (C): vanillin (slow). 119
Figure 5.6: DPPH radical scavenging activities by vitamin C as a function of the number of moles of vitamin C / mole DPPH•. 120
Figure 5.7: Calibration curve of DPPH˙ using microplate reader and UV-Vis spectrophotometer at different total assay volume size.. 128
Figure 5.8: Scavenging activity of DPPH radical by gallic acid as a function of the number of moles of gallic acid /mole DPPH• using plate reader and UV-Vis spectrophotometer. 130
Figure 5.9: Time course (1 h) of scavenging of DPPH free radical by lignin monomers (1.5 mM) dissolved in $[C_2mim][C_2SO_4]$ 131
Figure 5.10: Time course (1h) of scavenging of DPPH free radical by lignin monomers (10 mM) dissolved in $[C_2mim][C_2SO_4]$. 132
Figure 5.11: Time course (1 h) of scavenging of DPPH free radical by lignin monomers (1.5 mM) dissolved in [[DMEA][HCOO] 133
Figure 5.12: Time course (1h) of scavenging of DPPH free radical by lignin monomers (10 mM) dissolved in [DMEA][HCOO] 133
Figure 5.13: Scavenging activity of Trolox (300 μM) and syringol (320 μM) against DPPH radical performed in different mole percentages of methanol in $[C_2mim][C_2SO_4]$. 138
Figure 5.14: DPPH• remaining as a function of the number of moles of syringol /mole DPPH• in toluene, acetonitrile and methanol. 141
Figure 5.15: UV spectra of DPPH radical (60.86 μM) in methanol at different times and storage conditions. 144
Figure 5.16**:** Time dependence of DPPH• (60.86 μM) absorption spectra in $[C_2mim][C_2SO_4]$ at 25 °C. 145
Figure 5.17: UV spectra of DPPH (60.86 μM) in $[C_2mim][C_2SO_4]$ at a different time and different storage conditions. 146
Figure 5.18: Time dependence of DPPH• (60.86 μM) absorption spectra in [DMEA][HCOO] at 25 °C. 146
Figure 5.19: Absorption spectra of DPPH (60.86 μM) in selected solvents ([DMEA][HCOO], $[C_2mim][C_2SO_4]$ and methanol) at the initial time. 147
Figure 5.20: Absorption spectra of DPPH (60.86 μM) in selected solvents ([DMEA][HCOO], $[C_2mim][C_2SO_4]$ and methanol) after 5 h under light exposure at room temperature. 147
Figure 5.21: Absorption spectra of DPPH (60.86 μM) in $[C_2mim][C_2SO_4]$ with and without Trolox (10 mM) at the initial time and after 24 h of reaction recorded at 25 °C. 148
Figure 5.22: Absorption spectra of DPPH (60.86 μM) in [DMEA][HCOO] with and without Trolox (10 mM) at the initial time and after 24 h of reaction recorded at 25 °C. 149
Figure 5.23: Absorption spectra of DPPH (60.86 μM) in methanol with and without Trolox (10 mM) at the initial time and after 24 h of reaction recorded at 25 °C. 149
Figure 5. 24: Absorption spectra of Trolox (10 mM) in DPPH solution dissolved in selected solvents ([DMEA][HCOO], $[C_2mim][C_2SO_4]$ and methanol) at the initial time recorded at 25 °C. 150

Figure 5.25: The effect of syringol, vitamin C and Trolox concentration on the absorbance reduction of the $ABTS^{\bullet+}$ in phosphate buffer solution (pH 7.4) at 10 min and 37 °C. 151
Figure 5.26: Syringol and Trolox antioxidant potential as a vitamin C equivalent capacity (VCEAC) by ABTS assay 152
Figure 5.27: Electrochemically formation of ABTS radical cation in $[C_2mim][C_2SO_4]$ (A): Figure shows the blue-green colour intensity of ABTS radical formation after 24 h of reaction (B) disappeared of the blue-green colour after few minutes from removing from the electrochemical cell (24 h of reaction). 155

LISTS OF SCHEMES

Scheme 2.1: Reaction of an antioxidant with a radical induced in an antioxidant assay through hydrogen atom transfer. 31
Scheme 2.2: Reaction of an antioxidant through single electron transfer with a radical induced in an antioxidant assay..... 32
Scheme 2.3: Reaction of the stable radical DPPH• with an antiradical compound (ArOH) 33
Scheme 2.4: Generation of ABTS radical cation ($ABTS^{\bullet+}$) and its reaction with an antiradical compound (ArOH) (Oliveira *et al.*, 2014) 34
Scheme 2.5: $[Fe(III)(TPTZ)_2]^{3+}$, $[Fe(II)(TPTZ)_2]^{2+}$ reduction reaction for the FRAP assay 35
Scheme 2.6: Proposed reaction scheme for photogeneration of lophyl radicals ($L^{\bullet}$) and their recombination within the solvent cage or reaction with another lophyl radical after escape out of the solvent cage and diffusion through the ionic liquid matrix. k_{rec}= rate constant for radical recombination; k_{sep}= rate constant for radical separation 37
Scheme 4.1: Schematic representation of the reaction of ABTS and VA at the working electrode 85
Scheme 4.2: Proposed reaction scheme for the oxidation of phenol with ABTS cation radical 92

LISTS OF TABLES

Table 2.1: Solubility and extraction efficiency of lignin in various ILs. 10
Table 2.2: Lignin depolymerisation and degradation in ILs. 11
Table 2.3: Effect of ILs on laccase activity under different conditions. 22
Table 2.4:Electrochemical oxidation (cyclic voltammetry and bulk electrolysis) of lignin model compounds and lignin. 28
Table 3.1: Products obtained by extraction with different solvents after lignin degradation. 65
Table 3.2: Syringaldehyde concentration and non-polar product yields obtained from organosolv lignin treatment in $[C_2mim][C_2SO_4]$ after solvent extraction. 66
Table 4. 1: Composition of the solutions used in this chapter 73
Table 4.2: Diffusion coefficients of ABTS in different solvents using potential step chronoamperometry 83
Table 4.3: Syringaldehyde concentration and non-polar product yields obtained from bulk electrolysis of organosolv lignin in the IL after ethyl acetate extraction 95
Table 5.1**:** Characterisation of antiradical efficiencies of lignin-related compounds using DPPH• assay in methanol. 121
Table 5.2: O-H bond dissociation energy (BDE) values for lignin-related compounds and standards tested in this study. 124
Table 5.3**:** Comparison between the UV-Vis spectrophotometer and 96-well plate reader in the determination of antiradical efficiencies using DPPH assay. 129
Table 5.4: Viscosity measurements and water content. 137
Table 5.5**:** The effect of different solvents on the antiradical efficiencies of lignin-related compounds and standards using DPPH assay. 141
Table 5.6**:** Solubility of ABTS and AAPH in solvents tested. 154
Table 6. 1: Summary of types of solvent used and the major products obtained from different lignin process covered in this thesis 162

LIST OF ABBREVIATIONS

A	Electrode surface area
A_λ	Absorbance at certain wavelength (λ)
AAPH	2,2'-Azobis(2-methylpropionamidine) dihydrochloride
ABTS	2,2'-azino-bis(3-ethylbenthiazoline-6-sulfonic acid) diammonium salt
$ABTS^{\bullet+}$	ABTS radical cation
$ABTS^{2+}$	ABTS dication
$A_{compound}$	Peak area of the compound
AE	Antiradical efficiency =$(1/(EC_{50}T_{EC50}))$
Ag	Silver
AgTfO	Silver trifluoromethane sulfonate
A_{IS}	The peak area of the internal standard
APR	Antiradical power $(1/EC_{50})$
ATR-IR	Attenuated total reflectance Fourier transform infrared spectroscopy
BDE	Bond dissociation enthalpy
C	Bulk concentration of the redox species
[Ch][AA]	Cholinium amino acids
[DMEA][HCOO]	*N,N*-dimethyl ethanolammonium formate
CV	Cyclic voltammetry
D	Diffusion coefficient of the redox species
DCM	Dichloromethane
DHAP	3, 5-dimethoxy-4-hydroxyacetophenone
DHCD	3, 5-dimethoxy-4-hydroxycinnamaldehyde
DHPAA	3,5-dimethoxy-4-hydroxyphenyl acetic acid
DMBQ	2,6-dimethoxybenzoquinone
DPPH•	2,2-diphenyl-1-picrylhydrazyl
EC_{50}	Effective Concentration: the concentration of compound necessary to decrease the initial DPPH• concentration by 50%
EDTA	Ethylenediamine-N,N,N′,N′-tetraacetic acid
EMS	Electrolytic Mediator System
$E_{p,a}$	Oxidation peak
$E_{p,c}$	Reduction peak
ESR	Electron paramagnetic resonance
EtOH	Ethanol
F	Faraday constant
FRAP	Ferric ion reducing antioxidant power
G	Guaiacyl
GC-FID	Gas chromatography– flame ionisation detector
GC-MS	Gas chromatography-mass spectrometry
GPC	Gel permeation chromatography
h	Hour
H	Hydrogen
HAA	3-hydroxyanthranilic acid
HAT	Hydrogen atom transfer
HBA	4-hydroxybenzoic acid
HBD	Hydrogen bond donor
HBT	1-hydroxybenzotriazole
HMCD	4-hydroxy-2-methoxy cinnamaldehyde

HMQC	Heteronuclear multiple quantum coherence
HPLC	High-performance liquid chromatography
HSQC	Heteronuclear single quantum coherence
i	Current
ILs	Ionic liquids
IP	Ionisation potential
$i_{p,a}$	Oxidation peak current
$i_{p,c}$	Reduction peak current
IS	Internal standard
K_m	Michaelis-Menten constant
KSE	Kinetic solvent effect
L	Light path length
LAB	*Agaricus bisporus*
$LiClO_4$	Lithium perchlorate
LMS	Laccase-mediator system
LTV	Laccase from *Trametes versicolor*
MALDI-TOF	Matrix-assisted laser desorption/ionisation time-of-flight mass spectrometry
MeOH	Methanol
$MgSO_4$	Magnesium sulfate
$Mn(NO_3)_2$	Manganese (II) nitrate tetrahydrate
n	Number of electrons transferred/molecule
Na_2HPO_4	Sodium phosphate dibasic
Na_2S	Sodium sulfide
NaOH	Sodium hydroxide
NHE	Normal hydrogen electrode
NHPI	*N*-hydroxyphthalimide
NIST	National institute of standards and technology
NMR	Nuclear magnetic resonance
^{13}C NMR	Carbon NMR
^{1}H NMR	Proton NMR
o-Cl-HABI	*o*-chlorohexaarylbiimidazole
OSL	Organosolv lignin
p-H	*p*-Hydroxyphenyl propane
PIL	Protic ionic liquid
RF	Response factor
RT	Room temperature
[S]	Substrate concentration
S	Syringyl
SET	Single electron transfer
T	Time
TEAC	Trolox equivalent antioxidant capacity
T_{EC50}	Time needed to reach the steady state at the concentration corresponding to EC_{50}
TEMPO	2,2′,6,6′-tetramethylpiperidine-N-oxyl
T_g	Glass transition temperature
TPTZ	2,4,6-Tris(2-pyridyl)-s-triazine
Trolox	(±)-6-Hydroxy-2,5,7,8-tetramethylchromane-2-carboxylic acid
U	Unit
V	Potential
v/v	Volume per volume
v_0	Initial rate of reaction

VA	Veratryl alcohol
VCEAC	Vitamin C equivalent antioxidant capacity
VLA	Violuric acid
V_{max}	Maximum reaction rate
w/w	weight per weight
wt	Weight
β-O-4	Arylglycerol-*β*-aryl ether
δ_H	Hildebrand solubility parameter
ε	Molar extinction coefficient

IONIC LIQUIDS ABBREVIATIONS

Abbreviation	Ionic Liquid Name
$[C_1mim][C_1SO_4]$ ($[Mmim][MeSO_4]$)	1,3-dimethylimidazolium methyl sulfate
$[C_1mim][C_1C_1PO_4]$ ($[C_1mim][Me_2PO_4]$)	1,3-dimethylimidazolium dimethyl phosphate
$[C_2mim][C_1CO_2]$ ([Emim][OAc], ($[C_2mim][OAc]$)	1-ethyl-3-methylimidazolium acetate
$[C_2mim][C_2SO_4]$ ([Emim] $[EtSO_4]$)	1-ethyl-3-methylimidazolium ethyl sulfate
$[C_2mim][ABS]$ ([Emim][ABS])	1-ethyl-3-methylimidazolium xylenesulfonate
$[C_2mim][CF_3SO_3]$ ([Emim][OTf], $[C_2mim][$ OTf])	1-ethyl-3-methylimidazolium trifluoro methane sulfonate
$[C_2mim][C_1SO_3]$ ($[Emim][MeSO_3]$)	1-ethyl-3-methylimidazolium methane sulfonate
$[C_2mim][C_2C_2PO_4]$ ($[C_2mim][Et_2PO_4]$, EMIM DEP)	1-ethyl-3-methylimidazolium diethylphosphate
$[C_2mim][MDEGSO_4]$	1-ethyl 3-methylimidazolium 2-(2-methoxyethoxy) ethyl sulfate
$[C=C_2mim]Cl$ ([Amim][Cl])	1-allyl-3-methylimidazolium chloride
$[C_3mim]Br$ ([PrlMIM][Br])	1-propyl-3-methylimidazolium bromide
$[C_4mim]Cl$ ([Bmim][Cl])	1-butyl-3-methylimidazolium chloride
$[C_4mim][OTf]$ ($[Bmim][CF_3SO_3]$)	1-butyl-3-methylimidazolium trifluoro methane sulfonate
$[C_4mim][HSO_4]$ ($[C_4C_1im][HSO_4]$)	1-butyl-3-methylimidazolium hydrogen sulfate
$[C_4mim][C_1SO_4]$ ($[Bmim][MeSO_4]$)	1-butyl-3-methylimidazolium methyl sulfate
$[C_4mim]Br$ ([Bmim]Br)	1-butyl-3-methylimidazolium bromide
$[C_4mim][N(CN_2)]$	1-butyl-3-methylimidazolium dicyanamide
$[C_4mim][BF_4]$ ($[Bmim][BF_4]$)	1-butyl-3-methylimidazolium tetrafluoroborate
$[C_4mim][$ $PF_6]$ ($[Bmim][PF_6]$)	1-butyl-3-methylimidazolium hexafluoro phosphate
$[C_4mim][NTf_2]$ ($[Bmim][NTf_2]$)	1-butyl-3-methylimidazolium bis(trifluoromethylsulfonyl)-imide
$[C_6mim]Br$	1-octyl-3- methylimidazolium bromide
$[C_8mim]Cl$	1-octyl-3- methylimidazolium chloride

$[C_{10}mim]Cl$	1-decyl-3-methylimidazolium chloride
[Cyanomim]Br	1-(2-cyanoethyl)-3-methylimidazolium bromide (1-cyano-3-methylimidazolium bromide)
$[Bnmim][NTf_2]$	1-benzyl-3-methylimidazolium bis(trifluoromethylsulfonyl)-imide
$[C_1py][C_1C_1PO_4]$ ($[mPy][Me_2PO_4]$)	Methyl pyridinium dimethyl phosphate
$[C_1mmo][C_1C_1PO_4]$ ($[mmo][Me_2PO_4]$)	4,4-dimethylmorpholin-4-ium dimethyl phosphate
$[C_4mpyr][TfO]$	1-butyl 1-methylpyrrolidinium trifluoro methane sulfonate
[Ch][Lys]	Cholinium lysine
[DMEA][HCOO] (DMEAF)	*N*,*N*-dimethyl ethanol ammonium formate
$[DMEA][C_1CO_2]$ (DMEAA)	*N*,*N*-dimethyl ethanol ammonium acetate
[DMEA][glycolate] ($[DMEA][C_1OHCO_2]$, DMEAG)	*N*,*N*-dimethyl ethanol ammonium glycolate
[DMEA][succinate] (DMEAS)	*N*,*N*-dimethyl ethanol ammonium succinate
$[HN_{222}][C_1SO_3]$ ($[HNEt_3][MeSO_3]$)	Triethyl ammonium methane sulfonate
[TMA][TfO]	Tetra-methylammonium trifluoro methane sulfonate
$[4\text{-}BMP][BF_4]$	4-methyl-N-butyl-pyridinium tetrafluoroborate
$[N_{1222}][C_1C_1PO_4]$ ($[mtetn][Me_2PO_4]$)	*N, N*-diethyl-N-methylethanaminium dimethyl phosphate
$[P_{6,6,6,14}][Tf_2N]$	Tetradecyl(trihexyl) phosphonium bis[(trifluoromethane) sulfonyl] imide

Chemical structures of ILs can be found at Appendix A.1

CHAPTER ONE

OBJECTIVES AND THESIS OUTLINE

Lignin is a heterogeneous aromatic natural polymer comprising 15–30% of the total dry weight of lignocellulose, found in plant cell walls (Bugg *et al.*, 2011). The complexity of lignin in terms of composition and structure makes the transformation process of this macromolecule to valuable products complicated (Ibrahim *et al.*, 2013). In order to develop a sustainable and green biotechnological solution to lignin processing, the use of ionic liquids (ILs) as a solvent or co-solvent in lignin biodegradation can be used to facilitate this processing. Many ILs are able to dissolve lignin. Among the numerous ILs commonly available, 1-ethyl-3-methylimidazolium ethyl sulfate [C_2mim][C_2SO_4] has been demonstrated to effectively dissolve lignin and to be one of the best solvents for lignin valorisation (Mäki-Arvela *et al.*, 2010, Harwardt *et al.*, 2014).

The primary goal of the current study was to develop an improved method for the treatment or transformation of lignin to valuable products by using ILs to improve solvation. The first objective was to explore the potential for organosolv lignin transformation to high-value chemicals by using laccase from *Trametes versicolor* (LTV) with ABTS as a mediator in [C_2mim][C_2SO_4]. The second objective of this work was investigating the electrochemical oxidation of lignin (organosolv, Kraft and lignosulfonate) with the assistance of ABTS as a mediator in [C_2mim][C_2SO_4]. Details regarding the likelihood of repolymerisation of monomers, once cleaved, and the relative reactivity of different functional groups towards oxidation in the complex lignin mixture were unable to be delineated through this electrochemical oxidation approach. Therefore, the final objective was designed to explore the radical behaviour of lignin-related monomers in ionic liquids.

The outline of the thesis is as follows. Chapter two covers a general overview of lignin, e.g. the chemical structure of lignin, applications of lignin, the different isolation methods for lignin and the use of ionic liquids for lignin dissolution and degradation. Furthermore, the laccase-mediator system (LMS), laccase activity and stability are

reviewed. In addition, it provides a detailed review of the electrochemical oxidation of lignin and antiradical activity measurements.

In Chapter three, the use of laccase from *Trametes versicolor* (LTV) with ABTS as a mediator in $[C_2mim][C_2SO_4]$ as a solvent or co-solvent was explored for the transformation of lignin to high-value chemicals. The lignin treatment process was explored with respect to the reaction temperature, the concentration of IL and process design to find appropriate conditions for lignin treatment.

In Chapter four, particular attention has been given to the electrochemical behaviour of ABTS in oxidising the non-phenolic lignin model veratryl alcohol and three technical lignins: Kraft lignin, organosolv lignin and lignosulfonate, in $[C_2mim][C_2SO_4]$. Cyclic voltammetry was applied as a quick, accurate and efficient way to explore the ABTS-mediated oxidation process. In order to study the compounds formed during the electrochemical oxidation of lignin, bulk electrolysis of organosolv lignin in $[C_2mim][C_2SO_4]$ and lignosulfonate in sodium acetate buffer solution were also conducted in this chapter.

Chapter five deals with the behaviour of the free radicals of lignin-related compounds in ionic liquids. Three different approaches were trialled to evaluate the antiradical capacity of the lignin-related monomer compounds, including the FRAP assay, the DPPH radical scavenging assay and the ABTS assay. In this work, six lignin monomers; syringaldehyde, vanillin, vanillic acid, guaiacol, syringol and homovanillyl alcohol were chosen, based on the most common components identified from the lignin dissolution and treatment processes in the IL that have been discussed in Chapter three. Three well-known antioxidant standard compounds; vitamin C (ascorbic acid), Gallic Acid and Trolox (a water-soluble vitamin E analogue) were used to compare the antioxidant potentials.

Lastly, Chapter 6 summarises the main discussion and conclusions obtained from these studies. Recommendations for further studies are also included.

CHAPTER TWO

LITERATURE REVIEW

Lignocellulosic biomass is the most abundant renewable material on Earth. It is composed of three main biopolymers: cellulose (35–50%), hemicelluloses (up to 35%) and lignin (5–30%), the quantities of which vary depending on the type and species of plant source (Mäki-Arvela *et al.*, 2010, Sun *et al.*, 2013). The complex and rigid structure of these biopolymers make lignocellulose highly resistant to biological and chemical degradation processes (Sun *et al.*, 2013).

2.1 Lignin

Lignin is a complex, amorphous biopolymer that acts as a glue to hold together the hemicelluloses and cellulose of the plant (Cox and Ekerdt, 2012). It is created by enzymatic polymerisation of three phenylpropane monomers, guaiacyl (G) units from precursor coniferyl alcohol, syringyl (S) units from precursor sinapyl alcohol, and *p*-hydroxyphenyl propane (*p*-H) units from precursor *p*-coumaryl alcohol, as shown in Figure 2.1. The resulting structure is a unique and very complex macromolecule that contains a number of different types of linkages (Tejado *et al.*, 2007, Bugg *et al.*, 2011, Cox and Ekerdt, 2012). The dominant linkage is the *β*-aryl ether (β-O-4) representing 48-60% of linkages in lignin (Figure 2.2), depending on the type of wood material. Hardwood and softwood lignin have different structures; a typical softwood lignin consists mostly of G units and a small amount of *p*-H units. On the other hand, hardwoods are generally GS-type lignins, containing mixtures of G and S units with a small amount of *p*-H units (Mohan *et al.*, 2006, Brebu *et al.*, 2013, Zhu *et al.*, 2013).

2.2 Methods for Isolating Lignin

The complex structure of the lignin−hemicellulose network is the major reason for making the isolation of unaltered lignin for structural and/or compositional analyses a challenging task (Achyuthan *et al.*, 2010). Many processes are developed and used in the extraction and isolation of lignin from other constituents of plant material for paper and other products. These processes include physical pretreatment (i.e., ball milling),

solvent fractionation (i.e. organosolv process) chemical pretreatment (acidic, alkaline (Kraft) and oxidative) and biological treatment (Muhammad *et al.*, 2013, Zhu *et al.*, 2013). Recently, ionic liquids (ILs) have received attention as promising sustainable solvents for lignocellulose pretreatment or fractionation (Fu *et al.*, 2010).

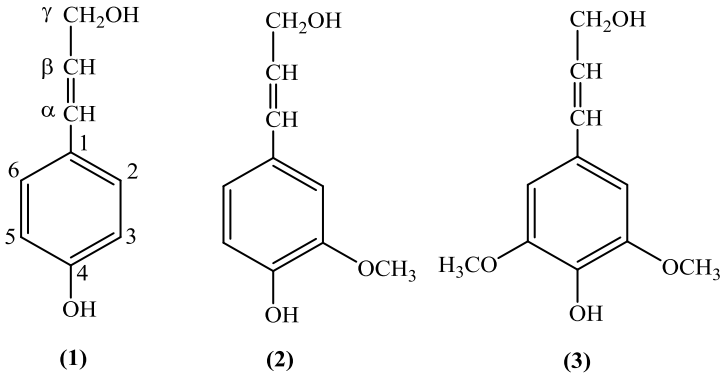


Figure 2.1: The three building blocks of lignin: (1) *p*-coumaryl alcohol (2), coniferyl alcohol and (3) sinapyl alcohol (Hossain and Aldous, 2012).

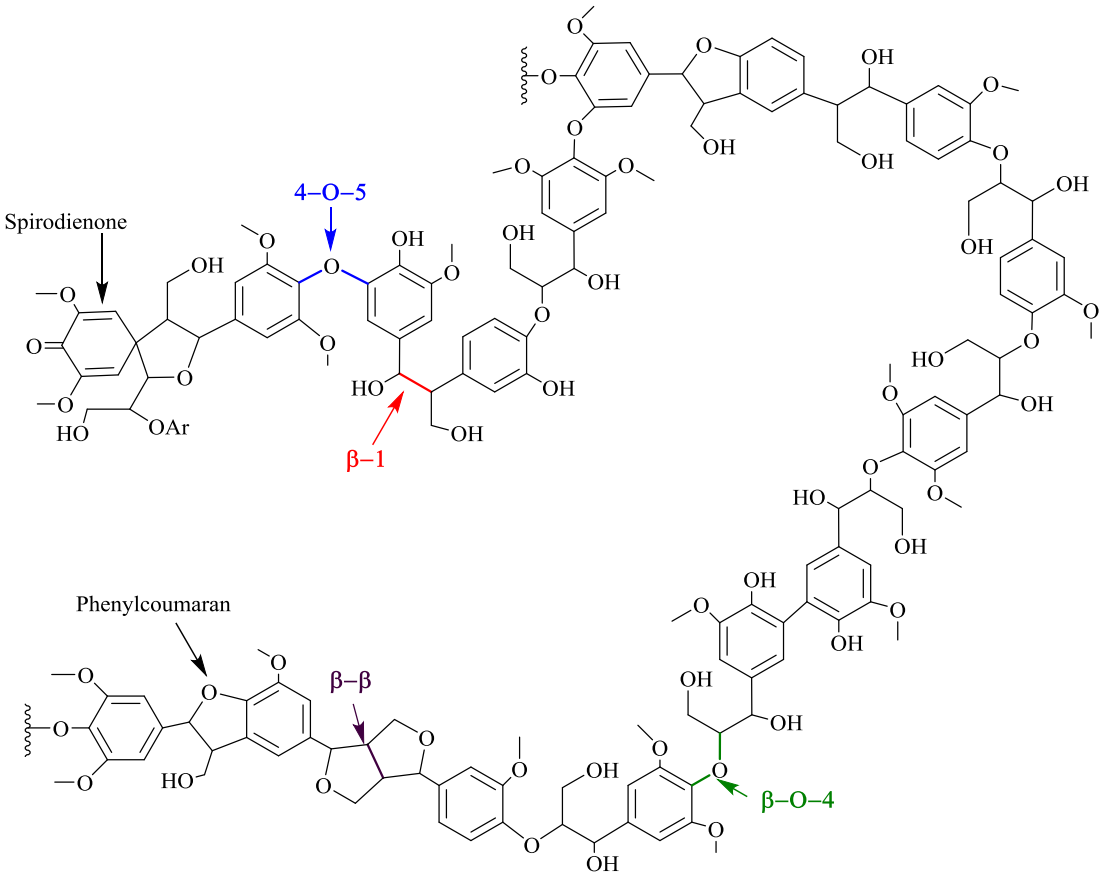


Figure 2.2: Schematic representation of a hardwood lignin structure highlighting the major linkage types. Adapted from (Zakzeski *et al.*, 2010a).

2.2.1 Kraft Lignin Process

The Kraft lignin process is the most dominant chemical pulping technique and accounts for nearly 85% of the total chemical wood pulp production (Tejado *et al.*, 2007, Cui *et al.*, 2013). It uses a combination of aqueous sodium hydroxide (NaOH) and sodium sulfide (Na_2S) at temperatures between 150-180 °C, and strong alkali for about 2 h to degrade lignin in a stepwise process (Rochefort *et al.*, 2004, Zakzeski *et al.*, 2010a). The major drawbacks associated with the Kraft process are pollution and odour problems, high amount of water needed, and large processing plant size (Tan *et al.*, 2009). Kraft lignin is structurally highly modified, as approximately 70–75% of the hydroxyl groups become sulfonated during standard Kraft pulping procedures (Lange *et al.*, 2013).

2.2.2 Sulfite (Lignosulfonate) Process

Lignosulfonates also called lignin sulfonate and sulfite lignin, are relatively common in the pulp and paper industry. The lignosulfonate process is conducted between pH 2 and pH 12 using sulfite. During the process, lignin is sulfonated, degraded and solubilised. The product is typically soluble in water and some highly polar organics and amines (Zakzeski *et al.*, 2010a, Lange *et al.*, 2013).

2.2.3 Organosolv Process

Organosolv lignin is obtained by the treatment of wood with either various organic solvents or their aqueous mixtures. Two of the most common organosolv processes are ethanol or ethanol-water mixture pulping (Alcell) and pulping with acetic acid containing a small amount of mineral acid, such as hydrochloric acid or sulfuric acid (Acetosolv) in a temperature range of 100–250 °C (Zhao *et al.*, 2009, Zakzeski *et al.*, 2010a). Organosolv lignin is hydrophobic, so it is insoluble in water and in acidic aqueous solutions, but will dissolve in basic solutions, and in many polar organic solvents (Lange *et al.*, 2013). In contrast to the lignosulfonate and Kraft processes, the organosolv process typically has no sulfur content, is environmentally friendly, has higher purity, low molecular weight and is a particularly attractive target for catalytic conversion. In addition, it contains many reactive side chains that can be available for

valorisation to high-value chemicals (Binder *et al.*, 2009, Vishtal and Kraslawski, 2011, Brebu *et al.*, 2013). Thus, organosolv lignin is used as a focus in this work.

2.3 Lignin Applications

Almost 98% of lignin is used by the paper and pulp industry as a fuel, so recovering its energy content (Chatel and Rogers, 2014). In addition, lignin is used in several applications such as dispersants, concrete additives, emulsifiers, a replacement for the phenol in phenol-formaldehyde resin synthesis, and in ion-exchange resins (Thielemans *et al.*, 2002, Tejado *et al.*, 2007, Hu *et al.*, 2011, Varanasi *et al.*, 2013). However, due to the very large generated quantities and the aromatic structure, lignin is increasingly considered as a potential renewable source of chemicals (Sun *et al.*, 2009).

2.4 Lignin Depolymerisation

Over the years, several methods have been explored and documented for the depolymerisation of lignin, such as pyrolysis (Huber *et al.*, 2006, Azadi *et al.*, 2013), chemical oxidation including electrochemical oxidation (Stärk *et al.*, 2010, Zakzeski *et al.*, 2011, Reichert *et al.*, 2012, Barta *et al.*, 2014, Zhu *et al.*, 2014), hydrolysis (Toledano *et al.*, 2012, Wang *et al.*, 2013), and enzymatic reactions. In nature, white-rot fungi produce a series of extracellular oxidative enzymes (peroxidases and laccases) that are able to degrade lignin (Hatakka, 2005, Ruiz-Duenas and Martinez, 2009, Bugg *et al.*, 2011). Among these methods, enzymatic reactions and electrochemical oxidation are preferable due to their environmentally friendly characteristics and lower energy demands. Therefore, both approaches were assessed in this work.

Recently, room-temperature ionic liquids (RTILs) have attracted significant attention as promising green and sustainable solvents in the field of lignocellulosic biomass utilisation. The use of ILs is currently concentrated on the dissolution of cellulose and the delignification process (i.e., pretreatment), however, a real challenge remains the valorisation of lignin to valuable chemicals (Chatel and Rogers, 2014).

2.5 Ionic Liquids (ILs)

Room temperature ionic liquids (RTILs), non-aqueous ionic liquids, molten salts, organic salts, and fused salts; all these words have been used to describe salts in the liquid phase (Hallett and Welton, 2011). Ionic liquids are substances composed of organic salts that are characterised by three main criteria: (Werner *et al.*, 2010) firstly, they consist only of ions (cation/anion pairs); secondly, they have melting points below 100 °C; and lastly, they exhibit extremely low vapour pressures below their temperatures of thermal decomposition.

2.5.1 Properties of ILs

ILs have many favourable properties in terms of processing, including negligible vapour pressure, a wide liquid range, non-flammability, high ionic and thermal conductivity, good dissolution power towards many substrates, excellent thermal and chemical stability, and a wide electrochemical potential window (Han and Row, 2010, Zhao, 2010). Furthermore, the physicochemical properties such as the viscosity, hydrophobicity, polarity, density, and solubility of ILs can be tuned by simply selecting different combinations of cations and anions. This has led to the concept of ionic liquids being "designer solvents" (Ohno, 2006, Moniruzzaman *et al.*, 2010b), which increases their potential applications.

2.5.2 Uses and Applications of ILs

There are a broad range of applications and uses for ILs due to their unique tunable properties including extraction, separation (Han and Row, 2010), organic synthesis and catalysis (Dupont *et al.*, 2002), inorganic synthesis (Plechkova and Seddon, 2008), preparation and stabilisation of nanomaterials (Rubim *et al.*, 2008), enzymatic reactions (van Rantwijk and Sheldon, 2007, Moniruzzaman *et al.*, 2010a, Rodriguez *et al.*, 2011), polymerisation (Schmidt-Naake *et al.*, 2008), engineering fluids (Ho *et al.*, 2014) and binders to prepare modified biosensors (Franzoi *et al.*, 2009a, Franzoi *et al.*, 2009b), electrochemistry (Galiński *et al.*, 2006, Reichert *et al.*, 2012) and their applications continue to expand. In particular, the application of environmentally benign ILs as media for biotransformation has received tremendous attention in the

past few years (Franzoi *et al.*, 2009b). Within the scope of this thesis, their applications as solvents for lignin processing and in activation and stabilisation of laccase are of primary interest.

2.6 Ionic Liquids as Solvents for Lignin

The ability of ionic liquids to dissolve biomass provides new opportunities for the pretreatment and conversion of lignocellulosic biomass. In this context, the efficacy of ILs in addressing the following current challenges are discussed below: the dissolution of lignin, as well as depolymerisation of lignin.

2.6.1 Lignin Dissolution and Isolation Using ILs

In recent years, many studies investigating lignin dissolution in ILs have conventionally utilised either whole biomass or commercially available Kraft lignin. However, the range of different lignin sources available makes direct comparison difficult (Lateef *et al.*, 2009, Lee *et al.*, 2009, Fu *et al.*, 2010, Wang *et al.*, 2010, Brandt *et al.*, 2011, Cheng *et al.*, 2012, Liu *et al.*, 2012, Moniruzzaman and Ono, 2012, Liu *et al.*, 2013a, Liu *et al.*, 2013b, Wen *et al.*, 2014); see Table 2.1 Three of the most commonly encountered ILs associated with lignin dissolution are $[C_2mim][C_1CO_2]$, $[C_4mim]Cl$ and $[C_1mim][C_1SO_4]$. A variety of ionic liquids can only partially dissolve wood chips, whereas ionic liquids such as $[C_4mim]Cl$ and $[C{=}C_2mim]Cl$ have good solvating power for wood chips under inert atmosphere (Kilpeläinen *et al.*, 2007).

The IL $[C_2mim][C_1CO_2]$ has been reported by Fu *et al.* (Fu *et al.*, 2010) as an effective solvent for lignin extraction from triticale straw, flax shives and wheat straw. A reported 52.7% of the original lignin in triticale straw was extracted by $[C_2mim][C_1CO_2]$ at 150 °C after a 90-minute exposure. The ionic liquid $[C_4mim]Cl$ is less efficient than $[C_2mim][C_1CO_2]$ for delignification of straw, whilst [DMEA][HCOO], $[DMEA][C_1CO_2]$, [DMEA][glycolate] and [DMEA][succinate] are not suitable for this purpose. Hou *et al.* (Hou *et al.*, 2012) used a similar method to study selective lignin extraction from rice straw using more environmentally-friendly cholinium-amino acid ILs ([Ch][AA]). Up to 71.4% lignin could be extracted by contact with a lysinate-based IL (cholinium lysine, ([Ch][Lys])) for 24 h at 130 °C.

Lee *et al.* (Lee *et al.*, 2009) found that [C_4mim][OTf] and [C_1mim][C_1SO_4] ILs preferentially dissolved lignin from lignocellulose while [C_4mim][PF_6] and [C_4mim][BF_4] do not favour high lignin solubility, as shown in Table 2.1. Maximum solubility was observed when the Hildebrand solubility parameter (δ_H) of the polymer and solvents were identical. It has been reported that [C_2mim][C_1CO_2] is a better solvent for the dissolution of wood than [C_4mim]Cl (Sun *et al.*, 2009), consistent with the results found for straw.

Recently, Moniruzzaman and Ono have demonstrated the use of ionic liquids [C_2mim][C_1CO_2] as a co-solvent as well as a pretreatment agent in the delignification of wood chips. In this study, the wood chips were pretreated with [C_2mim][C_1CO_2] for one hour then treated with laccase from *Trametes sp*., to remove lignin. Around 50% delignification of wood biomass was achieved after 24 h whereas only 10% delignification was obtained when original wood chips (without IL pretreatment) were used (Moniruzzaman and Ono, 2012).

An approach was taken by Cheng *et al.* (Cheng *et al.*, 2012) to study the shape of lignin subunits released from the treatment of three types of lignin (organosolv, Kraft and low sulfonate lignin) with [C_2mim][C_1CO_2]. One important finding that emerged from this study was that the sulfur content in sulfonate lignin could be reduced in the presence of this ionic liquid. [C_4mim][C_1SO_4] was identified as a potential delignification solvent, due to its ability to dissolve large quantities of lignin. In fact, solubilisation of up to 300 g lignin per kg of ionic liquid has been demonstrated using this IL (Wang *et al.*, 2010). The cyano substituted IL [cyanomim]Br has been used, but a less dramatic increase in solubility was observed (Lateef *et al.*, 2009).

The applicability of the IL [C_4mim][HSO_4] for lignocellulose pretreatment was also examined by Brandt *et al.* (Brandt *et al.*, 2011). It was found that ionic liquid liquors containing methyl sulfate, hydrogen sulfate and methane sulfonate anions were most effective in terms of lignin/cellulose fractionation and enhancement of cellulose digestibility (Brandt *et al.*, 2011).

Table 2.1: Solubility and extraction efficiency of lignin in various ILs.

Ionic Liquid[a]	Raw Materials	Solubility	Conditions	Reference
$[C_1mim][C_1SO_4]$	Kraft lignin	>500 (g/kg)	90 °C, 24 h	(Lee *et al.*, 2009)
$[C_4mim][OTf]$		>500 (g/kg)		
$[C_2mim][C_1CO_2]$		>300 (g/kg)		
$[C{=}C_2mim]Cl$ ([Amim][Cl])		>300 (g/kg)		
[Cyanomim]Br	Alkali, low sulfonate content lignin	95.3 (g/kg)	80–90 °C, 20 min	(Lateef *et al.*, 2009)
$[C_3mim]Br$		62.4 (g/kg)		
$[C_4mim]Cl$		87.8 (g/kg)		
[Ch][Lys]	Rice straw	71.4% lignin extraction	130 °C after 24 h incubation	(Hou *et al.*, 2012)
$[C_2mim][C_1CO_2]$	Kraft lignin (Indulin AT)	300 (g/kg)	90 °C, 24 h	(Fu *et al.*, 2010)
	Triticale straw	Lignin extraction 2.1 (g/kg)		
$[C_1mim][C_1SO_4]$	Softwood Kraft lignin	344 g/L	50 °C	(Wang *et al.*, 2010)
$[C_2mim][C_1CO_2]$	Alkaline lignin	30 g/kg	110–170 °C, 1–16 h	(Wen *et al.*, 2014)
$[C_4mim][HSO_4]$	Wood (*Miscanthus)*	Lignin yield 50%	120 °C after 13 h	Brandt *et al.*, 2011)

[a]: Chemical structures and full names of ILs can be found at Appendix A.1

2.6.2 Lignin Depolymerisation and Degradation Using ILs

Unlike hydrolysis and reduction reactions that disrupt the structure and remove chemical functionalities from lignin to produce simpler phenols, oxidation reactions form more complex platform aromatic compounds with additional functionalities or convert lignin directly to fine chemicals. Furthermore, generally the products can be easily separated through a filtration step (Chatel and Rogers, 2014).

The main lignin oxidation processing methods investigated in ILs are metal catalysis, and electrocatalysis. So far, the ILs used to study lignin oxidation and depolymerisation have been only those known to efficiently dissolve lignin. Table 2.2 summarises the different studies performed towards lignin depolymerisation using ionic liquids, indicating the experimental conditions, and ILs used.

Table 2.2: Lignin depolymerisation and degradation in ILs.

Ionic Liquid[a]	Raw Materials	Conditions	Products and Yield	Reference
$[C_4mim][C_1SO_4]$ and $[C_2mim][ABS]$	Organosolv lignin and Klason lignin	Cu/EDTA complex in the presence of a monomeric phenol (4-tert-butyl-2,6-dimethylphenol) at 180 °C	Formation of oligomers with molecular weight (1200-1700), the yield not specified	(Nanayakkara *et al.*, 2014)
$[C_1mim][C_1C_1PO_4]$	Organosolv lignin	$CuSO_4$ as a catalyst in the presence of O_2 at 175 °C for 1.5 h	100% of lignin conversion achieved and the total yield of the aromatic aldehydes was 29.7% Vanillin, syringaldehyde and *p*-hydroxybenzaldehyde	(Liu *et al.*, 2013b)
$[Bnmim][NTf_2]$	Lignin model compound (2-phenoxyacetophenone)	O_2 as the oxidant with H_3PO_4 as a catalyst	Benzoic acid with yield 89 wt % and phenol with yield 84 wt %	(Yang *et al.*, 2015)
$[Bnmim][NTf_2]$	Organosolv lignin	O_2 as the oxidant with H_3PO_4 as a catalyst	Benzoic acid (yield: 43 wt %) and benzaldehyde are the main products	(Yang *et al.*, 2015)
$[C_2mim][C_1CO_2]$	Kraft lignin, low sulfonate alkali, lignin, Pine, Switchgrass and Eucalyptus	160 °C after 6 h incubation	0.5–5.7 g non-polar products/kg of biomass Guaiacol, 4-ethyl guaiacol 4-vinyl guaiacol, eugenol, syringol, 4-(1-propenyl) guaiacol, vanillin, allyl syringol and guaiacylacetone	(Varanasi *et al.*, 2013)

$[C_2mim][OTf]$ $[C_2mim][C_2SO_4]$	Organosolv beech lignin	$Mn(NO_3)_2$ as a catalyst at 100 °C and 8.4 MPa air	Yield: 66.3% Vanillin, vanillic acid, syringaldehyde, syringol, syringic acid, sinapinic acid, DMBQ, coniferyl fragments, and some nonidentified lignin fragments. The predominant products DMBQ and syringaldehyde	(Stärk *et al.*, 2010)
$[HN_{222}][C_1SO_3]$	Alkali lignin	The electrolysis at several potentials in the range from 1.0 V to 1.5 V at 110 °C for 8 h	A wide range of aromatic compounds such as vanillin, benzaldehyde, 3-furaldehyde, m-tolualdehyde, acetovanillone, syringol, 2-methoxy-4-vinylphenol, diphenylether, and guaicol. The maximum yields of cleavage products were 6 wt % with respect to the initial lignin weight	(Reichert *et al.*, 2012)
$[C_2mim][C_2C_2PO_4]$	Alcell organosolv lignin and soda lignin	$CoCl_2 \cdot 6H_2O$, NaOH 80 °C for 3 h	Aldehydes and no monomeric products were formed	(Zakzeski *et al.*, 2010b)

[a]: Chemical structures and full names of ILs can be found at Appendix A.1

Oxidative depolymerisation of organosolv beech lignin has been investigated by Stärk *et al.* (Stärk *et al.*, 2010) using a multiparallel batch reactor associated with $Mn(NO_3)_2$ catalyst and, of four different ILs $[C_2mim][C_1SO_3]$, $[C_2mim][C_2SO_4]$, $[C_2mim][OTf]$ and $[C_1mim][C_1SO_4]$, $Mn(NO_3)_2$ in $[C_2mim][OTf]$ was found to be the most effective reaction system. Impressive yields (66.3%) of products were obtained, with the predominant product being either 2,6-dimethoxybenzoquinone (DMBQ) or syringaldehyde, depending upon reactor conditions. Promisingly, DMBQ could be isolated as a pure compound by basic extraction followed by recrystallisation (Stärk *et al.*, 2010). The use of ILs as solvents for the oxidative degradation of lignin or lignin-related model compounds with molecular oxygen and $CoCl_2 \cdot 6H_2O$ as a catalyst has also been achieved. Several of the alcohol functional groups in the lignin were oxidised to the corresponding aldehydes, but the absence of low molecular weight monomeric compounds suggested that O−C−O and C−C linkages remained intact (Zakzeski *et al.*, 2010b, Zakzeski *et al.*, 2011).

In order to use lignin as a renewable resource for the production of high added-value aromatic aldehydes, a novel approach has been proposed by Liu *et al.* (Liu *et al.*, 2013b). The concept is based on an extraction solvent, such as methyl isobutyl ketone, added to the IL (i.e. $[C_1mim][C_1C_1PO_4]$) system (see Figure 2.3), which prevents the aromatic aldehyde products from oxidising and improves their yields. The conversion of lignin reached a range of 86−100%, and the total yield into identified aromatic aldehydes (vanillin, syringaldehyde and *p*-hydroxybenzaldehyde) ranged from 19.3% to 29.7% in the coupled process (Liu *et al.*, 2013b). Compared with the traditional solvent NaOH aqueous solutions, the lignin conversion and the yields of aromatic aldehydes were higher in the IL process (Liu *et al.*, 2014). Moreover, the products and IL phase were easily separated, allowing the recycle and reuse of the IL phase containing the $CuSO_4$ catalyst with good activity six times (Liu *et al.*, 2013b).

Therefore, although the conversion and depolymerisation of lignin can be achieved, and even controlled by changing the structure of the IL or conditions, bulk separation of the products has only been reported for one pure compound, DMBQ (Stärk *et al.*, 2010).

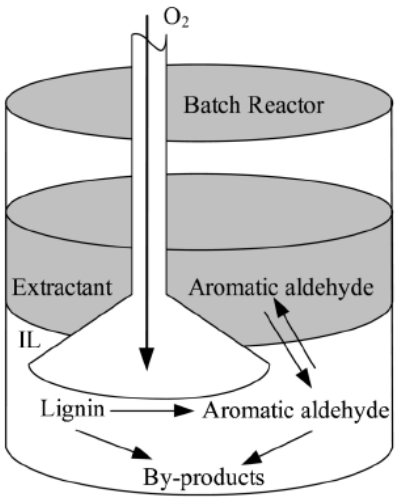


Figure 2.3: Batch process for the production of aromatic aldehydes from lignin coupled with the extraction process (Liu *et al.*, 2013b).

Nanayakkara *et al.* (Nanayakkara *et al.*, 2014) revealed recently that both organosolv lignin and Klason lignin can be extensively depolymerised under oxidative conditions using a Cu/EDTA catalyst complex *via* the redistribution mechanism in the presence of a monomeric phenol (4-tert-butyl-2,6-dimethylphenol) that is blocked from oxidative coupling in the *ortho* and *para* positions in ILs. Yang *et al.* (Yang *et al.*, 2015) had demonstrated a method for depolymerisation of the *β*-O-4 lignin model and organosolv lignin using an IL-based metal-free catalytic system. It was found that IL [Bnmim][NTf_2] combined with a small amount of H_3PO_4 and using O_2 as the oxidant are an excellent catalytic system that can promote the generation of the OOH free radical and thus efficiently transformed the *β*-O-4 lignin model compound 2-phenoxyacetophenone into benzoic acid and phenol and depolymerise organosolv lignin into benzoic acid, benzaldehyde, and some other unidentified compounds.

On the basis of the lignin electrochemistry in IL, Reichert and co-workers reported successfully depolymerisation of alkali lignin through electro-catalytic oxidative cleavage without using any mediator (Reichert *et al.*, 2012). They performed the depolymerisation in protic ionic liquid (PIL) triethylammonium methanesulfonate ([HN_{222}][C_1SO_3]) using an active ruthenium/vanadium/titanium mixed oxide electrode. This IL offered a suitable medium for lignin dissolution, ensured higher potential electrolysis and promoted an oxidative lignin cleavage. The proposed mechanism of the oxidative lignin cleavage involves the disruption of Cα–Cβ bonds within the

dominant β-O-4 linkage, which is prompted by single electron transfer (SET). After cleavage of the Cα–Cβ bond, a second electron transfer takes place, resulting in the deprotonation of the intermediate to form the aldehyde, see Figure 2.4. A wide range of aromatic compounds, such as aldehydes and ketones were identified as the cleavage products, as detected by gas chromatography-mass spectrometry (GC-MS) and high-performance liquid chromatography (HPLC) after diethyl ether extraction (Reichert *et al.*, 2012).

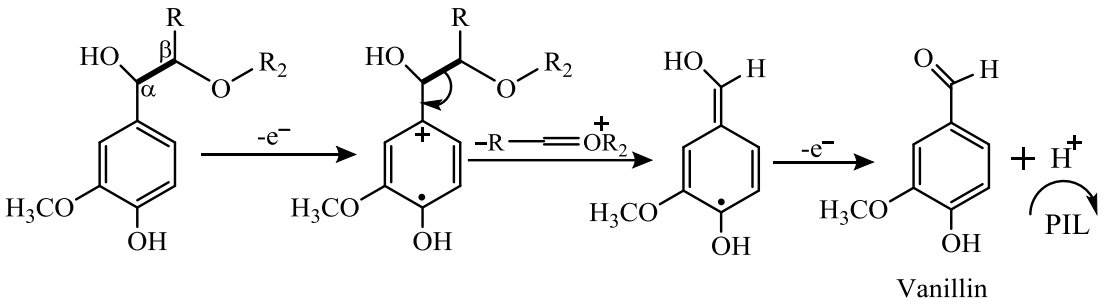


Figure 2.4: Proposed mechanism of the oxidative cleavage of the lignin Cα–Cβ bond in protic ionic liquids. Adapted from (Reichert *et al.*, 2012).

Recently, Varanasi *et al.* (Varanasi *et al.*, 2013) presented an approach to produce low molecular weight lignin and/or monomeric aromatic chemicals based on the selective breakdown of lignin during ionic liquid pretreatment without using any catalyst at high temperatures (120 °C and 160 °C). In this study, $[C_2mim][C_1CO_2]$ was used to produce monomeric aromatic compounds from two types of technical lignins (Kraft lignin and low sulfonate alkali lignin) and three types of lignocellulosic biomass (pine, switchgrass and eucalyptus) during pretreatment. Numerous guaiacyl monomers were obtained from the technical lignin and biomass samples after dissolution in $[C_2mim][C_1CO_2]$ at 160 °C for 6 h. Guaiacol was the main product achieved from both technical lignins and biomass. Syringyl monomers were produced on dissolution of switchgrass and eucalyptus. Moreover, different lignin-derived products could be obtained by tuning the process conditions. The total amount of non-polar lignin products ranged from 0.5–5.7 g/kg of biomass. The amount of vanillin formed ranged from 0.04–2.0 g/kg of biomass under the two processing temperatures tested (Varanasi *et al.*, 2013).

George *et al.* (George *et al.*, 2011) observed that the anion of ILs was shown to be the determining moiety in reducing lignin molecular weight and these ILs behaved as either reactants or catalysts. The size of the depolymerised lignin was decreased with the anionic component of ILs in order sulfates > lactate > acetate > chlorides > phosphates. Lee *et al.* (Lee *et al.*, 2009) also concluded that ILs containing large, non-coordinating anions like $[PF_6]^-$ and $[BF_4]^-$ are not suitable for dissolving lignin; and that methyl sulfate imidazolium-based ILs are effective for dissolution of lignin. Kilpelainen *et al.* (Kilpeläinen *et al.*, 2007) demonstrated that both the anion and cation of ILs played key roles in lignin dissolution. Lee *et al.* and Kilpelainen *et al.* did not cover the opportunities to transformation of lignin to valuable chemicals in their study.

2.7 Laccase

A number of different types of enzymes are available for the biodegradation of lignin, such as laccase. Laccase [EC 1.10.3.2, *p*-benzenediol: dioxygen oxidoreductases] belongs to the family of blue multicopper oxidases that are found in a variety of organisms from bacteria and fungi, to plants and insects. In nature, plant laccases biosynthesis lignin, and white-rot fungi laccases biodegrade lignin, although this role is unclear (Bugg *et al.*, 2011, Lahtinen *et al.*, 2013). Laccases use oxygen to catalyse the oxidation of a broad range of aromatic substrates (phenolic compounds preferentially) and even certain nonaromatic compounds with the concomitant reduction of oxygen to water (Tavares *et al.*, 2013). The laccase active site contains four copper atoms that each has different spectral and paramagnetic properties. The mononuclear Type 1 (T1) copper is responsible for the blue colour of these enzymes. The remaining copper atoms form a trinuclear cluster consisting of Type 2 (T2) copper and two Type 3 (T3) coppers. Substrate oxidation is thought to take place at the mononuclear T1 copper and electrons are transferred to the trinuclear T2/T3 centre where oxygen is reduced to water (Wong, 2009, Yu *et al.*, 2013), as shown in Figure 2.5.

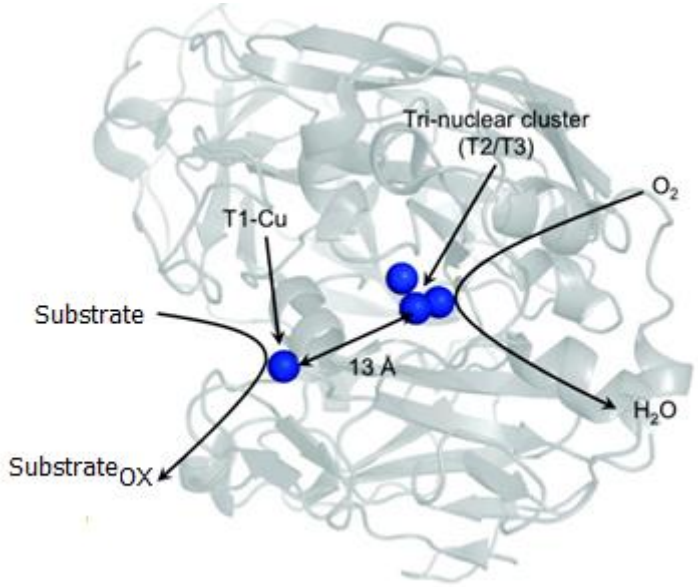


Figure 2.5: Structure of laccase from *Trametes versicolor (LTV)*. The four copper active sites are shown as blue spheres. Taken from (Chakraborty and Barton, 2011).

2.7.1 The Laccase-Mediator System (LMS)

Laccases have only a very limited effect on lignin degradation due to their low oxidation potentials (0.50 - 0.80 V *vs*. NHE) (Piontek *et al.*, 2002) and the limited substrate accessibility, meaning that they can oxidise the phenolic groups only but not the non-phenolic aromatic structures that comprise more than 80% of lignin. Laccases can react indirectly with non-phenolic compounds and potentially degrade lignin in the presence of a redox mediator (Bourbonnais and Paice, 1990, Piontek *et al.*, 2002, Rochefort *et al.*, 2004). A mediator is low-molecular weight compound that, once oxidised by the enzyme, diffuses away from the enzymatic pocket and then can oxidise other substrates, thus regenerating its reduced form. Overall, the laccase-mediator system acts as a catalyst to assist oxidation of lignin by the mediation of electron transfer from the oxidisable groups in lignin to oxygen molecules. This simplified mechanism is depicted in Figure 2.6 (Bourbonnais and Paice, 1990, Bourbonnais *et al.*, 1995, Bourbonnais *et al.*, 1998, Rochefort *et al.*, 2004, Aracri *et al.*, 2013, Christopher *et al.*, 2014). Generally, the ideal redox mediator should be a good laccase substrate, able to generate stable radicals upon oxidation that do not inhibit the enzymatic reaction, and also should not be consumed during the redox transformation (Rochefort *et al.*, 2004, Morozova *et al.*, 2007, Aracri *et al.*, 2013).

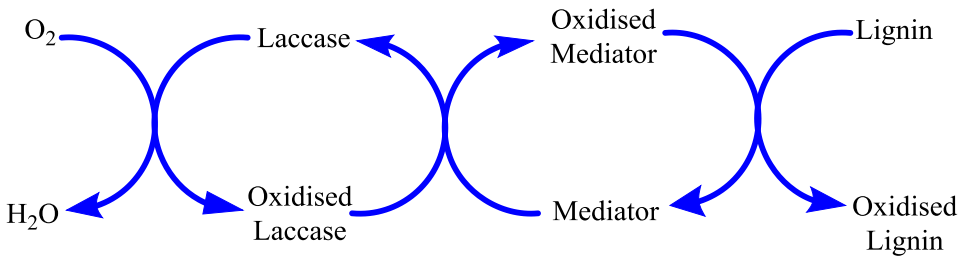


Figure 2.6: Schematic representation of lignin degradation by laccase and mediator system (Bourbonnais *et al.*, 1998).

In the past two decades, the range of compounds identified as mediators for the laccase-mediator system (LMS) has increased dramatically and 2,2'-azino-bis(3-ethylbenthiazoline-6-sulfonic acid) diammonium salt (ABTS, Figure 2.77) is currently regarded as the best mediator for laccase (Bourbonnais *et al.*, 1998, Fabbrini *et al.*, 2002, Rochefort *et al.*, 2002, Shumakovich *et al.*, 2006, Morozova *et al.*, 2007, Díaz-González *et al.*, 2011).

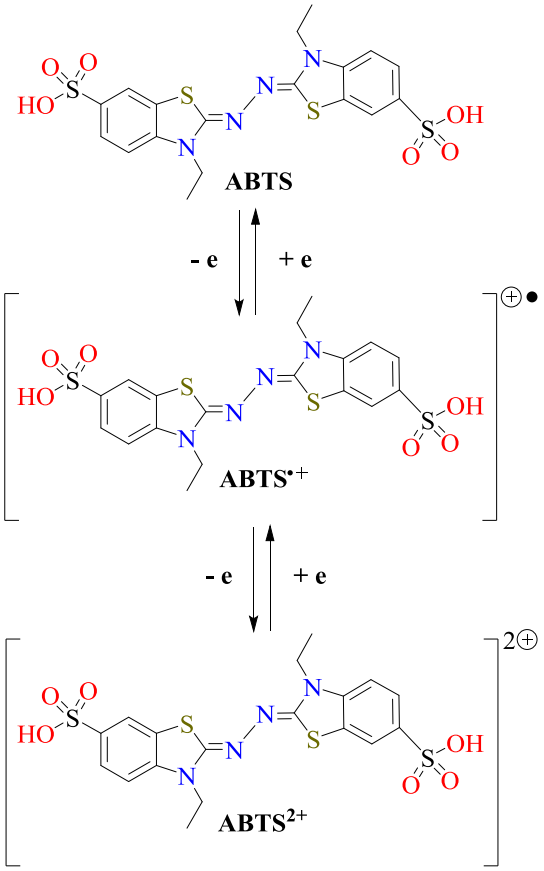


Figure 2.7: Chemical structure of ABTS mediator and formation of the cation radical and the dication by removal of one and two electrons, respectively, from ABTS (Fabbrini *et al.*, 2002).

2.7.2 Applications of Laccase

Laccases have received much attention in the last few decades for a wide number of biotechnological applications and with a broad range of substrates to transform or degrade. These applications include: delignification (biopulping and biobleaching) (Bourbonnais *et al.*, 1997, Christopher *et al.*, 2014), waste detoxification and decontamination, decolourisation of dyes (Baldrian, 2004), degradation of polycyclic aromatic hydrocarbons (Alcalde *et al.*, 2002), textiles (Kunamneni *et al.*, 2008a), the food industry (Osma *et al.*, 2010), as tools for medical diagnostics, as bioremediation agents to clean up herbicides, catalysts for the manufacture of anticancer drugs (Kunamneni *et al.*, 2008b), biosensors (Franzoi *et al.*, 2009b), biofuel cells (Guan *et al.*, 2015) and even as ingredients in cosmetics (Kunamneni *et al.*, 2008b).

2.8 Ionic Liquids as Solvents for Laccase

Although water is an excellent medium for laccase biocatalysis, laccases also exhibit potential use with water insoluble substrates by catalysing reactions in organic solvents. However, the use of conventional organic solvents for enzymatic reactions raises problems concerning solvent toxicity, flammability and low biodegradability (Shipovskov *et al.*, 2008, Tavares *et al.*, 2013).

In order to obtain green biotechnological solutions, the use of ionic liquids as solvents or co-solvents in biocatalytic reactions and processes has received a boost of attention within the past few years as very promising and environmentally friendly alternatives to harmful organic solvents. In addition, biocatalysis in non-aqueous media is a subject of interest to expand the possibilities of using enzymes with substrates that are not soluble in water like lignin, or to enhance the yields and process capacity of those with poor solubility. Enzyme reactions in ILs can exhibit excellent selectivity including the substrate, regio- and enantioselectivity, very high thermal and operational stability as well as better recoverability and recyclability (Moniruzzaman *et al.*, 2010b).

2.8.1 Effect of IL Types and Concentration on Laccase Activity and Stability

The activity and stability of laccase in aqueous ILs solutions have been reported by several researchers (Table 2.3). Shipovskov *et al.* (Shipovskov *et al.*, 2008) have investigated the influence of $[C_4mim]Br$, $[C_4mim][N(CN_2)]$ and $[C_4mim][BF_4]$ on laccase (LTV and LAB). They observed that $[C_4mim][BF_4]$ has an inhibitory effect on laccase, while $[C_4mim]Br$ and $[C_4mim][N(CN_2)]$ could enhance laccase activity, depending on their concentrations. There are many reports demonstrating the effect of the alkyl chain of ILs on the stability and activity of laccase. Tavares *et al.* (Tavares *et al.*, 2012) observed that laccase activity and stability appeared to decrease as the alkyl chain length increased from methyl (C_1) to butyl (C_4) at pH 9 and IL concentration of 50% v/v. The same behaviour was shown by Rodríguez *et al.* (Rodríguez *et al.*, 2011), where the laccase activity, stability, and kinetics decreased with the increased length of alkyl side chains used in imidazolium-based ILs ($[C_{10}mim]Cl$, $[C_8mim]Cl$ and $[C_4mim]Cl$). The same group also noted that among the short alkyl-chain ILs used ($[C_2mim][C_2SO_4]$, $[C_2mim][C_1SO_3]$ and $[C_2mim][MDEGSO_4]$), $[C_2mim][MDEGSO_4]$

was the most promising IL for laccase, maintaining a higher activity after 7 days of incubation than for other ILs (Tavares *et al.*, 2008).

Hinckley *et al.* (Hinckley *et al.*, 2002) have investigated the influence of [4-BMP][BF_4] and [C_4mim][PF_6] on laccase. They found that substitution of [4-BMP][BF_4] for *tert*-butanol as a medium could increase the yield of the oxidation product of the oxidation of anthracene catalysed by laccase.

In general, laccase stability diminishes as the size of the alkyl substituent in the methylimidazolium ring increases. Higher concentrations of ionic liquids cause more destabilisation than lower ones. Thus, low concentrations of [C_2mim][C_2SO_4] allowed enzymatic stability to be maintained. [C_4mim]Cl appears to have a stabilising effect on laccase, with little activity decay observed within three weeks. In contrast, [C_6mim]Br caused a sharp activity loss. However, the enzyme deactivation was so fast in [C_{10}mim]Cl that no activity was detected after very short incubation time (Domínguez *et al.*, 2011). Recently, Yu *et al.* (Yu *et al.*, 2013) found that high levels of either [C_4mim][OTf] or [C_4mpyr][OTf] destabilises laccase, while [TMA][OTf] stabilises laccase.

It is apparent from Table 2.3 that there is a limited number of ILs that are efficient in lignin depolymerisation and at the same time not inhibit the laccase, so, on this basis, [C_2mim][C_2SO_4] was chosen as a focus in this thesis.

Table 2.3: Effect of ILs on laccase activity under different conditions.

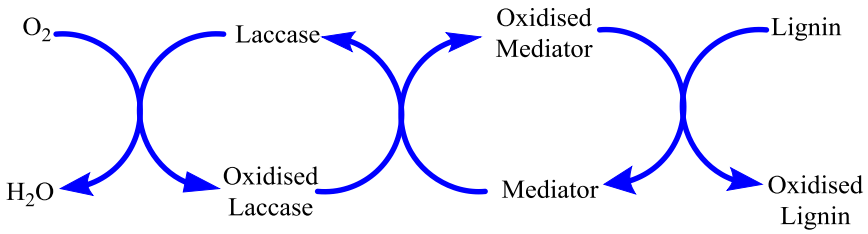
Enzyme Type	Ionic Liquid	Concentration of IL	Conditions	Reference
Laccase, *Trametes versicolor* (LTV)	$[C_4mim]Br$	Activates the laccase until 10% (v/v) then decrease (i.e. max at 10% (v/v) in activity)	Catechol oxidation, 22 °C pH 6.0 for LAB and 4.5 for LTV	Shipovskov) (*et al.*, 2008
	$[C_4mim][N(CN_2)]$	Max at 60% v/v		
	$[C_4mim][BF_4]$	Inhibition occurs even in low concentration (10% (v/v))		
Agaricus bisporus (LAB)	$[C_4mim]Br$	Activate the laccase until 20% (v/v) then decrease (i.e. max at 20% (v/v) in activity)		
	$[C_4mim][N(CN_2)]$	Max at 50% (v/v)		
	$[C_4mim][BF_4]$	Maximum at (10% (v/v))		
Commercial laccase from *Aspergillus* (Novozymes)	$[C_4mim]Cl$	(5% (v/v), 10% (v/v), 20% (v/v) and 40% (v/v) IL/buffer) 10% (v/v) is the best and $[C_4mim]Cl$ is the best IL	T= 40 °C Different pH values; pH 5, 7, and 9 Best pH at 9 for all types of ILs	Rodríguez *et*) (*al.* 2011
	$[C_8mim]Cl$			
	$[C_{10}mim]Cl$			
Commercial laccase from *Aspergillus* (Denilite base II, Novozymes)	$[C_2mim][C_2SO_4]$	(0% (v/v), 25% (v/v), 50% (v/v), 75% (v/v) and 100% (v/v)) Maintain its activity until 75% (v/v) IL/buffer	Immobilised on modified silica pH = 7 at 25 °C	(Tavares *et al.*, 2013)
		(0% (v/v), 25% (v/v), 50% (v/v), 75% (v/v) and 100% (v/v)) Maintain its activity until 50% (v/v)	Free enzyme pH = 7 at 25 °C	

Commercial laccase from *Aspergillus* (Denilite base II, Novozymes)	$[C_2mim][MDEGSO_4]$	(0% (v/v), 25% (v/v), 50% (v/v), 75% (v/v)) Laccase was most active at pH 7.0–9.0 $[C_2mim][MDEGSO_4]$ was the best at pH 9	T= 40 °C Different pH values; pH 5, 7, and 9 No activity was obtained at 75% (v/v) (enzyme precipitates)	(Tavares *et al.*, 2008)
	$[C_2mim][C_1SO_3]$			
	$[C_2mim][C_2SO_4]$			
Laccase from *Trametes versicolor*	$[C_4mim][C_1SO_4]$	10, 25, and 50% (v/v) The activity of laccase was approximately the same for both ILs up to 25% (v/v). For 50% (v/v), the inhibition of laccase was more sensitive to $[C_4mim][C_1SO_4]$ than $[C_1mim][C_1SO_4]$ at pH 9.0	pH 5.0, 7.0, and 9.0 25, 35, 45, 55 °C	(Tavares *et al.*, 2012)
	$[C_1mim][C_1SO_4]$			
Laccase from *Trametes versicolor* CBS 100.29 (CECT20148)	$[C_2mim][C_2SO_4]$ $[C_4mim]Cl$ $[C_6mim]Br$ $[C_{10}mim]Cl$	5%, 10 %, 25%, 50% (v/v) $[C_4mim]Cl > [C_2mim][C_2SO_4] > [C_6mim]Br$ $[C_{10}mim]Cl$	pH 4.5 at 40 °C	(Domínguez *et al.*, 2011)
Laccase from *Trametes versicolor*	$[C_4mim][OTf]$	(0.05, 0.2 and 1.0 mol L^{-1}) [TMA][TfO] stabilise laccase	pH 5.0 at 35 °C	(Yu *et al.*, 2013)
	$[C_4mpyr][OTf]$			
	[TMA][OTf]			
Laccase C from *Trametes sp.*	$[4\text{-}BMP][BF_4]$	25% (v/v)	pH 5.6 at 25 °C	(Hinckley *et al.*, 2002)
	$[C_4mim][PF_6]$			

2.9 Electrochemical Oxidation of Lignin

The oxidation reactions of lignin in the laccase-mediator system (LMS) and electrolytic mediator system (EMS) have been proposed as eco-friendly processes (Figure 2.8) (Shiraishi *et al.*, 2013). The use of EMS has two advantages over LMS, in that (1) a wide range of pH and temperature conditions can be selected (Rochefort *et al.*, 2004, Aracri *et al.*, 2013); and (2) a mediator with a high redox potential can be used (Shiraishi *et al.*, 2013).

a) Laccase-mediator system (LMS)



b) Electrolytic mediator system (EMS)

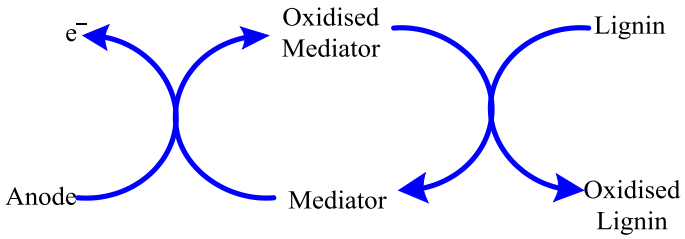


Figure 2.8: a) Laccase-mediator system (LMS) and b) electrolytic mediator system (EMS) (Shiraishi *et al*., 2013).

Cyclic voltammetry is a simple, rapid and powerful technique for studying the electrochemical oxidation of lignin or a lignin model compound by mediators/enhancers (electrochemically unstable intermediates). Some authors have assessed the efficiencies of a number of natural phenols as mediators or enhancers for the oxidation of either lignin or a lignin model compound (veratryl alcohol (VA)) in buffer solution (Table 2.4) (Díaz-González *et al.*, 2009, González Arzola *et al.*, 2009, Díaz-González *et al.*, 2011, Aracri *et al.*, 2013). The laccase mediator system can mediate lignin or lignin model oxidation only after being oxidised by laccase, or, as in the work presented in this thesis, by an electrode replacing it, which greatly simplifies the experimental design. On the other hand, using the IL, which is able to dissolve lignin, affords an advantage compared to the use of aqueous solutions.

As reported in Table 2.4, most of the published studies describe the role of mediator towards the electrochemical oxidation of either lignin model or lignin in aqueous buffer solution, and a few studies have investigated the impact of either lignin model or lignin in the buffer solution or IL without a mediator. To date, none of these studies has investigated the effect of the mediator on the electrolysis of either lignin model or lignin in ILs. Such an assessment is therefore presented in Chapter 4 of this thesis.

Many fundamental studies on electrochemical oxidation have been performed with lignin model compounds in an aqueous buffered medium. Bourbonnais *et al.* (Bourbonnais *et al.*, 1998) characterised the electrochemical properties of the two mediators ABTS and HBT, and their intermediates responsible for lignin oxidation. They also investigated the mechanism of oxidation of lignin model by ABTS and HBT using cyclic voltammetry and bulk electrolysis in an aqueous buffered medium. Fabbrini *et al*. (Fabbrini *et al.*, 2002) compared the mechanism of oxidation of non-phenolic compound (4-methoxybenzyl alcohol) by twelve mediators using cyclic voltammetry. Among them, TEMPO was found to be the most effective mediator. According to Rochefort *et al.* (Rochefort *et al.*, 2002), EMS and LMS gave different results with the same mediator. It has been shown that only the oxidation of phenyl-methyl-pyrazolones and *N*-hydroxynaphthalimide yielded several high-potential intermediates (the potentials of half-oxidation higher than 500 mV) capable of oxidising veratryl alcohol, whereas derivatives of benzoic acid were not able to oxidise the lignin model compound due to the low-potential (redox potential < 450 mV) of the intermediate obtained from electrochemical experiments (Shumakovich *et al.*, 2006). On the other hand, all phenolic compounds studied by means of cyclic voltammetry (sixteen compounds, twelve of which were derived from lignin), showed a catalytic effect on the veratryl alcohol (Díaz-González *et al.*, 2009). Two years later, the same group further demonstrated the ability of these phenolic compounds for oxidation of Kraft and flax lignins by using cyclic voltammetry. The results revealed that the best performing phenolic enhancers for the electrochemical oxidation of lignins were sinapinaldehyde, vanillin, acetovanillone, and syringic acid (Díaz-González *et al.*, 2011).

Similarly, the electrochemical properties of eighteen natural (see Table 2.4) and synthetic compounds (ABTS and violuric acid (VLA)) were evaluated in an aqueous

buffered medium using cyclic voltammetry to differentiate between redox mediators and enhancers. The major difference between a mediator and an enhancer is the oxidised intermediates obtained from the enhancer are electrochemically unstable and only a small number of redox cycles would be occurred between its oxidised and reduced states. Additionally, cyclic voltammetry was also applied to assess the catalytic efficiency of those compounds that oxidise veratryl alcohol and Kraft lignin. It has been demonstrated that, with the exception of gallic acid and catechol, all assayed compounds were capable of oxidising veratryl alcohol with varying catalytic efficiency using cyclic voltammetry. However, only some of them were able to oxidise Kraft lignin. Acetovanillone was found to be efficient in oxidising veratryl alcohol and Kraft lignin, even better than the synthetic mediators TEMPO, violuric acid or ABTS (González Arzola *et al.*, 2009).

In order to solve the electrode fouling attributed to polymerisation, four different IrO_2- based electrodes ($Ti/Ta_2O_5{-}IrO_2$, $Ti/SnO_2{-}IrO_2$, $Ti/RuO_2{-}IrO_2$, and $Ti/TiO_2{-}IrO_2$) were fabricated and their stability and electrochemical activity for lignin degradation were systematically studied to produce vanillin and vanillic acid. It was demonstrated that the $Ti/RuO_2{-}IrO_2$ electrode displayed the highest activity and stability for electrochemical oxidation of lignin without the presence of a mediator (Tolba *et al.*, 2010).

The electrochemical behaviours and catalytic efficiencies of seven natural phenols and two synthetic compounds for oxidising veratryl alcohol and sulfonated lignin were assessed as a function of pH (pH 3-8). The results obtained revealed the potential of using natural enhancers to improve the oxidative efficiencies of a broad range of laccases acting in acidic, neutral, and alkaline conditions (Aracri *et al.*, 2013).

Shiraishi *et al.* (Shiraishi *et al.*, 2013) proposed the use of a system based on bulk electrolysis for the selective oxidation of non-phenolic lignin model compounds in the presence of a mediator. Excellent yields were achieved, especially for the C_α- carbonylation of non-phenolic β-O-4 structures in lignin. Zhang and co-workers (Zhang *et al.*, 2014) developed a new process for lignin degradation to 2,6-bis(1,1-dimethylethyl)-4-methylphenol (BHT) by Pb/PbO_2 electrode anode electrochemical catalysis in an alkaline solution after 3 h. Zhu and co-workers (Zhu *et al.*, 2014)

designed a non-diaphragm electrolytic cell, in which the lignin in alkaline solution was oxidised by the electro-generated H_2O_2 oxidation and anodic oxidation. More than 20 kinds of low-molecular-weight aromatic compounds containing hydroxyl, aldehyde, carbonyl and carboxyl groups were generated.

On the basis of the lignin electrochemistry in ionic liquids, an electro-catalytic oxidative process was recently envisaged from Kraft lignin in the presence of a special protic ionic liquid (PIL), triethylammonium methane sulfonate ($[HN_{222}][C_1SO_3]$), using an active ruthenium/vanadium/titanium mixed oxide electrode without any mediator. A wide range of aromatic compounds such as vanillin, benzaldehyde, 3-furaldehyde, m-tolualdehyde, acetovanillone, syringol, 2-methoxy-4-vinylphenol, diphenylether, and guaicol were identified by gas chromatography−mass spectrometry (GC-MS) and high-performance liquid chromatography (HPLC). In this work, the PIL offered a suitable medium for lignin dissolution that ensured higher potential electrolysis, as well as promoting the oxidative cleavage mechanism (Reichert *et al.*, 2012).

Cyclic voltammetry was used to explore the reaction kinetics between the ABTS mediator and veratryl alcohol in different IL concentrations ($[C_2mim][C_2SO_4]$ and $[C_2mim][C_1CO_2]$). It has been demonstrated that the reaction rate of ABTS mediator with veratryl alcohol was increased at low IL concentrations (up to 15% (v/v)) due to increasing in conductivity. On the other hand, further increasing IL concentrations (up to 30% (v/v)) lead to higher viscosities and correspondingly, lowered the reaction rate (Harwardt *et al.*, 2014). However, only the lignin model compound (veratryl alcohol) was used in their study using different IL concentrations up to 40% (v/v). To expand the scope of ILs for cyclic voltammetry of lignin, three types of lignin (organosolv, Kraft and lignosulfonate), in addition to veratryl alcohol, in 100% $[C_2mim][C_2SO_4]$ were used in this thesis.

Table 2.4: Electrochemical oxidation (cyclic voltammetry and bulk electrolysis) of lignin model compounds and lignin.

Lignin/Lignin Model	Mediator	Solvent	Reaction Conditions		Bulk Elec.	Reference
			T (°C)	pH		
Veratryl alcohol (VA), vanillyl alcohol and Kraft lignin (Indulin)	ABTS 1-hydroxybenzotriazole (HBT)	Buffer	-	4.0	Yes (VA)	(Bourbonnais *et al.*, 1998)
4-methoxybenzyl alcohol	ABTS, HBT, violuric acid (VLA), N-hydroxyphthalimide (NHPI), 2,2′,6,6′-tetramethylpiperidine-N-oxyl (TEMPO), 3-hydroxyanthranilic acid (HAA), phenothiazine, triphenylamine , methyl viologen , 4-acetamido-TEMPO and 4-hydroxy-TEMPO,3-carbamoyl-PROXYL-ene	0.1 M $LiClO_4$ in 4% (v/v) CH_3CN	RT	4.7	No	(Fabbrini *et al.*, 2002)
Veratryl alcohol, 1-(3,4-dimethoxyphenyl)-2-(2-methoxyphenoxy) propane-1,3-diol, and 1-(3,4-dimethoxyphenyl)-2-phenylethanediol	ABTS, HBT, potassium octacyanomolybdate (IV) (MoCN) and *N*-hydroxyacetanilide	Buffer	-	4.5	No	(Rochefort *et al.*, 2002)
Veratryl alcohol	1-phenyl-3methyl- pyrazolone-5 (PP), 1-(3'-sulfophenyl)-3methyl-pyrazolone-5 (SPP-m), 1-(4'-sulfophenyl)-3methyl-pyrazolone-5 (SPP-p), 1-phenyl-2,3- dimethyl--4-amino-pyrazolone-5 (PPA), 1-phenyl-3-methyl–4-methylamino-	Buffer + 2% ethanol	-	5	No	(Shumakovich *et al.*, 2006)

	-pyrazolone-5-N(4)-methanesulfonate (PPA-Na), N hydroxyphthalimide N-(OH) PhI, 1, 8 N-hydroxynaphthalimide N-(OH) NaPhI and 3-amino-(6-hydroxy)-benzoic acid					
Veratryl alcohol	4-Hydroxybenzoic acid (HBA), vanillin, acetovanillone, syringaldehyde, vanillic acid, methyl syringate, p-Coumaric acid, acetosyringone, ferulic acid, coniferyl aldehyde, mesitol, syringic acid, sinapic acid, sinapinaldehyde, caffeic acid and gallic acid	Buffer + 2% ethanol	50	4	No	(Díaz-González *et al.*, 2009)
Veratryl alcohol Kraft lignin	Acetosyringone, gallic acid, vanillyl alcohol, vanillin, syringic acid, *p*-coumaric acid, syringaldehyde, acetovanillone, HAA, catechol, 2,6-dimethoxyphenol (DMP), NHPI, TEMPO, 1-(3′-sulfophenyl)-3 methyl-pyrazolone-5 (SPP-m), 1-(4′-sulfophenyl)-3 methyl-pyrazolone-5 (SPP-p), VLA, HBT and ABTS	Buffer	RT and 37	6	No	(González Arzola *et al.*, 2009)
Kraft Lignin (100 ppm)	No	Electrolyte: 0.5 M NaOH	2, 20, 40 & 60		Yes	(Tolba *et al.*, 2010)

Veratryl alcohol Kraft lignin Flax lignin	ABTS, VLA, gallic acid, caffeic acid (CA), HBA, vanillin, vanillic acid, *p*-coumaric acid, syringic acid, sinapic acid, acetovanillone, acetosyringone, ferulic acid, syringaldehyde, coniferyl aldehyde, mesitol and methyl syringate	Buffer (50 mM tartrate)	50	4	No	(Díaz-González *et al.*, 2011)
Alkali lignin (Kraft)	No	$[HN_{222}][C_1SO_3]$	110	-	Yes	(Reichert *et al.*, 2012)
Veratryl alcohol and Sulfonated lignin	Syringaldehyde, syringic acid, sinapic acid, sinapyl aldehyde, coniferyl aldehyde, ferulic acid, VLA, HBT and methyl syringate	Buffer	RT	3−8	No	(Aracri *et al.*, 2013)
Non-phenolic lignin model compounds	ABTS, NHPI, HBT, TEMPO and VLA	0.1 M $LiClO_4$ in CH_3CN/H_2O = 7/3 (v/v)	28	6 and 8	Yes	(Shiraishi *et al.*, 2013)
Veratryl alcohol	ABTS	15% (v/v) $[C_2mim][C_1CO_2]$ and 15% (v/v) $[C_2mim][C_2SO_4]$ in buffer solutions	22	4.5	No	(Harwardt *et al.*, 2014)
Lignin	No	0.5 M NaOH	-	-	Yes	(Zhang *et al.*, 2014)
Crude lignin	No	Alkaline solution (1.0 M NaOH)	RT	12	Yes	(Zhu *et al.*, 2014)

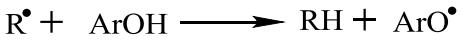
RT: room temperature

Chemical structures of mediators and compounds can be found at Appendix A.1 and Appendix A.2.

2.10 Antioxidant Reaction Mechanisms and Evaluation Methods

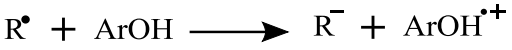
Both laccase mediated oxidation and electrochemical oxidation of lignin are believed to proceed *via* free-radical processes. Such processes govern the kinetics of both breakdown and repolymerisation, and, as such, to optimise these in the context of lignin processing, a detailed understanding of the radical reactions involved is helpful and can help to avoid processing challenges. In particular, lignin components, including breakdown monomers, are often phenolic-based and can act as antioxidant molecules, reacting with radicals as they are formed to form stable species and precursors for repolymerisation. There are two main mechanisms by which an antioxidant-like molecule can react with radicals; hydrogen atom transfer (HAT), and single electron transfer (SET). Assays exist that allow these mechanisms to be distinguished, providing the possibility of rapid mechanistic assessment and understanding to develop a way of controlling specific aspects of the radical process.

HAT-based methods for assessing antioxidant activity measure the ability of an antioxidant (ArOH) to quench free radicals *via* hydrogen donation, relative to the reaction of a defined substrate with the same radical (Scheme 2.1:).



Scheme 2.1: Reaction of an antioxidant with a radical induced in an antioxidant assay through hydrogen atom transfer.

Effective antioxidants must generate a relatively stable free radical, and should react rapidly with free radicals (R•) induced in the assay, but slowly with the substrate (e.g. lipids, fats and protein) to be oxidised. Relative reactivity in HAT methods is evaluated by the bond dissociation enthalpy (BDE) scale for the H-donating group (ArOH) in the potential antioxidant, since the weaker the OH bond, the easier will be the transfer of a hydrogen atom to the free radical. This mechanism is pH independent and is usually quite rapid, typically finished in seconds to minutes. Antioxidant reactivity or capacity measurements are based on monitored competition kinetics (Wright *et al.*, 2001, Leopoldini *et al.*, 2004, Prior *et al.*, 2005).



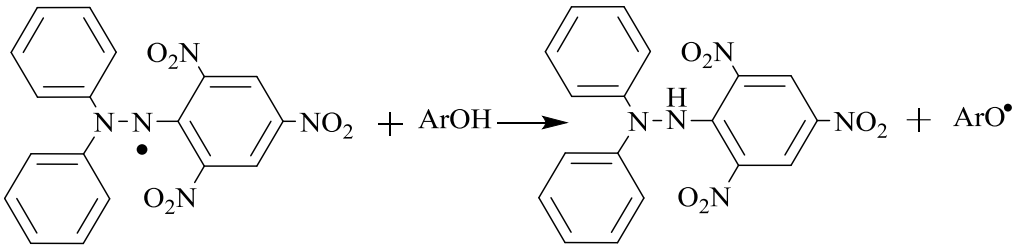
Scheme 2.2: Reaction of an antioxidant through single electron transfer with a radical induced in an antioxidant assay.

In an assay based on the electron transfer method (Scheme 2.2), the radical cation formed must be stable, so that it is unlikely to react with the substrate molecules. The ionisation potential (IP) is the most significant energetic factor for the estimation of the scavenging activity because the lower the ionisation potential, the easier the electron abstraction step. SET reactions are pH dependent and usually slow and require long times to reach completion. Both HAT and SET mechanisms almost always occur in parallel, but with different rates, with the balance determined by the antioxidant structure and pH (Wright *et al.*, 2001, Leopoldini *et al.*, 2004, Huang *et al.*, 2005, Prior *et al.*, 2005).

2.10.1: 2, 2-Diphenyl-1-picrylhydrazyl 1 (DPPH) Assay

The DPPH• radical (Scheme 2.3) is one of the few stable and commercially available organic nitrogen radicals and has a dark purple colour. An assay involving DPPH to assess radical reactivates of molecules was developed by Blois (Blois, 1958) and is based on the measurement of the reducing ability of antioxidants toward DPPH•. The DPPH radical shows an intense UV–Vis absorption maximum within the range 515– 520 nm (purple). The colour turns from purple to yellow due to formation of DPPH-H upon reaction with hydrogen/electron donor compounds and the reaction is conventionally monitored by a spectrophotometer. The method is technically simple, inexpensive, fast, accurate and extensively used to measure the ability of a compound to act as a free radical scavenger or hydrogen donor since the DPPH radical is stable and does not need to be generated *in situ*. The DPPH assay is typically run using the procedure that is discussed in detail in materials and methods section in Chapter 5 of this thesis. The colour of DPPH changes from deep purple to light yellow by either radical reaction (HAT) or reduction (SET) as well as unrelated reactions (reducing agents), which can contribute to inaccurate interpretations of antioxidant capacity, and thus results must be interpreted cautiously. In addition, the steric accessibility of the DPPH radical is a major determinant of the reaction mechanism therefore, small molecules that have better access to the radical site could show higher apparent

antioxidant capacity (Brand-Williams *et al.*, 1995, Sanchez-Moreno *et al.*, 1998, Molyneux, 2004, Prior *et al.*, 2005, Kedare and Singh, 2011).

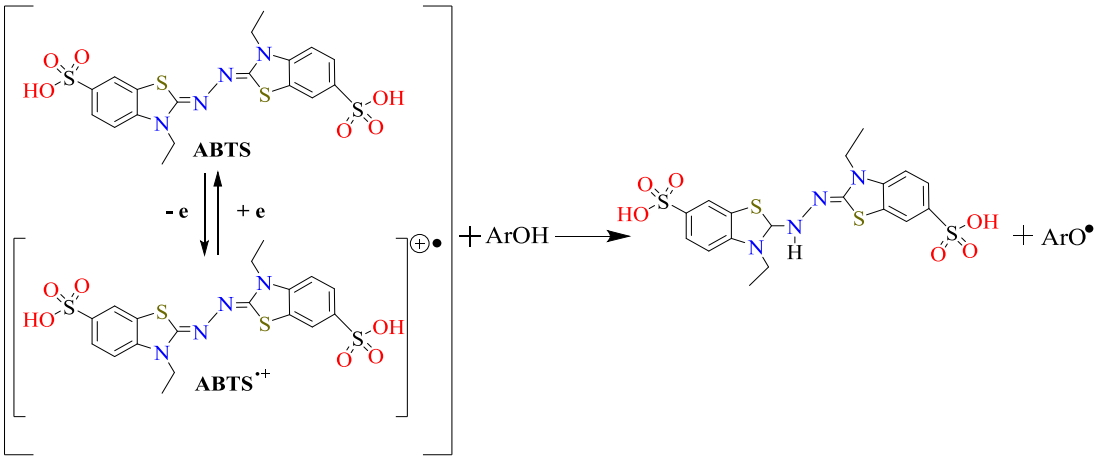


DPPH• DPPH-H

Scheme 2.3: Reaction of the stable radical DPPH• with an antiradical compound (ArOH) (Huang *et al.*, 2005).

2.10.2: 2, 2'-Azino-bis(3-ethylbenthiazoline-6-sulfonic acid) Diammonium Salt (ABTS) Assay

The ABTS method is also known as Trolox equivalent antioxidant capacity Assay (TEAC) and is based on the scavenging ability of antioxidants in reaction with the long-life radical cation $ABTS^{\bullet+}$. In this assay, ABTS is oxidised by either chemical reaction [e.g., 2,2'-azobis(2-methylpropionamidine) dihydrochloride (AAPH) (van den Berg *et al.*, 1999, Kim *et al.*, 2002); potassium persulfate (Re *et al.*, 1999)], enzyme reactions (Miller *et al.*, 1993) or electrochemically (Bourbonnais *et al.*, 1998). A metastable radical cation ($ABTS^{\bullet+}$) is formed, which is intensely coloured (blue-green) (Scheme 2.4). The addition of test compounds to this pre-generated radical cation ($ABTS^{\bullet+}$) reduces the cation to ABTS, thereby decolourising the reaction mixture to an extent and on a time-scale that reflects the antioxidant activity, the concentration of the antioxidant and the duration of the reaction. The relative ability of compounds to scavenge $ABTS^{\bullet+}$ can be easily measured spectrophotometrically at 734 nm. Results of test compounds can be expressed relative to Trolox (TEAC) or vitamin C (VCEAC). The TEAC or VCEAC is equal to the millimolar concentration of either a Trolox or a vitamin C solution, respectively, having the antioxidant capacity equivalent to a 1.0 mM solution of the tested substance under the same conditions (Miller *et al.*, 1993, van den Berg *et al.*, 1999, Antolovich *et al.*, 2002, Kim *et al.*, 2002, Huang *et al.*, 2005, Prior *et al.*, 2005, Floegel *et al.*, 2011).



Scheme 2.4: Generation of ABTS radical cation ($ABTS^{\bullet+}$) and its reaction with an antiradical compound (ArOH) (Oliveira *et al.*, 2014)

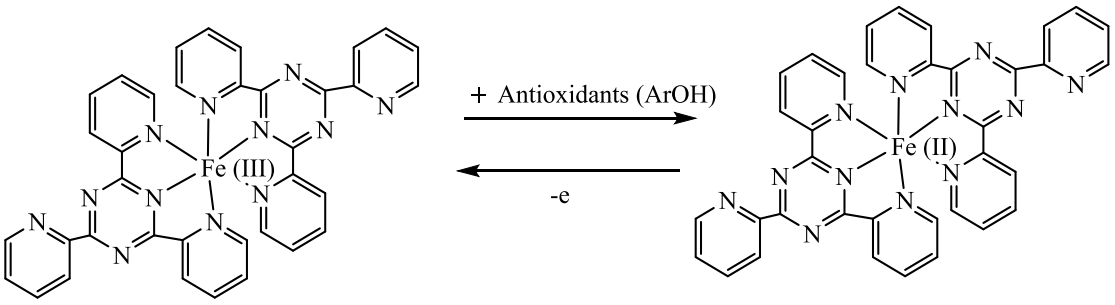
The ABTS assay can be performed at a wide pH range and thus the effect of pH on antioxidant mechanisms can be explored (Prior *et al.*, 2005). A drawback of the assay concerns the quantitation of the assay. By using an endpoint of short duration (4 or 6 minutes), the reaction rate differences between antioxidants and oxidants are not revealed and can result in an underestimation of TEAC values for slow reactions (Huang *et al.*, 2005). Nevertheless, this assay can provide a ranking order of antioxidants (Prior *et al.*, 2005).

2.10.3: Ferric Ion Reducing Antioxidant Power (FRAP) Assay

The FRAP method is a totally electron transfer based (SET-based) method, rather than mixed SET and HAT. It measures the ability of antioxidants to reduce the Fe^{3+} complex of tripyridyltriazine $Fe(TPTZ)^{3+}$ to the intensely blue coloured Fe^{2+} complex $Fe(TPTZ)^{2+}$ in acidic medium (pH 3.6) (Scheme 2.5). Results can be obtained as absorbance increases at 593 nm and can be expressed as micromolar Fe^{2+} equivalents or relative to an antioxidant standard. A FRAP unit is defined as the reduction of 1.0 mol of Fe^{3+} to Fe^{2+} (Benzie and Strain, 1996, Benzie and Strain, 1999, Antolovich *et al.*, 2002, Huang *et al.*, 2005, Prior *et al.*, 2005).

Since the FRAP mechanism is entirely electron transfer-based, it can be very useful in distinguishing dominant mechanisms with different types of antioxidants in combination with other methods. It is good for fast-reacting phenols (4 min) that bind

the iron or break down to compounds with lower or different reactivity. However, it is inappropriate for some polyphenols that react more slowly and require longer reaction times for detection. Thus, it has to be considered that not all antioxidants are able to reduce Fe^{3+} within four minutes (Ou *et al.*, 2002, Huang *et al.*, 2005, Prior *et al.*, 2005). Moreover, compounds including thiols and proteins that quench radicals differently (H transfer) cannot be detected by FRAP (Prior *et al.*, 2005). Another limitation concerns the maximum absorption of Fe (TPTZ)$^{2+}$ at 593 nm. Thus the oxidised antioxidant and its secondary reaction products should have no absorption at 593 nm (Ou *et al.*, 2002).



Scheme 2.5: [Fe (III)$(TPTZ)_2]^{3+}$, [Fe (II)$(TPTZ)_2]^{2+}$ reduction reaction for the FRAP assay (Prior *et al.*, 2005).

2.10.4 Radicals Reactions in Ionic Liquids

Nowadays, a large number of free radicals are reactive species in numerous processes and the increased application of ionic liquids in these processes results in a need to understand more about the interactions between radicals and ionic liquids. Stable radicals (sterically hindered radicals) have been used as useful models for investigation of ionic liquid radical interactions (Strehmel *et al.*, 2008, Strehmel *et al.*, 2010, Strehmel *et al.*, 2014a). Strehmel and co-workers (Strehmel *et al.*, 2008, Strehmel *et al.*, 2010, Strehmel *et al.*, 2014a) reported that the electron spin resonance (ESR) measurements over a broad temperature range on 2,2′,6,6′-tetramethylpiperidine-N-oxyl (TEPMO) derivatives containing different polar substituents at the 4-position with respect to the nitroxyl group are beneficial to describe and investigate the interactions between radicals and ionic liquids. A wide range of ionic liquid anions and cations was covered in their study. The result shows the stable radicals interact with the ionic liquids not only *via* the radical structure. Additional interactions occurred between the substituent bound at the stable radicals and the ionic liquids *via* hydrogen bonding or

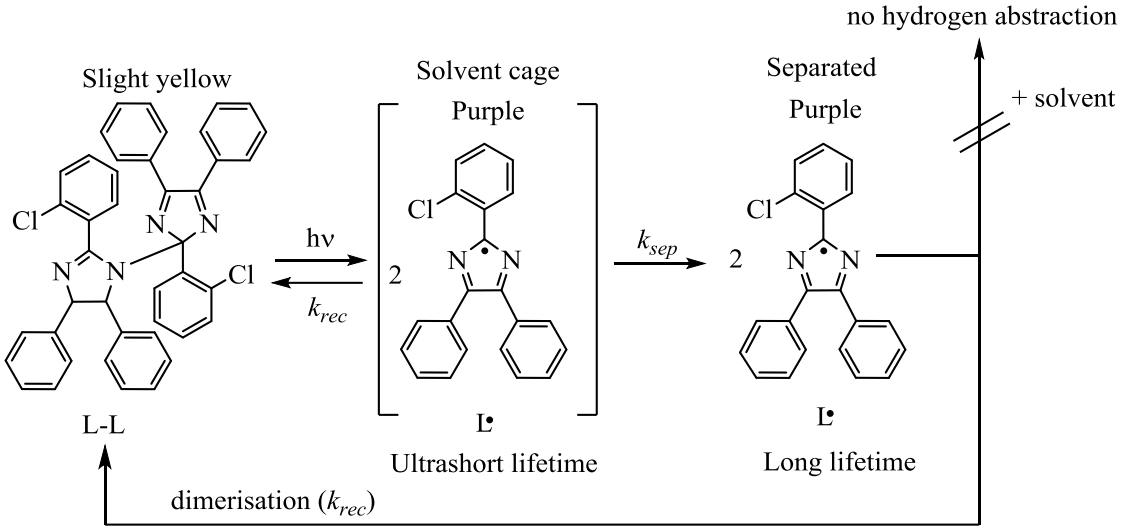
ionic interactions. They also concluded that the mobility of radicals in the ionic liquid depends strongly on the type of the substituent at the solute and on the temperature and therefore on the interactions through the nitroxyl group of the spin probe and the individual ions of the ionic liquid.

The same group also investigated the recombination reaction rates and cage escape yields of lophyl radicals in imidazolium-based and pyrrolidinium-based ionic liquids of varying viscosities in comparison with a conventional organic solvent (dimethylsulfoxide) using laser flash photolysis. Cage escape yields were reduced significantly in the ILs relative to dimethylsulfoxide due to strong ionic interactions between the individual ions of the ionic liquids, indicating longer cage retention times in the ILs and facilitating a faster recombination rate. Moreover, the rate constants of the photolytically generated lophyl radical recombination varied between individual ionic liquids indicating differences in the solvent cage between the ionic liquids. In contrast, the rate constant for lophyl radical recombination increases with temperature in each of individual solvents, which is attributed to a decrease in the solvent viscosity (Strehmel *et al.*, 2009, Strehmel, 2012, Berdzinski *et al.*, 2013, Strehmel *et al.*, 2014a).

Lophyl radicals are obtained from photogeneration of *o*-chlorohexaarylbiimidazole (*o*- Cl-HABI). After lophyl radicals formed, they can either recombine within the solvent cage resulting in back formation of *o*-Cl-HABI or they can escape out from the solvent cage diffusing through the solvent matrix resulting in separated long-living lophyl radicals where they can dimerise with another lophyl radical (Scheme 2.6). As a result, two dimerisation reactions should be taken into account. These are fast dimerisation within the solvent cage and dimerisation after diffusion through the matrix. The latter is strongly influenced by the solvent viscosity (Strehmel *et al.*, 2014a, Strehmel *et al.*, 2014b, Berdzinski *et al.*, 2015).

Exploration of lophyl radical reactions in ionic liquids may contribute to further understanding of free radical reactions in ILs and understand the role of these solvents in radical polymerisation reactions. This role includes the influence of ILs on the molecular weight of the polymers formed, in which the resulting products in ILs possessed higher molecular weight than those polymers obtained using conventional

organic solvents (Strehmel *et al.*, 2009, Strehmel, 2012, Berdzinski *et al.*, 2013, Strehmel *et al.*, 2014a, Strehmel *et al.*, 2014b).



Scheme 2.6: Proposed reaction scheme for photogeneration of lophyl radicals (L•) and their recombination within the solvent cage or reaction with another lophyl radical after escape out of the solvent cage and diffusion through the ionic liquid matrix. k_{rec}= rate constant for radical recombination; k_{sep}= rate constant for radical separation (Berdzinski *et al.*, 2015).

In general, therefore the previous studies have focused on using both stable radicals and photogenerated radicals to investigate the interaction and behaviour of free radicals in ILs, which have been monitoring by ESR spectroscopy. The understanding of radical reaction processes in ILs is vital to understanding lignin-based reactions under both laccase and electrochemical conditions. To do this, a way of probing transient radicals and their relative reactivity would be valuable but has not yet been implemented in the literature. Therefore adoption of the standard assays described above could provide an indirect solution, and this approach is examined in Chapter 5.

CHAPTER THREE

ENZYMATIC TREATMENT OF ORGANOSOLV LIGNIN IN $[C_2mim][C_2SO_4]$

3.1 Introduction

One of the main obstacles to the degradation of lignin is its insolubility in most commonly-used solvents. In recent years, ionic liquids (ILs) have been used for the dissolution of biomass. Very high solubility of lignin has been achieved using 1-ethyl-3-methylimidazolium acetate ($[C_2mim][C_1CO_2]$), 1-butyl-3-methylimidazolium chloride ($[C_4mim]Cl$) and 1-ethyl-3-methylimidazolium ethyl sulfate ($[C_2mim][C_2SO_4]$) (Lee *et al.*, 2009, Sun *et al.*, 2009, Mäki-Arvela *et al.*, 2010) and this good solubility provides new opportunities for lignin degradation.

The main goal of the current study, described in this chapter, was to develop a more effective method for the depolymerisation or transformation of lignin to valuable products in ILs. The use of laccase from *Trametes versicolor* (LTV) with ABTS as a mediator in $[C_2mim][C_2SO_4]$ was explored for the transformation of lignin to high- value chemicals. It is important to bear in mind that there are several factors that contribute towards the efficiency of the enzymatic conversion of lignin in the ionic liquid, which is complex from both the chemical and biological points of view.

As a first step, suitable ILs for lignin dissolution and/or depolymerisation that also did not inhibit laccase were identified from a review of the literature. Accordingly, the ionic liquid ($[C_2mim][C_2SO_4]$) was then selected for this study. Subsequently, the lignin dissolution process was explored with respect to the reaction temperature, IL concentration and process design to find the best conditions for lignin treatment.

3.2 Materials and Methods

3.2.1 Chemicals

Organosolv Lignin was supplied by Lignol Innovations Ltd, Canada. Laccase from *Trametes versicolor* (LTV) ≥ 10 U/mg, the ionic liquid [C_2mim][C_2SO_4] (≥95% purity), 2, 2'-azino-bis-(3-ethylbenzothiazoline-6-sulfonic acid) diammonium salt (ABTS) and all other chemicals and solvents used in this study were purchased from Sigma-Aldrich (UK) and used without any further purification.

3.2.2 Sodium Acetate Buffer Preparation

For the preparation of 0.1 M sodium acetate buffer solution, anhydrous sodium acetate (0.82 g) was dissolved in distilled water (100 mL). The pH was adjusted to pH 5.0 by adding sodium acetate solution (70 mL) to acetic acid solution (0.1 M, 30 mL) at 30 °C. The pH of this mixture was measured using a pH meter. The solution was then stored in a glass bottle at room temperature for future use.

3.2.3 Laccase from *Trametes versicolor* (LTV)

Laccase (0.01 g) was added to sodium acetate buffer solution pH 5.0 at 30 °C (10 mL) to make 1.0 mg/mL LTV solution. This solution was then pipetted into 1.0 mL-tube, where each tube contained 300 µl LTV. These tubes were stored in the freezer (-18 °C) for future use. Each tube was diluted to the desired concentration during a routine experiment and was used once, then discarded after use.

3.2.4 Activity of LTV

Laccase activity was determined spectrophotometrically by the oxidation of ABTS (Wolfenden and Willson, 1982) at 420 nm ($\varepsilon = 36\ mM^{-1}\ cm^{-1}$) in sodium acetate buffer solution (0.1 M, pH 5.0). The concentration of the reagents were: 4 mM ABTS; with 0.1 mg/mL LTV (see Appendix A.4). The oxidation was performed at 30 °C by using a temperature-controlled water-bath (Grant Instruments (Cambridge) Ltd.) with the rotary tube attached to the spectrophotometer. To study the effect of ABTS

concentration, the activity was determined over a range of substrate concentrations varying from 0.004 to 0.8 mM as a final concentration in the reaction system. Protein concentration was estimated spectrophotometrically using Biorad reagent (Appendix A.5). All spectrophotometric measurements were carried out using an Agilent 8453 UV-Vis spectrophotometer (Agilent Technologies Ltd., UK). Enzyme activity was expressed in units where one unit was defined as the amount of enzyme that oxidised 1 μmol of ABTS per min. All experiments were performed at least in triplicate and errors were calculated as the standard deviation. Catalytic constants were determined by fitting the experimental data onto the Michaelis–Menten model applying the Eadie-Hofstee plot.

3.2.5 Treatment of Organosolv Lignin in Sodium Acetate Buffer with LTV

Organosolv lignin with 10 wt % loading rate (0.2 g lignin) was dissolved in sodium acetate buffer (0.1 M, pH 5.0, 1.8 g). LTV (0.25 mg/mL, 10 μL) was then added to the lignin solution. The reaction was started by addition of ABTS solution (4 mM, 200 μL) and the mixture was shaken at 200 rpm in an incubator shaker for 6 h at 30 °C. The effect of LTV and mediators toward organosolv lignin was compared with the control experiments: (1) organosolv lignin under the same conditions but without ABTS, (2) organosolv lignin in buffer without LTV and ABTS, (3) organosolv lignin in buffer with ABTS but without LTV. All the experiments were carried out in triplicate.

3.2.6 The Activity of LTV at Different Concentrations of [C_2mim][C_2SO_4]

The measurement of LTV activity was performed according to the methodology described by Rehmann *et al*., (Rehmann *et al.*, 2012) with some modification. Laccase activity was measured in 96-well quartz plates (Hellma Quartz, Hellma Ltd., UK) using a BMG FLUOstar Optima Microplate reader (BMG Labtech Ltd., UK). The assay was prepared with a 200 μL total volume in each well containing LTV solution (1 μL, 0.1 mg/mL) and IL at different concentrations (either 10, 20, 30 and 50% (v/v) in sodium acetate buffer, or sodium acetate buffer for the control). The assay was incubated without shaking (22 min) to equilibrate the mixtures and then shaken for (1 min) to ensure proper mixing of the solutions. The reaction was started by adding ABTS solution (20 μL, 4 mM in sodium acetate buffer) and the absorbance was

monitored at 420 nm until the reaction reached a steady state at 30 °C. All experiments were performed at least in triplicate and errors were calculated as the standard deviation.

3.2.7 Treatment of Organosolv Lignin in 100% (v/v) [C_2mim][C_2SO_4]

Organosolv lignin with 10 wt % loading rate (0.2 g in 1.8 g of [C_2mim][C_2SO_4]) was dissolved in [C_2mim][C_2SO_4]. The mixture was then placed in a silicon oil bath and heated up to 160 °C using a hot plate with magnetic stirring for 6 h. The selected temperature for dissolution was monitored by a thermometer inside the oil. For lignin treatment at 30 °C, the mixture was shaken at 200 rpm by using incubator shaker (Innova 40, New Brunswick Scientific Co., Inc, USA). Each reaction mixture was incubated in triplicate.

3.2.8 Treatment of Organosolv Lignin in 30% (v/v) [C_2mim][C_2SO_4]/buffer mixtures with LTV

Organosolv lignin with 10 wt % loading rate (0.2 g lignin) was dissolved in [C_2mim][C_2SO_4] (0.6 g) and sodium acetate buffer (0.1 M, pH 5.0, 1.4 g). LTV (0.25 mg/mL, 10 µL) was then added to the lignin solution. The reaction was started by addition of ABTS solution (4 mM, 200 µL) and was shaken at 200 rpm by using incubator shaker for 6 h at 30 °C. The effect of LTV and mediators toward organosolv lignin in 30% (v/v) IL/buffer mixtures was compared with the control experiments shown in Figure 3.1: (1) organosolv lignin under same conditions but without ABTS, (2) organosolv lignin in [C_2mim][C_2SO_4]/buffer mixtures without LTV and ABTS, (3) organosolv lignin in [C_2mim][C_2SO_4]/buffer mixtures with ABTS without LTV. All the experiments were carried out in triplicate.

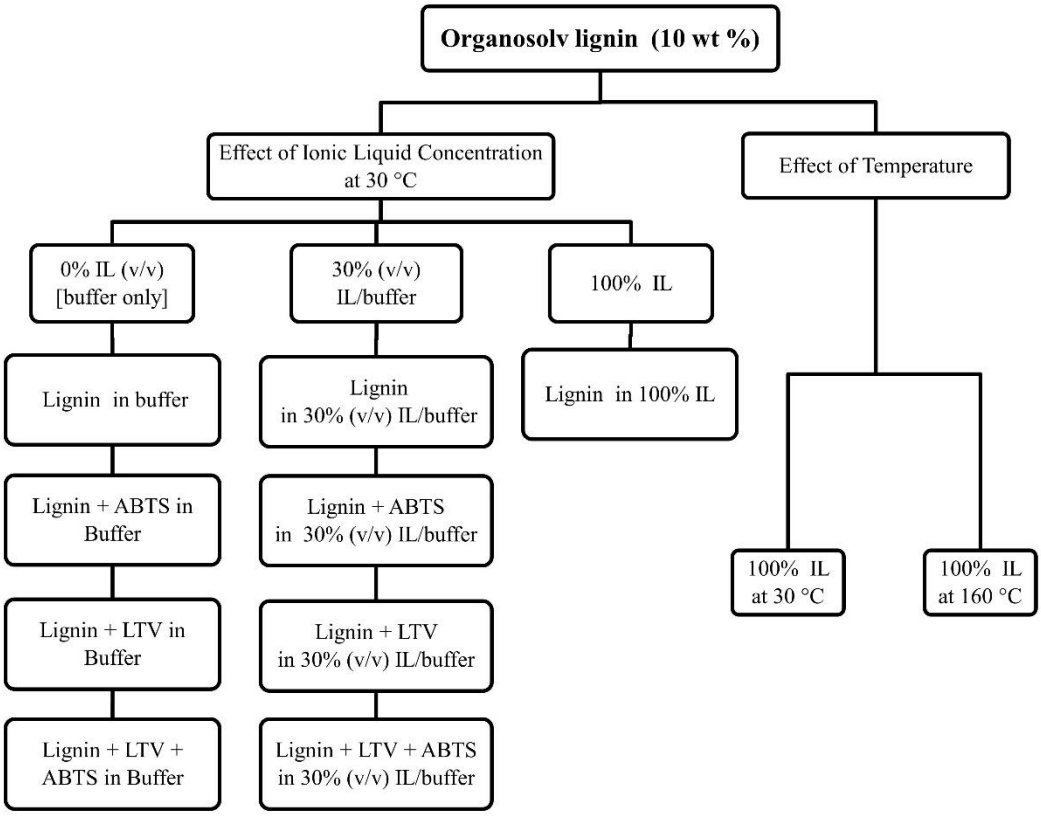


Figure 3.1: Schematic diagram for organosolv lignin treatment in the IL experiment set up.

3.2.9 Extraction of Non-Polar Lignin Breakdown Products by Benzene

Since ILs and water are both polar, benzene was used for the recovery of non-polar lignin breakdown products from the solution (Varanasi *et al.*, 2013). After the time of treatment had exceeded 6 h, water (7 mL, 95 °C) was added to the sample to precipitate the non-solubilised lignin. The mixture of $[C_2mim][C_2SO_4]$, water and lignin were then centrifuged to separate the solid. After the collection of supernatant ($[C_2mim][C_2SO_4]$ and water), the biomass was further washed ten times with water. A total of 2 mL of benzene was added to the supernatant in two steps. The resultant mixture (benzene and sample) was mixed thoroughly and was then phase-separated using a centrifuge. This benzene solution was further concentrated under nitrogen to a final volume of 0.5 mL. For quantification using GC-MS analysis, anthracene-d_{10} (30 μL) was added as an internal standard (IS) to this mixture, as illustrated in Figure 3.2.

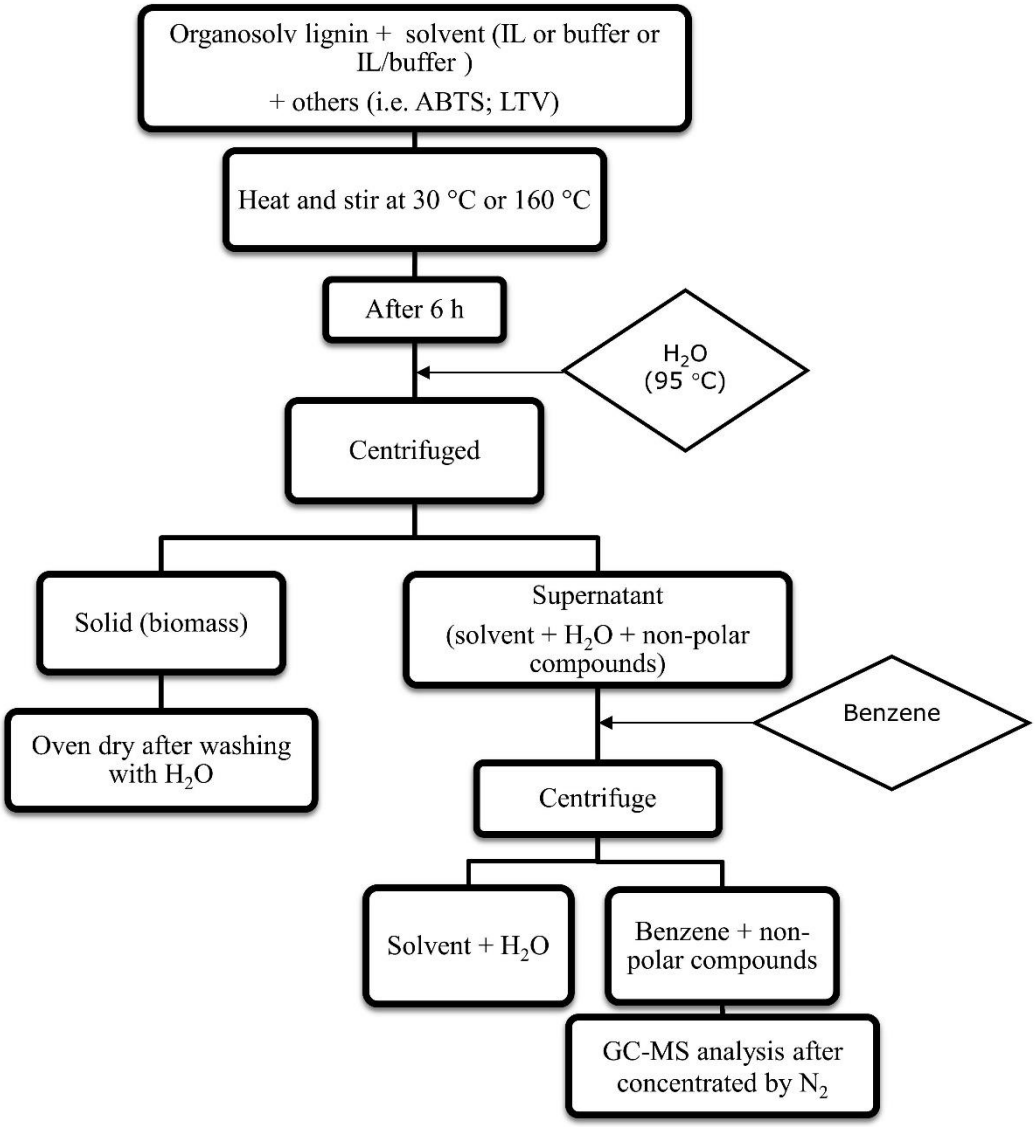


Figure 3.2: Flowchart of extraction process after organosolv lignin treatment with IL as a solvent or co-solvent.

3.2.10 Extraction of Non-Polar Lignin Breakdown Products Using Different Solvents

The main objective of this experiment was to find a suitable solvent for extracting lignin degradation products from IL/lignin mixtures to replace the benzene to avoid the health and safety issues associated with benzene. In addition, the previous benzene extraction process, analysis and qualification methods with GC-MS were modified. Five different solvents (methyl isobutyl ketone, diethyl ether, toluene, dichloromethane and ethyl acetate) were selected based on the literature. Firstly, their solubility in the

IL ([C_2mim][C_2SO_4]) at room temperature was recorded, based entirely on visual observation (where 0.5 mL solvent was added to 1.0 mL of IL followed by gently mixing).

Secondly, the extraction efficiency of the solvents was tested, where organosolv lignin with 10 wt % loading rate was dissolved in [C_2mim][C_2SO_4]. The mixture was shaken at 200 rpm using an incubator shaker (Innova 40, New Brunswick Scientific Co., Inc, USA) for 6 h at 30 °C. After the time had exceeded 6 h, the lignin was precipitated from the reaction mixture by adding 3.5 volume equivalents of distilled water (with regard to the volume of IL) (Figure 3.3). The mixture of [C_2mim][C_2SO_4], water and lignin was then centrifuged to separate the solid. After the collection of supernatant ([C_2mim][C_2SO_4] and water), the biomass was washed with distilled water and extracted with the solvent in triplicate. A total of one volume equivalent of solvent (with regard to the volume of the IL) was added to the supernatant. The resultant mixture (solvent and sample) was mixed thoroughly and was then phase separated using a centrifuge. The combined organic phases were washed with distilled water and dried over anhydrous magnesium sulfate ($MgSO_4$). Then the solvent was evaporated to dryness under vacuum yielding a quantity of brown powder. For the GC-MS analysis, the powder was dissolved in dichloromethane (DCM). Before injection, the sample was filtered with a special filter designed for organic solvents (Sartorius filter Minisart SRP, Scientific Laboratory Supplies) with a 0.2 µm pore size.

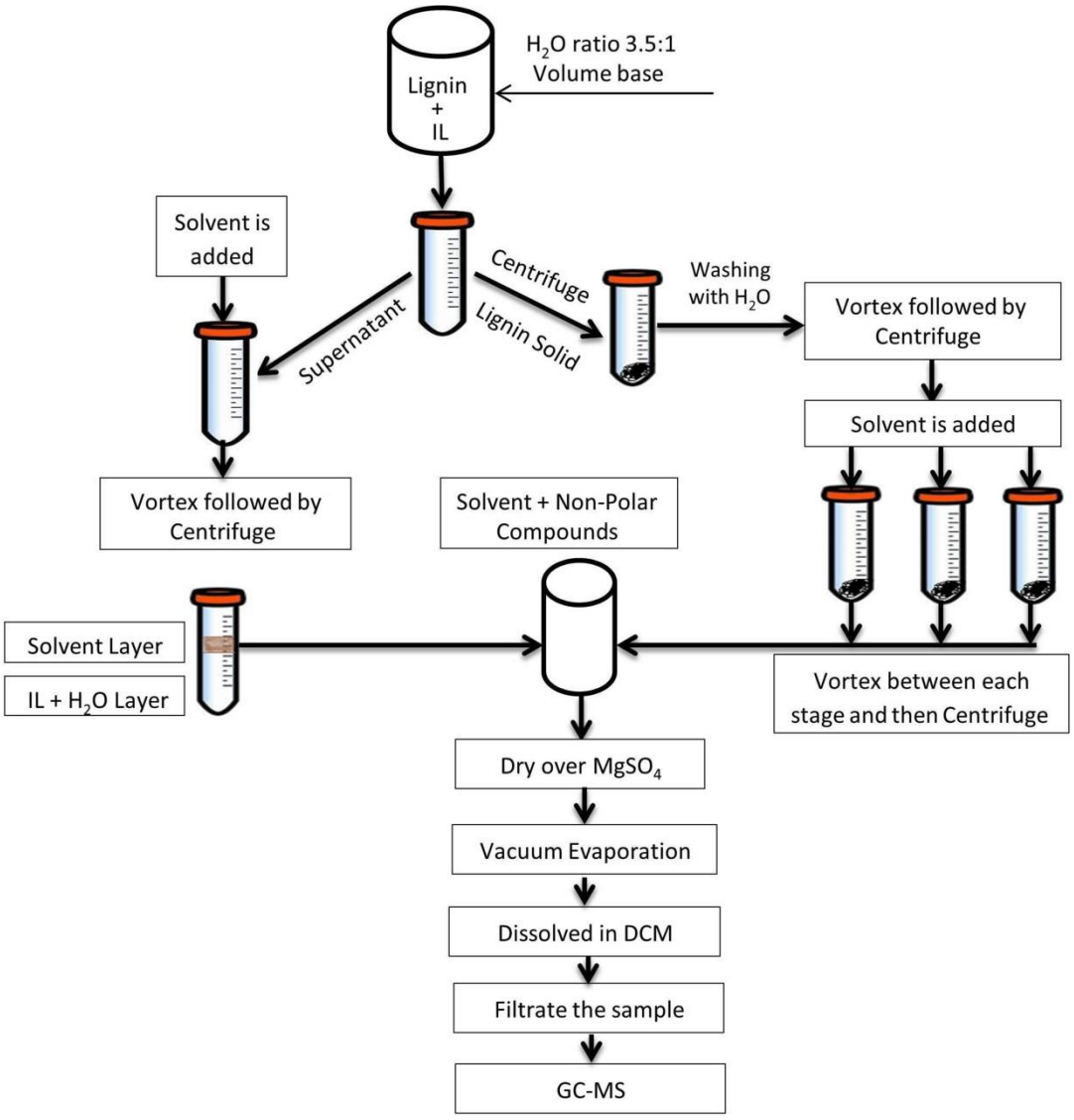


Figure 3.3: Flowchart for extracting lignin degradation products from lignin/IL mixtures.

3.3 Analytical Methods

3.3.1 Gas Chromatography–Mass Spectrometry (GC-MS)

3.3.1.1 GC-MS Analysis of Lignin Breakdown Compounds after Benzene Recovery

The analysis of the (non-polar) lignin breakdown compounds present after benzene recovery was performed using a GC-MS (Agilent Technologies 7890A) coupled to a MS-5975C triple-axis mass spectrometry detector (MS) and integrated auto sampler (model number 7693). The compounds were separated using a HP-5MS (Agilent Technologies) (30 m, 0.25 mm ID, with 0.25 μm of film thickness) chromatographic

column. Samples (1 μL) were injected into the GC at an inlet temperature of 220 °C and was operated in split mode (split flow of 30 mL/min, split ratio = 50). High purity helium was used as a carrier gas with a constant flow rate of 1.2 mL/min. The temperature of the GC was held at 45 °C for 1 min and then was increased at a rate of 10 °C/min up to 280 °C and was held at this temperature for 1 min. The MS was used until the end of the GC run with a solvent delay of 4 min. The ion source was maintained at a temperature of 250 °C and the MS was operated in scan mode. Anthracene-d_{10} was used as the internal standard as it is not present in the biomass samples (Varanasi *et al.*, 2013). The standards of vanillin and syringaldehyde were used to calculate the individual response factor. The response factor of other compounds could not be calculated since the standards were not available. Therefore, the identification of these compounds was based on the National Institute of Standards and Technology (NIST) library.

3.3.1.2 GC-MS Analysis of Lignin Breakdown Compounds after Organic Solvent Recovery

The analysis of the lignin breakdown compounds present after solvent extraction was performed using the same method as mentioned in the previous section (Section 3.3.1.1) with some modifications. Samples (1 μL) were injected into the GC at an inlet temperature of 220 °C and it was operated in a split mode (split flow of 12 mL/min, split ratio = 10). High purity helium was used as a carrier gas with a constant flow rate of 1.2 mL/min. The temperature of the GC was held at 45 °C for 1 min and then was increased at a rate of 10 °C/min up to 300 °C and was held at this temperature for 1 min. The MS was used until the end of the GC run with a solvent delay of 4.6 min. The ion source was maintained at a temperature of 250 °C, and the MS was operated in scan mode. Identification of syringaldehyde was based on both retention time of the authentic standard and NIST database hit.

3.4 Quantification

3.4.1 Calculation of Product Yield after Benzene Extraction by Using Single-Point Internal Standard Method

Single-point internal standard calibration was applied to estimate the response factor (RF) of the eluted compounds with respect to the internal standard (IS). Standards containing the compound (2 mM) and IS (30 μL, 1 mg/mL) in 0.5 mL of benzene were used for calibration. The response factor (RF) was calculated according to equation 3.1.

$$RF = \left(\frac{A_{compound}}{A_{IS}}\right) X \left(\frac{weight\ of\ IS\ injected}{weight\ of\ compound\ \ injected}\right) \quad (3.1)$$

where RF is the response factor of the compound, $A_{compound}$ is the peak area of the compound found from the GC-MS chromatogram and A_{IS} is the peak area of the internal standard found from the GC-MS chromatogram.

Then, the actual concentration of each compound in the injected sample was calculated using equation 3.2 and the RF obtained from equation 3.1.

$$\text{Weight of compound in the injected sample} = \left(\frac{A_{compound}}{A_{IS}}\right) X \left(\frac{weight\ of\ IS\ injected}{RF}\right) \quad (3.2)$$

After that, the amount of each compound (product) with respect to the initial amount of lignin was estimated using equation 3.3 as:

$$\frac{Amount\ of\ product\ A\ in\ the\ supernatant\ (g)}{Amount\ of\ the\ initial\ lignin\ (kg)} \quad (3.3)$$

Since the standards were not available for all the compounds produced from the organosolv lignin reaction in IL, the area ratio (A/A_{IS}) term was used for comparison, where A is the peak area of the compound found from the GC-MS chromatogram, and A_{IS} is the peak area of the internal standard found from the GC-MS chromatogram.

3.4.2 Amount of Syringaldehyde after Solvent Extraction Using the Calibration Curve

Syringaldehyde was the main product obtained from mixtures of organosolv lignin in 30% (v/v) IL/buffer at 30 °C after benzene extraction. According to this result, the efficiency of the solvent recovery was based on the amount of syringaldehyde formed and on the yield obtained. The syringaldehyde peak area is proportional to the amount of the syringaldehyde in the sample. Therefore, the peak area was used with the calibration curve (Appendix A.6) to quantify the amount of the syringaldehyde in the sample.

3.4.3 Determination of Michaelis-Menten Parameters

The enzyme kinetics in this study was characterised by the Michaelis-Menten kinetic parameters (K_m and V_{max}), as well as the initial rate of reaction (v_o) (Johnson and Goody, 2011). In order to find the Michaelis-Menten kinetic parameters, the initial rate of reaction (v_o) values were determined at several substrate (ABTS) concentrations. The values of the initial rates (v_o) were measured in mM/s from the slopes of the initial linear portions of the absorbance at 420 nm versus time curves. The Michaelis-Menten curve can be described by equation 3.4:

$$v_0 = \frac{V_{max}[S]}{[S] + K_m} \tag{3.4}$$

where v_0 is the initial rate of reaction (mM/s), V_{max} is the maximum reaction rate (mM/s) that is observed at saturating substrate concentrations; K_m is the value of substrate concentration at half of V_{max} (mM) and [S] is the ABTS concentration (mM). Then equation 3.4 can be rearranged to give an Eadie-Hofstee plot, which affords equation 3.5:

$$v_0 = V_{max} - K_m \frac{v_0}{[S]} \tag{3.5}$$

A plot of v_o against v_o/[S] will hence yield V_{max} as the y-intercept, V_{max}/K_m as the x- intercept, and K_m as the negative slope. However, before the values of K_m and V_{max} can be obtained, it is necessary to estimate the value of v_o.

The absorbance (A) of the reaction can be obtained spectrophotometrically at a specified wavelength (420 nm). From this, the absorbance data versus time was plotted. The value of v_o at each substrate concentration was calculated by using the changes in absorbance per unit time that correspond to the slope of this graph. The absorbance value at 420 nm can be converted to an actual concentration by Beer-Lambert law, presented in equation 3.6:

$$A_\lambda = \varepsilon c L \tag{3.6}$$

In these conditions, the transmittance and absorbance (A) at the certain wavelength (λ) of the sample depends on the molar concentration (c), light path length in centimetres (L) and extinction coefficient (ε) for the dissolved substance. The standard laboratory spectrophotometers are fitted for use with 1 cm wide sample cuvettes, hence the path length is assumed to be equal to one, with 36 mM^{-1} cm^{-1} as the molar extinction coefficient (ε) (Childs and Bardsley, 1975). Equation 3.6 was rearranged to give equation 3.7:

$$c = \frac{A_\lambda}{\varepsilon L} \tag{3.7}$$

The initial rate of reaction (v_o) is the concentration of the products formed (mM) per unit time, t (s), therefore the following relationships (equations 3.8-3.10) are possible:

$$v_0 = \frac{c}{t} \tag{3.8}$$

$$v_0 = \frac{A_\lambda}{\varepsilon L t} \tag{3.9}$$

$$v_0 = \frac{Slope}{\varepsilon L} \tag{3.10}$$

3.5 Results and Discussion

3.5.1 LTV Kinetics using the Michaelis-Menten Relationship

The rate of ABTS oxidation by LTV is influenced by the ABTS concentration, the operating temperature and also the pH of the buffer (Rancaño *et al.*, 2003). The optimum pH for laccase has been reported as strongly dependent on the substrate, temperature and laccase types. When using ABTS as the laccase substrate, the optimum pH was found to be in the range between pH 3 and pH 5 (Heinzkill *et al.*, 1998, Baldrian, 2006). The optimum temperature for laccase from various sources was found to be between 30-60 °C (Rancaño *et al.*, 2003, Baldrian, 2006). Therefore, the organosolv lignin experiments with LTV were performed at pH 5 and 30 °C. As shown in Figure 3.4, the relationship between the initial rate of reaction (v_0) and the concentration of ABTS follows the Michaelis-Menten relationship. At low concentration of ABTS, there is a steep increase in the initial rate of reaction with increasing ABTS concentration. However, as the concentration of ABTS increases, the LTV active sites become saturated with substrate (ABTS) and no further increase in the initial rate of the reaction is obtained at the same conditions (pH and temperature). Thus, the rate of product formation depends on the activity of the enzyme itself and is independent of the ABTS concentration. It is apparent from Figure 3.4 that there was no significant increase in the rate of reaction when the final concentration of ABTS was increased to 0.2 mM.

The Michaelis–Menten model using Eadie-Hofstee plot was applied to the experimental data in order to obtain the kinetic parameters of the ABTS oxidation by LTV. The value of K_m was estimated to be 0.0200 ± 0.0007 mM for ABTS oxidation and V_{max} was found to be 9.0 (± 0.2) x 10^{-5} mM.s^{-1} at 30 °C and pH 5.0 (Appendix A.7). These values were in good agreement with the values reported in the literature (Rehmann *et al*., 2012). The enzymatic activity of laccase was 51 U/mg (on ABTS at pH 5, 30 °C), and protein concentration 1.073 (± 0.008) x 10^{-4} mg/mL in the cuvette, measured with the Bio-Rad DC protein assay kit (see Appendix A.5). The enzymatic activity of laccase (51 U/mg) was higher than the activity mention by the supplier (activity ≥ 10 U/mg). This result is likely to be related to impurities present in

commercial laccase. Therefore, further research should be undertaken to purify the commercial laccase.

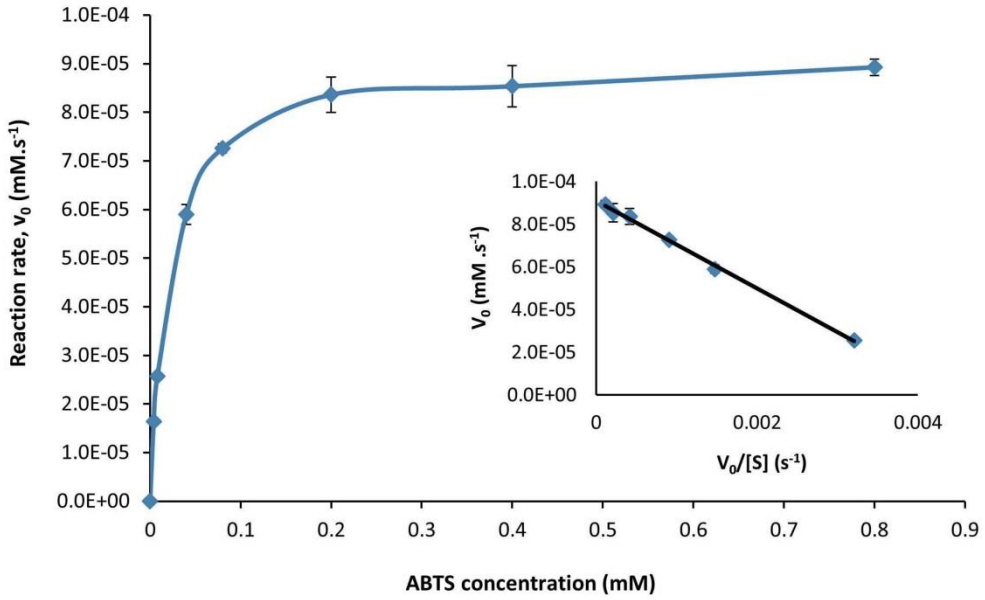


Figure 3.4: Effect of ABTS concentration on the reaction rate by LTV. ABTS was added to start the reaction containing sodium acetate buffer (0.1 mM, pH 5) and LTV (0.1 mg/mL). The change in absorbance at 420 nm was recorded at 30 °C. The inset shows the Eadie-Hofstee plot. Values are means ± standard deviations (n=3).

3.5.2 Effect of LTV on Organosolv Lignin Treatment in Sodium Acetate Buffer Solution

The reaction mixtures containing organosolv lignin, LTV and ABTS were incubated at 30 °C for 6 h. To verify the effect of any enzymatic treatment, controls without ABTS, without LTV, and without both ABTS and LTV were carried out in parallel under the same conditions. As can be seen from GC-MS chromatograms (Figure 3.5), no difference was observed between the reaction sample and the controls performed. Moreover, neither product formation (lignin monomers) nor lignin depolymerisation was detected under these experimental conditions. This result may be explained by the fact that the organosolv lignin is insoluble in water and acidic buffer, so the mass transfer might be very low. Another possible explanation for this is that repolymerisation might have occurred during the reaction. However, with a small sample size (2 mL), caution must be applied, as the findings might be influenced by the sample size.

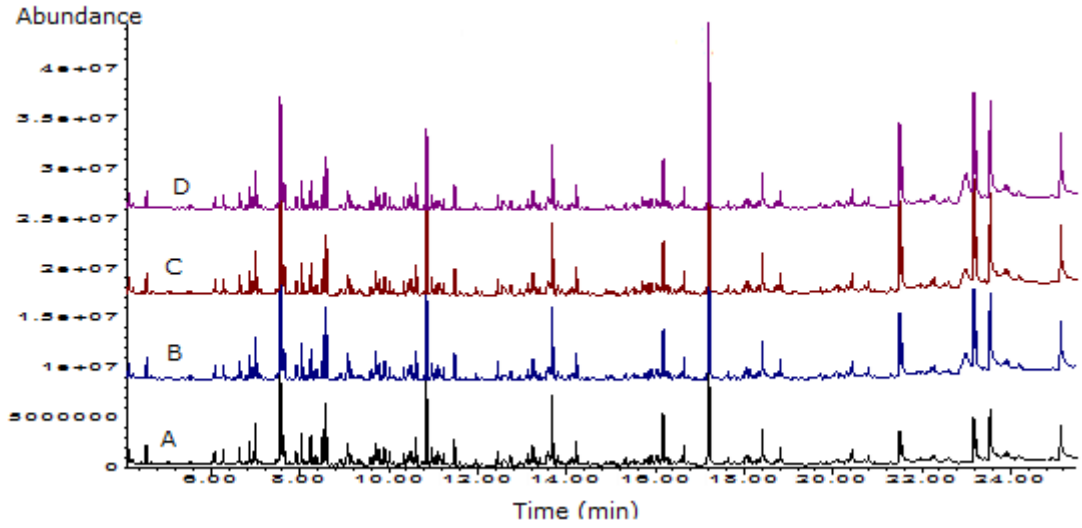


Figure 3.5: The GC-MS chromatograms of products that have been extracted in benzene. The samples were incubated in sodium acetate buffer under identical conditions (at 30 °C for 6 h, shaken at 200 rpm). Benzene extract fraction of organosolv lignin after treatment with (A) LTV and ABTS (B) LTV only (C) ABTS only and (D) benzene extract fraction of organosolv lignin only.

3.5.3 The Activity of LTV at Different Concentrations of [C_2mim][C_2SO_4]

As was mentioned in the previous section 3.5.2, it is clear that the solubility of lignin in the reaction system has the potential to play an important role in the detection of lignin products in the presence of the laccase-mediator system. Accordingly, the IL ([C_2mim][C_2SO_4]) was selected as a reaction medium for this study due to its high capacity to dissolve lignin (Stärk *et al.*, 2010, Liu *et al.*, 2013a), the low inhibitory effect of the IL anion and cation on laccase activity (Tavares *et al.*, 2008, Domínguez *et al.*, 2011, Tavares *et al.*, 2013), and low interference on the ABTS activity detection system (Liu *et al.*, 2013a). Moreover, this IL provides many desirable properties, such as being liquid at room temperature, water miscible, and only moderately viscous (96.6 ± 4.4 mPa.s at 22 °C), allowing it to be pipetted accurately into the assay (Gómez *et al.*, 2006).

First, the effect of [C_2mim][C_2SO_4] on the activity of LTV using ABTS as a substrate was studied by measuring LTV activity over a range of ionic liquid concentrations from 0 to 50% (v/v) in sodium acetate buffer (pH 5.0). The results of the catalytic activity measurements of laccase in this reaction (Figure 3.6) show that the enzyme tolerates moderate concentrations of this water-miscible ionic liquid ([C_2mim][C_2SO_4]).

Increasing concentrations of this solvent resulted in a decrease of the laccase activity, causing enzyme inhibition at concentrations of $[C_2mim][C_2SO_4]$ above 50% (v/v). Good agreement was found between this experimental result and those reported in the literature (Tavares *et al.*, 2008, Domínguez *et al.*, 2011). Thus, the treatment of lignin in $[C_2mim][C_2SO_4]$/buffer mixtures with LTV was carried out at 30% (v/v) of $[C_2mim][C_2SO_4]$.

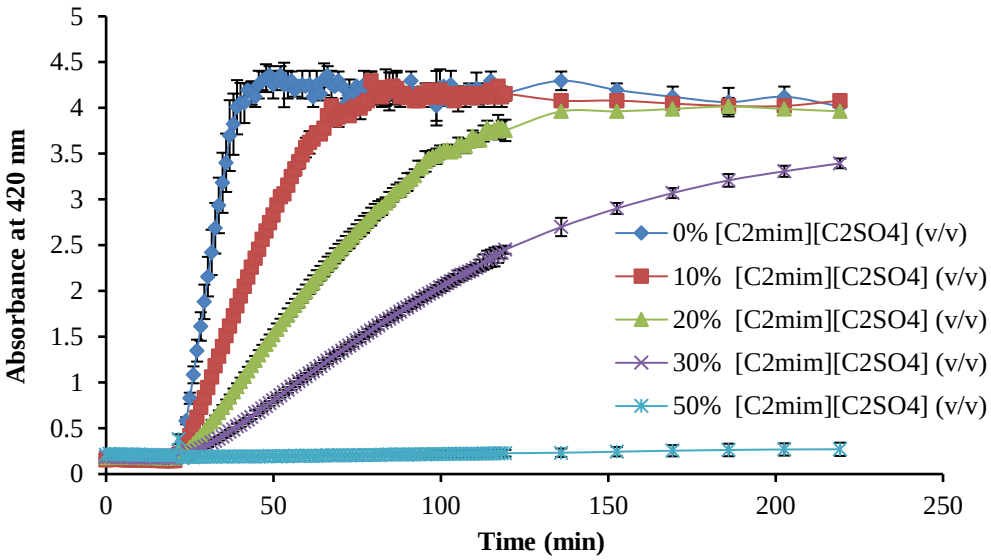


Figure 3.6: Time courses for ABTS oxidation in sodium acetate buffer (pH 5.0) containing various amounts of $[C_2mim][C_2SO_4]$ (0-50% (v/v)) at 30 °C. The reaction was started by adding ABTS after 22 min. Values are means ± standard deviations (n=3).

3.5.4 Effect of LTV on Organosolv Lignin in a $[C_2mim][C_2SO_4]$/Buffer Mixture

The feasibility of using LTV to maximise the yield and selectivity towards the breakdown of lignin was assessed in the presence of IL as a co-solvent. Organosolv lignin was used to gain an understanding of the interaction between laccase and lignin. Reaction mixtures containing sodium acetate buffer (pH 5.0), IL ($[C_2mim][C_2SO_4]$), organosolv lignin and LTV were shaken for 6 h at 30 °C. To verify the effect of the enzymatic treatment process on the organosolv lignin, the lignin was treated using the same conditions, but without LTV.

As shown in Figure 3.7 there was a significant increase of up to 9.4-fold in the amount of 2,6-dimethoxybenzoquinone (DMBQ) identified, compared to the control (lignin only) during the organosolv lignin dissolution process when LTV was used, along with

a slight increase in the amount of furfural, vanillin and syringaldehyde by 1.6-fold, 1.2- fold, and 1.3-fold, respectively (Figure 3.7 and Figure 3.8). These results seem to be consistent with other research that found that DMBQ was formed from lignin by using laccase (Higuchi, 2004). It can therefore be concluded that the use of LTV has enhanced the breakdown of the organosolv lignin in IL/buffer mixtures.

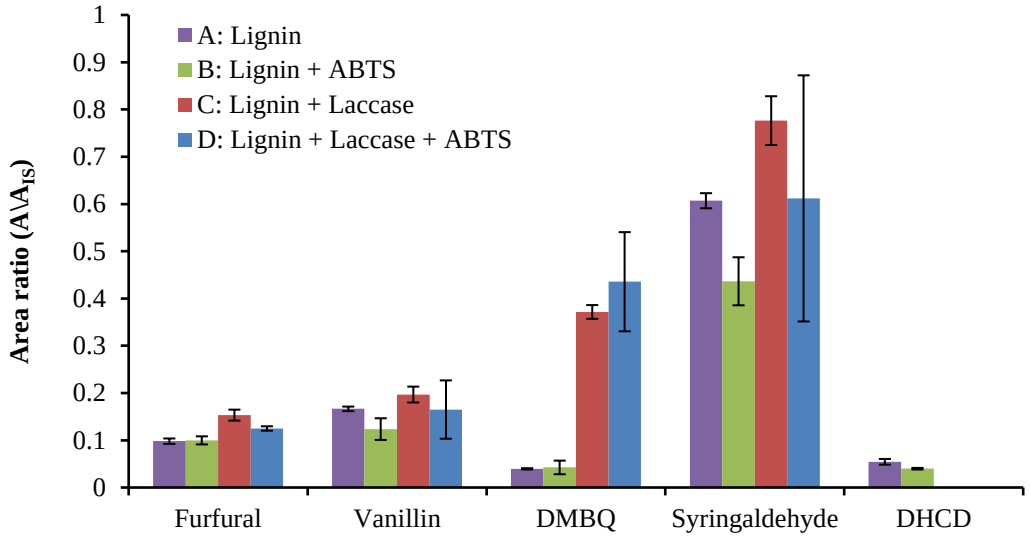


Figure 3.7: Major and minor lignin breakdown products from lignin after dissolution with 30% (v/v) of [C_2mim][C_2SO_4] with LTV and without LTV at 30 °C for 6 h. Identification of products was based on the NIST library data. The data represent the mean of three replicates. The GC-MS ion chromatograms can be found in Appendix A.8.

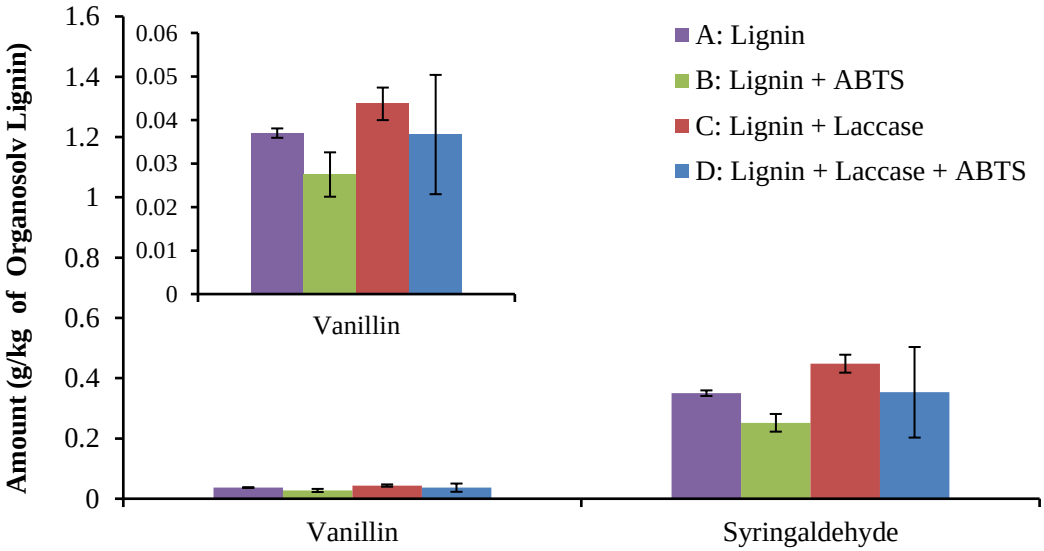


Figure 3.8: Lignin breakdown products (vanillin and syringaldehyde) after dissolution with 30% (v/v) IL/buffer at 30 °C for 6 h. Identification of products was based on the NIST library data and single-point internal standard method. The inset shows the amount of vanillin obtained. The data represent the mean of three replicates.

The specific catalytic mechanism of laccase in these reactions is still unclear. It is possible that many phenoxy radicals are produced from the inner lignin structures accessed by the laccase (Riva, 2006). It was previously shown that laccase alone has only a very limited effect on lignin degradation because laccase can only oxidise the phenolic constituents of lignin by single electron transfer steps, with the simultaneous reduction of dioxygen to water. Also, due to its size, laccase is unable to diffuse rapidly into the fibre wall to reach the remaining fragments of lignin (Barreca *et al.*, 2004, Rochefort *et al.*, 2004). Those studies have demonstrated the efficiency of laccase in the buffer solution, and not in the IL as a solvent or co-solvent. Thus, the co-solvent can be seen to significantly affect the laccase activity.

Laccase plays different roles in different solution systems, Zhang *et al.* (Zhang *et al.*, 2011) found that laccase played a role in lignin polymerisation in the $[C_4mim]Cl/H_2O$ homogeneous solution. However, in the heterogeneous IL solution laccase played a role in lignin biodegradation. The current study has found that lignin biodegradation for organosolv lignin occurred in IL/buffer solution, as evidenced by DMBQ formation, while lignin biopolymerisation may occur in a buffer solution or mass transfer may be problematic because of the low solubility of organosolv lignin in aqueous solution. Thus the addition of ionic liquid has a positive effect on the laccase reaction with organosolv.

3.5.5 Effect of ABTS on Organosolv Lignin in $[C_2mim][C_2SO_4]$/Buffer Mixture

Reaction mixtures containing sodium acetate buffer, IL, organosolv lignin and ABTS were shaken for 6 h at 30 °C. To verify the effect of ABTS on organosolv lignin; the lignin was treated using the same conditions, but without ABTS.

Surprisingly, the total amount of product identified from the dissolution of organosolv lignin in 30% (v/v) $[C_2mim][C_2SO_4]$ with ABTS was observed to be lower than that produced under the same conditions but without ABTS (Figure 3.7). After the treatment of organosolv lignin by ABTS, the amount of syringaldehyde and vanillin was reduced by 28% and 26%, respectively (Figure 3.8). It was found that ABTS radical cation and dication are responsible for lignin degradation (Bourbonnais *et al.*, 1998). Thus, ABTS first must be oxidised by using laccase or electrochemically into a radical and dication

that can then oxidise the lignin (Bourbonnais *et al.*, 1998). This suggests that the material is being further converted, likely through an ABTS mediated reaction. This is consistent with another work where the major inhibitors to lignin depolymerisation were found to be the repolymerisation of lignin fragments and the most common reaction for this repolymerisation was alky–aryl radical coupling (Cox and Ekerdt, 2012). However, the effect of ABTS alone without laccase has not previously been described.

3.5.6 Effect of Laccase-Mediator System (LMS) on Organosolv Lignin in $[C_2mim][C_2SO_4]$/Buffer Mixture

Figure 3.7 shows that the production of DMBQ was higher than the other products when organosolv lignin was exposed to the LMS. Figure 3.7 reveals that there has been a marked increase of up to 11-fold in DMBQ formation during the organosolv lignin dissolution process with LMS. In general, therefore, it seems that the DMBQ was only formed from lignin oxidation by using laccase. However, no significant changes in vanillin and syringaldehyde amounts were identified compared with the control (Figure 3.8).

There was an increase by 14.7% in the formation of DMBQ and a decrease by 26.9% in syringaldehyde formation during the organosolv lignin dissolution with LMS compared to the treatment of the organosolv lignin with LTV only, indicating that syringaldehyde may have been oxidised to give DMBQ. These results seem to be consistent with other research which found that syringaldehyde was transformed to DMBQ (Faure *et al.*, 1996, Stärk *et al.*, 2010).

Although many studies have considered the degradation of non-phenolic lignin structures by the laccase/ABTS system, the mechanism of this process is not fully understood. ABTS oxidation has been demonstrated to occur in two stages: first ABTS is oxidised to the cation radical ($ABTS^{\bullet+}$), followed by the formation of dication ($ABTS^{2+}$). The two oxidised species are relatively stable and electrochemically reversible. The ABTS dication is responsible for the oxidation of the non-phenolic lignin model compound, whereas the ABTS cation radical has been shown to react only with phenolic structures in lignin (Bourbonnais *et al.*, 1998).

In a study that set out to investigate the adsorption of laccase on alkali lignin and the effect of mediator (ABTS) on the adsorption process, Lai *et al.* (Lai *et al.*, 2013) found that ABTS enhanced the adsorption rate and adsorption affinity of laccase. As such, the amount of laccase adsorbed to alkali lignin was higher in the presence of ABTS than in its absence. Although extensive research has been carried out on LMS in the buffer solution, no studies exist that adequately cover LMS in pure IL or IL/buffer mixtures.

3.5.7 Influence of Temperature on Organosolv Lignin in [C_2mim][C_2SO_4]

Temperature is an important variable in dissolving lignin for subsequent processing steps, both in terms of quantity and time taken. The effects of incubation temperature on the quantity and type of chemicals identified from lignin dissolved in [C_2mim][C_2SO_4] were investigated. The quantification was conducted using GC-MS. It is clear from Figure 3.9 that, the patterns of identified products are very different at different processing temperatures. Furfural, 2, 6-dimethoxybenzoquinone (DMBQ), 4-hydroxy-2-methoxy cinnamaldehyde (HMCD) and 3, 5-dimethoxy-4-hydroxycinnamaldehyde (DHCD) were identified only at 30 °C, while 3, 5-dimethoxy-4-hydroxyacetophenone (DHAP) was produced only at 160 °C (Appendix A.9.1 and Appendix A.9.2). Comparing the two results, the product concentrations were higher at 30 °C than at 160 °C and it can be seen that syringaldehyde was the main product at both processing temperatures tested, followed by vanillin. From the data in Figure 3.9, it was apparent that the furfural was only obtained at 30 °C, whilst no furfural was detected at 160 °C. It is necessary to mention that the starting material organosolv lignin contains less than 0.5 wt % furfural. These results are likely to be related to the evaporation of furfural from the reaction mixture at high temperatures since the boiling point of furfural is 162 °C. When the temperature of the organosolv lignin dissolution process was changed from 160 °C to 30 °C, the detection of vanillin and syringaldehyde increased dramatically by 52-fold and 47-fold, respectively (Figure 3.10). It is difficult to explain this result, but it might be related to repolymerisation reactions that may be promoted during treatment at high temperatures. Chemical structures of products identified from organosolv lignin treatment with [C_2mim][C_2SO_4] are shown in Figure 3.11.

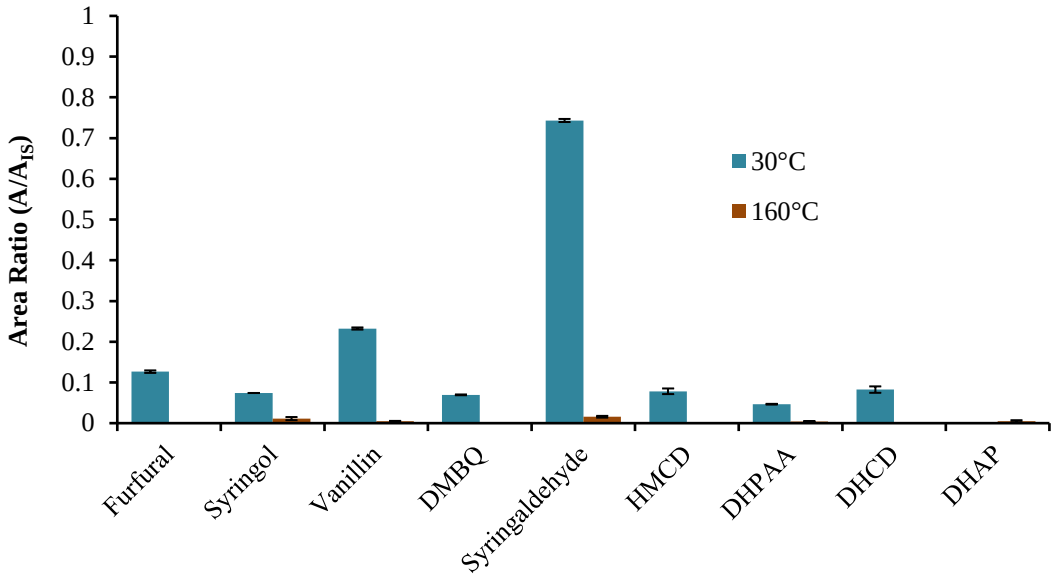


Figure 3.9: Major and minor lignin breakdown products from organosolv lignin after dissolution with [C_2mim][C_2SO_4] at 30 °C and 160 °C for 6 h. Identification of the compounds were based on the NIST library. Identification of vanillin and syringaldehyde were based on a single-point internal standard method and NIST library data.

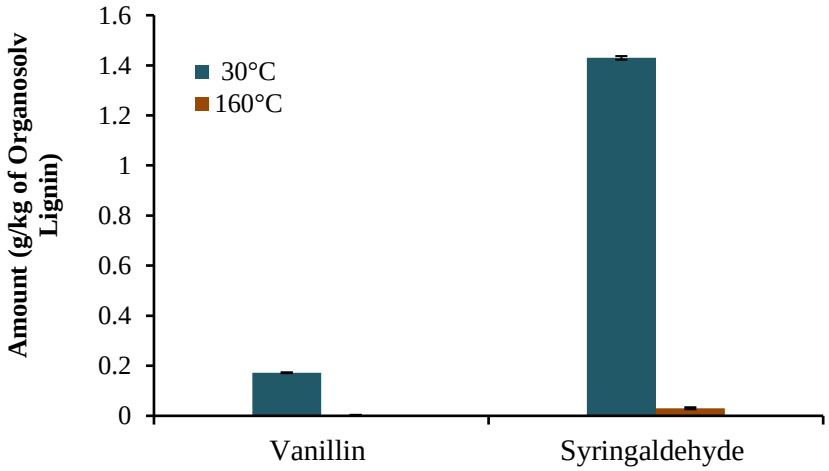


Figure 3.10: Organosolv lignin products (vanillin and syringaldehyde) after dissolution with [C_2mim][C_2SO_4] at 30 °C and 160 °C for 6 h. Identification of products was based on the NIST library data and single-point internal standard method.

Previous studies have reported that different underivatised lignin preparations have glass transition temperature (T_g) values between 90 °C and 180 °C, depending on the source of lignin, with the higher values usually corresponding to softwood Kraft lignin and the lower ones to organosolv lignin (Tejado *et al.*, 2007). Cui *et al.* (Cui *et al.*, 2013) mention that radicals are able to be produced at a temperature above the T_g and that the radical coupling reaction rates are significantly increased due to the reduced viscosity of lignin at this temperature. This is consistent with a higher repolymerisation

rate of lignin-based components, as proposed as an explanation for the quantities of materials identified in Figure 3.9.

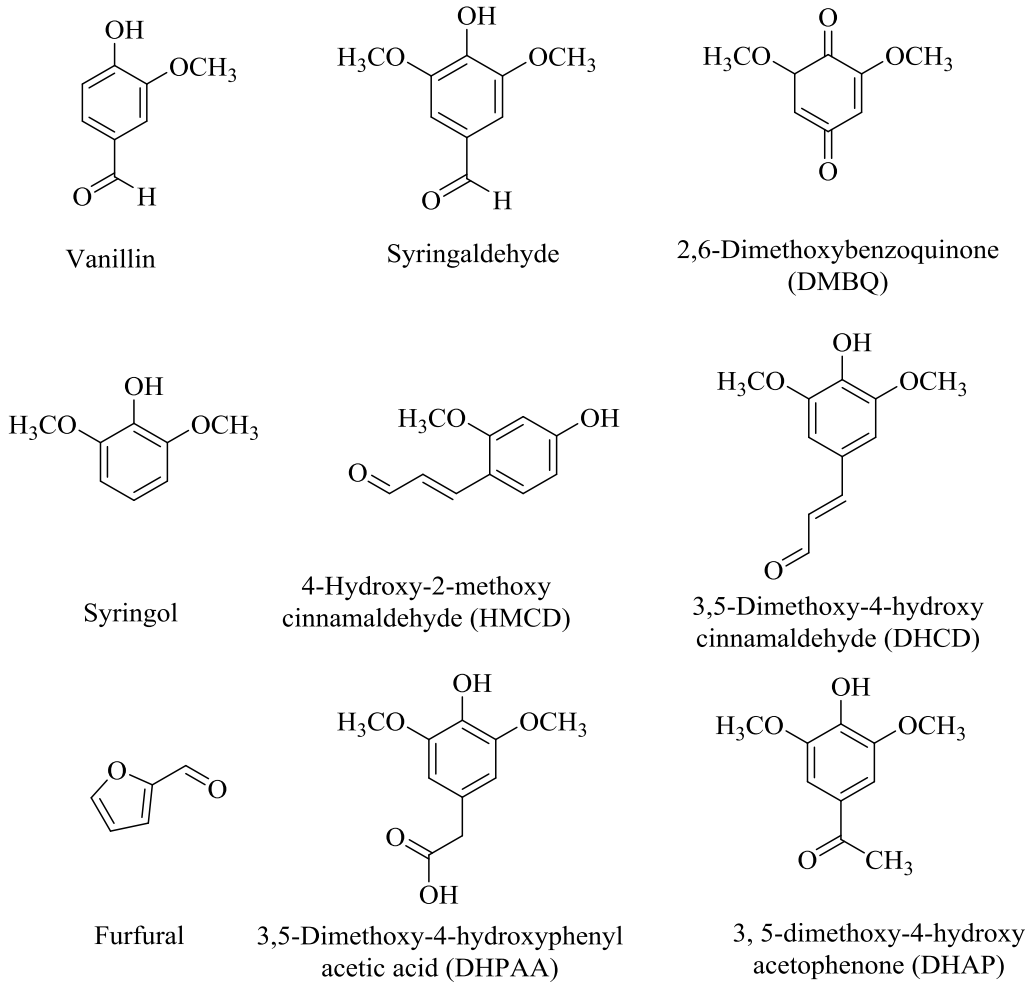


Figure 3.11: Chemical structures of products produced from organosolv lignin degradation in $[C_2mim][C_2SO_4]$ at 30 °C and 160 °C.

Repolymerisation reactions are believed to be one of the main problems in lignin monomer production. Therefore, decreasing the rate of repolymerisation reactions will have to be taken into consideration when proposing to enhance the yields of lignin monomers during the lignin processing. Further research should be undertaken to investigate the effect of process time under a wide temperature range on both the lignin dissolution and the ability for repolymerisation reactions to occur under these conditions.

Varanasi *et al.* (Varanasi *et al.*, 2013) have recently developed a methodology for the dissolution of biomass and technical lignin in 1-ethyl-3-methylimidazolium acetate

([C_2mim][C_1CO_2]). Several guiacyl monomers were found to be present in the supernatant of technical lignin and biomass samples after dissolution in [C_2mim][C_1CO_2], at 160 °C for 6 h, also consistent with the results reported here for organosolv in [C_2mim][C_2SO_4].

In reviewing the literature, very little was found on the dissolution of organosolv lignin in ILs. A considerable amount of literature has been published on ILs in the biomass field, but these works focus on the impact of ILs on the delignification and the crystalline nature of cellulose, while little attention has been paid to the valorisation of lignin.

3.5.8 Effect of [C_2mim][C_2SO_4] Concentration on Dissolution of Organosolv Lignin

The solubility of lignin will strongly influence the efficiency of treatment methods. To clarify that and to find the effect of water content on the lignin dissolution process, dissolution using three different concentrations of [C_2mim][C_2SO_4] 0% (buffer only), 30% (v/v) and 100% (v/v) was investigated. Samples were prepared by incubating organosolv lignin at different concentrations of IL in sodium acetate buffer (pH 5.0) at 30 °C for 6 h and analysing by GC-MS. A higher quantity of syringaldehyde (1.430 ± 0.007 g/kg of lignin) was identified at a 100% (v/v) IL concentration when compared to a 30% (v/v) IL concentration (0.35 ± 0.01 g/kg of lignin) (Figure 3.12 and Figure 3.13). Other products like furfural, syringol, vanillin, DMBQ, HMCD, DHCD and 3,5-dimethoxy-4-hydroxyphenyl acetic acid (DHPAA) were also identified at smaller concentrations. Similar compounds were observed by Stärk *et al.* (Stärk *et al.*, 2010) from the oxidative depolymerisation of beech lignin in [C_2mim][C_2SO_4] using $Mn(NO_3)_2$ as a catalyst. It is apparent from Figure 3.12 that there is no detection of any of the lignin derivatives observed in the sample without IL (in buffer only).

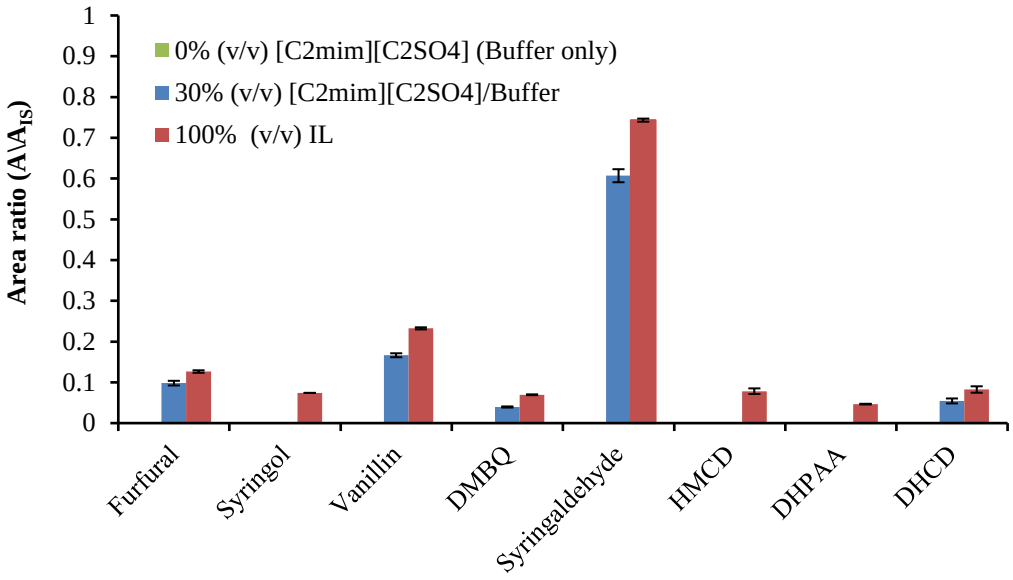


Figure 3.12: Major and minor lignin breakdown products from organosolv lignin after dissolution with 100%, 30% and 0% (v/v) [C_2mim][C_2SO_4] at 30 °C for 6 h without presence of LTV. Identification of the compounds was based on the NIST library. The data represents the mean of three replicates.

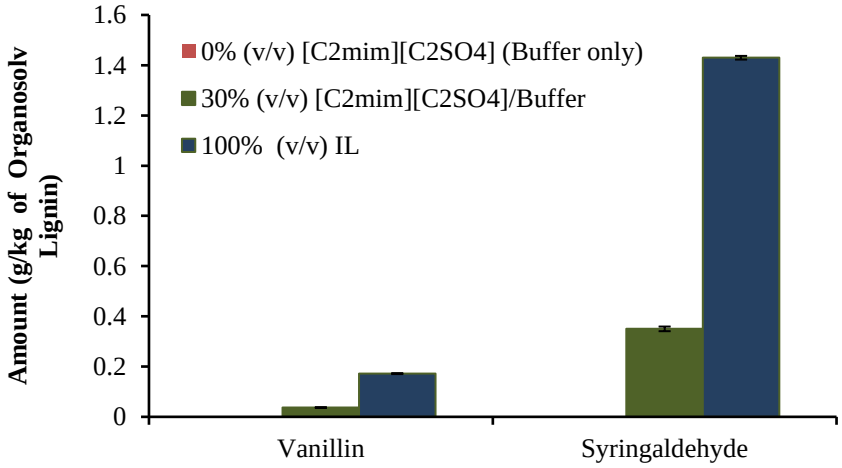


Figure 3.13: Lignin breakdown products (vanillin and syringaldehyde) after dissolution with 100%, 30% and 0% (v/v) [C_2mim][C_2SO_4]/sodium acetate buffer at 30 °C for 6 h without presence of LTV. Identification of products was based on the NIST library data and single-point internal standard method. The data represent the mean of three replicates.

The increase in extraction of aromatic materials at higher IL concentrations may be rationalised as follows. At low water concentrations (high IL concentrations), water interacts selectively with -SO_3 in the ethyl sulfate anion ([C_2mim] [C_2SO_4]), while, at high concentrations (mole fraction of water equal to or greater than 0.6 (0.97 in our case)), it can also form hydrogen bonds directly with the imidazolium ring forming a stable new complex. Therefore, the presence of water competes with lignin in the

interaction with IL (Zhang *et al.*, 2010). Organosolv lignin is insoluble in water, so the mass transfer and dissolution processes decrease in the presence of a high concentration of water, such as 70% (v/v).

The role of water (both its presence and absence) in the IL is significant. ILs, such as 1-allyl-3-methylimidazolium chloride ([C=C_2mim]Cl), interact with lignin mainly *via* hydrogen bonds (H bonds). Therefore, the interaction of the IL with lignin is stronger than that of lignin with lignin. However, the IL prefers to form H bonds with water molecules, and the number of H bonds tends to increase with an increase in the water content. Thus, the H bonds between the IL and lignin are weakened or even destroyed by the addition of water. With the increase of the water concentration, the H bonds between lignin monomers form again and the lignin precipitates from the IL-lignin solution (Ji *et al.*, 2012). The point at which this occurs will be of course vary with the exact nature of each IL.

By opening up the lignin structure in this way with an IL, trapped breakdown products may potentially be released. This may be an additional explanation for the larger quantities of organic materials identified subsequent to the dissolution process when treated with increasing quantities of IL.

To determine the pattern and concentration of compounds present in the starting material (at T = 0) before the reaction, the samples were prepared by dissolving organosolv lignin in [C_2mim][C_2SO_4], [C_2mim][C_2SO_4]/buffer mixture or buffer only, then immediately followed by extraction using benzene and analysed by GC-MS.

If compared to the initial time, the production of syringaldehyde and vanillin were dramatically increased to 16-fold and 8-fold, respectively, when organosolv lignin was dissolved in 30% (v/v) [C_2mim][C_2SO_4] after 6 h of incubation at 30 °C. The total amount of vanillin and syringaldehyde produced from lignin dissolution in 100% (v/v) IL (1.6 g/kg of lignin) was higher than that produced from lignin dissolution in 30% (v/v) IL (0.39 g/kg of lignin) (Figure 3.14). On the other hand, syringaldehyde and vanillin were not detected in buffer dissolution process at both the initial time and after 6 hours of incubation. Stärk and co-workers (Stärk *et al.*, 2010) reported that the total product (syringol, vanillin, DMBQ, syringic acid, syringaldehyde and sinapinic

acid) extracted from the oxidative depolymerisation of lignin in $[C_2mim][C_2SO_4]$ using $Mn(NO_3)_2$ as a catalyst was 28.8 wt %.The yields of cleavage products (including vanillin and syringaldehyde) obtained from electro-catalytic oxidation of lignin in $[HN_{222}][C_1SO_3]$ using an active ruthenium/vanadium/ titanium mixed oxide electrode was 6 wt % with respect to the initial mass of lignin (Reichert *et al.*, 2012).

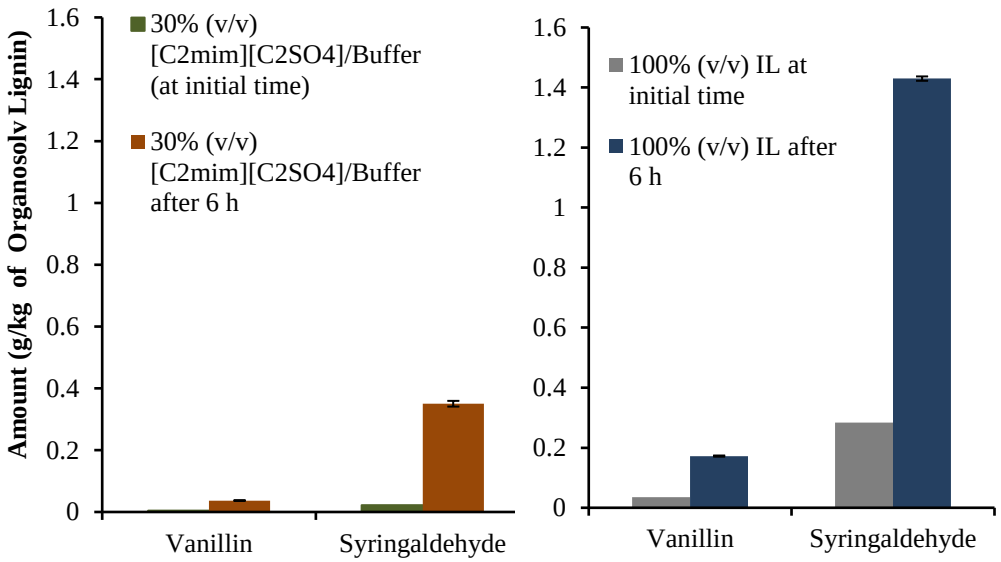


Figure 3.14: The effect of incubation time on product formation during lignin dissolution process in the IL at different concentration, 100% $[C_2mim][C_2SO_4]$ and 30% (v/v) $[C_2mim][C_2SO_4]$/buffer. Identification of products was based on the NIST library data and single-point internal standard method. The data represents the mean of three replicates.

The total amount of vanillin and syringaldehyde obtained from the dissolution of organosolv lignin for both concentration, 100% $[C_2mim][C_2SO_4]$ and 30% (v/v) $[C_2mim][C_2SO_4]$/buffer, increased after 6 h of incubation. In future investigations, it might be possible to use a different process time to explore the effect of process time on the lignin monomers generation during the dissolution process in the ILs.

3.6 Lignin Product Identification - Extraction Process

For the extraction of non-polar products from the mixtures examined, solvents with good solubility towards aromatic aldehydes were investigated, specifically, those that were used previously in separation processes utilising ILs and lignin or lignin models. These solvents included methyl isobutyl ketone, benzene, diethyl ether, toluene, dichloromethane and ethyl acetate (Table 3.1). Methyl isobutyl ketone was selected and used for extraction and separation of the aromatic aldehydes produced from the oxidation of organosolv lignin in four dimethyl phosphate-based ILs (Liu *et al.*, 2013b). Among four extraction solvents (pentane, hexane, heptane and benzene) tested, benzene enabled the most recovery of non-polar products from lignin dissolution in $[C_2mim][C_1CO_2]$. The yields were changed using different solvents, but the patterns of lignin degradation and recovery were similar for all the solvents tried (Varanasi *et al.*, 2013). Stärk and co-workers (Stärk *et al.*, 2010) applied a sequence of extractions to recover the products from the oxidation of organosolv lignin in four ILs. The solution was first contacted with toluene, then with dichloromethane and finally with ethyl acetate. However, the yields and patterns of products recovery were different using different solvents. In an attempt to isolate any possible low molecular weight, monomeric products formed during the oxidation of lignin in $[C_2mim][C_2C_2PO_4]$. Zakzeski *et al.* (Zakzeski *et al.*, 2010b) found that both ethyl acetate and diethyl ether efficiently extracted the products from the ionic liquids, but the extraction efficiencies of ethyl acetate were higher compared to diethyl ether. Reichert and co-workers (Reichert *et al.*, 2012) reported that diethyl ether was a suitable solvent for extraction of a wide range of lignin cleavage products from electrolysis in the IL.

Table 3.1: Products obtained by extraction with different solvents after lignin degradation.

Solvent	IL[a]	Lignin Type	Experimental conditions	Products Obtained	Analysis Method	Reference
Methyl isobutyl ketone (3 times)	$[C_1mim][C_1C_1PO_4]$ $[C_1py][C_1C_1PO_4]$ $[N_{1222}][C_1C_1PO_4]$ $[C_1mmo][C_1C_1PO_4]$	Organosolv lignin	$CuSO_4$ as a catalyst 2.5 MPa O_2 175 °C for 1.5 h	Syringaldehyde, vanillin and *p*-hydroxybenzaldehyde	HPLC	(Liu *et al.*, 2013b)
Pentane, hexane, heptane and benzene	$[C_2mim][C_1CO_2]$	Switchgrass pine, eucalyptus, Kraft and low sulfonate alkali	160 °C and 120 °C for 6 h	Several guiacyl monomers	GC-MS	(Varanasi *et al.*, 2013)
Sequence of extraction: Toluene → acidified with sulfuric acid (pH 1) → dichloromethane → ethyl acetate	$[C_2mim][CF_3SO_3]$ $[C_1mim][C_1SO_4]$ $[C_2mim]$ $[C_2SO_4]$ $[C_2mim][C_1SO_3]$	Organosolv-beech-lignin	10 wt % of lignin $Mn(NO_3)_2$ as a catalyst 100 °C for 24 h	Syringaldehyde, DMBQ syringol and vanillin	GC-MS	(Stärk *et al.*, 2010)
Ethyl acetate Diethyl ether	$[C_2mim][C_2C_2PO_4]$	Alcell organosolv lignin and soda lignin	$CoCl_2 \cdot 6H_2O$, NaOH 80 °C for 3 h	Aldehydes and no monomeric products were formed	GC-MS	(Zakzeski *et al.*, 2010b)
Diethyl ether	$[HN_{222}][C_1SO_3]$	Kraft lignin	Electrochemistry 1.0, 1.3 and1.5 V 110 °C for 8 h	Vanillin and some other aromatic compounds such as; benzaldehyde, syringol, acetovanillone, and guaiacol	HPLC and GC-MS	(Reichert *et al.*, 2012)

[a:] Chemical structures of ILs can be found at Appendix A.1

The solubility of the selected organic solvents (methyl isobutyl ketone, benzene, diethyl ether, toluene, dichloromethane and ethyl acetate) in the IL $[C_2mim][C_2SO_4]$ at room temperature was assessed by direct observation. The results indicated that dichloromethane had a good solubility in the IL (Table 3.2), making phase separation untenable.

Table 3.2: Syringaldehyde concentration and non-polar product yields obtained from organosolv lignin treatment in $[C_2mim][C_2SO_4]$ after solvent extraction.

Solvent	**Solubility in IL**	**Syringaldehyde Concentration (mM)**	**Yield (wt %)[a]**
Benzene	None observed	1.21 ± 0.09	13.0 ± 2.3
Dichloromethane	Yes	-	
Diethyl ether	None observed	0.26 ± 0.03	0.9 ± 0.1
Ethyl acetate	None observed	1.18 ± 0.09	10.6 ± 0.9
Methyl isobutyl ketone	None observed	1.53 ± 0.07	7.0 ± 2.0
Toluene	None observed	0.364 ± 0.006	6.55 ± 0.07

[a:] Yield: with respect to the mass of the initial organosolv lignin.

In all organic solvents used, syringaldehyde, vanillin, syringol, DHPPA and DHCD were isolated but in different quantities, as can be observed in Figure 3.15. Chemical structures of products identified from organosolv lignin treatment with $[C_2mim][C_2SO_4]$ after extraction with different solvents are shown in Figure 3.16. Furthermore, syringaldehyde was obtained as a major product for all the studied solvents. All the lignin monomers compounds can be extracted by benzene and ethyl acetate with different yields. The extraction efficiency of vanillin by ethyl acetate was very low, while methyl isobutyl ketone presented high selectivity toward vanillin. It can therefore be suggested that further investigation of each compound (control extraction) has to be undertaken in order to know better about the maximum extraction efficiency and the selectivity of these products in a different extracting solvent. It could be concluded that type of extracting solvent is an essential factor in isolated and recovery of products obtained from lignin dissolution process in IL.

The yields of the products obtained were changed according to the extracting solvent used (Table 3.2). The lowest extraction yields were observed from diethyl ether. However, out of the solvents tried ethyl acetate afforded the highest recovery yields and selectivity overall of lignin monomer compounds and hence ethyl acetate was selected and used for the separation and extraction of lignin-based products from the lignin/IL or lignin/buffer mixtures for all further experiments.

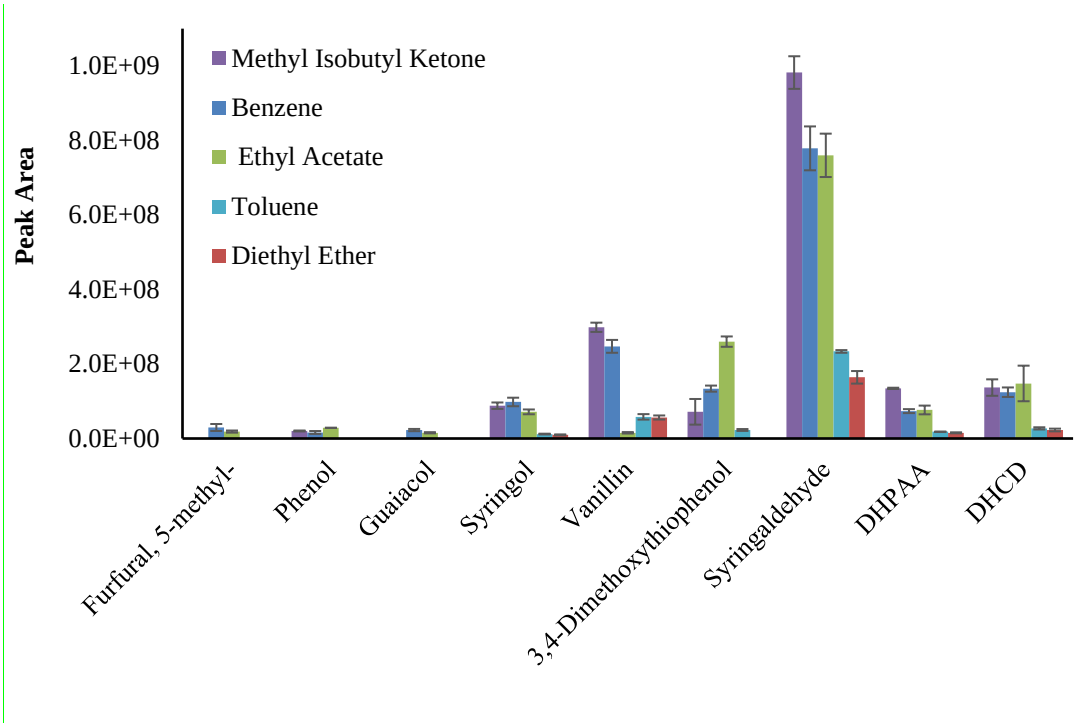


Figure 3.15: Major and minor lignin products obtained by extraction with different solvents after the dissolution of organosolv lignin in $[C_2mim][C_2SO_4]$ at 30 °C for 6 h. Identification of the compounds was based on the NIST library. The data represent the mean of three replicates. The GC-MS ion chromatograms can be found in Appendix A.10.

In conclusion, the choice of extracting solvent applied to isolate lignin monomers formed during the dissolution process involving IL is based on several parameters. These include (1) type of IL used, (2) lignin type, and (3) the extraction process (i.e., the sequence of extraction, and time of extraction).

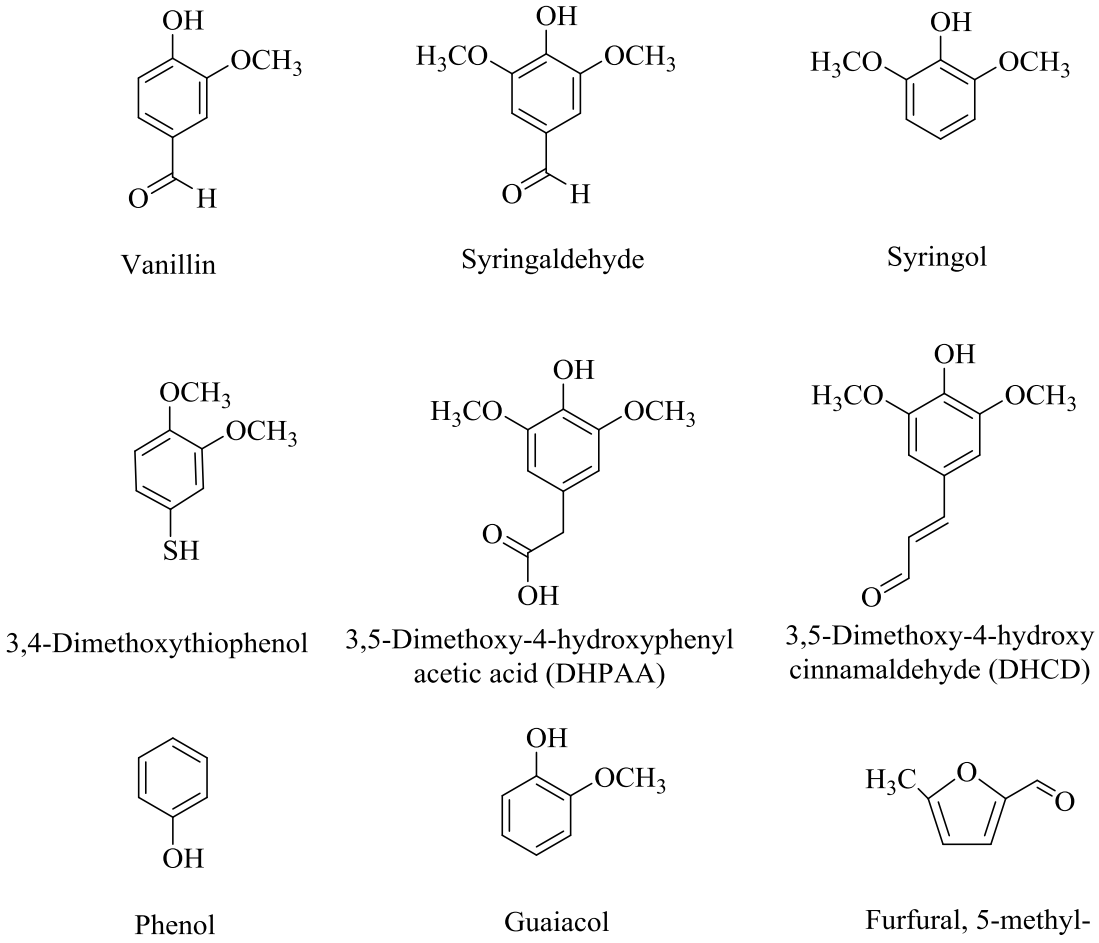


Figure 3.16: Chemical structures of products obtained from organosolv lignin dissolution in $[C_2mim][C_2SO_4]$ after extraction with different solvents.

3.7 Summary and Conclusions

One of the more significant findings to emerge from this study was that breakdown products were identified from the mixture of ionic liquid $[C_2mim][C_2SO_4]$ and oraganosolv lignin under mild conditions (30 °C) and without the assistance of LTV and ABTS.

The patterns of identified products were very different under different processing conditions, so different lignin-derived products could be generated by tuning the process conditions. The largest quantity of product was obtained when dissolving organosolv lignin in 100% IL at 30 °C, followed by treatment of lignin with the assistance of the LTV in 30% (v/v) IL/buffer at the same temperature. Enzymatic

conversions were also higher in 30% IL/buffer mixtures compared to aqueous media under the same conditions. These results are consistent with an increase the organosolv lignin solubility. This improved solubility extended to IL/buffer mixtures and thereby, enzymatic access to lignin is also assumed to be improved.

Vanillin, syringaldehyde or other lignin monomer compounds were not detected during the dissolution process in buffer solution. This latter result may be explained by the fact that the organosolv lignin is insoluble in sodium acetate buffer (pH 5).

Syringaldehyde was found to be a major product throughout all IL experiments performed and the ratio between the amount of syringaldehyde produced and the amount of vanillin formed was in the range of 9-10. These results are likely to be related to the raw woody biomass sources of organosolv lignin. The organosolv lignin in this study was produced from mixed hardwoods which consist of both guaiacyl (G) and syringyl (S) units. It was found that the quantities of syringaldehyde vary from the very small amount of lignin obtained from softwoods to a considerable amount of the lignin obtained from hardwoods (Wu *et al.*, 1994). It is expected that the reactivity of S and G units is different under different process conditions. The current results are consistent with the idea that lignin is included as aggregates of fairly regular basal subunits that connect to each other *via* intermolecular forces (aggregation) and/or covalent bonds (polymerisation) (Cheng *et al.*, 2012). Another important finding that emerged from this study was that the 2,6-dimethoxybenzoquinone (DMBQ) was obtained from organosolv lignin oxidation using laccase only, indicating that these enzymes are both active and could be utilised in the production of specific renewable chemicals.

Importantly, laccase (from *Trametes versicolor*) was shown to possess catalytic activity for the degradation of organolsov lignin in systems containing $[C_2mim][C_2SO_4]$. Surprisingly, no significant differences were found in the total amounts of products obtained from organosolv lignin treatment with LMS compared to the treatment with laccase only. In addition, no increase in the total amount of products was detected after the organosolv lignin dissolution process with ABTS assistance in 30% (v/v) IL/buffer mixtures. Thus, further research should be undertaken to understand the role of free radicals resulting from oxidation of ABTS and how these may interact with lignin. This

work also raises questions about the ABTS mechanism, which are discussed in Chapter Four of this thesis.

There is no suitable method for the analysis of the complex mixture of products formed after the reaction of organosolv lignin, especially in ionic liquid mixtures. Thus, extraction was used to assess the quantity and identity of non-polar compounds formed during processing. As was pointed out in the materials and methods section to this chapter, after the extraction step, three fractions were obtained from organosolv lignin treatment: a solid residue, an organic solvent extract containing non-polar compounds and an aqueous fraction. All the products reported in this work only represent the nonpolar compounds that were soluble in organic solvent after dissolution. The analysis and recovery of polar lignin breakdown compounds in the aqueous fraction afford significant challenges since the separation efficiency of the GC-MS column renders it not suitable for aqueous and ionic liquid solvents. Further studies need to be carried out in order to extract and quantify polar lignin products, and to develop alternative and more effective methods for analysis if a full picture of lignin interaction with solvents is to be achieved.

CHAPTER FOUR

TOWARDS UNDERSTANDING MEDIATOR BEHAVIOUR IN $[C_2mim][C_2SO_4]$

NOTE: Chapter 4 (Section 4.1-Section 4.3) summarises material from paper (Eshtaya *et al.*, 2016), which is appended at the end of the thesis (Appendix 23).

4.1 Introduction

The laccase-mediator (LMS) system acts as a catalyst to assist oxidation of lignin by mediation of electron transfer from the oxidisable groups in lignin to oxygen molecules (Bourbonnais and Paice, 1990, Bourbonnais *et al.*, 1995, Bourbonnais *et al.*, 1998, Rochefort *et al.*, 2004, Aracri *et al.*, 2013, Christopher *et al.*, 2014). Despite the obvious advantages, LMS has some of the drawbacks such as high cost of the enzymes and their sensitivity to the experimental conditions (pH, temperature and inhibitors). Furthermore, there are difficulties associated with the use of LMS in a conventional solvent (Lorenzo *et al.*, 2005, Kunamneni *et al.*, 2008b, Shipovskov *et al.*, 2008, Tavares *et al.*, 2008). In contrast to LMS, an electrolytic mediator system (EMS) could provide a promising and effective alternative for lignin depolymerisation. Instead of using a laccase to oxidise the mediator, the mediator can be oxidised electrochemically instead. By avoiding the requirement for a sensitive enzyme, the electrochemical process can be performed under a broad range of pH and temperature conditions with mediators that have a high redox potential (Rochefort *et al.*, 2004, Aracri *et al.*, 2013, Shiraishi *et al.*, 2013).

Unlike conventional organic solvents, room temperature ILs have many favourable properties in electro-organic synthesis including low vapour pressure at room temperature, a wide liquid range, inherent conductivity, non-volatility, good dissolving power towards many substrates, and excellent thermal and chemical stability. Also, they possess a wide window of electrode potential, and no addition of supporting electrolyte is required, which can assist electrochemical processes such as the oxidation

of lignin (Chen *et al.*, 2010, Zhao, 2010). When compared to conventional solvents, however, ILs are commonly 10–100 times more viscous, and the diffusion rates of species in these media are lowered accordingly (Chen *et al.*, 2010, Harwardt *et al.*, 2014).

ABTS (Figure 4.1) was used in this study because it is currently regarded as the best mediator for laccase. Several studies have been done on the electrochemical behaviour of ABTS in aqueous solutions (Bourbonnais *et al.*, 1998, Fabbrini *et al.*, 2002, Rochefort *et al.*, 2002, Shumakovich *et al.*, 2006, Morozova *et al.*, 2007, González Arzola *et al.*, 2009, Díaz-González *et al.*, 2011, Shiraishi *et al.*, 2013) but to our knowledge, no study of the electrochemical behaviour of ABTS for oxidising either lignin or a lignin model compound in ionic liquids has so far been reported.

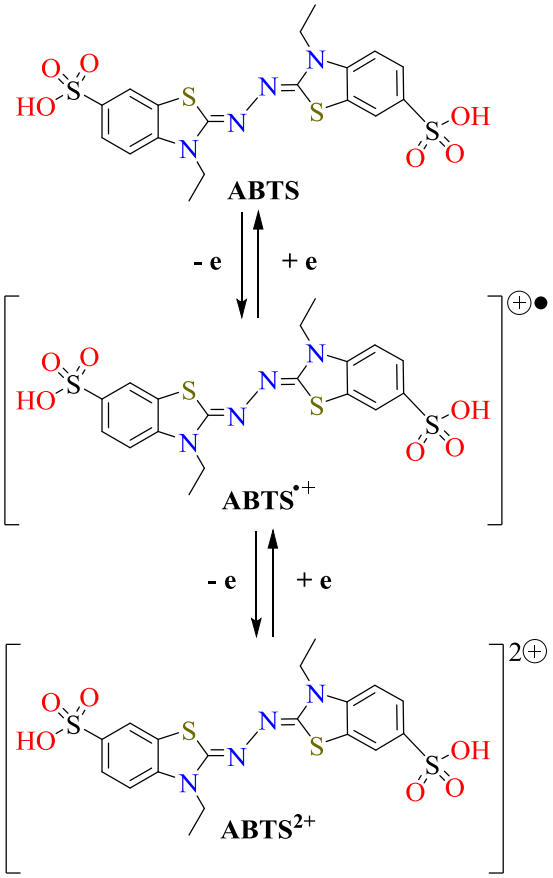


Figure 4.1: Chemical structure of ABTS mediator and formation of the cation radical and the dication by removal of one and two electrons from ABTS, respectively (Fabbrini et al., 2002).

This work is aimed at studying the electrochemical behaviour of ABTS in oxidising the non-phenolic lignin model veratryl alcohol and three technical lignins: Kraft lignin,

organosolv lignin and lignosulfonate lignin in [C_2mim][C_2SO_4]. Due to its high capacity to dissolve lignin, [C_2mim][C_2SO_4] was chosen in this study (Stärk *et al.*, 2010, Liu *et al.*, 2013a). Cyclic voltammetry was applied as a quick, accurate and efficient way to explore the ABTS-mediated oxidation process (Eshtaya *et al.*, 2016). In order to study the compounds formed during the electrochemical oxidation of lignin, bulk electrolysis of organosolv lignin in [C_2mim][C_2SO_4] and lignosulfonate in sodium acetate buffer solution were also conducted.

4.2 Materials and Methods

4.2.1 Chemicals

Sodium lignosulfonate, alkali (Kraft) lignin, 3,4-dimethoxybenzyl alcohol (veratryl alcohol), silver trifluoromethane sulfonate (AgTfO) (≥98% purity) and all other chemicals and solvents used in this study were purchased from Sigma-Aldrich (UK) and used without any further purification.

4.2.2 Buffer Preparation

For the preparation of 0.1 M sodium acetate buffer solution, anhydrous sodium acetate (0.82 g) was dissolved in distilled water (100 mL). The pH was adjusted to pH 4.5 by adding sodium acetate solution (40 mL) to acetic acid solution (0.1 M, 60 mL) at room temperature. The pH of this mixture was measured using a pH meter.

Table 4. 1: Composition of the solutions used in this chapter

Solution type	Composition
Sodium acetate buffer (pH 4.5)	Sodium acetate solution + acetic acid solution
15% (v/v) [C_2mim][C_2SO_4]/Buffer	15% (v/v) [C_2mim][C_2SO_4] + sodium acetate buffer
[C_2mim][C_2SO_4]	As-received [C_2mim][C_2SO_4]
Alkaline aqueous solution	0.05 Sodium phosphate dibasic (Na_2HPO_4) solution + 0.1 M NaOH
5% (v/v) alkaline solution/[C_2mim][C_2SO_4]	5% (v/v) alkaline aqueous solution + [C_2mim][C_2SO_4]

4.2.3 Viscosity and Water Content Measurements

The viscosities of $[C_2mim][C_2SO_4]$, 0.1 M sodium acetate buffer solution (pH 4.5), 15% (v/v) $[C_2mim][C_2SO_4]$/buffer solution and lignin/$[C_2mim][C_2SO_4]$ mixtures were measured at room temperature with a Kinexus pro$^+$ rotational rheometer (Malvern Instruments Ltd., UK) provided with cone-and-plate geometry (40 mm in diameter; with a cone angle of 4° and a gap of 150 μm). A strain rate sweep was performed from 1.0 to 1000 s^{-1}. The water content in $[C_2mim][C_2SO_4]$ was measured by Karl Fischer coulometric titration apparatus (Mitsubishi CA100). For further details see (O'Mahony *et al.*, 2008, Dominguez *et al.*, 2010).

4.2.4 Cyclic Voltammetry (CV) Measurements

Cyclic voltammetry (CV) is the most common technique to gain preliminary information about an electrochemical process. Cyclic voltammetry and chronoamperometry were carried out using Autolab Type III potentiostat/galvanostat from EcoChemie (Metrohm, Netherlands) controlled by the Autolab GPES software, version 4.9, in an undivided three-electrode cell. A glassy carbon disc electrode (3.0 mm in diameter) was used as the working electrode, which was polished prior to use and between each measurement using aqueous alumina (0.05 μm) suspensions. After polishing, the electrode surface was rinsed with deionised water. The reference electrode was an IL-based Ag/Ag^+ electrode, which has been described previously (10 mM AgTfO, $[C_2mim][C_2SO_4]$) (Snook *et al.*, 2006) and a graphite rod as the counter electrode. All the solutions were degassed with nitrogen prior to measuring, and all experiments were performed at room temperature (Eshtaya *et al.*, 2016).

The electrochemical characterisation of ABTS was first carried out alone in either 0.1 M sodium acetate buffer solution (pH 4.5), 15% (v/v) $[C_2mim][C_2SO_4]$/buffer solution or as-received $[C_2mim][C_2SO_4]$ at different scan rates see Table 4.1 for solution composition. The voltammetric responses of ABTS mediator were also recorded separately at the same potential scan rate in the presence of either the lignin model compound veratryl alcohol (13.8 mM) in 15 % (v/v) $[C_2mim][C_2SO_4]$/buffer solution or $[C_2mim][C_2SO_4]$, or lignin (Kraft, organosolv and lignosulfonate) (5 wt %) dissolved in $[C_2mim][C_2SO_4]$. The current response of ABTS-mediated organosolv

lignin at different concentrations of alkaline aqueous solution in $[C_2mim][C_2SO_4]$ was also measured. Finally, the voltammograms of the ABTS in the presence of lignosulfonate, either in sodium acetate buffer solution or in 15% (v/v) $[C_2mim][C_2SO_4]$/buffer solution, were recorded (Eshtaya *et al.*, 2016).

4.2.5 Bulk Electrolysis

4.2.5.1 Bulk Electrolysis of Organosolv Lignin in $[C_2mim][C_2SO_4]$

Electrochemical oxidation of organosolv lignin (5 wt %) and ABTS (10 mM) in the IL ($[C_2mim][C_2SO_4]$) was performed in a 40 mL glass cell. The cell consisted of a graphite rod (6.38 mm diameter) as a working electrode, a graphite rod (4.88 mm diameter) as a counter electrode that was isolated from the cell by a glass frit and filled with IL (see Figure 4.2), and an Ag/Ag^+ electrode (10 mM AgTfO, $[C_2mim][C_2SO_4]$) as a reference electrode. The initial suspension (5 wt % organosolv lignin, 10 mM ABTS) was dissolved in 13.0 mL IL with stirring for 1 h. Electrolysis was carried out at a fixed potential (1.0 V *vs.* Ag/Ag^+) for 6 h. Two control experiments were also undertaken as shown in Figure 4.3. First, organosolv lignin was reacted in the presence of ABTS in the IL under the same conditions but without bulk electrolysis for 6 h. Second, to verify the effect of extracting solvent on the process, organosolv lignin was dissolved in ethyl acetate in the presence of ABTS but without IL at the initial time.

Analysis of the reaction solution was conducted by first performing ethyl acetate extraction in an attempt to isolate non-polar lignin degradation products formed during the reaction (Figure 4.4) for the GC-MS analysis method. After the time had exceeded 6 h, the lignin was precipitated from the reaction mixture by adding 3.5 volume equivalents of distilled water (with regard to the volume of the IL). The mixture of $[C_2mim][C_2SO_4]$, water and lignin were then centrifuged to separate the solid. After the collection of supernatant ($[C_2mim][C_2SO_4]$ and water), the biomass was washed with distilled water and extracted with the solvent in triplicate. A total of one volume equivalent of solvent (with regard to the volume of the IL) was added to the supernatant. The resultant mixture (solvent and sample) was mixed thoroughly and was then phase separated using a centrifuge. The combined organic phases were washed

with distilled water and dried over anhydrous magnesium sulfate ($MgSO_4$). Then the solvent was evaporated to dryness under vacuum yielding an amount of brown powder.

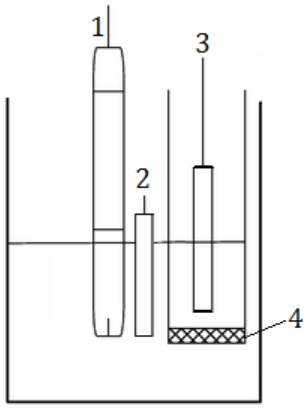


Figure 4.2: Schematic diagram of the electrochemical cell: (1) graphite rod working electrode (2) Ag/Ag^+ reference electrode (3) graphite rod counter electrode (4) glass frit.

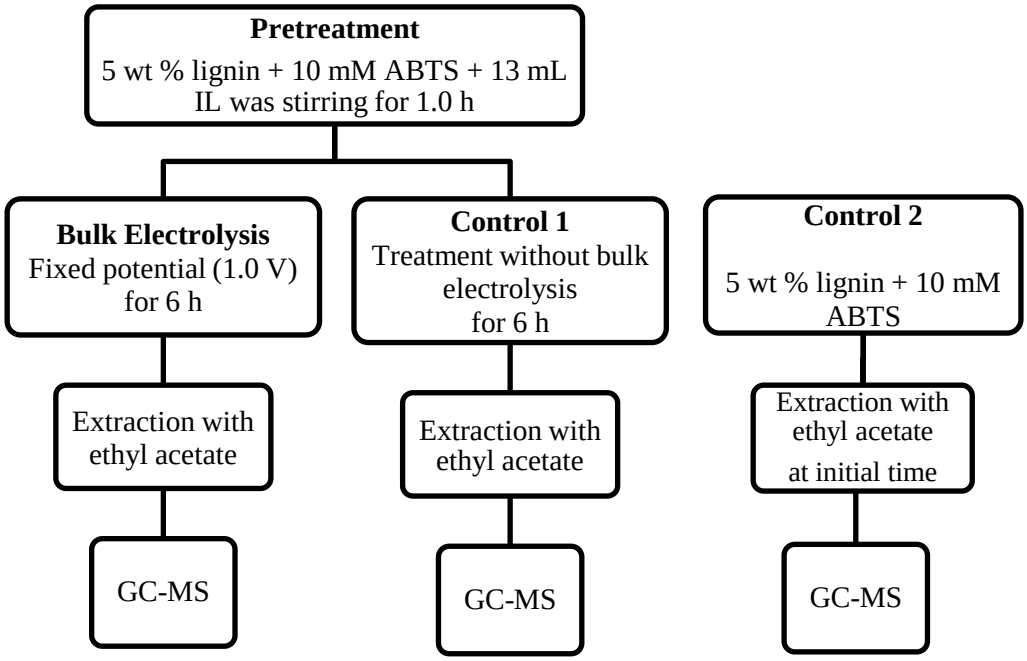


Figure 4.3: Flowchart of electrochemical oxidation experiments-bulk electrolysis of organosolv lignin in the IL with the presence of ABTS.

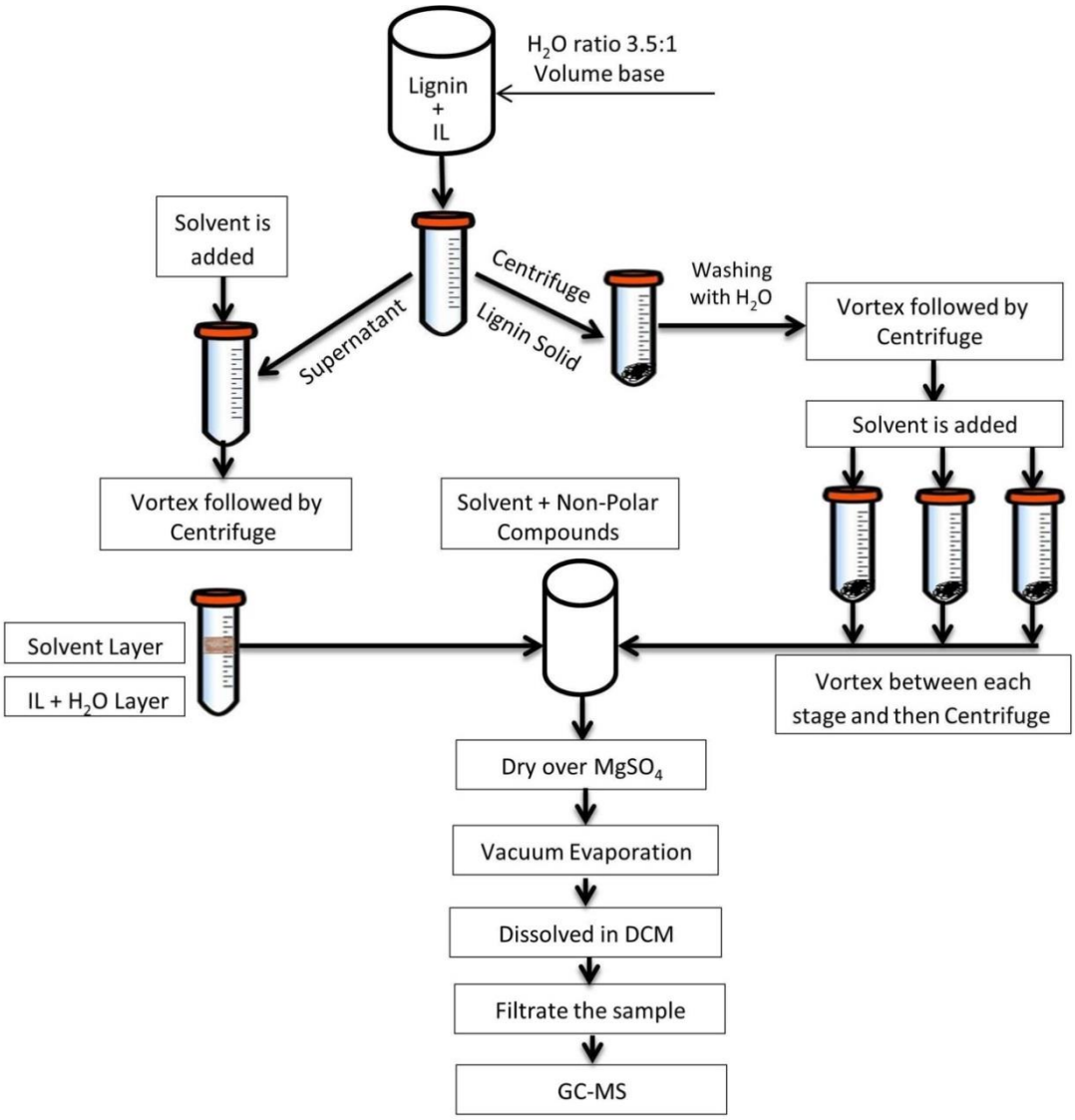


Figure 4.4: Flowchart for extracting lignin degradation products from lignin/IL mixtures.

4.2.5.2 Bulk Electrolysis of Lignosulfonate in Buffer

Electrochemical oxidation of lignosulfonate (6.7 wt %) and ABTS (10 mM) in the sodium acetate buffer (pH 4.5) was performed in a 40 mL glass cell as discussed previously in the above section (Section 4.2.5.1). The initial suspension (6.7 wt % lignosulfonate and 10 mM ABTS) was dissolved in $[C_2mim][C_2SO_4]$ (15.0 mL) with stirring for 1 h. Electrolysis was carried out at a fixed potential (1.0 V) for 8 h. Three control experiments were also undertaken as shown in Figure 4.5. First, lignosulfonate was reacted in the presence of ABTS in the buffer under the same conditions but without bulk electrolysis for 8 h. Second, to verify the effect of extracting solvent on the process, lignosulfonate was dissolved in ethyl acetate in the presence of ABTS but

without a buffer at the initial time. Third, lignosulfonate was dissolved in the buffer under the same conditions but without ABTS and without bulk electrolysis for 8 h.

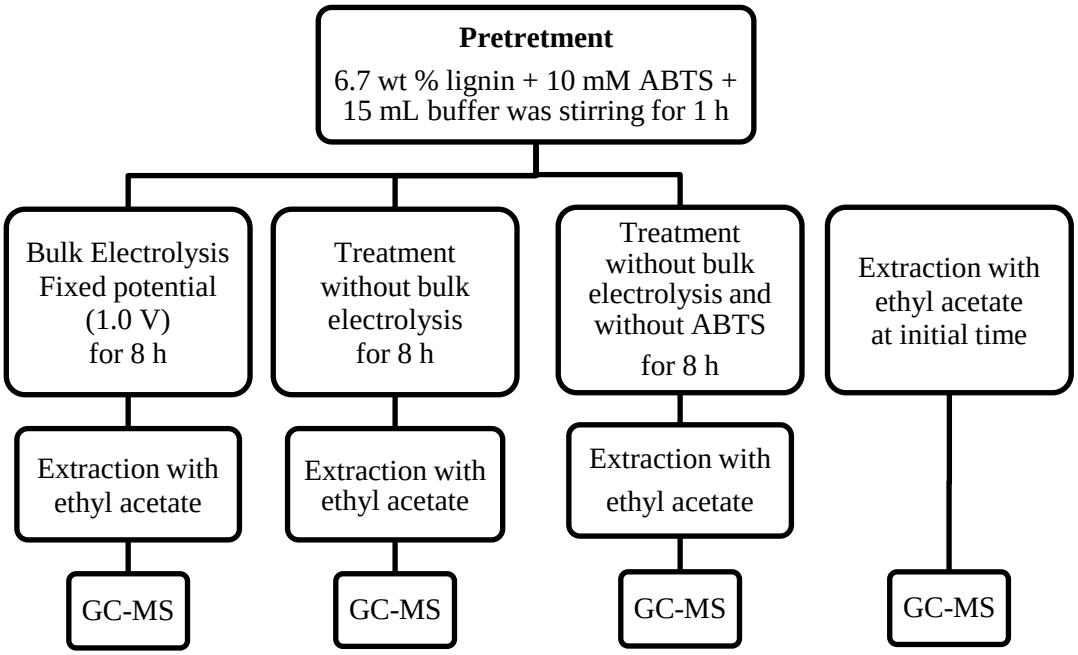


Figure 4.5: Flowchart of electrochemical oxidation experiments-bulk electrolysis of lignosulfonate in sodium acetate buffer (pH 4.5).

After the time had exceeded 8 h, the solution formed was firstly adjusted to pH 2.0. Then a total of 15 mL of ethyl acetate was added. The resultant mixture (solvent and sample) was mixed thoroughly and was then phase separated using a centrifuge. The extraction was repeated three times and the combined organic phases were washed with distilled water and dried over anhydrous magnesium sulfate ($MgSO_4$). Then the solvent was evaporated to dryness under vacuum, yielding a quantity of brown powder.

4.2.6 Gas Chromatography–Mass Spectrometry (GC-MS)

The powder that formed after vacuum drying of both types of lignin extract (Section 4.2.5) was dissolved in dichloromethane. Before GC-MS injection, the sample was filtered with a special filter designed for organic solvents (Sartorius filter Minisart SRP, Scientific Laboratory Supplies) with a 0.2 μm pore size.

The analysis of the lignin breakdown compounds (non-polar) present after ethyl acetate recovery was performed using a GC-MS (Agilent Technologies 7890A) coupled to a MS-5975C triple-axis mass spectroscopy detector (MS) and integrated auto sampler (model number 7693). The compounds were separated using a HP-5MS (Agilent Technologies) (30 m, 0.25 mm ID, with 0.25 μm of film thickness) chromatographic column. Sample (1 μL) was injected into the GC at an inlet temperature of 220 °C and was operated in a split mode (split flow of 30 mL/min, the split ratio of 50). High purity helium was used as a carrier gas with a constant flow rate of 1.2 mL/min. The temperature of the GC was held at 45 °C for 1 min and then was increased at a rate 10 °C/min up to 300 °C and was held at this temperature for 1 min. The MS was used until the end of GC run with a solvent delay of 4.6 min. The ion source was maintained at a temperature of 250 °C and the MS was operated in scan mode. For electrochemical oxidation of organosolv lignin in the IL, the identification of syringaldehyde was based on both retention time of the authentic standard (see Appendix A.11) and NIST database hit. The identification of other compounds was based on NIST library data only. However, the identification of products obtained by the electrochemical cleavage of lignosulfonate was based on the combination of authentic standards (see Appendix A.12) and the NIST library data. Some of the GC-MS identified products remained unquantified because they were not commercially available and therefore their calibration could not be carried out. All the authentic standards were soluble in dichloromethane except vanillic acid, so it was dissolved in ethyl acetate.

4.2.7 Lignosulfonate Pretreatment

First, lignosulfonate was solubilised in methanol (MeOH) to precipitate out the desired high molecular weight lignin, followed by stirring at 25 °C for about 30 minutes. Afterwards, the mixture was centrifuged using an Eppendorf centrifuge 581OR (2000 rpm, 10 °C for 15 min) to precipitate the solid residue (MeOH-insoluble lignin). Then, the supernatant was removed, and MeOH-insoluble lignin was washed with excess methanol three times, and the final cake (MeOH-insoluble lignin) was dried in a vacuum oven at 50 °C until constant weight. The remaining supernatant (MeOH-lignin solution) was evaporated to collect MeOH-soluble lignin (Saito *et al.*, 2014).

The isolated yield of MeOH-insoluble lignin was 68.1 (± 0.4)%, therefore, the yield of MeOH-soluble lignin was assumed as 31.9 %.

4.3 Results and Discussion

4.3.1 Electrochemical Behaviour of ABTS in [C_2mim][C_2SO_4]

The cyclic voltammogram of 10 mM ABTS in [C_2mim][C_2SO_4] with a scan rate of 200 mV/s is shown in Figure 4.6. Two oxidation peaks ($E_{p,a}$) at potentials of 0.500 V (A) and 0.815 V (B) were detected, corresponding to the oxidation of ABTS to its cation radical ($ABTS^{\cdot+}$) and subsequently to its dication ($ABTS^{2+}$), as per Equation 4.1. The reverse scan showed two reduction peaks ($E_{p,c}$) at 0.738 V (C) and 0.423 V (D) for the reduction of the dication and the cation radical, respectively. Analysis of the two redox couples at a range of scan rates (see inset in Figure 4.6) revealed that the oxidation ($i_{p,a}$) and reduction ($i_{p,c}$) peak currents were proportional to the square root of the scan rate. Additionally, at each scan rate, the ratio of $i_{p,a}$ to $i_{p,c}$ was close to one, indicating that the mass transport of ABTS to the electrode surface was diffusion controlled in [C_2mim][C_2SO_4] and confirmed that the radical cation $ABTS^{\cdot+}$, dication $ABTS^{2+}$ and [C_2mim][C_2SO_4] do not interact with one another, e.g. *via* ion pairing or proton transfer, to a significant extent. These observations are consistent with the electrochemical behaviour of ABTS in aqueous systems reported by Bourbonnais *et al.* (Bourbonnais *et al.*, 1998).

$$\text{ABTS} \rightarrow ABTS^{\cdot+} \rightarrow ABTS^{2+} \qquad (4.1)$$

For an electrochemically-reversible reaction with a one-electron transfer process, the peak-peak potential separation ($\Delta E_p = E_{p,a} - E_{p,c}$) for each redox couple at each scan rate should be approximately 59 mV at room temperature and independent of the scan rate. However, the ΔE_p for the ABTS radical cation and dication in [C_2mim][C_2SO_4] were significantly greater than 59 mV and increased as the scan rate increased (77 mV at 50 mV/s and 101 mV at 1000 mV/s), indicating a quasi-reversible redox process. These results might indicate slow electron transfer kinetics, and may also be partly attributed to the effect of the uncompensated ohmic resistance of the electrolyte and the measuring circuit (Lovelock *et al.*, 2011).

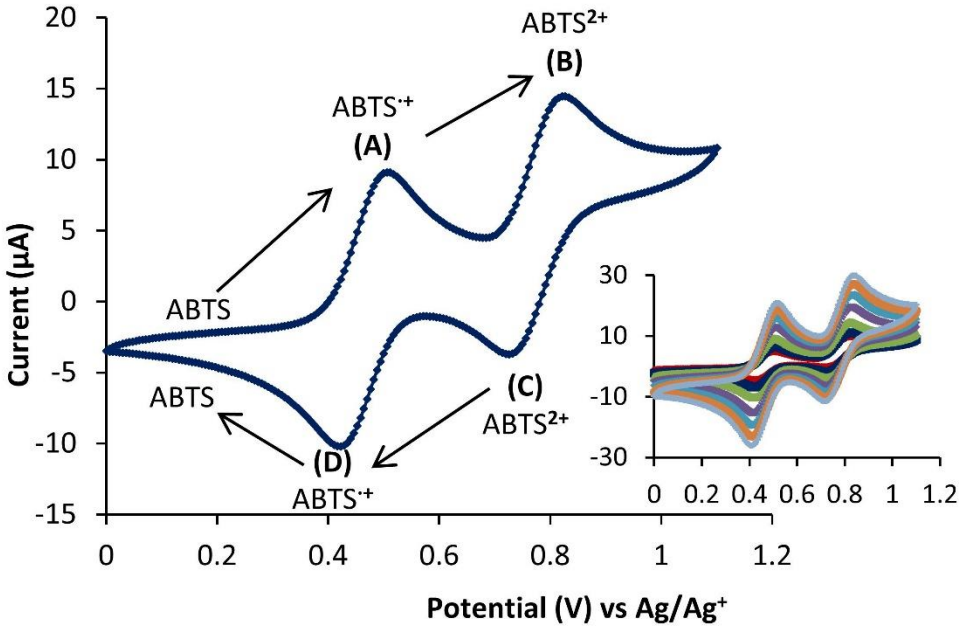


Figure 4.6: Cyclic voltammogram of 10 mM ABTS in $[C_2mim][C_2SO_4]$ recorded at a scan rate of 200 mV/s. The inset shows the cyclic voltammogram of 10 mM ABTS in $[C_2mim][C_2SO_4]$ with varying scan rates (from inside to outside (mV/s): 50, 100, 200, 400, 600, 800 and 1000) (Eshtaya *et al.*, 2016).

The CV features observed at high (200 mV/s) and low (50 mV/s) scan rates differed markedly, as shown in Figure 4.7. Thus, at a low scan rate and a higher concentration of ABTS (50 mM), no cathodic signal corresponding to the reduction of the ABTS dication was detected. Instead, the intensity of the $ABTS^{\cdot+}$ reduction peak was about 1.4 fold that of its oxidation peak ($i_{p,a}/i_{p,c}$ = 1.4). This behaviour was previously observed in aqueous solutions and attributed to the comproportionation reaction between ABTS and its dication with the formation of $ABTS^{\cdot+}$ as shown in Equation 4.2, which has resulted in the disappearance of a cathodic peak due to the reduction of $ABTS^{2+}$ (Bourbonnais *et al.*, 1998). This comproportionation reaction depends on the concentration of the electroactive species close to the surface of the electrode so that, in the case when the concentration of ABTS is high, the comproportionation reaction of the dication will take place before its reduction at the electrode surface.

$$\mathrm{ABTS} + ABTS^{2+} \underset{disproportionation}{\overset{comproportionation}{\rightleftharpoons}} 2ABTS^{\cdot+} \qquad (4.2)$$

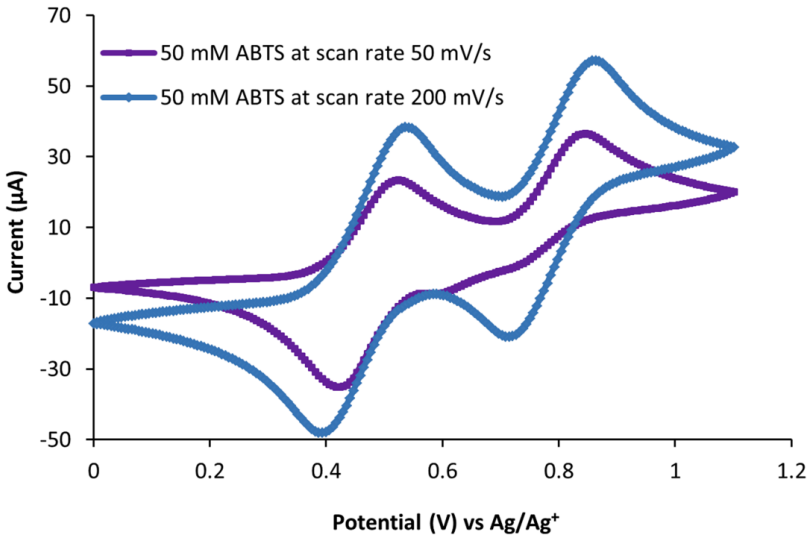


Figure 4.7: Cyclic voltammograms of 50 M ABTS in $[C_2mim][C_2SO_4]$ recorded at scan rates of 50 mV/s and 200 mV/s (Eshtaya *et al.*, 2016).

4.3.1.1 Diffusion Coefficient of ABTS in $[C_2mim][C_2SO_4]$

The impact of solvent viscosity on the oxidation reaction can be related to the diffusivity of the substrate. Single potential step chronoamperometry was employed in order to determine the diffusion coefficient of ABTS in $[C_2mim][C_2SO_4]$. Figure 4.8A shows a typical chronoamperogram obtained using 10 mM ABTS in $[C_2mim][C_2SO_4]$ after a potential step from a potential where no faradaic reaction occurred to a potential at which the oxidation of ABTS was diffusion controlled. The current, *i*, is proportional to $t^{-0.5}$ as shown by the Cottrell equation, (Equation 4.3)

$$i(t) = \frac{nFACD^{0.5}}{\pi^{0.5}t^{0.5}} \qquad (4.3)$$

where *i* is the peak current, *n* the number of electrons transferred/molecule, A the electrode surface area, C the bulk concentration of the redox species, D the Diffusion coefficient of the redox species and F the Faraday constant. Figure 4.8B shows the corresponding Cottrell profile of *i(t) vs* $t^{-0.5}$ and, from the gradient of the straight line best-fit to the plot, the diffusion coefficient of $ABTS/ABTS^{\cdot+}$ in $[C_2mim][C_2SO_4]$ was calculated to be 1.9 (± 0.3) x 10^{-8} cm^2s^{-1}, which is typical for molecular species in viscous ILs (O'Toole *et al.*, 2007, Lovelock *et al.*, 2011). A similar analysis was performed to find the diffusion coefficients of ABTS in sodium acetate buffer solution and the 15% (v/v) $[C_2mim][C_2SO_4]$/buffer mixture. Table 4.2 also shows the viscosity

of these solvents. There was a good agreement between the diffusion coefficients of ABTS and the viscosity of both buffer solutions and [C_2mim][C_2SO_4] with literature values (Schroder *et al.*, 2003, Lovelock *et al.*, 2011). The value of the diffusion coefficient of ABTS in [C_2mim][C_2SO_4] was almost three orders of magnitude lower than that determined in the buffer solution (3.5 (± 0.2) x 10^{-6} cm^2s^{-1}), which is consistent with the high viscosity of this IL and reflects the low mass transport rate of the ABTS in [C_2mim][C_2SO_4], compared to that in the buffer solution.

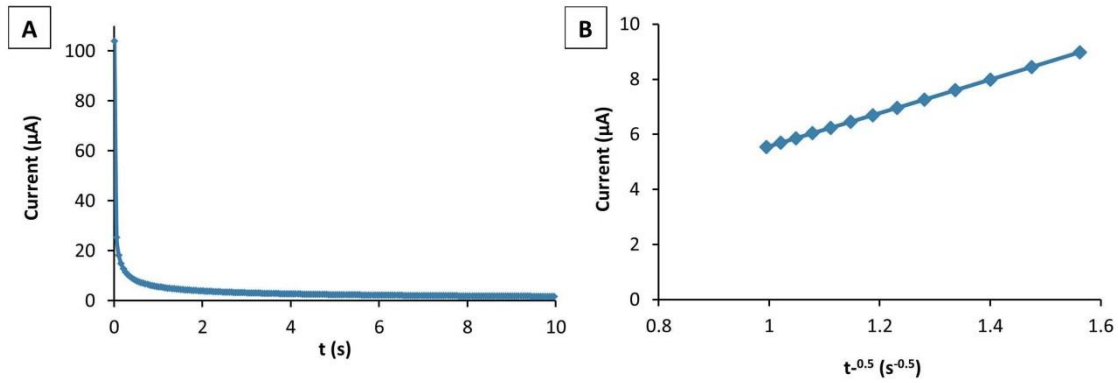


Figure 4.8: (A) Potential step chronoamperogram obtained at a 3 mm diameter glassy carbon disk electrode in 10.0 mM ABTS in [C_2mim][C_2SO_4]. The potential was stepped from 0.3 V to 0.6 V *vs*. ABTS /$ABTS^{\cdot+}$ and held for 10 s. (B) Cottrell plot of *i (t) vs.* $t^{-0.5}$ for the oxidation process (Eshtaya *et al.*, 2016).

Table 4.2: Diffusion coefficients of ABTS in different solvents using potential step chronoamperometry (Eshtaya *et al.*, 2016).

Solution type	**Diffusion Coefficient (cm^2s^{-1})**	**Viscosity (mPa.s)**
1 mM ABTS in sodium acetate buffer	3.5 (± 0.2) x 10^{-6}	0.76 ± 0.02
1 mM ABTS in 15% (v/v) [C_2mim][C_2SO_4]/Buffer	1.74 (± 0.04) x 10^{-6}	1.23 ± 0.01
1 mM ABTS in [C_2mim][C_2SO_4]	2.6 (± 0.1) x 10^{-8}	96.6 ± 4.4
10 mM ABTS in [C_2mim][C_2SO_4]	1.9 (± 0.3) x 10^{-8}	96.6 ± 4.4

4.3.2 Cyclic Voltammetry of Veratryl Alcohol (VA)

The redox reaction between the mediator, ABTS and the non-phenolic lignin model compound veratryl alcohol (VA) was also included in this study as a benchmark and was analysed using CV. At first, the behaviour of the ABTS and VA was studied in IL-

buffer solution. As can be seen in Figure 4.9, VA alone did not show any oxidation peak below 900 mV but, in the presence of ABTS, the recorded peak height increased by more than four-fold at the appropriate potential, indicating the $ABTS^{2+}$ dication catalysing VA oxidation. No oxidation of this lignin model occurred in the potential range corresponding to the formation of the $ABTS^{\cdot+}$ between 0.70 and 0.95 V. This CV finding is consistent with those previously reported in the literature (Harwardt *et al.*, 2014). The effect of VA on redox catalysis of an electrochemical reaction, as described by Bourbonnais *et al.* (Bourbonnais *et al.*, 1998) is for the ABTS dication to oxidise the VA to veratryl aldehyde with concurrent regeneration of the ABTS radical, resulting in an increase in the peak current compared to that seen on the CV of the ABTS solution without veratryl alcohol (Scheme 4.1 and Equation 4.4).

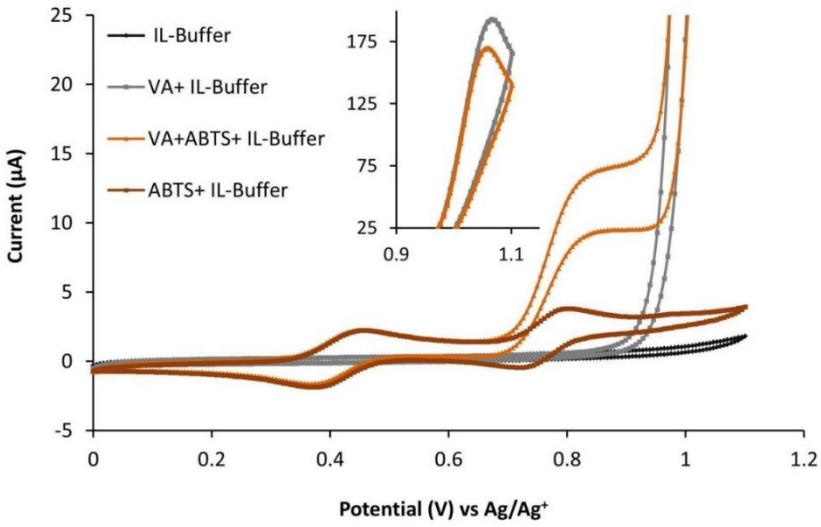
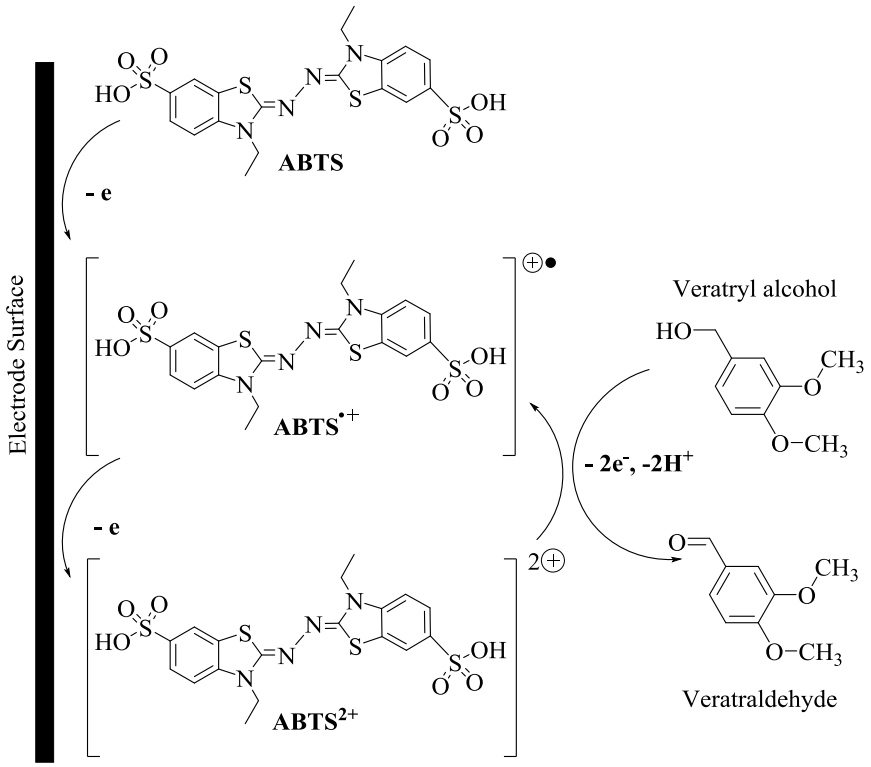


Figure 4.9: Cyclic voltammograms of 1 mM ABTS, 13.8 mM veratryl alcohol 4, 13.8 mM veratryl alcohol 4 mixed with 1 mM ABTS in 15% (v/v) $[C_2mim][C_2SO_4]$ in 0.1 M sodium acetate buffer (pH 4.5) recorded at a scan rate of 10 mV/s. The inset shows the portion of the CVs with current above 25 µA between 0.9 and 1.1 V (Eshtaya *et al.*, 2016).

The electrochemical behaviour of ABTS in the presence of VA was also explored in $[C_2mim][C_2SO_4]$. Figure 4.10 shows the CVs of ABTS (1.0 mM), veratryl alcohol (13.8 mM) and the two compounds mixed together in $[C_2mim][C_2SO_4]$ under the same conditions as described above for the 15% (v/v) $[C_2mim][C_2SO_4]$/buffer mixture. The resulting CVs confirm the stability of $[C_2mim][C_2SO_4]$ in the oxidative potential range of 0 to 1.1 V *vs.* Ag/Ag^+. As with the 15% (v/v) $[C_2mim][C_2SO_4]$/buffer mixture, the simultaneous electrochemical oxidation of ABTS and VA resulted in an increase of the second oxidation peak of ABTS, indicating a regeneration of ABTS at the electrode.

However, the peak current of the second oxidation in the presence of the VA is reduced by 10 fold in the $[C_2mim][C_2SO_4]$, compared with in 15% (v/v) $[C_2mim][C_2SO_4]$/buffer mixture and therefore the reaction rate between ABTS and VA oxidation in 15% (v/v) $[C_2mim][C_2SO_4]$/buffer mixture may be higher than in $[C_2mim][C_2SO_4]$ as can be seen by comparing Figures 4.9 and 4.10. This is probably due to the high viscosity of $[C_2mim][C_2SO_4]$ (96.6 mPa.s at 22 °C, Table 4.2), and can be explained by VA diffusion through the higher viscosity solvent becoming slower and hindering the transport of analytes towards the working electrode. Therefore, lower peak currents were measured. Figures 4.9 and 4.10 also indicate that the electrochemical behaviour of ABTS in the $[C_2mim][C_2SO_4]$ was different to that found in 15 % (v/v) $[C_2mim][C_2SO_4]$/buffer mixtures. Whereas the ABTS showed reversible electrochemical behaviour in 15 % (v/v) $[C_2mim][C_2SO_4]$/buffer mixtures, the CVs of ABTS in the $[C_2mim][C_2SO_4]$ did not show the cathodic peak corresponding to the reduction of the dication ($ABTS^{2+}$) at this particular ABTS concentration and at the scan rate used.

$$ABTS^{2+} + veratryl\ alcohol \rightarrow ABTS^{\cdot+} + veratryl\ aldehyde \qquad (4.4)$$



Scheme 4.1: Schematic representation of the reaction of ABTS and VA at the working electrode (Bourbonnais *et al.*, 1998).

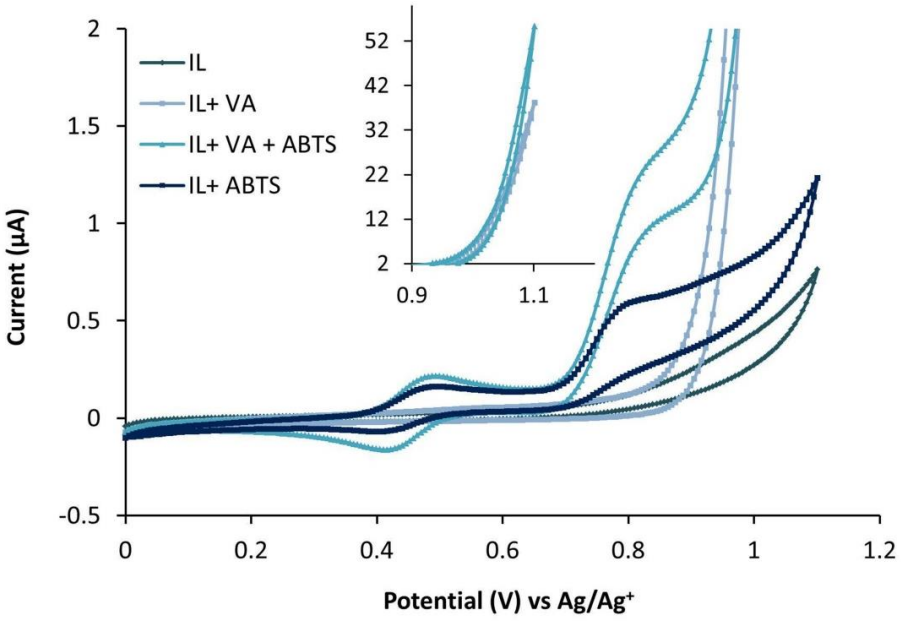


Figure 4.10: Cyclic voltammograms of 1 mM ABTS, 13.8 mM veratryl alcohol, 13.8 mM veratryl alcohol mixed with 1 mM ABTS in [C_2mim][C_2SO_4] recorded at a scan rate of 10 mV/s. The inset shows the portion of the CVs with current abo ve 2.0 µA between 0.9 and 1.1 V (Eshtaya *et al.*, 2016).

4.3.3 Cyclic Voltammetry of Different Lignins in [C_2mim][C_2SO_4]

Mainly because of the structural complexity of lignin (Figure 4.11), most of the studies reported to date have been performed using lignin model compounds. However, the challenge is to valorise the widely available authentic lignins that are by-products of cellulose isolation. Therefore, the reactions of ABTS with three types of technical lignin (organosolv, Kraft and lignosulfonate) were studied by cyclic voltammetry in [C_2mim][C_2SO_4] to determine the reactivities of the two oxidised states of ABTS, and towards lignin (from Figure 4.12 to Figure 4.15). Initially, the voltammetric response of ABTS (10 mM) in [C_2mim][C_2SO_4] was assayed alone at different scan rates and then the voltammetric responses of each type of lignin (5 wt %) were also recorded separately at the same potential scan rate. Each lignin (5 wt %) was dissolved in the [C_2mim][C_2SO_4] and then, the mixture was stirred at 60 °C for 2 h in order to ensure complete dissolution. Subsequently, nitrogen was purged through the resultant solutions before CVs were measured to reduce potential interference from oxygen. Finally, the CVs of the ABTS (10 mM) in the presence of lignin (5 wt %) in [C_2mim][C_2SO_4] were recorded as indicated above.

As can be seen in Figure 4.12, an increase in the oxidation current was detected at potentials around 1.0 V for all types of lignin in the absence of ABTS. This is possibly related to the oxidation of the hydroxyl (OH) group on either the α-carbon or γ-carbon (see Figure 4.11) (Chen *et al.*, 2010). ABTS behaved differently in response to the addition of different lignins, as shown in Figures 4.13 to 4.15. Its behaviour was fairly electrochemically reversible in the presence of lignosulfonate and Kraft lignin in $[C_2mim][C_2SO_4]$ (Figures 4.14 and 4.15). However, organosolv lignin caused a significant increase in the second oxidation peak of ABTS (Figure 4.13).

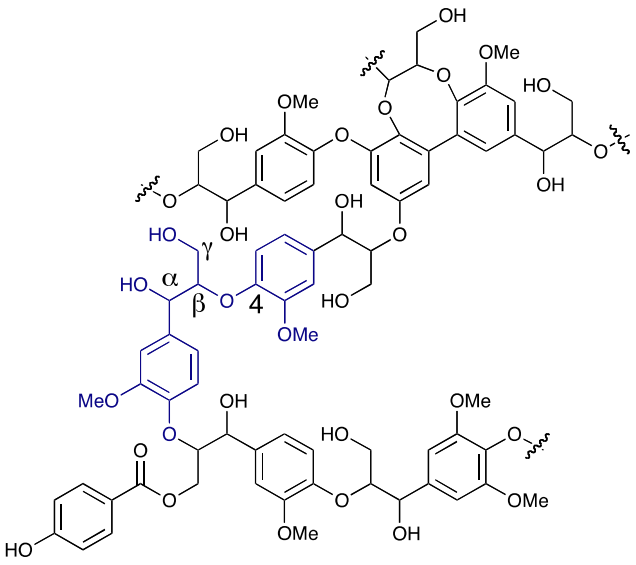


Figure 4.11: Representative structure of a fragment of lignin (Rahimi *et al.*, 2014).

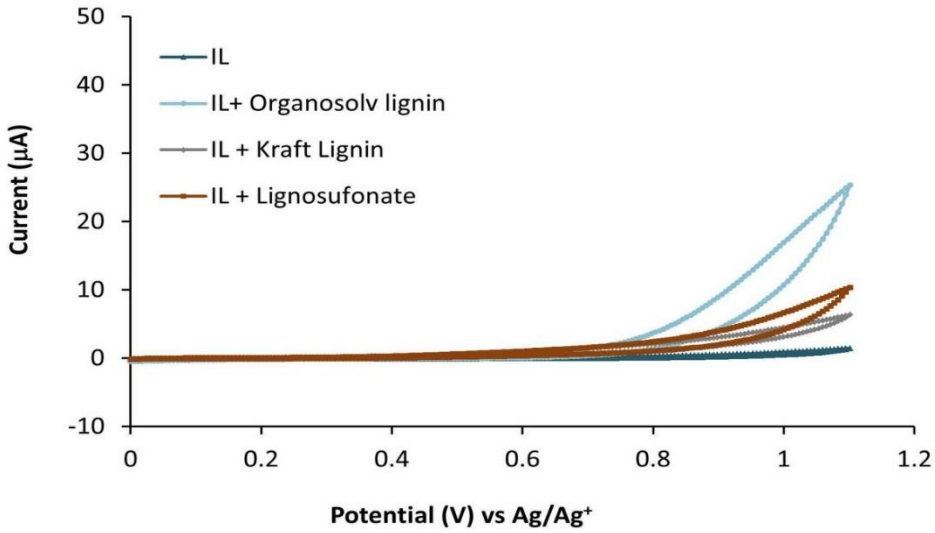


Figure 4.12: Cyclic voltammograms of organosolv, Kraft and lignosulfonate lignin (5 wt %) in $[C_2mim][C_2SO_4]$ recorded at a scan rate of 50 mV/s (Eshtaya *et al.*, 2016).

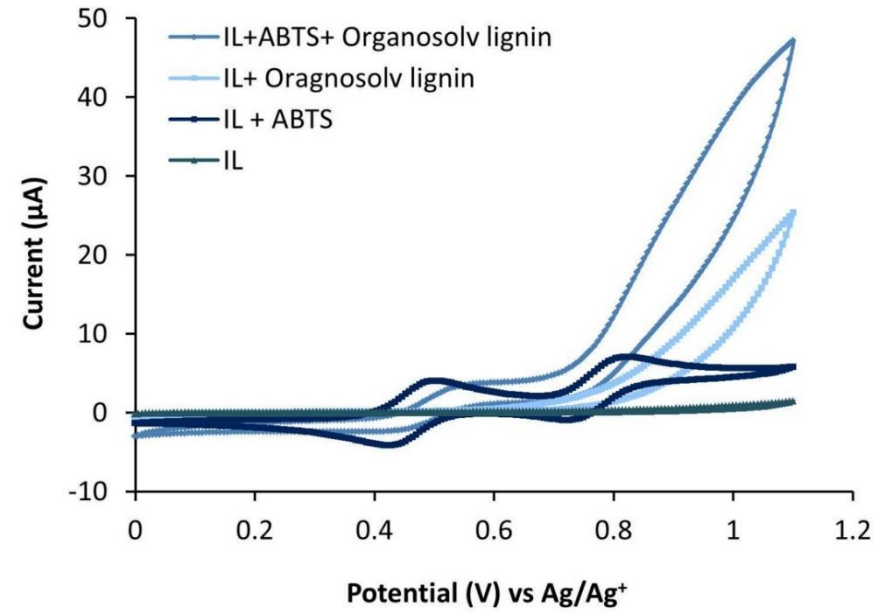


Figure 4.13: Cyclic voltammograms of ABTS (10 mM), organosolv lignin (5 wt %) and organosolv lignin (5 wt %) mixed with 10 mM ABTS in $[C_2mim][C_2SO_4]$ recorded at scan rate of 50 mV/s (Eshtaya *et al.*, 2016).

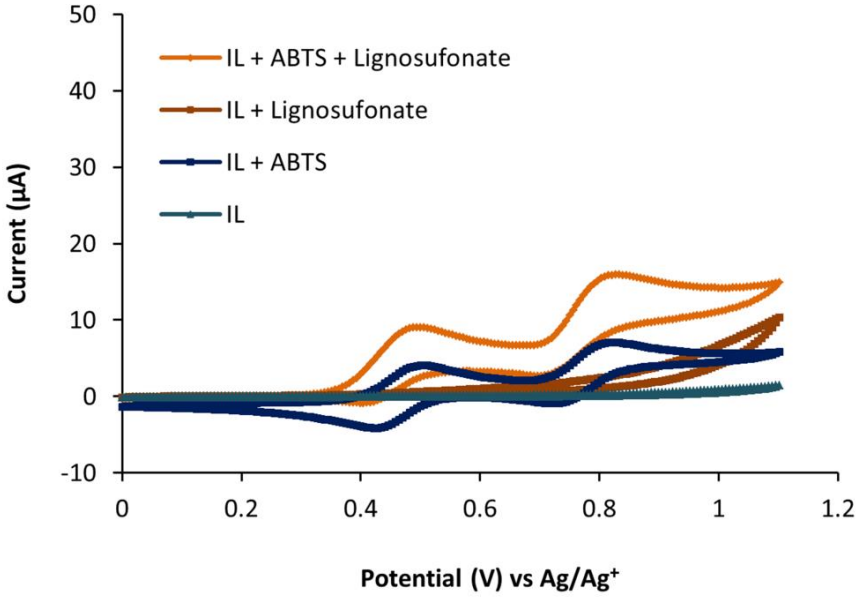


Figure 4.14: Cyclic voltammograms of ABTS (10 mM), lignosulfonate (5 wt %) and lignosulfonate (5 wt %) mixed with 10 mM ABTS in $[C_2mim][C_2SO_4]$, recorded at a scan rate of 50 mV/s (Eshtaya *et al.*, 2016).

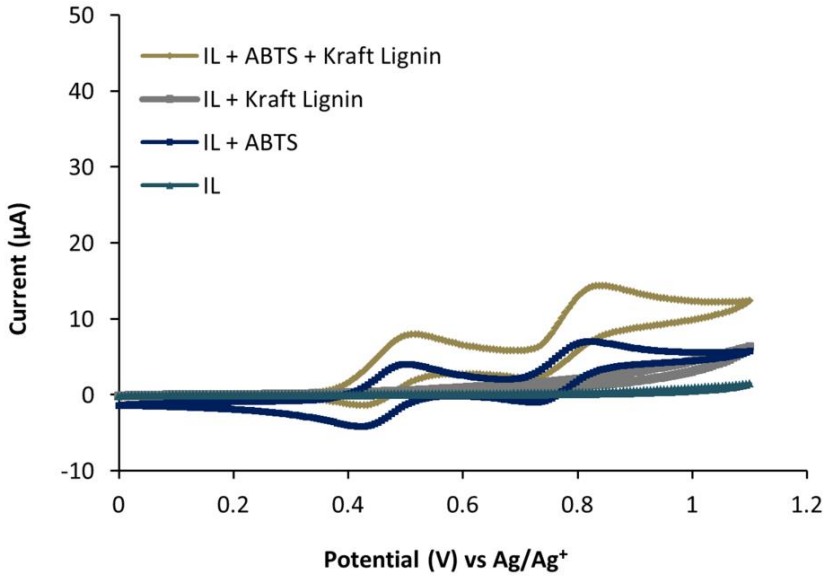


Figure 4.15: Cyclic voltammograms of ABTS (10 mM), Kraft lignin (5 wt %) and Kraft lignin (5 wt %) mixed with 10 mM ABTS in $[C_2mim][C_2SO_4]$ recorded at a scan rate of 50 mV/s (Eshtaya *et al.*, 2016).

In Figure 4.13, the anodic current corresponding to formation of the radical cation decreased slightly and shifted towards more positive potentials. These features seem to indicate direct interactions between ABTS and organosolv lignin, which may be due to the high polydispersity of organosolv lignin and the presence of low molecular weight fractions that could activate cascade reactions between their phenolic and non-phenolic structures (González Arzola *et al.*, 2009, Aracri *et al.*, 2013, Nanayakkara *et al.*, 2014). Generally, however, organosolv lignin contains less contaminants than lignin obtained from other processes, such as Kraft lignin or lignosulfonate (Cybulska *et al.*, 2012) and is also closest in structure to native lignin.

It can also be seen in Figure 4.13 that the dication formation current peak seemed to have merged into, and also enhanced the current from the oxidation of organosolv lignin. This CV response was highly likely caused by the peak potential for formation of the ABTS dication being very close to the current onset potential for the oxidation of organosolv lignin. Nonetheless, the significantly greater currents between 0.7 and 1.1 V on the CV of the mixed solution of ABTS and organosolv lignin than those on the CVs individually recorded is still evidence for the ABTS dication to be responsible for the mediated or catalytic oxidation of organosolv lignin. A possible factor of influence on the differing oxidation behaviour of organosolv lignin with ABTS is that,

because organosolv lignin comprises relatively low molecular weight lignin units, relative to the other lignins examined herein, it is also the most amenable to the IL treatment to afford a more deconstructed lignin, thus making it more accessible to ABTS (George *et al.*, 2011).

The CVs of ABTS in the presence of lignosulfonate and Kraft lignin were quite similar, as can be seen in Figures 4.14 and 4.15. In these two cases, both the peak currents for the formation of the radical cation and dication of ABTS increased noticeably after addition of either lignosulfonate or Kraft lignin. These results indicate possible interactions between the lignin and both the oxidised ABTS species and, leading to the increase of the oxidation currents. However, in comparison with Figures 4.13, 4.14 and 4.15, whilst these interactions might have caused depolymerisation of the lignin, the effect, if any, was insignificant and controlled by diffusion. It is possibly due to a solubility issue. Organosolv lignin is soluble in $[C_2mim][C_2SO_4]$ at room temperature, but lignosulfonate and Kraft lignin exhibit low solubility, or the dissolution is kinetically very slow in $[C_2mim][C_2SO_4]$ at room temperature. A mixing process at 60 °C for about 2 h was needed to make sure these two lignins completely dissolved. This heating step could potentially initiate adverse coupling reactions of the phenols in the lignin structure. Additionally, in contrast to organosolv lignin, Kraft lignin and lignosulfonate contain sulfur groups and therefore, a strong interaction between $[C_2mim][C_2SO_4]$ and sulfur species on the lignin could have possibly occurred in such a way that it limits the accessibility of ABTS to the lignin macromolecules. Thus, further studies are required to understand the intermolecular interactions between the lignin and ABTS mediator with the IL ions to explain the differences between the reactivity of ABTS with each of these types of lignin.

4.3.4 Cyclic Voltammetry of Lignosulfonate (LS)

In order to elucidate the effect of viscosity on the ABTS catalytic efficiency (as defined later), CVs of lignosulfonate in the sodium acetate buffer (pH 4.5) and the 15% (v/v) $[C_2mim][C_2SO_4]$/buffer mixtures were studied. Most of the lignins available are practically water insoluble. However, sodium lignosulfonate contains hydrophilic functional groups, which make this type of lignin water-soluble. Therefore, sodium lignosulfonate was used in this part of the study. Figure 4.16 shows the CV of

lignosulfonate (1 wt %) at a low potential scan rate (10 mV/s) in the 15% (v/v) [C_2mim][C_2SO_4]/buffer solution. The increase in the anodic peak currents of ABTS in the presence of lignosulfonate, compared with those measured in the presence of ABTS alone, indicate that both the cation radical and dication were involved in the redox reactions of lignosulfonate. This finding is consistent with the results obtained by Bourbonnais and co-workers for electrochemical oxidation of Kraft lignin (Indulin) in buffer solutions (Bourbonnais *et al.*, 1998, Rochefort *et al.*, 2004). The increase of the peak current for formation of the ABTS cation radical has been related to the quantity of more easily oxidisable residues in lignin such as phenolic groups, whereas the increase of the peak current for formation of the ABTS dication corresponds more likely to (non-phenolic) groups in lignin with higher redox potentials (Bourbonnais and Paice, 2004). The reaction mechanism is already known for the oxidation of phenols by ABTS cation radical and consists of at least two homogeneous chemical reactions: fast and reversible electron transfer (Scheme 4.2), consistent with the increase in the cation radical peak in Figure 4.16, followed by the reaction of the formed phenoxy radicals with another ABTS-derived radical cation (Campos and Lissi, 1997, Schroder *et al.*, 2003).

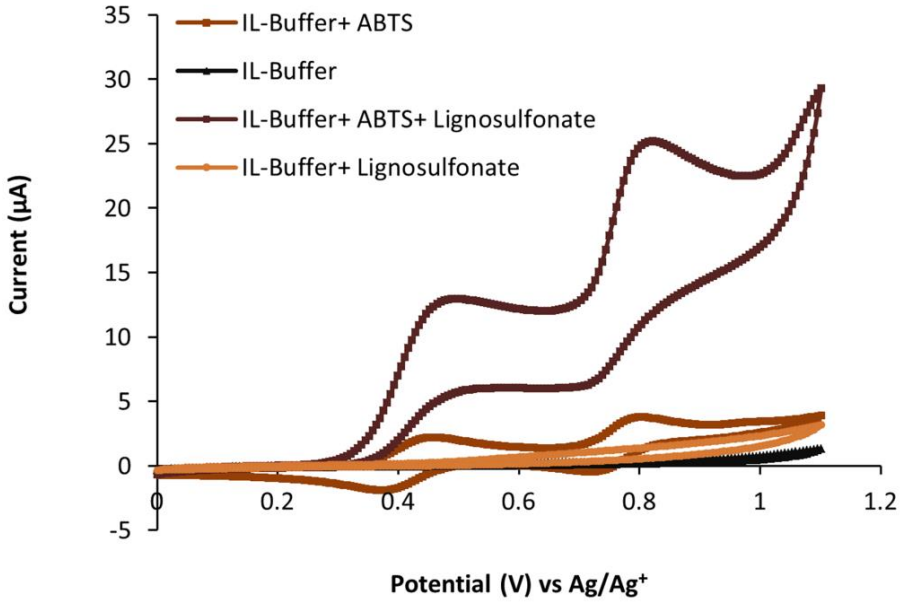
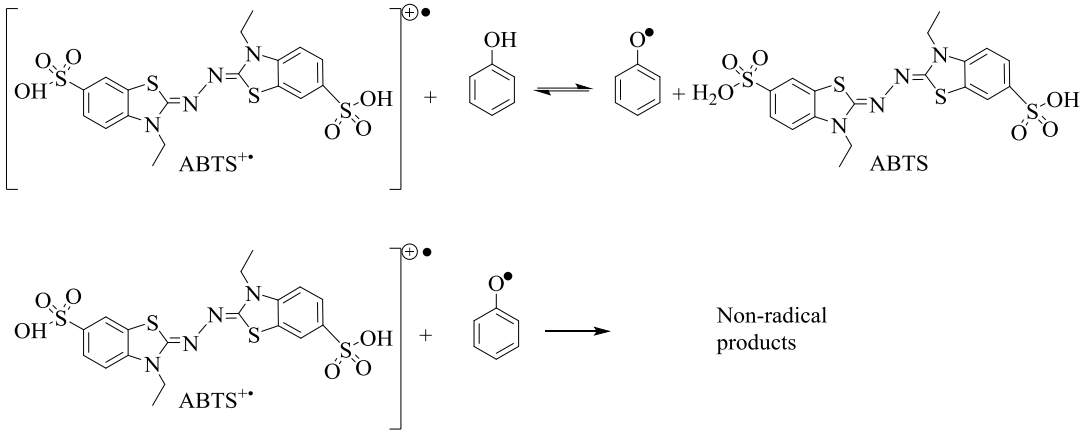


Figure 4.16: Cyclic voltammograms of 1 mM ABTS, 1 wt % lignosulfonate, 1 wt % lignosulfonate mixed with 1 mM ABTS in 15% (v/v) [C_2mim][C_2SO_4] in 0.1 M sodium acetate buffer (pH 4.5) recorded at a scan rate of 10 mV/s (Eshtaya *et al.*, 2016).



Scheme 4.2: Proposed reaction scheme for the oxidation of phenol with ABTS cation radical (Eshtaya et al., 2016).

Additionally, in the presence of lignosulfonate the CVs present well-shaped oxidation peaks (Figure 4.16), but only one small reduction peak was observed, indicating the absence of ABTS regeneration. A likely explanation is that a portion of the ABTS dication, and almost all of the radical cation formed, coupled with phenoxy radicals and other reactive intermediates produced during the reaction to form covalently-linked derivatives (Matsumura *et al.*, 1986).

The catalytic efficiency of ABTS can be expressed by the ratio i_k/i_c, where i_k (catalytic current) is the anodic peak current of the ABTS in the presence of lignin, and i_c (diffusion current) is the anodic peak current of the ABTS alone (Bourbonnais *et al.*, 1998, González Arzola *et al.*, 2009, Shiraishi *et al.*, 2013). According to this relationship, the catalytic efficiencies of the two oxidised species of ABTS, ABTS cation radical and dication, in the presence of lignosulfonate in 15% (v/v) IL/buffer solution were calculated. On this basis, the anodic current corresponding to the ABTS radical cation increased by 5.9-fold and the ABTS dication by 6.7-fold, reflecting that the oxidation capability of ABTS dication is higher than that of the ABTS cation radical.

The absence of the radical cation peak, as well as the presence of only one small reduction peak, were observed on the CVs of lignosulfonate oxidation (1 wt %) by ABTS in the buffer solution (Figure 4.17). Noticeably, the dication peak rose strongly in the buffer solution and its catalytic efficiency being intensified by 17.6-fold. The

strong current increase at 809 mV indicates that the reaction between $ABTS^{2+}$ and lignosulfonate is relatively fast compared to the reaction with ABTS radical cation.

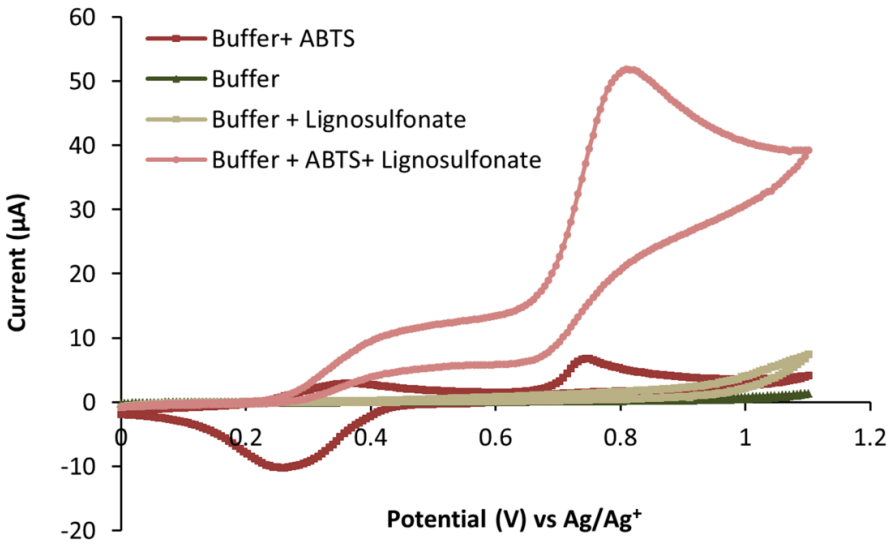


Figure 4.17: Cyclic voltammograms of 1 mM ABTS, 1 wt % lignosulfonate, 1 wt % lignosulfonate mixed with 1 mM ABTS in 0.1 M sodium acetate buffer (pH 4.5) recorded at a scan rate of 10 mV/s (Eshtaya *et al.*, 2016).

Electrochemical oxidation of ABTS at a concentration of 1.0 mM was irreversible in the buffer solution at the scan rate of 10 mV/s (Figure 4.17). However, when the scan rate was increased to 400 mV/s, ABTS (1.0 mM) exhibited a more reversible oxidation process (Appendix A.13). This can be explained by the comproportionation reaction between ABTS and its dication to give two equivalents of the radical cation at the slower scan rate. This ABTS behaviour was also found in ionic liquid and discussed previously in the context of the electrochemical oxidation behaviour of ABTS in $[C_2mim][C_2SO_4]$.

It is likely that the viscosity effect could be the reason behind the high increases in anodic peak currents of ABTS in the presence of lignosulfonate in the buffer solution, compared with 15% (v/v) $[C_2mim][C_2SO_4]$/buffer solutions, where the viscosity of buffer is around half that of the mixture containing 15% (v/v) IL (Table 4.2). Through this decrease in viscosity, a significant increase, about two-fold, in the diffusion coefficient of ABTS in the buffer solution would promote the mass transfer at the electrode surface-bulk solution interface and thus also increase the catalytic efficiencies.

4.3.5 Cyclic Voltammograms of Organosolv Lignin in Alkaline Aqueous Solution/[C_2mim][C_2SO_4] at Different Concentrations

The reaction between the ABTS and organosolv lignin at different concentrations of alkaline aqueous solution in ionic liquid was also explored. As shown in Figure 4.18, the addition of alkaline aqueous solution to the IL resulted in an increase in the second oxidation peak of ABTS. The likely reason behind the initial increase in the dication peak current is a dilution effect, whereby the viscosity of the IL is reduced, resulting in improved mass transfer. This is consistent with the similar electrochemical behaviour seen in solutions of 5% (v/v) alkaline solution/IL, 7% (v/v) alkaline solution/IL and 10% (v/v) alkaline solution/IL since small quantities of water are known to dramatically affect viscosity. For example, the addition of only a 5% (v/v) of water to [C_2mim][C_2SO_4] could lead to a reduction in the IL viscosity by 30% (Rodriguez and Brennecke, 2006, Harwardt et al., 2014). Increasing the concentration of alkaline aqueous solution by more than 10% (v/v) lowered the peak current measured for ABTS. The reduced peak current was most likely caused by a solubility effect since the organosolv lignin is insoluble in the alkaline aqueous solution. A layer of organosolv lignin could have then formed at the working electrode surface, hence either slowing or preventing ABTS accessing the electrode. These results, taken together, emphasise that viscosity and solubility are important driving factors to consider in lignin-based electrochemical oxidation.

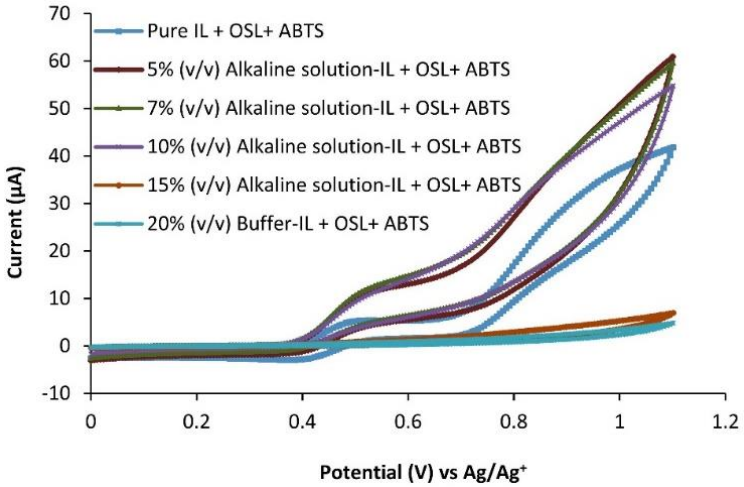


Figure 4.18: Cyclic voltammograms of organosolv lignin (OSL) (5 wt %) mixed with 10 mM ABTS in pure [C_2mim][C_2SO_4], 5% (v/v) alkaline solution/[C_2mim][C_2SO_4], 7% (v/v) alkaline solution/[C_2mim][C_2SO_4], 10% (v/v) alkaline solution/[C_2mim][C_2SO_4], 15% (v/v) alkaline solution/[C_2mim][C_2SO_4] and 20% (v/v) alkaline solution/[C_2mim][C_2SO_4] recorded at a scan rate of 50 mV/s (Eshtaya *et al.*, 2016).

4.4 Bulk Electrolysis

4.4.1 Bulk Electrolysis of Organosolv Lignin

In order to study the intermediates and compounds resulting from the electrochemical oxidation process, a large surface area working electrode was used (graphite rod). This electrode replaces the enzyme/O_2 biocatalyst as the oxidising agent in the laccase-mediator system, thus acting as an enzyme-free model for this process. The results of the CV studies revealed that only organosolv lignin had a notable increase of its anodic current peak in the presence of the ABTS mediator in [C_2mim][C_2SO_4] (Figure 4.13). Therefore, this lignin was used to perform bulk electrolysis. Organosolv lignin (5 wt %) was oxidised by ABTS (10 mM) in the IL and its oxidation products can then be analysed using GC-MS after an ethyl acetate extraction process, which was described in the materials and methods section. The main results were reported in Table 4.2, whilst the GC-MS ion chromatograms can be found in Appendix A.14.

Table 4.3: Syringaldehyde concentration and non-polar product yields obtained from bulk electrolysis of organosolv lignin in the IL after ethyl acetate extraction

Experiment	**Syringaldehyde Concentration[a] (mM)**	**Yields[b] of products (wt %)**
Bulk Electrolysis for 6 h	0.562 ± 0.030	14.40
Control 1: Treatment without bulk electrolysis for 6 h	0.635 ± 0.034	13.31
Control 2: Ethyl acetate extraction at initial time	1.466 ± 0.083	61.63

[a]Syringaldehyde concentration was obtained from the calibration curve.
[b]Yield: Weight formed after extraction and drying/initial weight of lignin in the sample.

After bulk electrochemical oxidation (6 h) at 1.0 V, analysis of the end product showed the presence of syringaldehyde together with other compounds (see Figure 4.19). Unfortunately, the other lignin cleavage products could not be confirmed because the IL is able to contaminate the GC-MS system and this method was not utilised further. The product portfolio was not significantly influenced by the method of reaction and

treatment, and the product formation did not exhibit an enhancement with the bulk electrolysis. Surprisingly, the concentration of syringaldehyde (1.47 ± 0.08 mM), as shown in Table 4.2, produced from the initial extraction of organosolv lignin without using the IL and without bulk electrolysis, was higher than the electrochemical oxidation of organosov lignin in the IL by 2.6-fold and dissolution of lignin in the IL without bulk electrolysis by 2.3-fold. The results in Table 4.2 also show that the yields of products from the dissolution of organosolv lignin in the IL using bulk electrolysis and without using bulk electrolysis were similar at approximately 14.4 wt % and 13.3 wt %, respectively, with respect to the mass of the initial lignin. On the other hand, the yield from the initial extraction without bulk electrolysis was significantly higher. A possible explanation for these results may be due to the high solubility of organosolv lignin or breakdown products in ethyl acetate. Also, the partitioning of the lignin monomers between the ethyl acetate and IL phases may limit the extent of products extraction. Another possible explanation for this is that repolymerisation of the lignin monomeric products may be occurred during the treatment of lignin in the IL.

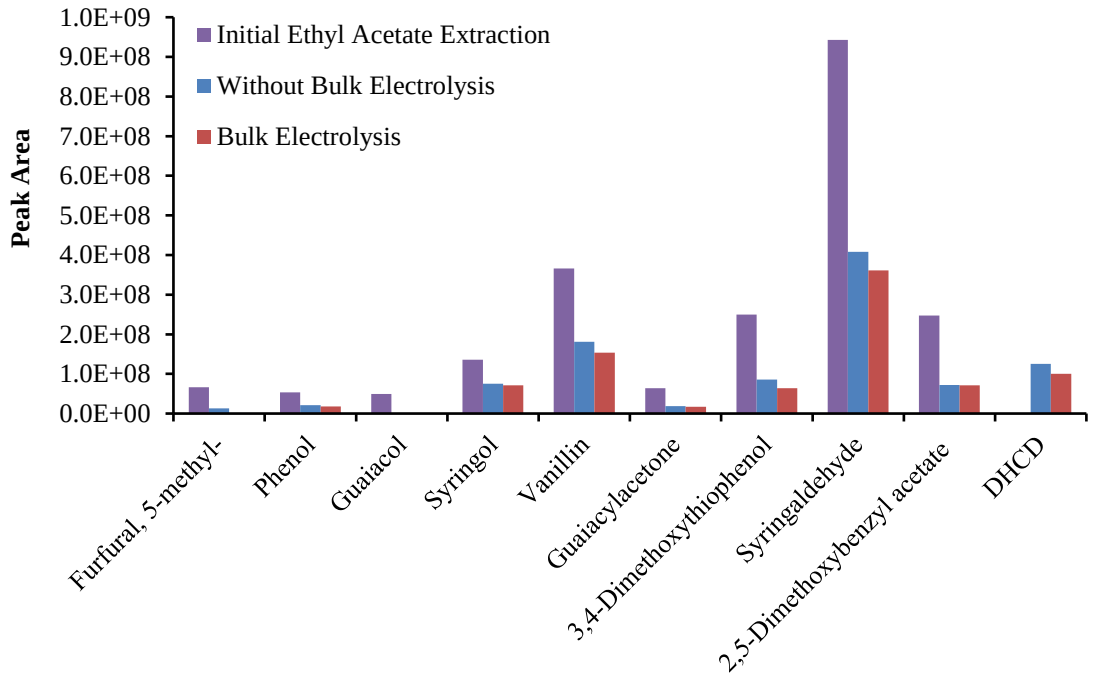


Figure 4.19: Major and minor lignin breakdown products from organosolv lignin after electrochemical oxidation in $[C_2mim][C_2SO_4]$ for 6 h. Identification of the compounds was based on the NIST library. Identification of syringaldehyde was based on authentic standard and NIST library database.

As can be clearly seen from Figure 4.19, the peak area of all products obtained after initial ethyl acetate extraction of organosolv lignin without electrolysis was significantly higher than the other two treatment groups. The chemical structures of the identified compounds are presented in Figure 4.20. On the other hand, there were no significant differences between the peaks areas of all products obtained from electrochemical oxidation and without electrochemical oxidation of organosolv lignin in the IL after 6 h of reaction. This result may be explained by radical oxidative coupling mechanisms occurring during the reaction and hence polymerisation. Polymerisation of lignin during chemical or electrochemical oxidation reactions has been previously reported (Pardini *et al.*, 1991, Stiefel *et al.*, 2016). The by-product 3,5-dimethoxy-4-hydroxycinnamaldehyde (DHCD) was only obtained from the dissolution of organosolv lignin in the IL, indicating the effect of the IL in opening up the structure. Presumably, the absence once electrolysis has taken place corresponds to either repolymerisation of the aldehyde to the lignin or further oxidation to the acid. Guaiacol was detected only at the initial time, and this result is likely to be related to the conversion of guaiacol to new compounds during the dissolution process of organosolv lignin in the IL. However, these compounds could not be detected by GC-MS. The major cleavage products in all cases were syringaldehyde and vanillin, indicating the disruption of C_α-C_β bonds in the propyl side chain of the phenylpropane building blocks (C9 units) of lignin. These results are in line with the results obtained from the dissolution of organosolv lignin in $[C_2mim][C_2SO_4]$ or 30%(v/v) $[C_2mim][C_2SO_4]$/sodium acetate buffer at 30 °C, as shown earlier in Chapter 3. From the data in Figure 4.19, it was apparent that furfural was not detected in the electrochemical oxidation of organosolv lignin, indicating either the conversion of furfural to new compounds during the reaction or that the limit of detection had been reached with this analytical approach since the organosolv lignin starting material contained less than 0.5 wt % of furfural.

Figure 4.19, shows that the intensity of peak area of initial syringaldehyde, vanillin obtained from organosolv lignin was reduced up to 2-fold after electrochemical oxidation and after the dissolution of lignin without electrochemical oxidation in the presence of IL. A possible explanation for this might be related to repolymerisation or further oxidation could occur during the process. Thus, further studies, which take these variables into account, will need to be undertaken.

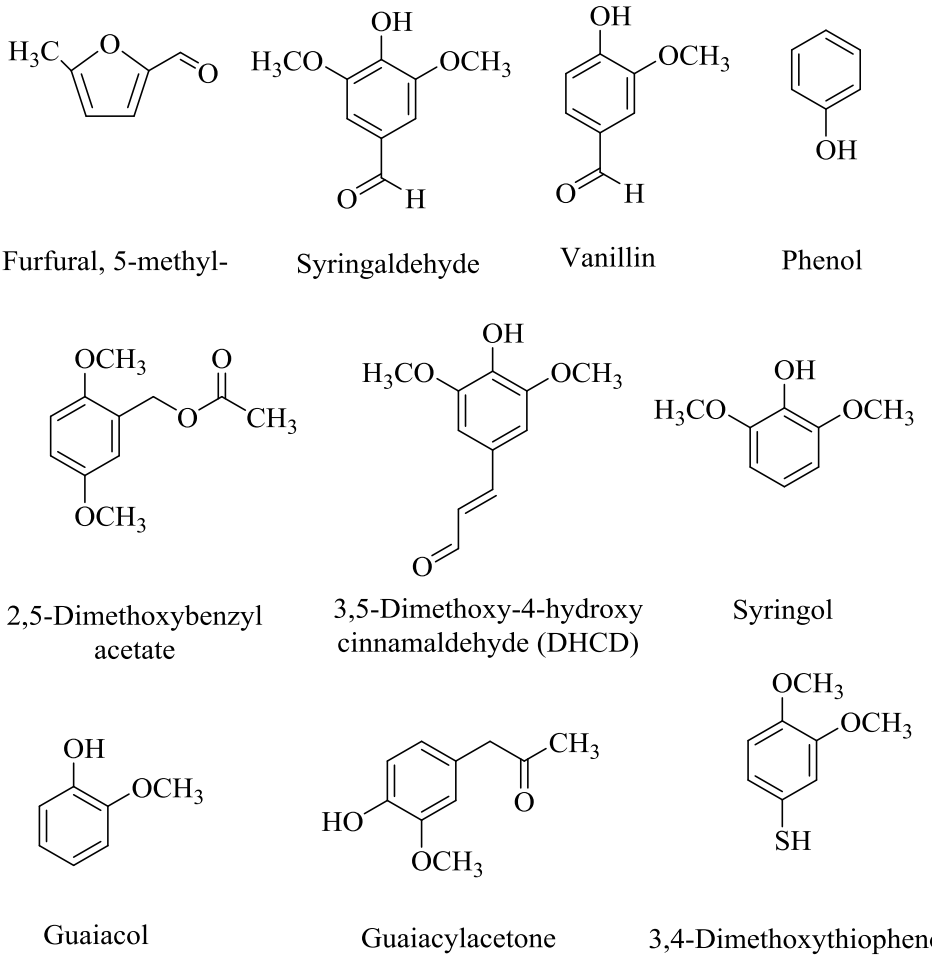


Figure 4.20: Chemical structures of products produced from organosolv lignin chemical oxidation in [C_2mim][C_2SO_4].

4.4.2 Bulk Electrolysis of Lignosulfonate without Pretreatment

The results of the CV studies show (Figure 4.17) that lignosulfonate had a notable increase in the anodic current peak, in the presence of the ABTS mediator in sodium acetate buffer. Thus, bulk electrolysis was also performed on this sample due to the oxidative response. Lignosulfonate was electrochemically treated by ABTS (10 mM) in buffer solution and the oxidation products obtained from the process analysed using GC-MS after an ethyl acetate extraction process. The GC-MS ion chromatograms can be found in Appendix A.15.

The highest peak area of products in the ethyl acetate fraction was produced from the dissolution of lignosulfonate in buffer solution without addition of ABTS and without

performing the bulk electrolysis. Specifically, the intensity peak area of homovanillyl alcohol obtained from treatment of lignosulfonate, without the addition of ABTS and without electrochemical processing, was 4.3-fold higher than the peak area obtained by the electrochemical oxidation of lignosulfonate in the presence of ABTS, as reflected in Figure 4.21. There was no significant difference observed in the peak area of products formed after the dissolution of lignosulfonate in buffer without electrochemical oxidation if compared to the initial amount, suggesting that the result from bulk electrolysis in the presence of ABTS must arise from depletion of lignin-based analytes.

With respect to other analytes, methyl-(2-hydoxy-3-ethoxy-benzyl) ether was detected with low probability, according to the NIST library database, at two different retention times, namely 14.6 min and 15.8 min. The identification of these peaks was unable to be confirmed because a standard was not available, preventing their calibration.

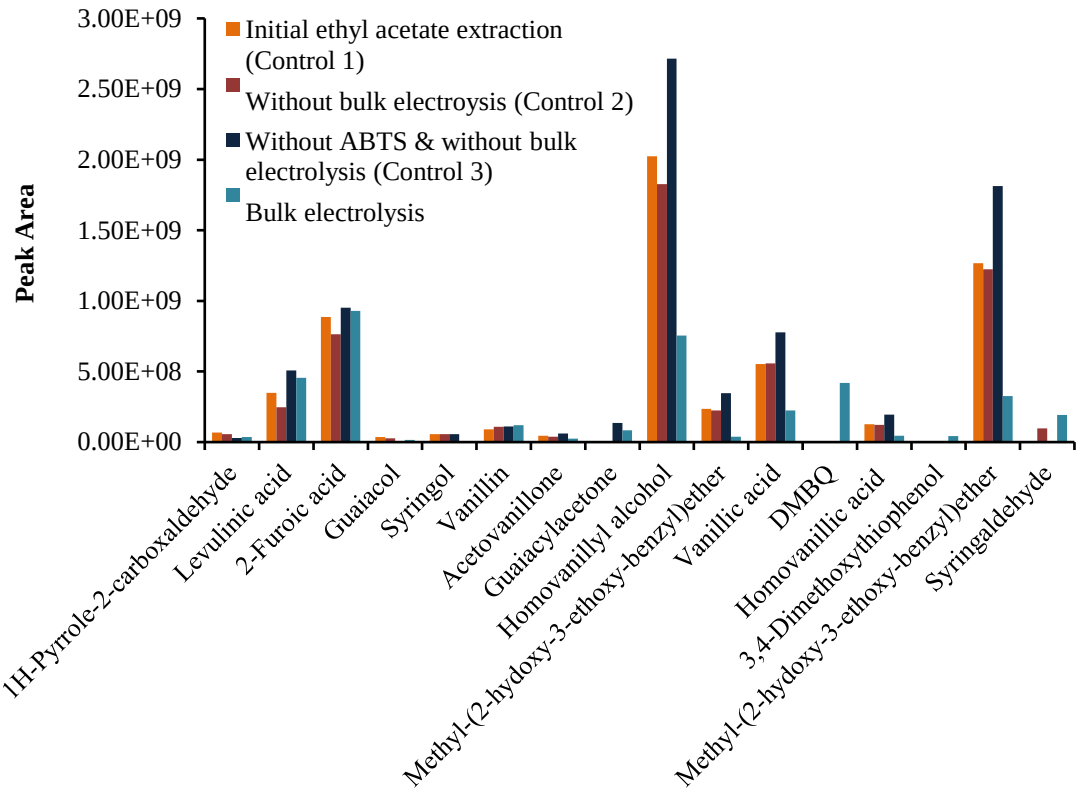


Figure 4.21: Major and minor lignin breakdown products from the electrochemical oxidation of as-received lignosulfonate in sodium acetate buffer pH 4.5 for 8 h. Identification of the compounds was based on the NIST library database.

As shown in Figure 4.22, 2-furoic acid, vanillic acid, homovanillyl alcohol, homovanillic acid and levulinic acid were identified as the major products in all cases. A small amount of vanillin, syringol and acetovanillone were also detected. Interestingly, 2,6-dimethoxybenzoquinone (DMBQ) was only produced from the electrochemical oxidation of lignosulfonate and was not observed in any of control experiments, consistent with the products from the LMS (Chapter 3). Shin and Lee (Shin and Lee, 1999) also found that DMBQ was obtained from oxidation of lignosulfonate by peroxidase of *Pleurotus ostreatus*. This suggests that the use of electrochemically oxidised ABTS may well be a good model for the enzymic process since DMBQ appears only to be generated under the mediator-driven conditions.

Syringaldehyde was obtained from the dissolution of lignosulfonate in the buffer solution in the presence of ABTS (bulk electrolysis and without bulk electrolysis). The chemical structures of products formed from electrochemical oxidation of lignosulfonate are shown in Figure 4.23. In her thesis, Hamidi (Hamidi, 2013) found that guaiacol, vanillin, acetovanillone, vanillic acid, homovanillyl alcohol, phenol, 4-methyl benzaldehyde, catechol, p-toluic acid, 4-hydroxybenzaldehyde, tyrosoI, isovanillin, and 3-hydroxy-l-(4-hydroxy-3-methoxyphenyl) propan-l-one could be identified, and vanillic acid and vanillin were the major products after enzymatic depolymerisation of sodium lignosulphonate using *Trametes versicolor* (LTV) in the presence of ABTS at 60 °C and after 6 h of reaction. This compares well with the patterns of products observed for the EMS system here.

The most surprising aspect of the results is the concentrations of the major compounds obtained from the dissolution of lignosulfonate without bulk electrolysis and without the addition of ABTS were the highest. The treatment of lignosulfonate did thus not exhibit a significant enhancement with the electrolysis process. In fact, the amount of vanillic acid, acetovanillone homovanillyl alcohol and homovanillic acid were decreased in electrochemical oxidation of lignosulfonate compared with the initial amount. This result may be attributed to the repolymerisation of these compounds during the reaction and/or further oxidation of products. The amount of vanillic acid and homovanillyl alcohol obtained from electrochemical oxidation of lignosulfonate was reduced by 1.3-fold and 2.7-fold, respectively, compared to the initial quantities prior to oxidation. Since vanillic acid was dissolved in ethyl acetate instead of

dichloromethane, as per the other standards, the amount of vanillic acid obtained may be underestimated.

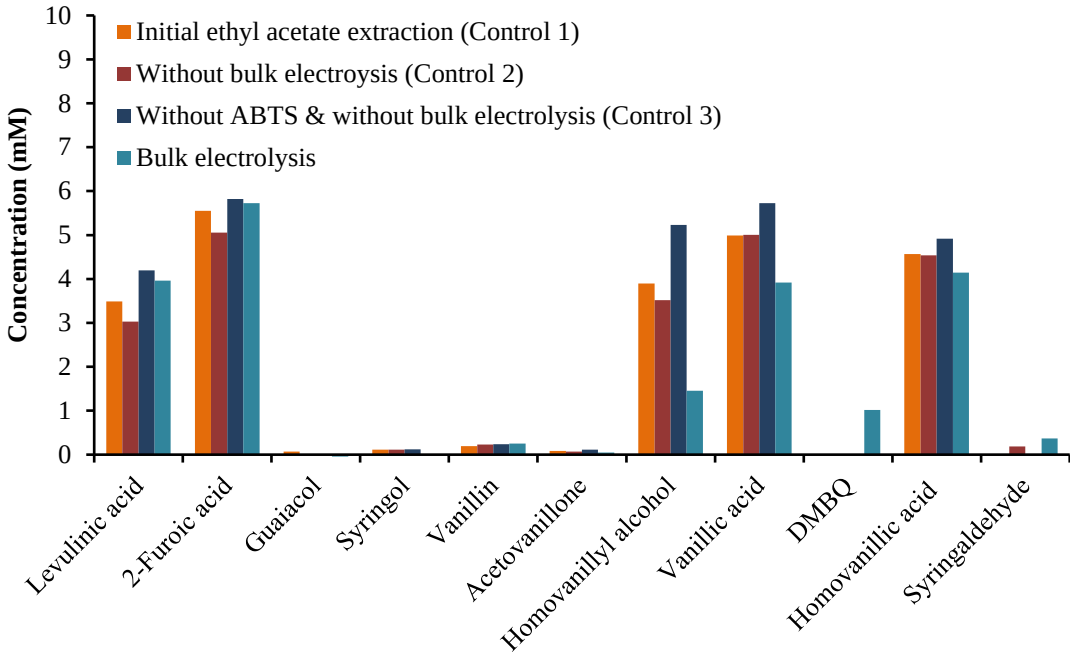


Figure 4.22: Major and minor lignin breakdown products by concentration, from electrochemical oxidation of as-received lignosulfonate in sodium acetate buffer pH 4.5 for 8 h. Identification of the compounds was based on authentic standards and the NIST library database.

Depolymerisation of lignosulfonate probably is introduced by the oxidation of the free phenolic group to form a phenoxy radical. Then this radical would produce a range of compounds via C_α-C_β cleavage, C_α-oxidation and alkyl-phenyl cleavage (Shin and Lee, 1999).

It can be seen that the patterns of the products formed during the electrochemical oxidation of organosolv lignin were significantly different from those obtained from electrochemical oxidation of lignosulfonate (see Figure 4.19 and Figure 4.21). Whereas, syringaldehyde and vanillin were the major products obtained from electrochemical oxidation of organosolv lignin (Figure 4.19), 2-furoic acid, vanillic acid, homovanillyl alcohol, homovanillic acid and levulinic acid were the main products of electrochemical oxidation of lignosulfonate. This result may be explained by the fact that the lignosulfonate from softwood was used as the substrate in this study so most of the lignosulfonate products detected were guaiacyl (G) derivatives as expected. On the other hand, organosolv lignin in this study was produced from mixed

hardwoods, which consist of both guaiacyl (G) and syringyl (S) units and thus was more likely to produce more syringaldehyde and vanillin.

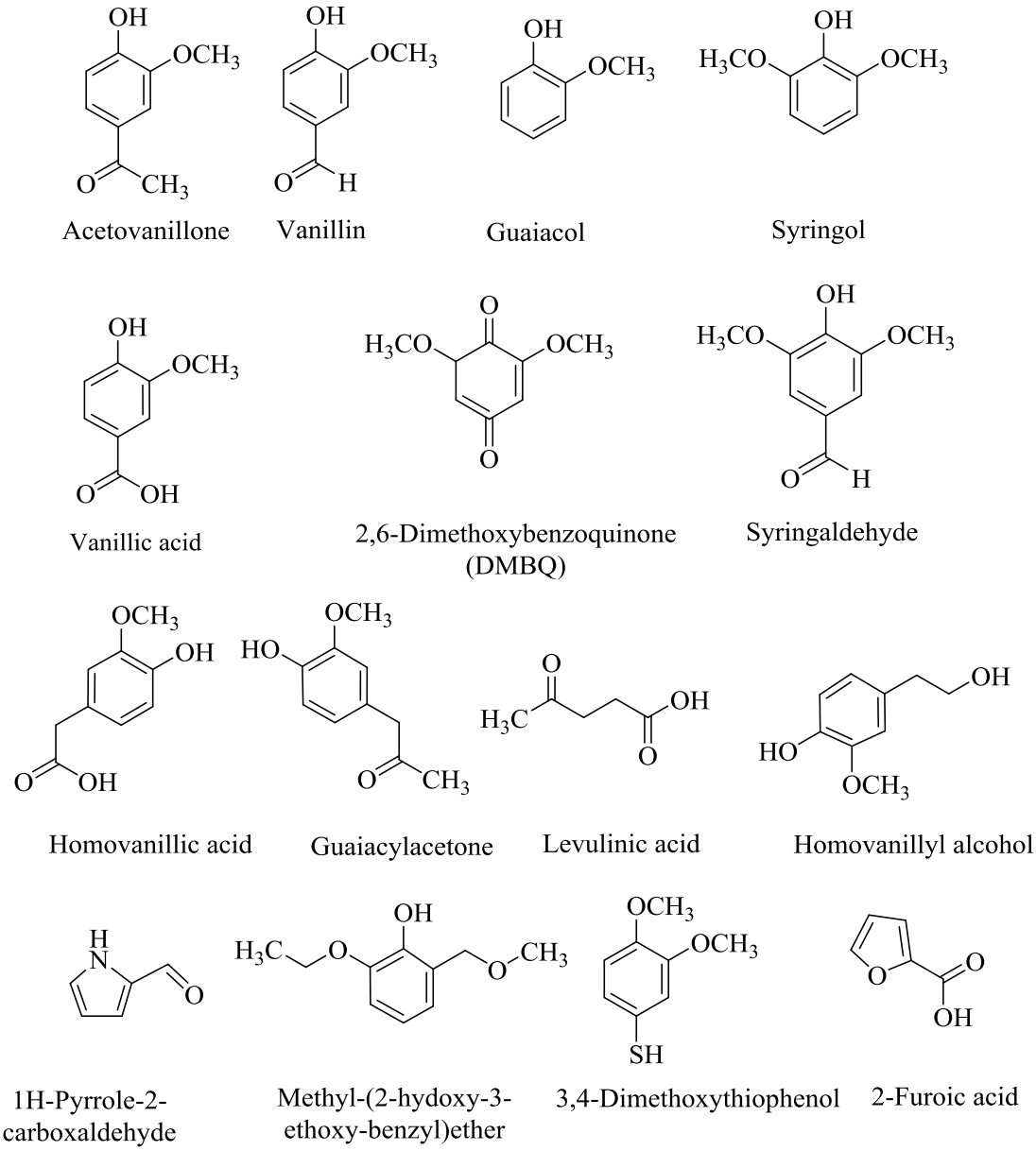


Figure 4.23: Chemical structures of products obtained from lignosulfonate electrochemical oxidation in sodium acetate buffer (pH 4.5).

4.4.3 Bulk Electrolysis of Lignosulfonate after Pretreatment

Solvent fractionation of lignosulfonate using methanol can be used in order to increase the molecular weight of starting materials and to remove any low molecular weight compounds and impurities if they present in the lignosulfonate starting materials. After washing with methanol, the methanol-insoluble portion of the lignosulfonate was

electrochemically oxidised by ABTS (10 mM) in a buffer solution, followed by the extraction process using ethyl acetate. The oxidation products were analysed using GC- MS. The GC-MS ion chromatograms can be found in Appendix A.16. It is apparent from Figure 4.24 and Figure 4.25; there was no significant difference observed in major product concentrations obtained from electrochemical oxidation of lignosulfonate after pretreatment with methanol compared with electrochemical oxidation of lignosulfonate without any pretreatment. The amount of vanillic acid and homovanillic acid were increased only by 1.3-fold and 1.2-fold, respectively, after MeOH pretreatment. Syringaldehyde was only observed after electrochemical oxidation of as-received lignosulfonate, suggesting that this breakdown product was removed, and is not formed as part of the electrochemical reaction.

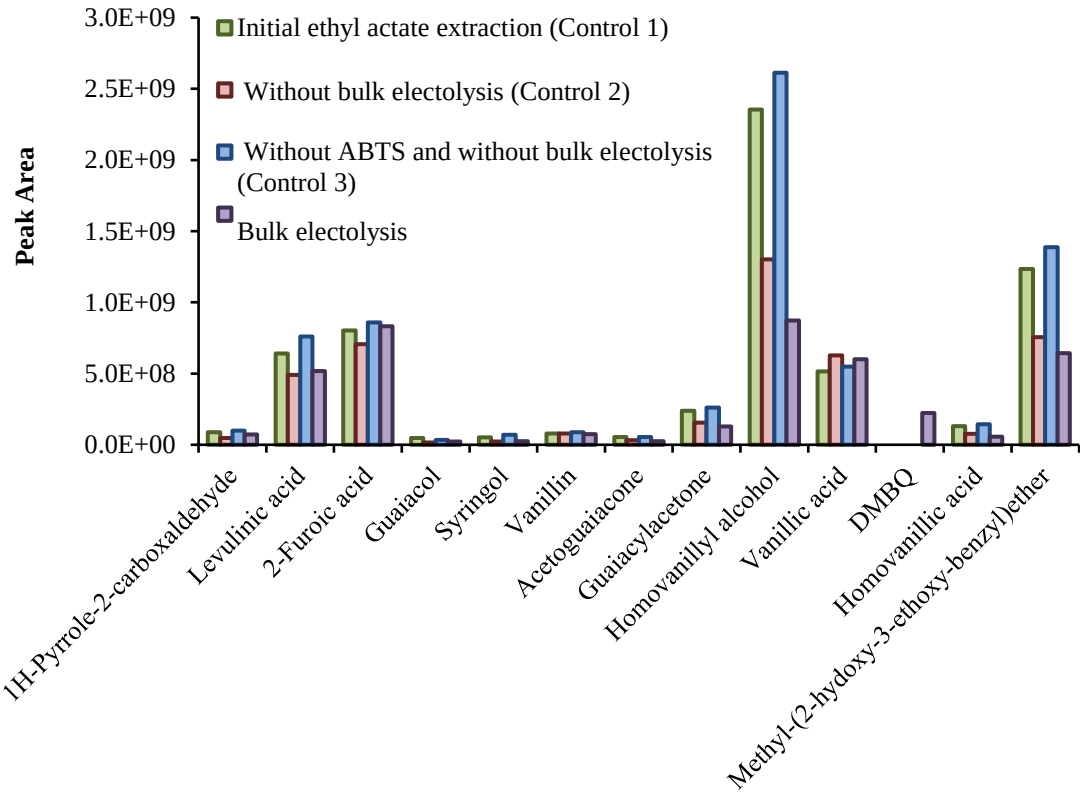


Figure 4.24: Major and minor lignin breakdown products from the electrochemical oxidation of washed-lignosulfonate in sodium acetate buffer pH 4.5 for 8 h. Identification of the compounds was based on the NIST library database.

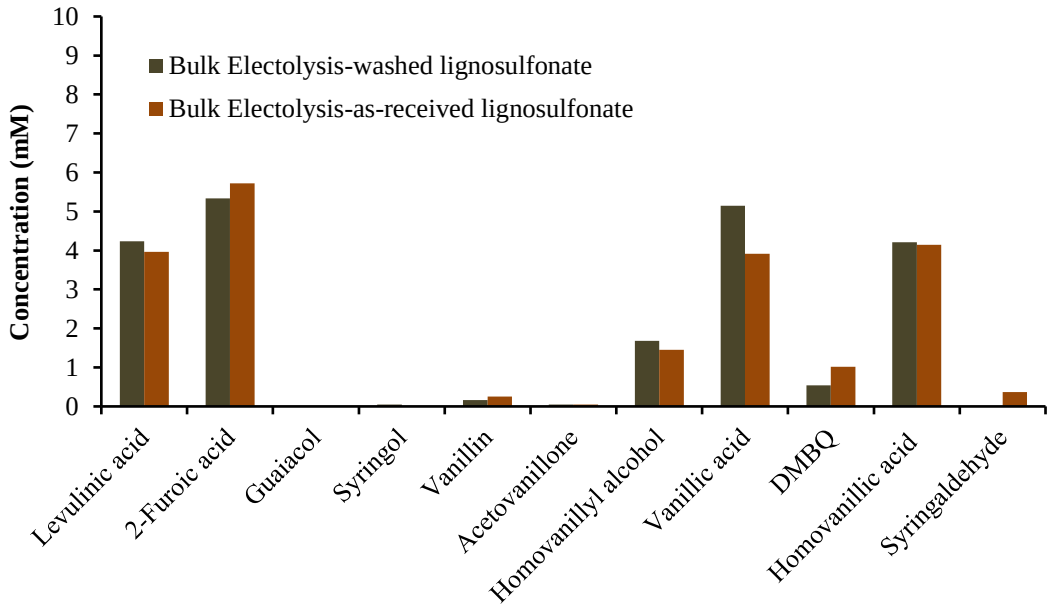


Figure 4.25: Major and minor lignin breakdown products concentration from washed-lignosulfonate and as-received lignosulfonate after electrochemical oxidation in sodium acetate buffer pH 4.5 for 8 h. Identification of the compounds was based on authentic standards and the NIST library database.

To date, there are few studies that have investigated the electrochemical oxidation of lignin using bulk electrolysis. To the best of our knowledge, no study has been performed on the bulk electrolysis of organosolv lignin in the IL with the presence of a mediator. Recently, Reichert and co-workers successfully depolymerised alkali lignin through electro-catalytic oxidative cleavage without using any mediator. They performed the depolymerisation in a special protic ionic liquid ($[HN_{222}][C_1SO_3]$), using an active electrode of mixed ruthenium/vanadium/titanium oxides. The PIL offers a suitable medium for lignin dissolution that ensures a higher potential during electrolysis, as well as promoting the oxidative cleavage mechanism through protonation. A wide range of aromatic compounds, such as aldehydes and ketones were identified in the mixture, as detected by GC-MS and HPLC after diethyl ether extraction (Reichert *et al.*, 2012). Another study performed by Zhu *et al.* (Zhu *et al.*, 2014) achieved electro-oxidative cleavage of lignin in alkaline solutions (2 wt %) by anodic oxidation coupled with electro-generated H_2O_2 oxidation in a non-diaphragm electrolytic cell. Owing to the effective breakage of the C–C and C–O–C linkages among C9 units, lignin macromolecules were depolymerised into low molecular weight aromatic products with different functional groups, such as aldehydes, ketones, phenols and acids (Zhu *et al.*, 2014). More recently, Stiefel *et al.* (Stiefel *et al.*, 2016)

demonstrated the use of 3D-structured electrode materials for the electrochemical depolymerisation of Kraft lignin with a subsequent membrane filtration in order to increase product yield under mild conditions. However, the authors in the above studies did not show any control experiment to support their findings that these products were indeed formed through the electrocatalytic process.

On the basis of the yields of products obtained during electrochemical oxidation of lignin, Reichert and co-workers (Reichert *et al.*, 2012) found that the maximum yields of cleavage products were 6 wt % with respect to the initial lignin weight. Zhu *et al.* (Zhu *et al.*, 2014) reported that 59.2 % of lignin (based on organic and aqueous phases) was depolymerised into low molecular weight aromatic products after 1 h electrolysis. Low yields (0.5 wt %) of individual compounds (vanillin, acetovanillone and syringaldehyde) were obtained by Stiefel *et al.* (Stiefel *et al.*, 2016). While the yields of products obtained from treatment of organosolv lignin in the IL using bulk electrolysis were 14.4 wt % with respect to the mass of the initial lignin in this current study.

4.5 Conclusions

Electrochemical oxidation using CV has been explored for the potential degradation of three types of lignin (lignosulfonate, Kraft and organosolv) in $[C_2mim][C_2SO_4]$, utilising the mediator ABTS. The electrochemical behaviour of ABTS alone in $[C_2mim][C_2SO_4]$ was studied and is quite similar to that previously seen in buffered aqueous solutions, in terms of proportionality of peak currents to the square root of the scan rate and the ratio of anodic to cathodic peak currents.

The oxidation currents on the CVs for the formation of either or both of the ABTS radical cation and the ABTS dication were observed to increase after addition of all types of lignin, proving ABTS to be an effective mediator for electrochemical oxidation of lignin. However, the use of ABTS was found to affect more significantly the oxidation of organosolv lignin, which is consistent with the greater solubility of this lignin in the utilised IL over the other types of lignin examined in this study. Similarly, the solubility of this lignin decreased dramatically at around 10% (v/v) buffer concentration and resulted in a concomitant reduction in the oxidation peak current.

The solubility of lignin and viscosity of both the solvent and solution are likely to play a vital role in the electrochemical oxidation reaction of lignin. The viscosity and interactions of ionic liquid-lignin solutions influence the mass transfer of ABTS from the electrode surface into the bulk solution, and IL-solute interactions have potential to limit the electron transfer kinetics, as has been shown for other reaction types (Yau *et al.*, 2008, Yau *et al.*, 2009, Yau *et al.*, 2013). Overall, the rates of heterogeneous and homogeneous electron-transfer reactions are lower in $[C_2mim][C_2SO_4]$ compared to those measured in the buffer solution. The CV studies of ABTS mediator with lignin demonstrate a high level of catalytic efficiency toward lignosulfonate in buffer (dication 17.6-fold) and 15% (v/v) $[C_2mim][C_2SO_4]$/buffer (cation 5.9-fold and dication 6.7-fold) but there was no increase in catalytic efficiency associated with presence of the $[C_2mim][C_2SO_4]$. A future study investigating the molecular interactions between ABTS/ionic liquid/lignin and lignin/ionic liquid would help to clarify the influence of ionic liquids, both in terms of their solubilisation of lignin components, specific solute-solvent interactions, and viscosity, and delineate their impact on reactivity.

One of the more significant findings emerging from this study is that the electrochemical techniques can be quickly and easily applied to study ionic liquid/lignin/mediator systems for prediction and selection of an appropriate ionic liquid and mediator combination for the lignin degradation process. This may lead in future to optimised electrochemical processes for improved utilisation of lignolytic biomass in an energy efficient manner.

A wide range of lignin cleavage products from bulk electrolysis of lignosulfonate in buffer solution and organosolv lignin in the IL have been identified. No significant enhancement of lignin depolymerisation has been identified as occurring under bulk electrolysis conditions for both types of lignin, compared with the control experiments. A future study investigating the effects of temperature and reaction time on electrochemical oxidation of lignin using bulk electrolysis would be very interesting.

One of the greatest challenges remaining in this study was to complete identification and quantification of the produced low-molecular-weight compounds from the

complex mixtures of lignin formed after bulk electrolysis reaction, especially in the IL. Only the products from ethyl acetate extraction were characterised using GC-MS. Syringaldehyde was the only product identified, while the other lignin cleavage products could not be confirmed because the use of the IL was incompatible with the GC-MS system available. In general, therefore, further investigation would be needed to further and robustly identify the compounds in aqueous and solid fractions, or to find a direct method to identify and detect the products obtained from the reaction mixtures without doing an extraction process prior to the analysis.

Finally, this research provides a framework for the exploration of depolymerisation of lignin using electrochemical oxidation process with the presence of ionic liquid. Further investigation and experimentation using different types of ionic liquids are strongly recommended.

CHAPTER FIVE

UNDERSTANDING THE RADICAL BEHAVIOUR OF LIGNIN RELATED COMPOUNDS IN IONIC LIQUIDS

5.1 Introduction

Free radicals are molecules or fragments of molecules that contain at least one unpaired electron in an atomic outer orbital. Many radicals are unstable and highly reactive and tend to transfer either an electron or hydrogen atom from other molecules to gain chemical stability (Lobo *et al.*, 2010). The antioxidant can be defined as ‘‘any substance that, when present at low concentrations compared to those of an oxidisable substrate, significantly delays or prevents oxidation of that substrate’’ (Halliwell and Gutteridge, 1995).

There are two major mechanisms that are possible for radical reactions and are probed through different assays to measure the total antioxidant activity; assays based on the single electron transfer (SET) reaction and assays based on a hydrogen atom transfer (HAT). Both mechanisms can occur in the same reactive mixture. For SET, the antioxidant can give an electron to the free radical to generate a radical cation. In the second mechanism, the free radical removes a hydrogen atom from the antioxidant, which in turn becomes a radical. However, there is no simple standard method by which antioxidant capacity can be measured accurately and quantitatively (Wright *et al.*, 2001, Leopoldini *et al.*, 2004, Huang *et al.*, 2005, Prior *et al.*, 2005). In this present study three different types of assays including FRAP, DPPH and ABTS were adopted to assess the free radical activity of lignin-related compounds in ionic liquids. These assays are described in more detail in the literature review (Section 2.10).

5.1.2 Objective

One of the most important findings that has emerged from the previous chapter (Chapter 4) investigating the electrochemical oxidation of lignin with the assistance of ABTS as a mediator in the ionic liquid, was that although electrochemical oxidation was shown to take place in the ionic liquid and be different for different types of lignin,

the exact nature of this reaction and products was extremely difficult to follow. In particular, details regarding the likelihood of repolymerisation of monomers, once cleaved, and the relative reactivity of different functional groups towards oxidation in the complex lignin mixture, were unable to be delineated through this approach. This information is key in designing new and more efficient approaches to depolymerisation in ionic liquid solvents, along with the selection of improved solvents.

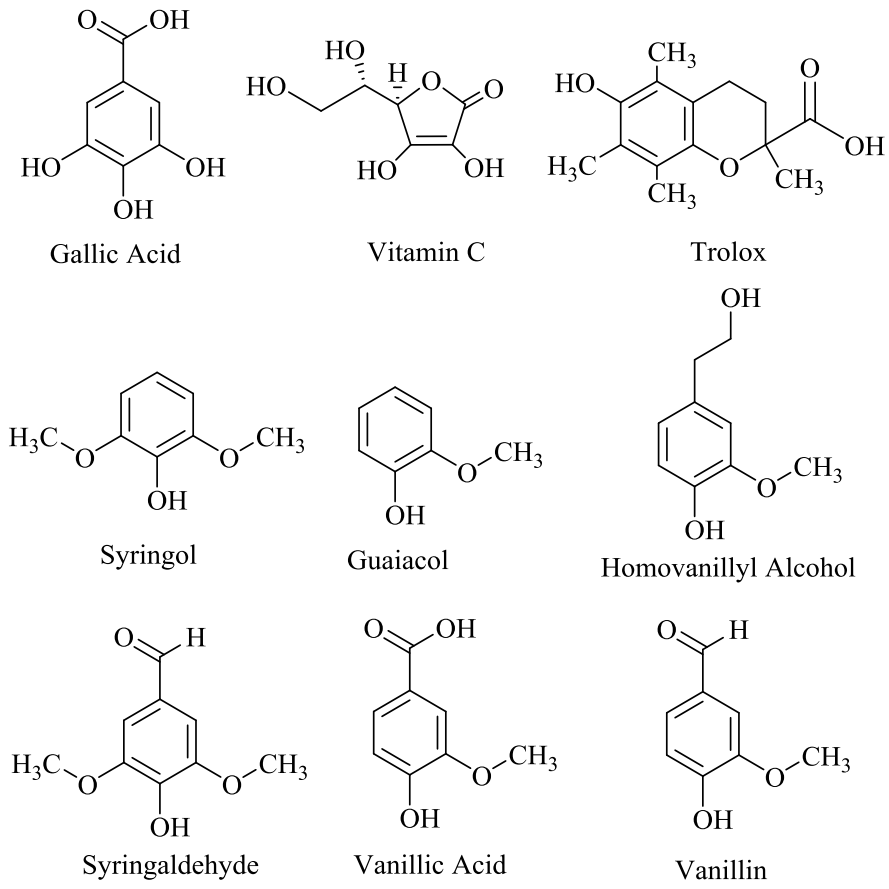
To approach these gaps, a better fundamental understanding of the behaviour of the free radicals of lignin-related compounds in ionic liquids is required. In reviewing the literature, no data was found on either the specific free radical behaviour or detailed reaction of the lignin depolymerisation process in ionic liquids. Therefore, the work presented in this chapter was designed to explore the radical behaviour of lignin-related monomers in ionic liquids. To do this in the first instance, three different methods were carried out to evaluate the antiradical capacity of the lignin-related monomers compounds, including FRAP assay, DPPH radical scavenging and ABTS assay. In this work, six lignin monomers; syringaldehyde, vanillin, vanillic acid, guaiacol, syringol and homovanillyl alcohol were chosen, based on the most common components identified from the lignin dissolution process in the ionic liquid that have been discussed in previous chapters. Three well-known antioxidant standard compounds; vitamin C (ascorbic acid), gallic acid and Trolox (a water-soluble vitamin E analogue) were used to compare the antioxidant potential. The chemical structures of lignin- related monomers and standards compounds are shown in Scheme 5.1.

5.2 Materials and Methods

5.2.1 Chemicals

Acetonitrile, methanol and toluene were obtained from VWR International Ltd (UK) as HPLC grade. The stable radical 2, 2-Diphenyl-1-picrylhydrazyl (DPPH•) was purchased from Alfa Aesar (A Johnson Matthey Co., Lancashire, UK). tetradecyl(trihexyl) phosphonium bis[(trifluoromethane) sulfonyl] imide ($[P_{6,6,6,14}][Tf_2N]$) was obtained from Iolitec (IOLITEC Ionic Liquids Technologies GmbH, Heilbronn, Germany), 3,4,5-Trihydroxybenzoic acid (gallic acid), L-ascorbic acid (vitamin C), (±)-6-Hydroxy-2,5,7,8-tetramethylchromane-2-carboxylic acid (Trolox), 2,2'-Azobis(2-methylpropionamidine) dihydrochloride (AAPH), 2,4,6-

Tris(2-pyridyl)-s-triazine (TPTZ) and all other chemicals and solvents used in this study were purchased from Sigma-Aldrich (UK) and used without any further purification.



Scheme 5.1: Chemical structures of the tested compounds, including literature standards and lignin monomers.

5.2.2 DPPH Assay Using 96 Well Plate Reader

The measurement of the DPPH radical scavenging activity assay was performed according to the methodology described by Brand-Williams *et al.* (Brand-Williams *et al.*, 1995) with some modification. The stock solution was prepared by dissolving 20 mg DPPH with 20 mL solvent (methanol, toluene, acetonitrile $[C_2mim][C_2SO_4]$ or [DMEA][HCOO]) degassed with nitrogen and then stored at -20 °C until needed. The DPPH solution (6×10^{-5} M) in the solvent was prepared fresh daily before UV measurements. The solutions of the test compounds/standards (25 μL) at different concentrations were added to 975 μL of DPPH• solution and then 200 μL of each mixture was added to three separate wells of a 96-well plate. All experiments were

repeated at least three times. In the control (ionic liquids experiments), the volume of sample was replaced by the same volume of solvent. Quartz plates (QG Hellma) were used for ionic liquid, acetonitrile and toluene solutions, to avoid leeching of plasticisers from plastic plates, and a disposable plate (NUNC) was used for methanol. The decrease in absorbance at 520 nm was monitored using a BMG FLUOstar Optima Microplate reader (BMG Labtech Ltd., UK) until the reaction reached a steady state reached at 25 °C.

5.2.3 DPPH Assay Using UV-Vis Spectrophotometer

The DPPH solution in methanol (6×10^{-5} M) was prepared as described in the previous section. The sample (0.1 mL) at different concentrations was mixed with 3.9 mL of DPPH solution and thereafter 200 μL of this mixture were added in triplicate to wells of a 96-well plate (NUNC). The decrease in absorbance at 520 nm was monitored using a BMG FLUOstar Optima Microplate reader (BMG Labtech Ltd., UK). For UV-Vis spectrophotometer a 1.0 mL of the same mixture (0.1 mL sample and 3.9 mL DPPH solution) was transferred to a disposable cuvette (1 cm path length) and then the decrease in absorbance at the same wavelength (520 nm) was monitored using a UV- Vis spectrophotometer (UV-2600, Shimadzu) until the reaction reached a steady state at 25 °C.

5.2.4 ABTS Assay Using UV-Vis Spectrophotometer

The ABTS assay was performed according to the method developed by Van den Berg *et al.* (van den Berg *et al.*, 1999). An $ABTS^{\bullet+}$ solution was prepared by mixing 1.0 mM AAPH with 2.5 mM ABTS in 100 mM phosphate buffered saline solution (pH 7.4), containing 150 mM NaCl. The mixture was heated in a water bath at 68 °C for 40 min. A fresh $ABTS^{\bullet+}$ stock solution was prepared daily in order to maintain consistency and prevent the degradation in the assay. The resulting blue-green $ABTS^{\bullet+}$ solution was cooled to room temperature, filtered through nylon syringe filters and adjusted to an absorbance of 0.650 ± 0.004 at 734 nm. The sample solution of 20 μL was added to 980 μL of the resulting blue-green ABTS radical solution. The mixture, protected from light with aluminium foil, was incubated in a water bath at 37 °C for 10 min. The decrease in absorbance at 734 nm was measured using a UV-Vis spectrophotometer

(UV-2600, Shimadzu) at the endpoint of 10 min. The control sample consisted of 20 μL of phosphate buffer in 980 μL of $ABTS^{\bullet+}$ solution. All experiments were performed at least in triplicate and in a concentration range between 0.2 and 2.0 μg/mL, final concentration.

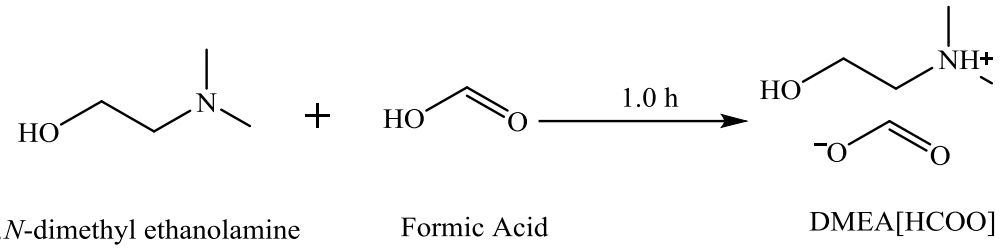
5.2.5 FRAP Assay Using 96 Well Plate Reader

The FRAP assay was performed according to the method developed by Benzie and Strain with some modifications (Benzie and Strain, 1996, Benzie and Strain, 1999). The FRAP reagent was prepared by mixing solution A [300 mM acetate buffer (pH 3.6) prepared by dissolving sodium acetate trihydrate (3.1 g/L) and glacial acetic acid (16 mL/L) in distilled water and stored at 4 °C], solution B [31.2 mg of TPTZ dissolved in 10 mL of 40 mM HCl at 50 °C in a water bath] and solution C [540 mg of ferric chloride hexahydrate dissolved in 100 mL distilled water] in a volume ratio of 10:1:1, respectively. The freshly prepared FRAP reagent was warmed to 37 °C before use. The samples (20 μL) were each added to three wells of a 96-well quartz plate (QG Hellma). The assay was started by adding 180 μL of FRAP reagent to each well. Appropriate blanks were prepared from the FRAP reagent only and run simultaneously with the samples. The plate was immediately shaken in a BMG FLUOstar Optima Microplate reader (BMG Labtech Ltd., UK) for 30 seconds and the reaction was allowed to run for 60 min, after which the plate was read on the plate reader (595 nm). A reference ferrous compound, ferrous sulfate ($FeSO_4.7H_2O$, 0-0.1 mM in distilled water as a final concentration in test system), was run simultaneously and used to generate the calibration curve by linear regression. The absorbance of the samples were compared to a $FeSO_4$ standard curve (prepared daily), and the FRAP values were expressed as Ferrous Equivalent. One FRAP unit is arbitrarily defined as the reduction of 1.0 mole of Fe(III) to Fe(II).

5.2.6 Preparation of *N,N*-dimethyl ethanol ammonium Formate ([DMEA][HCOO])

[DMEA][HCOO] was prepared by adapting the procedure used by Idris *et al*. (Idris *et al.*, 2014) The neutralisation method was used for [DMEA][HCOO] preparation, as illustrated in Scheme 5.2. An equimolar amount of formic acid was (34.0 g, 0.74 mol) added dropwise to *N,N*-dimethyl ethanolamine (65.96 g, 0.74 mol) whilst stirring

rapidly in an ice bath. The mixture was stirred for one h, and a colourless liquid was formed as a final product with 99.5% yield.



N,N-dimethyl ethanolamine Formic Acid DMEA[HCOO]

Scheme 5.2: Preparation of *N*,*N*-dimethyl ethanol ammonium formate.

^{1}H NMR and ^{13}C NMR spectra of the *N*,*N*-dimethyl ethanol ammonium formate were recorded at 400 MHz on a Bruker AV400 spectrometer as solutions in deuterated chloroform. ^{1}H NMR (ppm, 400MHz, $CDCl_3$) δ_H: 8.91 (2H, s, $^{+}$NH, OH), 8.37 (1H, s, $HCOO^{-}$), 3.73 (2H, q, CH_2), 2.92 (2H, t, CH_2), 2.61 (6H, s, 2 CH_3).^{13}C NMR (ppm, 400 MHz, $CDCl_3$) δ_C: 169.04, 59.91, 56.38, 43.36. NMR spectra of *N*,*N*- dimethyl ethanol ammonium formate can be found in Appendix A.17.

5.2.7 Water Content Measurements

The water content in [C_2mim][C_2SO_4] and [DMEA][HCOO] was measured by Karl Fischer Coulometric titration apparatus (Mitsubishi CA100) For further details see (O'Mahony *et al.*, 2008, Dominguez *et al.*, 2010). All experiments were performed at least in triplicate.

5.2.8 Viscosity Measurements

The viscosity measurements of ionic liquids ([C_2mim][C_2SO_4] and [DMEA][HCOO]) and methanol/[C_2mim][C_2SO_4] mixtures were carried out at 25 °C using a Malvern Kinexus pro^{+} rotational rheometer (Malvern Instruments Ltd., UK) equipped with cup and bob (cup size C14 (DIN), bob diameter 14 mm). A strain rate sweep was performed from 1.0 to 1000 s^{-1}. For pure ionic liquids, no dependence of the viscosity on shear rates could be observed within the range from 1 to 1000 s^{-1} at 25 °C and both ionic liquids ([C_2mim][C_2SO_4] and [DMEA][HCOO]) appear to be Newtonian fluids. However, shear-rate-dependent viscosity measurements of methanol/[C_2mim][C_2SO_4] mixtures showed an influence of the shear rate on the viscosity measured at shear rates lower than 10 s^{-1}. Selection of a shear rate equal to or higher than 10 s^{-1} resulted in

viscosity data independent of shear rate. Therefore, shear rates of between 10-250 s^{-1} were selected for methanol/[C_2mim][C_2SO_4] mixture viscosity measurements. The viscosity of pure methanol was measured at a shear rate of 250 s^{-1}. All the samples were prepared immediately prior to performing viscosity measurements to avoid variations in composition due to either evaporation of methanol or pickup of water by the hygroscopic ILs.

5.2.9 Generation of ABTS Radical Cation in Ionic Liquid

Electrochemical formation of ABTS radical cation (12 mM) in [C_2mim][C_2SO_4] was performed in a 40 mL glass cell with 15 mL as a working volume. The cell consisted of a graphite rod (10 mm diameter) as a working electrode, a graphite rod (10 mm diameter) as a counter electrode, isolated from the cell by a glass frit, and filled with [C_2mim][C_2SO_4] (see Figure 5.1), and an Ag/Ag^+ electrode (10 mM AgTfO, [C_2mim][C_2SO_4]) as a reference electrode. Electrolysis was carried out at a fixed potential (1.0 V) for 24 h.

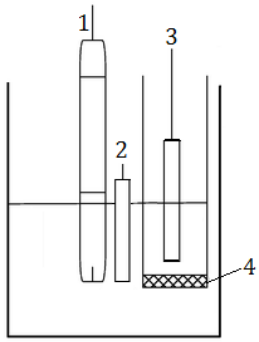


Figure 5.1: Schematic diagram of electrochemical cell (1) graphite rod working electrode (2) Ag/Ag^+ reference electrode (3) graphite rod counter electrode (4) glass frit.

5.3 Results and Discussion

5.3.1 FRAP Assay

A first order regression model in relation to the absorbance at 595 nm versus different concentrations of gallic acid and vitamin C was obtained for all solvents tested (Appendix A.18). The standard curve (Figure 5.2) that relates the concentration of ferrous sulfate and the absorbance was used to calculate ferrous sulfate equivalents based on the absorbance of gallic acid and vitamin C. The antioxidant capacity of gallic

acid and vitamin C also showed a first-order relationship with ferrous sulfate equivalents (Figure 5.3).

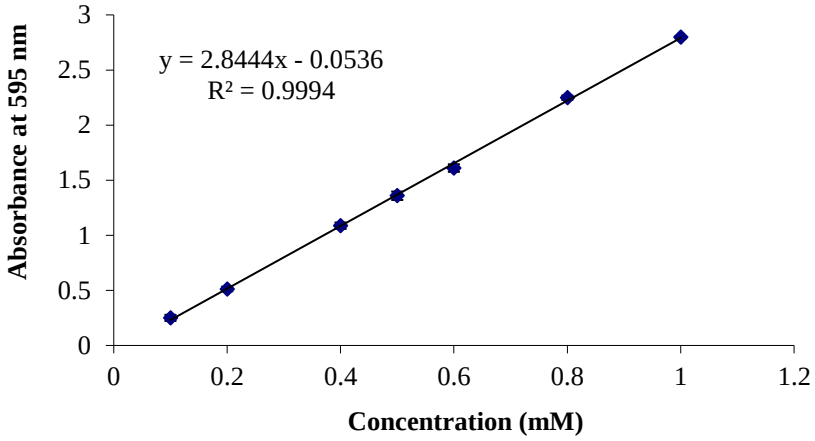


Figure 5.2: Example of a calibration curve for FRAP assay using ferrous sulfate as standard. Values are means ± standard deviations (n=3).

The rates of increase in absorbance at 593 nm (Appendix A.19) for vitamin C did not reach an endpoint within the monitoring period (60 min) in all solvents investigated even for high concentrations. These results seem to be inconsistent with other research that has found that the reaction of FRAP reagents with vitamin C is very fast and reaches completion in less than 1.0 min (Benzie and Strain, 1996). However, these results are consistent with research was done by Pulido *et al.* (Pulido *et al.*, 2000) that found the absorption for polyphenols and vitamin C increased slowly, even after several hours. Thus, the FRAP values of these compounds cannot be obtained accurately after 4.0 min of reaction time used in some assays. The reaction with gallic acid was faster than that of vitamin C, reaching the endpoint within 30-40 min (depending on the concentration and solvent used) in all solvents investigated (Appendix A.19).

Figure 5.3 compares the antioxidant activity of vitamin C and gallic acid dissolved in different types of solvents ($[C_2mim][C_2SO_4]$, isopropanol and water) using the FRAP assay. For these assays, the antioxidant solvent was only used for sample preparation so appears in the final mixture at only 10% v/v, whilst the aqueous FRAP reagent was used in all cases to maintain low pH (pH 3.6). In all solvent systems investigated, gallic acid showed much higher values of antioxidant activity compared to vitamin C. These results were in line with those of previous studies (Pulido *et al.*, 2000, Schlesier *et al.*, 2002). The stoichiometric factors or relative activity (defined as the ability of 1.0 mole of the compound to reduce 1.0 mole of Fe(III) to Fe(II)), which is can be found from

slope in Figure 5.3 of gallic acid in isopropanol, $[C_2mim][C_2SO_4]$ and water were estimated to be 4.2, 3.8 and 5.1, respectively. The stoichiometric factors of vitamin C were found in isopropanol, $[C_2mim][C_2SO_4]$ and water; 1.85, 0.77 and 0.40 respectively. These results seem to be consistent with other research that found that the FRAP values are influenced by the types of solvents used to prepare the samples and the Fe(II) calibration standard solution (Pulido *et al.*, 2000). According to Benzie and Strain, vitamin C has a stoichiometric factor of 2.0 (1.0 mole of vitamin C can reduce 2.0 mole of Fe(III) in aqueous solution using FRAP assay (Benzie and Strain, 1999). This inconsistency may be due to the reaction time, where the reaction of vitamin C in the present study does not reach steady state even after 60 min, while the reaction reached the end point within a few seconds in the Benzie and Strain study. Another possible explanation for this variation in the result is that the final concentrations of Fe(III) and sample in the reaction solution were modified to consider the effect of dilution in the thesis. However, there was no mention in the Benzie and Strain study of the values related to the sample concentrations either before dilution in the cuvette or after the dilution.

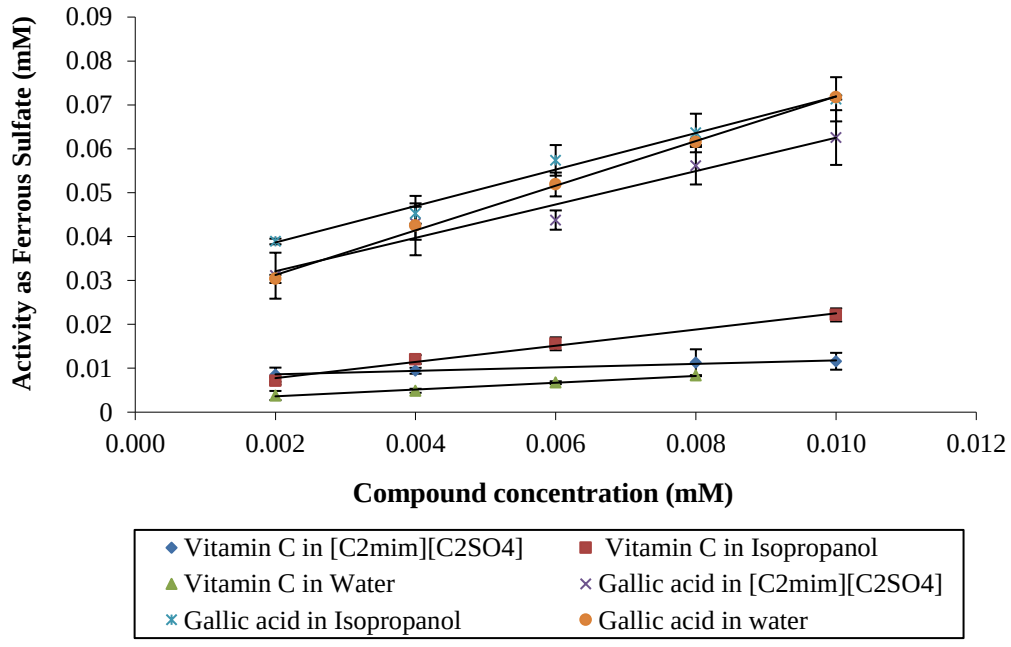


Figure 5.3**:** The relative activity of gallic acid and vitamin C (expressed as Ferrous sulfate (μM) equivalents) using different concentration dissolved in three solvents in FRAP assay after 60 min of reaction. Values are means ± standard deviations (n=3).

Although the FRAP assay is simple and does not require specialist equipment, many reagents are required for this assay. Potential problems may arise specifically with ionic

liquids, as the ions could interact with Fe(III) to form complexes that may not react the same with antioxidants. In addition, the reaction should be monitored until reaching the steady state.

To provide a contrast to the FRAP approach, and to ensure consistency in the observations, the DPPH and ABTS methods were adopted with a view to obtaining further mechanistic information on the free radical behaviour of lignin-related compounds in ionic liquids.

5.3.2 Radical Activity Scavenging of Lignin-Related Monomers by DPPH in Methanol Using 96 Well Plate Reader

The antioxidant activity of lignin-related monomers and standards was measured in terms of hydrogen donating or radical scavenging ability, using the stable radical DPPH. The exact DPPH• concentration ([DPPH•]) in the reaction medium at any one time was calculated from a calibration curve (the calibration curve prepared daily prior the measurements to increase the accuracy of the results see e.g. Figure 5.4) using equation 5.1, determined by linear regression.

$$\text{Absorbance (520 nm)} = a\,[\text{DPPH}\bullet] + b \qquad (5.1)$$

where a is the slope of the line, b is the y-intercept and [DPPH•]: was expressed as mM

Example (Figure 5.4) Absorbance (520 nm) = 0.0085 [DPPH•] + 0.0942

The percentage of remaining DPPH• was calculated using the following equation 5.2:

$$\%DPPH\bullet_{remaining} = \frac{[DPPH\bullet]_t}{[DPPH\bullet]_{t=0}} \qquad (5.2)$$

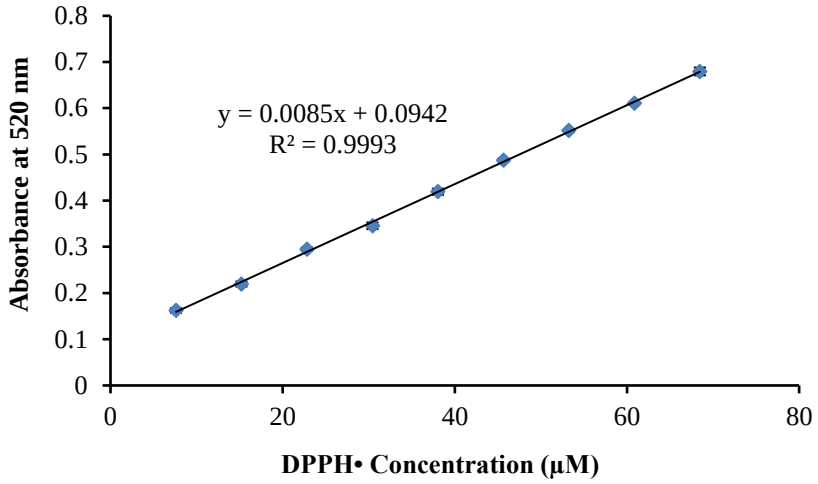


Figure 5.4: Example of the calibration curve of DPPH•. Values are means ± standard deviations (n=3).

For each of the lignin monomer or standard concentrations tested, the reaction kinetics were plotted (see Figure 5.5 as an example and the rest of the results can be found in Appendix A.20). From these graphs, the percentage of DPPH• remaining at the steady state was determined and used to determine the percentage of residual DPPH• at the steady state as a function of the molar ratio of sample to DPPH•. The concentration of sample necessary to decrease the initial DPPH• concentration by 50% (Efficient Concentration = EC_{50} ((mole/L) lignin monomers/(mole/L) DPPH•) was determined with $1/EC_{50}$, or the antiradical power (ARP), calculated (see Figure 5.6 as an example and the rest of the results can be found in Appendix A.20). The stoichiometry values were also calculated as the number of DPPH• moles reduced by one mole of lignin/standard compound. Antiradical efficiency ($AE = 1/(EC_{50}T_{EC50})$) is an expression of results that takes into account both stoichiometry (in terms of EC_{50}) and time needed to reach steady state at the concentration corresponding to EC_{50} (T_{EC50}). The higher AE value indicates higher antioxidant activity. The AE method was shown to be a more discriminatory calculation of antioxidant scavenging capacity than EC_{50} since it takes into account kinetic properties of the antioxidant reactions (reaction time) (Brand-Williams *et al.*, 1995, Sanchez-Moreno *et al.*, 1998, Bortolomeazzi *et al.*, 2007). Sanchez-Moreno and co-workers (Sanchez-Moreno *et al.*, 1998) classified the kinetic behaviour of the antioxidant compound based on the T_{EC50} values as follows T_{EC50} < 5 min (rapid); 5- 30 min (intermediate) and >30 min (slow). This classification was adopted in this study with examples presented in Figure 5.5.

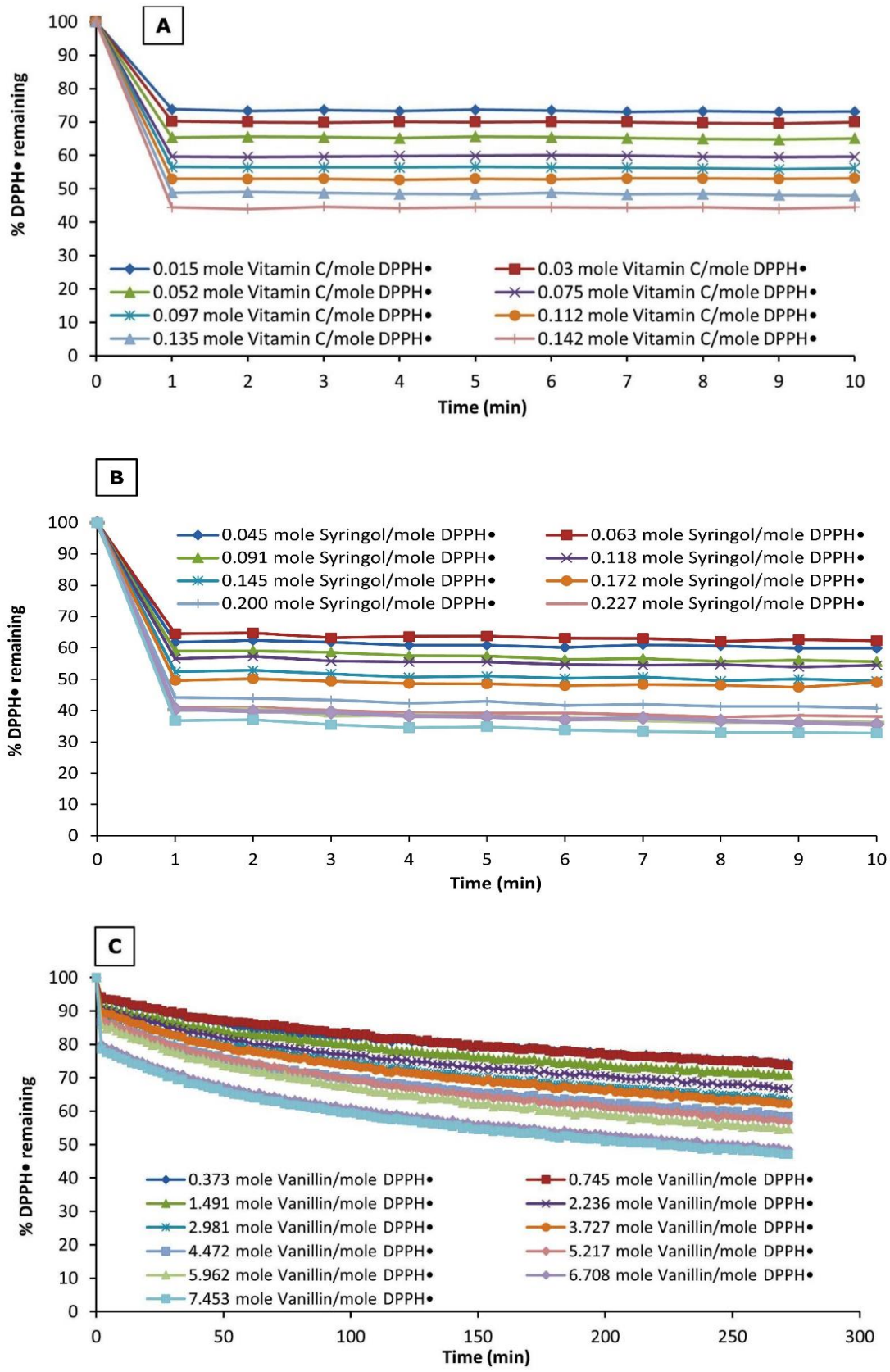


Figure 5.5: Examples of three reaction kinetics behaviour (A): Vitamin C (rapid) (B): Syringol (intermediate), and (C): vanillin (slow).

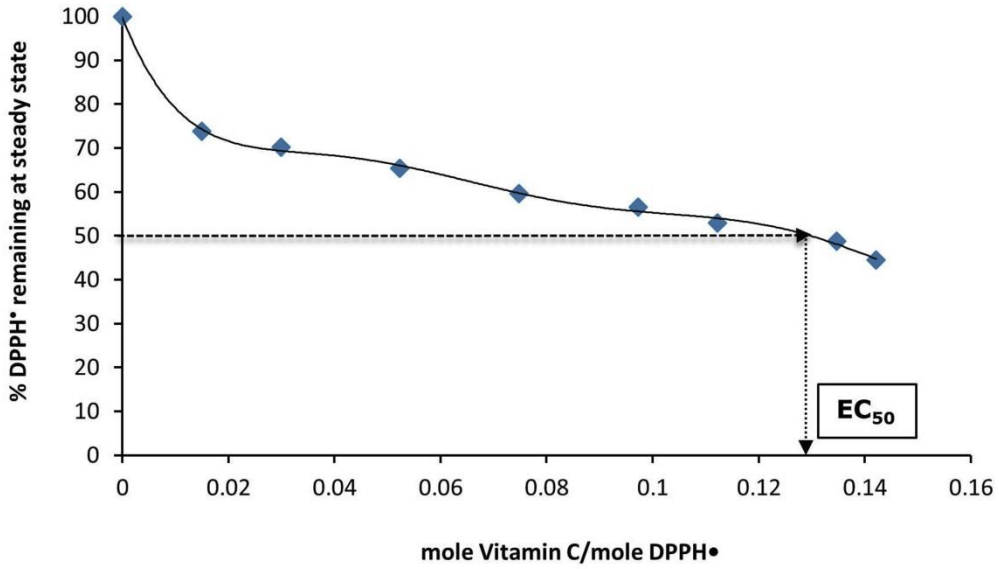


Figure 5.6: DPPH radical scavenging activities by vitamin C as a function of the number of moles of vitamin C / mole DPPH•.

The stoichiometry of each compound was obtained by multiplying the EC_{50} value by two which gives the theoretical efficient concentration of each compound needed to reduce 100% of the DPPH• (Table 5.1) (Brand-Williams *et al.*, 1995). However, the stoichiometric value alone does not explain all the aspects of antioxidant efficiency. For example, guaiacol appears to be the best antioxidant because 1.0 mol of guaiacol reduces about 14.0 mol of DPPH•, even though it reacts very slowly (reached the steady state after 5 h).

Antiradical efficiencies (AE), EC_{50} and T_{EC50} values of the substrates examined are shown in Table 5.1. All tested lignin-related monomers have the ability to quench DPPH radical in a concentration-dependent manner. vitamin C and Trolox reacted very quickly with the DPPH• reaching a steady state immediately (less than 1.0 minute, see Figure 5.5). Gallic acid and syringol reacted a little slower and reached a steady state within 17 min and 15 min, respectively. The remaining compounds reacted more slowly with the DPPH• reaching a steady state from 3 to 7 h. Based on the AE values, among the lignin-related compounds tested, syringol reacted faster than the other compounds and was the most effective DPPH radical scavenger. This was followed by guaiacol, homvanillyl alcohol, syringaldehyde and vanillic acid, while vanillin showed the lowest AE (Table 5.1 and Appendix A.20).

Table 5.1**:** Characterisation of antiradical efficiencies of lignin-related compounds using DPPH• assay in methanol.

Compound	**EC_{50}[a]**	**ARP[b]**	**T_{Range}[c] (min)**	**T_{EC50}[d] (min)**	**AE[e]**	**Classification**	**Stoichiometric Value**	**Number of reduced DPPH•**	**ARP (Reported)**
Vitamin C	0.118 ± 0.009	8.459 ± 0.639	0.5-1	1	8.455	Rapid	0.236	4.237	5.88 (Sanchez-Moreno *et al.*, 1998) 3.70 (Brand-Williams *et al.*, 1995)
Trolox	0.103 ± 0.002	9.680 ± 0.197	1-2	1	9.680	Rapid	0.206	4.854	3.846 (Bortolomeazzi *et al.*, 2007)
Gallic acid	0.048 ± 0.001	21.055 ± 0.313	6-17	17	1.239	Intermediate	0.096	10.417	12.5 (Brand-Williams *et al.*, 1995) 16.6 (Sanchez-Moreno *et al.*, 1998) 16.0 (Yoshida *et al.*, 1989)
Syringol	0.130 ± 0.007	7.704 ± 0.419	8.5-27	15	0.514	Intermediate	0.260	3.846	3.6[f] (Dizhbite *et al.*, 2004) 2.222 (Bortolomeazzi *et al.*, 2007)

Guaiacol	0.035 ± 0.001	28.771 ± 0.284	250-324	310	0.093	Slow	0.070	14.286	4.0 (Brand-Williams *et al.*, 1995) 2.6[f] (Dizhbite *et al.*, 2004)
Homovanillyl alcohol	0.099 ± 0.001	10.126 ± 0.130	105-169	166	0.061	Slow	0.198	5.051	
Syringaldehyde	0.580 ± 0.062	1.735 ± 0.184	366-444	420	0.004	Slow	1.160	0.862	0.855 (Bortolomeazzi *et al.*, 2007)
Vanillic acid	2.608 ± 0.101	0.384 ± 0.015	382-428	424	0.0009	Slow	5.216	0.192	0.17 (Brand-Williams *et al.*, 1995)
Vanillin	7.791 ± 0.593	0.128 ± 0.010	164-232	220	0.0006	Slow	15.582	0.064	0.05 (Brand-Williams *et al.*, 1995) 0.476 (Bortolomeazzi *et al.*, 2007)

[a] EC_{50}: Effective Concentration ((mole/L) compound/(mole/L)DPPH•)

[b] APR: Antiradical power (1/ EC_{50})

[c] T_{Range} : Range of time to reach steady state

[d] T_{EC50}**:** Time needed to reach the steady state at the concentration corresponding to EC_{50}

[e] AE: Antiradical efficiency =$(1/(EC_{50}T_{EC50}))$

[f] (10%) water/dioxane was used as a solvent instead of methanol

ARP values of all compounds investigated in this work were higher about 1.7-2.7-fold except for guaiacol (7.2-fold) than those reported by Brand-Williams *et al*. (Brand-Williams *et al.*, 1995). Higher values were obtained probably due to using smaller volume than as reported that might affect the accuracy of the relative volumes (1.0 mL as a final working volume was used in this study, while a 4.0 mL was used in Brand-Williams *et al*. study). The difference in guaiacol values may be due to the slow reaction of this compound. The guaiacol kinetics taking from 1 to 6 h to reach steady state in Brand-Williams *et al.* study while, the time required to reach steady state was 4 to 5 h in this study depending on the concentration (Brand-Williams *et al.*, 1995). However, it is difficult to compare our results on antioxidant activity with those of previous workers because their test methods have relied on quite different criteria from ours. In general, the results are highly dependent on initial DPPH concentration, the definition of steady-state time point, the concentration ratio between the antioxidants and DPPH• and the sample size (Sanchez-Moreno *et al.*, 1998, Molyneux, 2004).

The structure-antioxidant activity relationships of some phenolic compounds have been reported in the literature (Brand-Williams *et al.*, 1995, Sanchez-Moreno *et al.*, 1998, Wright *et al.*, 2001). The degree of phenolic antioxidant activity depends mainly on different structural features such as O-H bond dissociation energy (BDE). The lower the dissociation energy is, the more active the phenolic hydroxyl is said to be. Resonance delocalisation of the phenol radical and steric hindrance resulting from bulky groups substituting hydrogen in the aromatic ring all impact on the BDE (Sanchez-Moreno *et al.*, 1998).

The antiradical efficiency of monophenols was increased substantially by two methoxy substitutions in positions *ortho* to the OH. Despite syringol and guaiacol possess the same reactive structure, the AE of syringol was measured as higher than guaiacol by 5.5-fold. Also, it was observed that the AE of syringaldehyde was higher than vanillin. This result may be explained by the values of BDE were reduced in syringol and syringaldehyde (see Table 5.2) by the addition of methoxyl group (electron-donating) and hence enhance the antiradical activity (Dziedzic and Hudson, 1983, Dizhbite *et al.*, 2004).

Table 5.2: O-H bond dissociation energy (BDE) values for lignin-related compounds and standards tested in this study.

Compound	BDE (kcal mol^{-1})	Reference
Syringol	79.2	(Medina *et al.*, 2013)
Guaiacol	84.7	(Lucarini and Pedulli, 2010)
Syringaldehyde	79.9	(Medina *et al.*, 2013)
Vanillin	84.1	(Medina *et al.*, 2013)
Homovanilly alcohol	83.9	(Foti *et al.*, 2008)
Vanillic acid	84.6	(Medina *et al.*, 2013)
Gallic acid	3-OH 77.9 4-OH 78.0 5-OH 85.9	(Chen *et al.*, 2015)
Trolox	74.6	(Ardalan *et al.*, 2014)
Vitamin C	83	(Wang *et al.*, 2009)

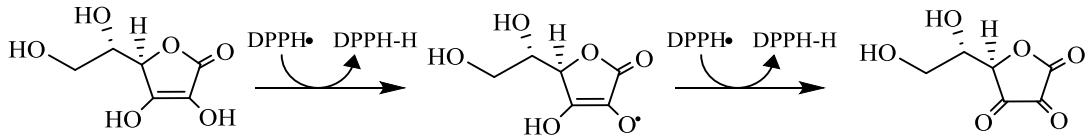
Surprisingly, the AE value of guaiacol was higher than the homovanillyl alcohol, vanillic acid and vanillin although the BDE value of guaiacol (84.7 kcal/mol) was higher than homovanillyl alcohol, vanillic acid and vanillin. The electron-withdrawing properties of the carboxylate group in (-COOH) in vanillic acid have a negative influence on the H-donating abilities. It was also noticed that the introduction of CHO moiety in vanillin lowered the value of AE by 155-fold compared to guaiacol despite the BDE value of vanillin (84.1 kcal/mol) being within close range to that of guaiacol (84.7 kcal/mol). The obtained AE value of homovanillyl alcohol was lower by 1.5-fold with respect to that of guaiacol by which is related to C-CH_2CH_2OH substitution. However, the BDE of homovanillyl alcohol was lower than that of guaiacol.

Vanillin and vanillic acid have the highly related structures with the AE of vanillic acid slightly higher than vanillin by 1.5-fold. The presence of the –CHO instead of a – COOH moiety has been shown to significantly hinder the activity of vanillin. In particular, phenolic acids are considered to be efficient hydrogen donors due to their characteristic carboxylic group (COOH) which is easily ionised (Palafox-Carlos *et al.*, 2012). It should be noted that a similar finding has also been reported for a syringaldehyde and syringic acid (Bountagkidou *et al.*, 2010). Brand-Williams *et al.* (Brand-Williams *et al.*, 1995) have attributed the low antiradical efficiency of syringaldehyde, vanillin and vanillic acid to the presence of an electron withdrawing group (CHO or COOH). However, for the slow kinetics reaction; syringaldehyde,

vanillic acid and vanillin, the low stoichiometric values (less than one) observed mean that it is difficult to interpret, and the mechanisms of the DPPH reaction with these compounds were not clear. Could also be interpreted by in terms of the accessibility of the radical centre of DPPH to each compound (Yoshida *et al.*, 1989).

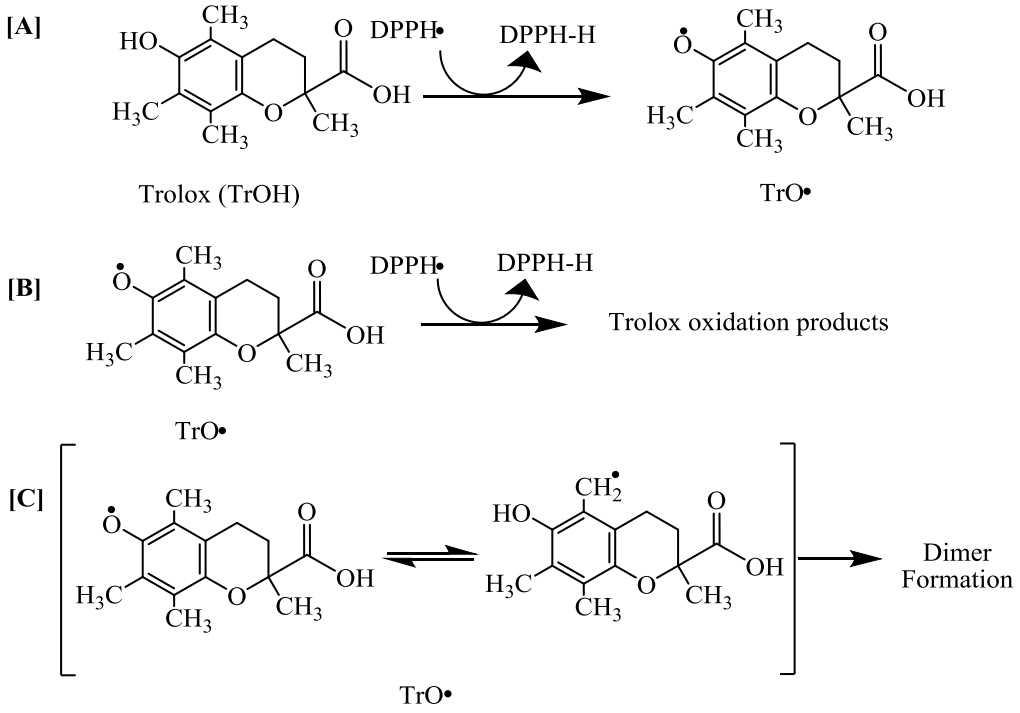
Vanillic acid reacted very slowly and poorly with DPPH•. The low DPPH• scavenging value obtained for this phenolic acid can be explained by vanillic acid possessing a high oxidation potential and is not expected, for thermodynamic reasons, to be effectively reduced by the weak DPPH• oxidant (Cirillo *et al.*, 2012).

A proposed chemical mechanism for the reaction between DPPH• and vitamin C was presented by Brand-Williams *et al*. (Brand-Williams *et al.*, 1995) and is illustrated in Scheme 5.3. From this reaction, one molecule of vitamin C reduces nearly two DPPH• molecules, which corresponds to the number of hydrogen atoms available for donation by the hydroxyl groups.



Scheme 5.3: Proposed mechanism for the DPPH• scavenging of vitamin C in methanol (Brand-Williams *et al.*, 1995).

The number of DPPH• molecules scavenged by Trolox, gallic acid, syringol, guaiacol and homovanillyl alcohol is larger than the number of phenolic hydroxyl groups in the compound. Trolox has a stoichiometry similar to vitamin C that can reduce two DPPH• molecules, although it possesses only one hydroxyl group available for H-atom donation. There are two possible pathways for Trolox / DPPH• reactions (Scheme 5.4). After the phenoxyl-type radical (TrO•) forms in the initial reaction step with DPPH• (A), the TrO• can react with remaining DPPH• *via* adduct formation (B) or self-dimerisation (C). The intermediate formed would then be able to reduce a second DPPH• molecule (Brand-Williams *et al.*, 1995, Friaa and Brault, 2006). In support of this, it was found that the presence of methyl group *para* to the functional hydroxyl group in the chromanol ring of Vitamin E was essential for the hydrogen donating ability (Rice-Evans *et al.*, 1996).

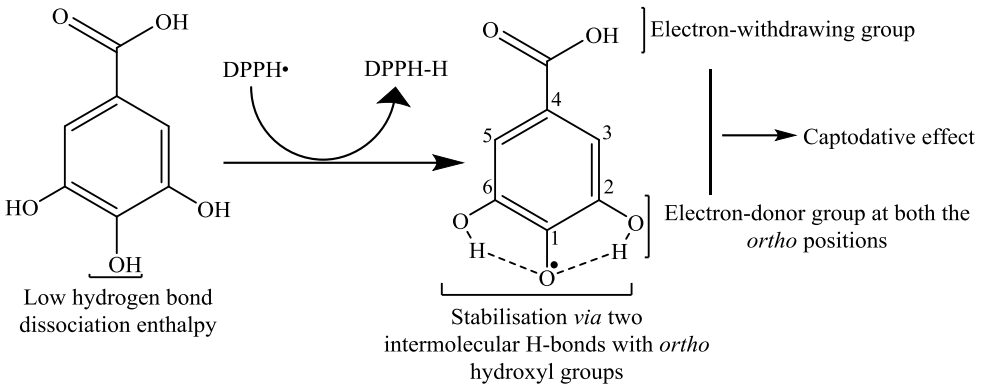


Scheme 5.4: Proposed mechanism of the reaction between DPPH• and Trolox (Friaa and Brault, 2006).

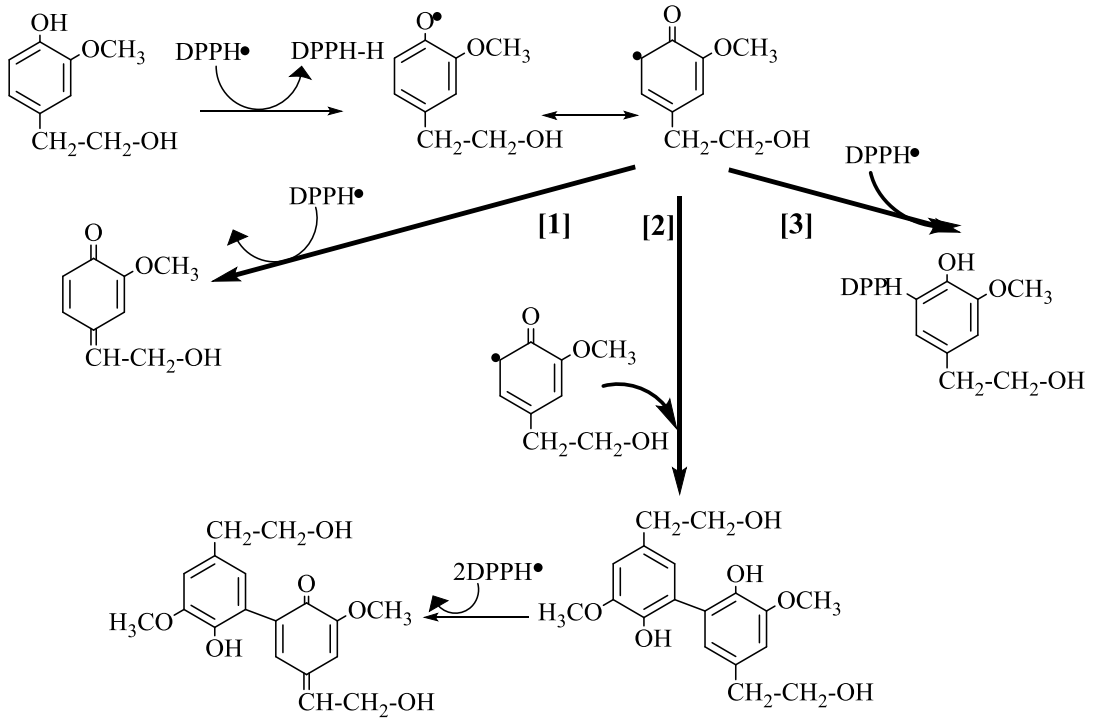
Gallic acid, with three hydroxyl groups (triphenolic), was observed to be a very active phenolic compound (Table 5.1). In general, the radical-scavenging activities of phenolic compounds depends on the number and position of hydroxyl moieties attached to the aromatic ring. It is known that polyphenols have a higher antiradical activity than monophenols (Brand-Williams *et al.*, 1995, Karamac *et al.*, 2005). In addition, the hydroxyl groups *ortho* to phenol tends to stabilise the radical formed in gallic acid, resulting in lower hydrogen bond dissociation enthalpy and hence enhanced the antioxidant capacity (Wright *et al.*, 2001). The type and the position of the substituents with respect to the hydroxyl group also enhanced the radical activity of polyphenols. For example, the presence of the easily ionisable carboxylic group (- COOH) in the *para* position with respect to the electron-donating OH group contributes toward the efficient hydrogen donation tendency of phenolic acids due to the push-pull or captodative effect (Scheme 5.5) (Leopoldini *et al.*, 2004, Badhani *et al.*, 2015).

Three hypotheses were suggested by Brand-Williams *et al.* (Brand-Williams *et al.*, 1995) in order to explain the reaction mechanism of monophenolic compounds in DPPH• solution, which can be applied to homovanillyl alcohol. The first hypothesis

suggests that a second hydrogen donation may occur after electron delocalisation onto the *para*-substituted (benzylic) group, as shown in reaction **[1]** of Scheme 5.6. The second hypothesis involves a dimerisation between two phenoxyl radicals with a free *ortho*-position (reaction **[2]**) with the new compound formed able to reduce a second DPPH• molecule. In the third hypothesis, one DPPH• molecule complexes with one aryl radical as indicated in reaction **[3]** of Scheme 5.6. The second and third hypotheses also can be applied to guiacol and syringol.



Scheme 5.5: Proposed mechanism for the DPPH• scavenging of gallic acid in methanol highlighting factors responsible for the high antiradical efficiency of the gallic acid molecule (Badhani *et al.*, 2015).



Scheme 5.6: Potential mechanism reaction DPPH• with homovanillyl alcohol [1]: donation of a second hydrogen, [2]: dimerisation, [3]: complexation.

5.3.3 Comparison between the UV-Vis Spectrophotometer and Microplate Reader for Determination the Antiradical Efficiencies Using DPPH Assay

As explained earlier, ARP values of lignin monomers and standards were higher by 1.7- 2.7 times, except guiacol by 7.2 times, than those reported by Brand-Williams *et al*. (Brand-Williams *et al.*, 1995). These higher values were thought to be due to using a smaller volume than that reported in the literature that may, in turn, affect the accuracy of the relative volumes (1.0 mL as a final working assay volume was used in this study, while a 4.0 mL was used in the Brand-Williams *et al*. study). In an attempt to confirm that a discrepancy in the methodology was leading to the difference, the effect of assay volume size and absorbance monitoring methods on the antiradical activity in DPPH• assay gallic acid and vitamin C were investigated.

Figure 5.7 compares the DPPH• calibration curves obtained using the microplate reader and UV-Vis spectrophotometer. It is apparent from this figure that no significant differences were found between the methods at the same total assay volume size (4.0 mL) and both obeyed the Beer-Lambert's law. However, there was a deviation from Beer- Lambert's law observed when the total assay volume was reduced to 1.0 mL using the microplate reader.

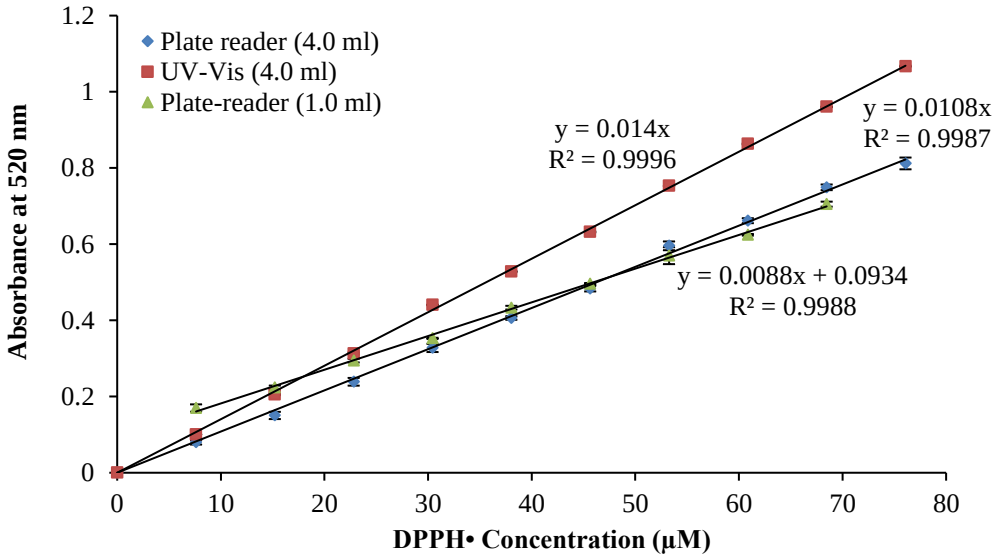


Figure 5.7: Calibration curve of DPPH• using microplate reader and UV-Vis spectrophotometer at different total assay volume size. Values are means ± standard deviations (n=3).

As shown in Table 5.3 and Figure 5.8, no differences were found in determining the EC_{50} values of gallic acid and vitamin C using the microplate reader and UV-Vis

spectrophotometer at the same assay volume size. However, the AE value of gallic acid at 4.0 mL using microplate reader was higher up to about 4-fold compared to UV- Vis spectrophotometer as the time needed to reach the steady state was higher (up to about 4-fold) in UV-Vis method. Additionally, it was observed that the EC_{50} values of gallic acid and vitamin C using the microplate reader were increased by about 2- fold in 1.0 mL assay working volume relative to 4.0 mL as a working volume under the same conditions. This highlights that the antiradical activity can be influenced by the assay volume size. Thus this must be considered when comparing with the literature values, as the results are dependent on the initial DPPH concentration, the concentration ratio between the antioxidants and DPPH•, sample size and total assay working volume.

Table 5.3**:** Comparison between the UV-Vis spectrophotometer and 96-well plate reader in the determination of antiradical efficiencies using DPPH assay.

Compound	**EC_{50}**	**ARP**	**T_{Range} (min)**	**T_{EC50} (min)**	**AE**
Gallic acid (UV-Vis)[(a)]	0.093 ± 0.001	10.811 ± 0.083	1.5-15	15	0.717
Gallic Acid (Plate reader)[(a)]	0.092 ± 0.0004	10.876 ± 0.046	4-9	4	2.717
Gallic acid (Plate reader)[(b)]	0.048 ± 0.001	21.055 ± 0.313	6-17	17	1.239
Vitamin C (UV-Vis)[(a)]	0.241 ± 0.026	4.176 ± 0.455	0.5	0.5	9.524
Vitamin C (Plate reader)[(a)]	0.247 ± 0.031	4.085 ± 0.516	0.5-1	0.5	8.097
Vitamin C (Plate reader)[(b)]	0.118 ± 0.009	8.459 ± 0.639	0.5-1	1	8.455

[(a)] 0.1 mL sample and 4.0 mL total assay volume.

[(b)] 25 µL sample and 975 µL total assay volume.

In general, 96-well microplate DPPH assays used less solution and were faster than the conventional assays (UV-Vis spectrophotometer). The 96-well assay also reduced the time needed to transfer the reactant solutions to the cuvettes in order to be manually read in the spectrophotometer and allowed for more replicates to be run at the same concentration than was possible with the conventional methods. As such, these assays have been shown to offer great potential for screening.

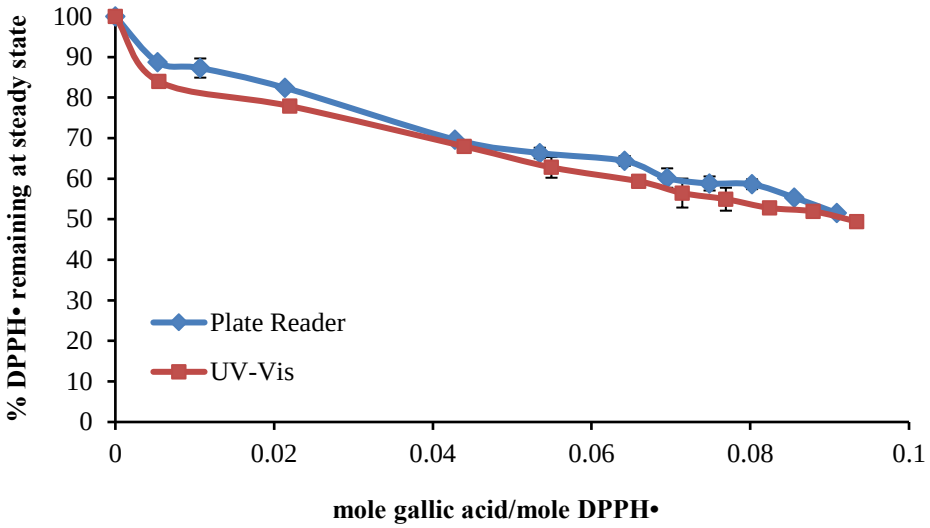


Figure 5.8: Scavenging activity of DPPH radical by gallic acid as a function of the number of moles of gallic acid /mole DPPH• using plate reader and UV-Vis spectrophotometer. Values are means ± standard deviations (n=3).

Further studies need to be carried out in order to validate the calibration process for microplate DPPH assay by normalising the microplate results to match the data obtainable with a 1-cm pathlength spectrophotometer, and this can be achieved by determining the molar absorptivity for pathlength correction. Furthermore, further research needs to examine more closely the links between preparation sample size, and total assay working volume using microplate DPPH assay.

5.3.4 Radical Scavenging Activity of Lignin Monomers in Ionic Liquids

As was pointed out in the previous sections, the DPPH assay has been successfully utilised for investigating the radical scavenging activity with all types of lignin monomers and standards in methanol. Thus, the DPPH assay was chosen to assess the radical scavenging activity of lignin monomers in ionic liquids. Both protic ([DMEA][HCOO]) and aprotic ([C_2mim][C_2SO_4]) ionic liquids were tested in this part of the study, as the solubility of organosolv lignin in these ILs were very high. Moreover, the electrochemistry of DPPH has been studied in [C_2mim][C_2SO_4] (Taylor *et al.*, 2012). [$P_{6,6,6,14}$][Tf_2N] was also tested since the DPPH was electrochemically more stable in [$P_{6,6,6,14}$][Tf_2N] compared to in [C_2mim][C_2SO_4] (Taylor *et al.*, 2012). However, the poor solubility of organosolv lignin and its monomers in [$P_{6,6,6,14}$][Tf_2N] limits its use in the DPPH assay. Figure 5.9 shows the time course of the DPPH• scavenging by lignin monomers and standards in [C_2mim][C_2SO_4] at 520 nm. All the

lignin-related monomers compounds and standards confirmed no detectable reaction with DPPH• at this wavelength, as shown in Figures 5.9-5.12, even after several hours of reaction time (8 h) and at very high concentrations (10 mM). The results up to 1 h of reaction shown here with the rest of the results up to 8 h in Appendix A.21. The percentage of DPPH scavenging activity was calculated using equation 5.3:

$$\%DPPH \bullet scavenging\ activity = \frac{Absorbance\ of\ the\ sample\ at\ any\ time}{Initial\ absorbance\ of\ DPPH\ solution} \quad (5.3)$$

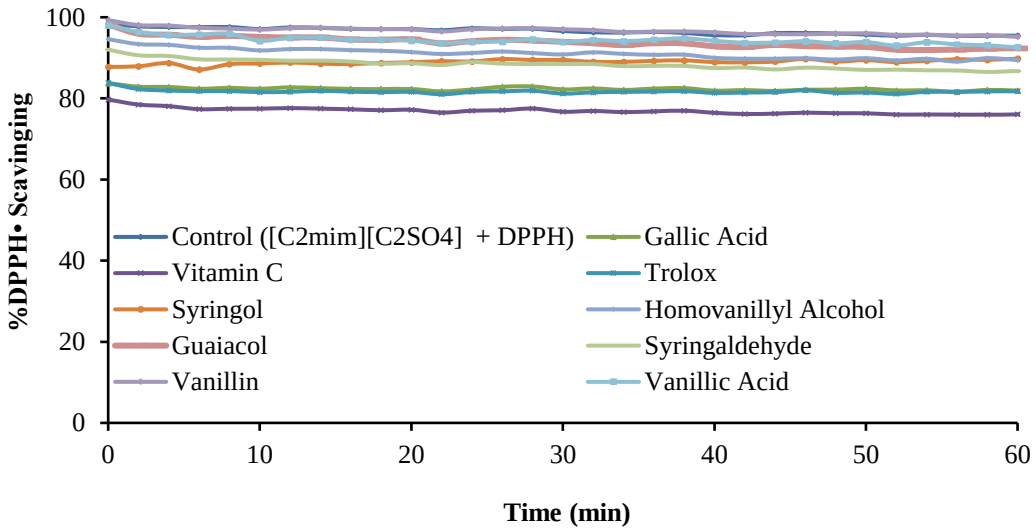


Figure 5.9: Time course (1 h) of scavenging of DPPH free radical by lignin monomers (1.5 mM) dissolved in $[C_2mim][C_2SO_4]$(error bars were not shown for figure clarity).

As shown in Figure 5.9, the apparent DPPH scavenging activity of lignin monomers and standards in $[C_2mim][C_2SO_4]$ at 1.5 mM decreased in the order of vitamin C >Trolox ≥ gallic acid > syringol > syringaldehyde > homovanillyl alcohol > vanillic acid ≥ guaiacol > vanillin. Similar orders have been found in methanol (Table 5.1) Surprisingly, a different order has been obtained in $[C_2mim][C_2SO_4]$ at high concentration of tested compounds (10 mM) (Figure 5.10), where the DPPH scavenging activity decreased in the order of homovanillyl alcohol ~ vitamin C ~ syringol ≥ gallic acid > Trolox >guaiacol > syringaldehyde >vanillin ≥ vanillic acid.

Only little DPPH scavenging activity was recorded for the standard compounds (vitamin C, gallic acid and Trolox) in $[C_2mim][C_2SO_4]$ at low concentration (1.5 mM). The difference between the control and vitamin C provides clues that some reaction may have occurred in this ionic liquid. It is important to note that vitamin C only had a

20% capacity for scavenging DPPH radicals at 1.5 mM concentration in [C_2mim][C_2SO_4]. However, only 0.315 mM of vitamin C was needed to quench 50% of initial DPPH•, when the dissolving solvent of DPPH radicals was methanol (Table 5.1). In addition, all the DPPH scavenging activities for tested compounds in [C_2mim][C_2SO_4] were independent on the reaction time. Vanillin did not react against DPPH• radical as can be seen from Figure 5.10.

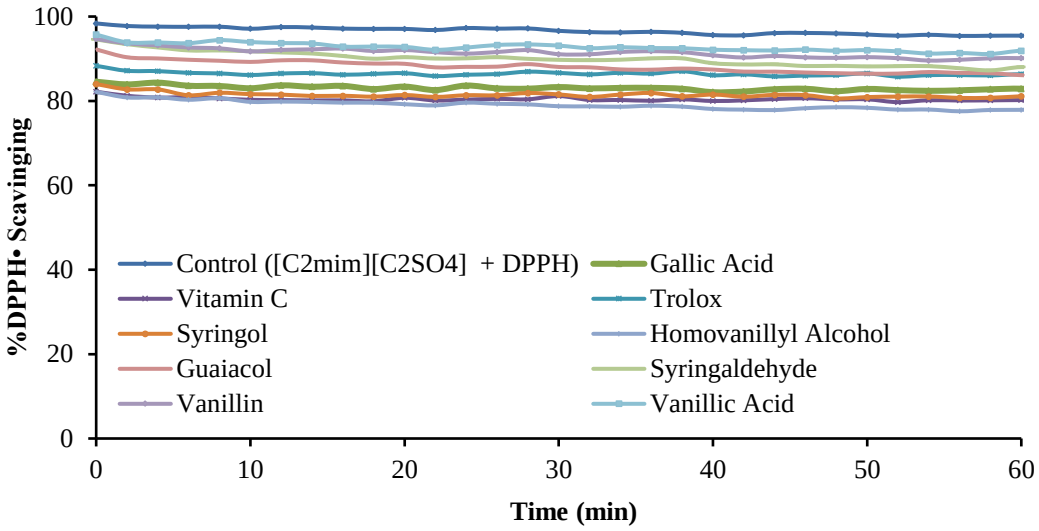


Figure 5.10: Time course (1h) of scavenging of DPPH free radical by lignin monomers (10 mM) dissolved in [C_2mim][C_2SO_4] (error bars were not shown for figure clarity).

No radical scavenging activities of lignin-related monomers compounds or standards were detected by DPPH• in [DMEA][HCOO] (Figure 5.11 and Figure 5.12) even after several hours of reaction time (8 h) and at very high concentrations (10 mM). Similar trends have been found at low concertation (1.5 mM). For all compounds investigated, the apparent DPPH scavenging activity of lignin monomers and standards in [C_2mim][C_2SO_4] was higher than in [DMEA][HCOO] under the same conditions.

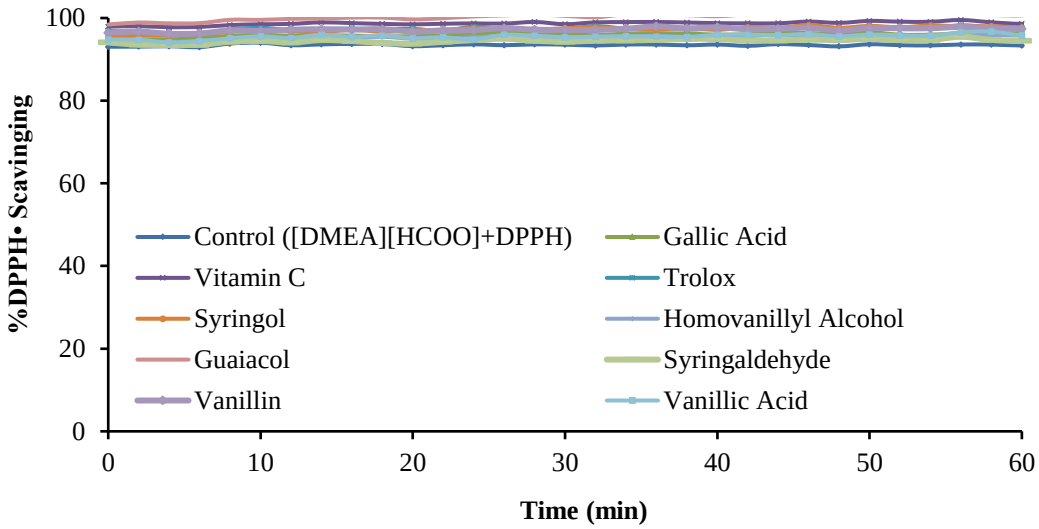


Figure 5.11: Time course (1 h) of scavenging of DPPH free radical by lignin monomers (1.5 mM) dissolved in [[DMEA][HCOO] (error bars were not shown for figure clarity).

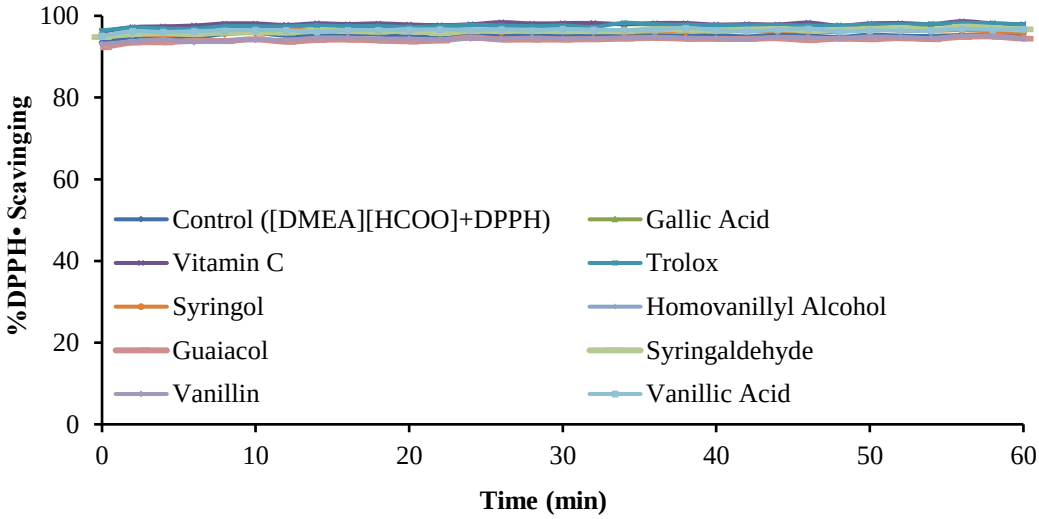
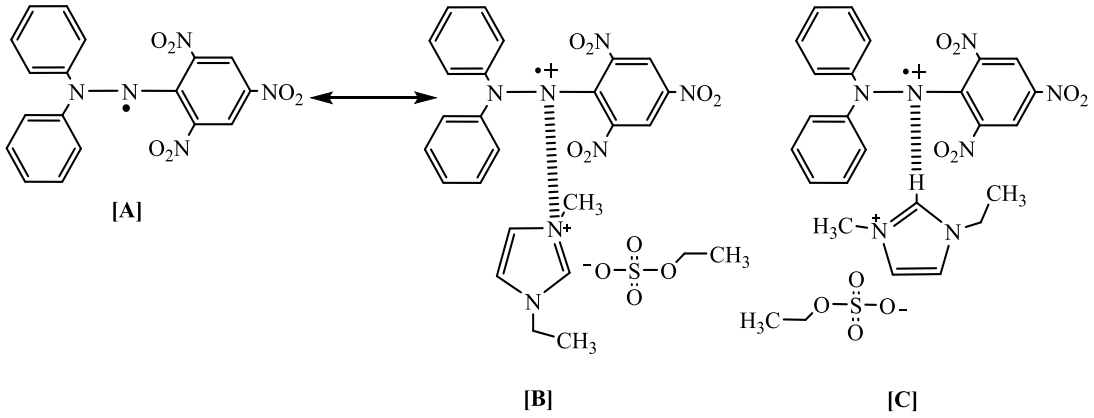


Figure 5.12: Time course (1h) of scavenging of DPPH free radical by lignin monomers (10 mM) dissolved in [DMEA][HCOO] (error bars were not shown for figure clarity).

There are several possible explanations for the apparent low antiradical activity of lignin monomers and standards obtained in ILs. The first explanation involves the interactions between individual ions of the ionic liquid and the radicals. There have been few previous studies that have examined behaviour of radicals in ionic liquids. Overall, these studies explored the interaction between the stable free radicals and ionic liquids. Mostly, the 2,2,6,6-tetramethylpiperidine-1-yloxyl (TEMPO) derivatives contain various substituents at the 4-position to the nitroxyl have been used for investigation of ionic liquids using electron paramagnetic resonance (ESR) spectroscopy. The results of these studies concluded that the stable radicals interact

with the ionic liquids not only *via* the radical structure. Additional interactions include hydrogen bonding or ionic interactions between the additional substituent bound at the stable radicals and the ionic liquids. Furthermore, it was found that the mobility of radicals in ionic liquid is strongly dependent on the nature and structure of substituents, the temperature, the structure and properties of the ionic liquid (viscosity and self-diffusion) and therefore on the interactions between the radicals and the individual ions of the ionic liquid (Strehmel *et al.*, 2008, Strehmel *et al.*, 2010, Strehmel, 2012).

Therefore, it would be expected that the DPPH radical interacts with ionic liquids not only through the radical centre. Such interactions include those between the radical structure and the ionic liquid through ionic interactions (Scheme 5.7, structure B) with the cation of the ionic liquid, and hydrogen bonding (Scheme 5.7, structure C) mainly with the acidic hydrogen atoms (C_2) of the imidazolium ring in [C_2mim][C_2SO_4]. Further research needs to examine more closely the interactions between DPPH radical and ionic liquids, as this result has not previously been described.

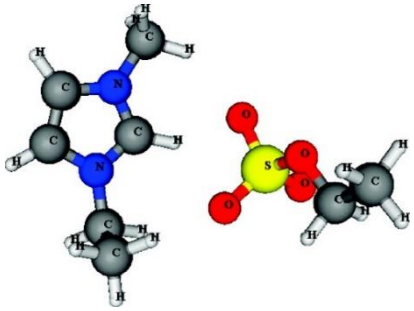


Scheme 5.7: Possible interactions between DPPH• radical and [C_2mim][C_2SO_4].

Recently, it was observed that the rate constant of all steps of the condensation reaction of benzaldehydes with hexylamine was increased in ionic liquid relative to acetonitrile under the same conditions leading to faster product formation rate. It was also concluded that the use of ionic liquids in simple condensation reaction accelerated the reaction due to an entropically favourable interaction between the cation of the ionic liquid and the nucleophilic nitrogen centre on the amine (Keaveney *et al.*, 2015a, b). It was also found that the interactions between the cation of the ionic liquid and pyridinic

nitrogen responsible for the rate acceleration of the reaction between the bromide and pyridine (Tanner *et al.*, 2013).

Accordingly, if the anion-cation interaction is high, it will be more difficult for the DPPH• to access the cation, causing a reduction in the enthalpic cost and entropic benefit. It is interesting to mention that the cation-anion interaction in 1-ethyl-3-methylimidazolium ethyl sulfate ($[C_2mim][C_2SO_4]$) (Scheme 5.8) is characterised by several interionic interactions *via* C-H---O hydrogen bonds, some of which exhibit bifurcated interactions (Dhumal *et al.*, 2011). On the other hand, [DMEA][HCOO] has a hydroxyl group attached to the cation so it would be expected that the extent of anion-cation interaction (*via* H-bonding) would increase. It has been demonstrated that the interaction between the –OH and the anion is preferentially stronger than the H- bonding between –OH and water (Tang *et al.*, 2012).



Scheme 5.8: Chemical structure of $[C_2mim][C_2SO_4]$ (Dhumal *et al.*, 2011).

It is necessary to consider any interaction between the IL and both reagents DPPH and lignin monomers/standards when exploring the reaction of DPPH scavenging reactions in ILs. Other interactions between the ionic liquid and phenolic compounds may also occur, including π-stacking interactions and hydrogen bonding between the phenolic O−H and the solvent hydrogen bond acceptor (HBA) moiety. It has been demonstrated that there is a strong interaction between ILs and phenolic compounds (Hou *et al.*, 2013). Moreover, the interaction between the intermediates and ILs may also occur. DPPH-PheO• species could be formed by complexation under the experimental conditions, as shown in the following equation:

$$DPPH• + PheO• \rightarrow DPPH\text{-}PheO$$

The above equations will compete with the PheO• coupling termination reaction (Sanchez-Moreno *et al.*, 1998):

$$PheO\bullet + PheO\bullet \rightarrow PheO\text{-}PheO$$

Another possible explanation for low activity of compounds in ILs is that the compounds accessibility to the radical centre of DPPH• could be restricted due to the high viscosity of the ILs. It was found that the diffusion and mobility of solutes in ILs is strongly depending on the structure and nature of the solute, its interaction with the IL, viscosity of the IL and by self-diffusion of the IL (Strehmel et al., 2008). Some lignin related compounds and standards shown little activities against DPPH radical in $[C_2mim][C_2SO_4]$ compared to [DMEA][HCOO], where no activity was detected. Nevertheless, the viscosity of [DMEA][HCOO] at 25 °C was lower than the viscosity of $[C_2mim][C_2SO_4]$ at the same temperature (Table 5.4). Thus, the behaviour of radicals in ILs can be influenced by the structures of the cation and the anion as well as the interactions between these ions.

Solvent cage effects of ILs and diffusion processes may also influence radical reactions in ILs. In general, the viscosity of the IL strongly affects the mobility of the radicals. Recently, Strehmel and co-workers examined the recombination of lophyl radicals in ILs and organic solvents. It was demonstrated that after lophyl radicals formed by photogeneration, they could either dimerise within the solvent cage or they escape out of the solvent cage diffusing through the matrix where they can recombine with another lophyl radical resulting in the back formation of the dimer. Therefore, two dimerisation reactions need to be taken into consideration. These are fast dimerisation within the solvent cage and dimerisation after diffusion through the matrix. The latter is influenced by the solvent viscosity. It also was found that the cage escape yields were reduced by half in the ILs relative to regular solvents. In contrast, the recombination of the lophyl radicals was significantly faster in the ionic liquids than in the traditional organic solvents tested (Strehmel *et al.*, 2009, Strehmel, 2012, Berdzinski *et al.*, 2013, Strehmel *et al.*, 2014a). It is possible to hypothesise that these conditions are less likely to occur in DPPH radical due to steric hindrance.

$$DPPH\bullet + DPPH\bullet \rightarrow DPPH\text{-}DPPH$$

There are, however, other possible explanations for the low activity of lignin monomers/standards in ionic liquids. The kinetic solvent effects (KSE) of ionic liquids on hydrogen atom abstraction from lignin monomers/standards to DPPH• may have a considerable effect. It was found that the rate constant for abstraction of hydroxylic

hydrogen atoms showed dramatic solvent effects. According to Valgimigli *et al.* (Valgimigli *et al.*, 1996, Valgimigli *et al.*, 1999) the reactivity of DPPH• in hydrogen atom abstractions was enhanced in tert-butyl alcohol by a factor of about 5 relatives to its reactivity in many other tested solvents including methanol and acetonitrile. Up to now, there is no study demonstrating the kinetic solvent effects (KSE) of ILs in radicals' reactions.

5.3.5 Radical Scavenging Activity of Trolox and Syringol in Methanol-Ionic Liquid Mixture

The radical activity of lignin monomers and standards in ILs obtained by DPPH was not high. A possible explanation for these results may be due to the effect of high viscosity of the IL. In general, the viscosity of the IL strongly affects the mobility of radicals. It has been reported and documented that the presence of co-solvents can strongly affect the physical and chemical properties of ILs such as viscosity, density as well as solvation and solubility properties (Rodriguez and Brennecke, 2006, Gong *et al.*, 2012). Therefore, in order to examine the effect of viscosity on the DPPH scavenging activity by lignin monomers compounds, a mixture of methanol in the IL at different mole concentration was used as a dissolving solvent for DPPH reaction.

Figure 5.13 outlines the influence of the methanol concentration on the viscosity of IL as well as the quenching of DPPH radical by Trolox and syringol at steady state as a function of the methanol mole fraction in the solvent mixture. The percentage of DPPH• remaining at the steady state was determined as follows:

$$\%DPPH \bullet remaining = \frac{Absorbance\ at\ steady\ state}{Initial\ absorbance\ of\ DPPH\ solution}$$

Table 5.4: Viscosity measurements and water content.

Solvent	Viscosity (mPa.s)			Water content (ppm)
	Cup-Bob	Plate-Cone	Theoretical value	
$[C_2mim][C_2SO_4]$	134.3 ± 0.8	96.6[a] ± 4.4	95.0 (Rodriguez and Brennecke, 2006)	767.2 ± 21.9
[DMEA][HCOO]	104.0 ± 0.1	61.4 ± 1.9	-	1129.5 ± 14.3
Methanol	0.573 ± 0.003	Not applicable	0.532 (Gong *et al.*, 2012)	-

[a]: viscosity at 22 °C

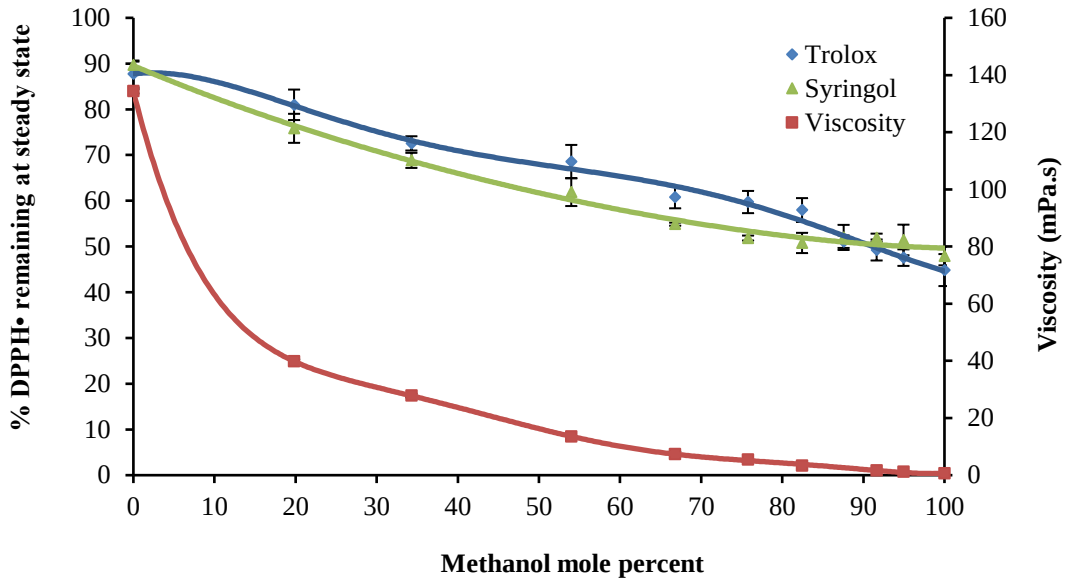


Figure 5.13: Scavenging activity of Trolox (300 μM) and syringol (320 μM) against DPPH radical performed in different mole percentages of methanol in $[C_2mim][C_2SO_4]$. Values are means ± standard deviations (n=3).

As shown in Figure 5.13, the viscosity was highest for the pure $[C_2mim][C_2SO_4]$ (134.3 ± 0.8 mPa.s). However, as the amount of the methanol in the reaction mixture was increased it was found that there was a gradual decrease in viscosity with the main changes in viscosity occurring between (0-50 mole %). The viscosity then reached a constant value at higher mole fractions, with a maximum decrease in viscosity relative to ionic liquid occurring between 60 mole % and 100 mole % of methanol. Moreover, as illustrated in Figure 5.13, the presence of small quantities of methanol strongly decreases the viscosity of the reaction mixture. For example, the addition of only a 10 mole % of methanol to $[C_2mim][C_2SO_4]$ leads to a reduction in the IL viscosity by two-fold.

Compared to literature, the viscosity value for pure $[C_2mim][C_2SO_4]$ was notably higher (by about 39.3 mPa.s) than that reported by (Rodriguez and Brennecke, 2006). This discrepancy could be attributed to the method used for viscosity measurements. As can be seen from the Table 5.4, great differences in the viscosity measured for investigated ILs ($[C_2mim][C_2SO_4]$ and [DMEA][HCOO]) have been observed using different types of measurements (plate-cone, cup-bob). For example, the viscosity [DMEA][HCOO] at 25 °C was found equal to 61.4 ± 1.9 mPa.s using plate-cone method compared to 104.0 ± 0.1 mPa.s) for cup-bob method, which corresponds to a

difference of 69%. The cup and bob method is particularly useful in measuring the low viscous fluid and no evaporation effects associated with this method, which is good for mixtures containing methanol, so this method was used in this study. It is also worth mentioning that the presence of water and impurities strongly decreases the viscosity of the ILs (Jacquemin *et al.*, 2006). It was found that the viscosity of pure methanol agrees with value was given by (Gong *et al.*, 2012). However, no previous data on the viscosity of $[C_2mim][C_2SO_4]$ mixtures with methanol has been found.

The drastic decrease of viscosity of the mixture by the addition of molecular solvents like methanol may be explained by the following facts. First, the diluting effect, lowering the viscosity of the molecular solvent relative to the pure IL leads to lowering of the bulk viscosity of the binary mixture significantly. Second, the dielectric behaviour of the solvent can reduce the electrostatic interaction among ions. Third, the ionic species are largely separated by the dissolved solvent molecules and thus decrease the Coulomb interaction and increase the fluidity of the liquid mixture (Gong *et al.*, 2012).

As predicted, the scavenging of DPPH radical by syringol and Trolox were found to increase with the proportion of the methanol in the reaction mixture (Figure 5.13). This may be caused by a considerable reduction of the viscosity of the reaction mixture resulting in faster diffusion of compounds and DPPH, and therefore, higher quenching of DPPH radicals by Trolox and syringol. No significant differences were observed between the scavenging activity of Trolox and syringol in the methanol-IL binary mixture. It was observed that the scavenging of DPPH radical by syringol and Trolox were enhanced by about 2-fold in methanol relative to the ionic liquid. When the methanol content was 70 mole % or higher in the reaction mixtures, the DPPH scavenging activity by syringol remained constant. However, there was a slight reduction in the DPPH scavenging activity by Trolox in the same range of methanol mole percent. Moreover, incorporation of 54 mole % methanol in the DPPH assay medium resulted in 31% greater DPPH scavenging activity than that determined in pure ILs for the same concentration of syringol. Overall, these results confirm the association between the viscosity and quenching of DPPH radicals.

The influence of the IL-methanol interactions on DPPH radical's reaction has to be taken into account, too. Zhang and co-workers reported that there is large interaction energy of [C_2mim][C_2SO_4] resulting from the electrostatic interaction of the cation and the anion. The interaction energy of [C_2SO_4]-H_2O is larger than that of [C_2mim]-H_2O, indicating that the interaction between H_2O and the ethyl sulfate anion is stronger than that between H_2O and the 1-ethyl-3-methylimidazolium cation. It is therefore likely that such interactions exist between cation/anion and methanol, and these interactions may compete with the other interactions occurring between the species in the reaction system such as IL-DPPH•, IL-intermediates and IL-compound previously discussed. They also demonstrated that the mode and intensity of hydrogen bonding interactions between water molecules and the cation/anion of [C_2mim][C_2SO_4] depend strongly on water mole fraction in [C_2mim][C_2SO_4]-water binary system. At low concentrations, water interacts selectively with -SO_3 in the ethyl sulfate anion, while at the mole fraction of water equal or greater than 0.6 it can also interact with the hydrogen atoms on the imidazolium ring, forming a stable new complex (Zhang *et al.*, 2010). These observations provide further support for the behaviour of quenching of DPPH radicals by Trolox and syringol at a high mole fraction of methanol in the reaction mixtures (Figure 5.13).

5.3.6 Influence of Solvent Type on the Quenching of the DPPH Radical by Lignin Monomers and Standards

Typically, the DPPH scavenging activity is determined in methanol. Toluene and acetonitrile, in addition to methanol, were used to assess the effect of solvents on radical behaviour using DPPH assay. Syringol was used as an example of a lignin monomer, and two standards (Trolox and gallic acid) were used in this part of the study. Gallic acid and Trolox are not soluble in toluene so acetonitrile and methanol could only be used in this case.

The quenching of DPPH• by syringol in toluene, acetonitrile and methanol are presented in Figure 5.14. As shown in Figure 5.14, EC_{50} values were altered by solvents used and the EC_{50} value of syringol in methanol was significantly less than in acetonitrile and toluene. However, there were no significant differences between EC_{50} values of syringol in acetonitrile and toluene.

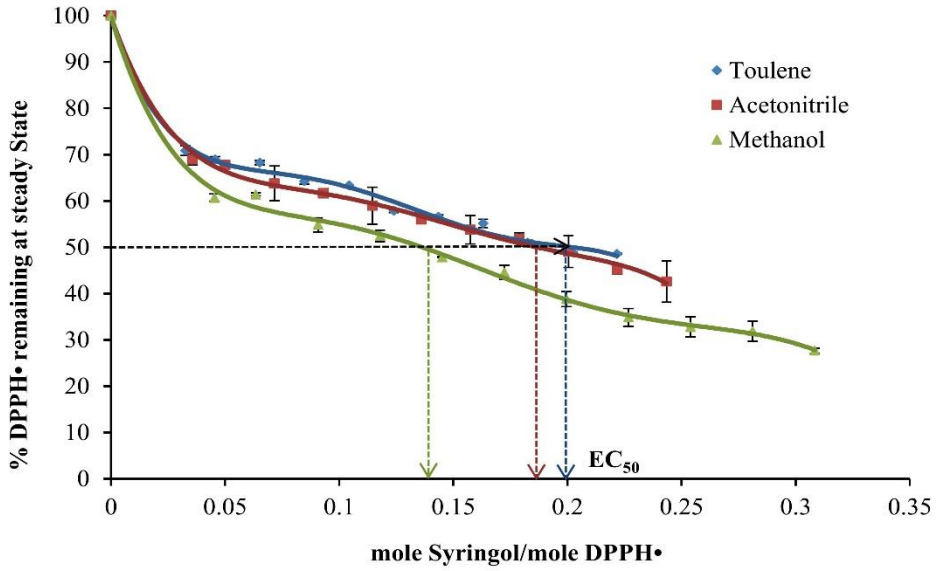


Figure 5.14: DPPH• remaining as a function of the number of moles of syringol /mole DPPH• in toluene, acetonitrile and methanol. Values are means ± standard deviations (n=3).

Table 5.5**:** The effect of different solvents on the antiradical efficiencies of lignin-related compounds and standards using DPPH assay.

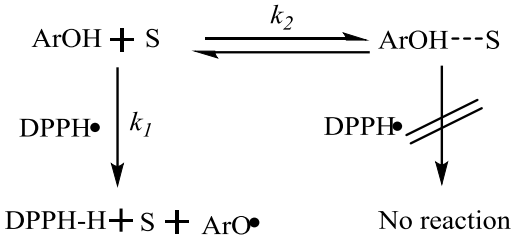
Compound	**EC_{50}**	**ARP**	**T_{Range} (min)**	**T_{EC50} (min)**	**AE**	**Solvent**
Syringol	0.130 ± 0.007	7.704 ± 0.419	8.5-27	15	0.514	Methanol
Syringol	0.192 ± 0.003	5.220 ± 0.083	85-91	88	0.059	Toluene
Syringol	0.193 ± 0.015	5.204 ± 0.408	72-82	82	0.063	Acetonitrile
Trolox	0.103 ± 0.002	9.680 ± 0.197	1-2	1	9.680	Methanol
Trolox	0.126 ± 0.004	7.930 ± 0.259	2	2	3.965	Acetonitrile
Gallic acid	0.046 ± 0.001	21.923 ± 0.585	20-36	27	0.812	Acetonitrile
Gallic acid	0.048 ± 0.001	21.055 ± 0.313	6-17	17	1.239	Methanol

Note: Gallic acid, Trolox and vitamin C are not soluble in toluene

Considerable differences in antioxidant behaviour were observed as a function of the DPPH• dissolving solvent. As can be seen from the data in Table 5.5, EC_{50} values were affected and altered by the solvents used (Figure 5.14). As the time taken to reach the

steady state is influenced by the solvents used, the values of AE were changed accordingly. Generally, the AE values obtained in methanol were the highest (Table 5.5). These results further support the idea that the reactivity of DPPH• was influenced significantly by the solvent types, and it was larger in methanol than in any other solvent (Sharma and Bhat, 2009, Gaikwad *et al.*, 2010). AE values estimated in the reaction of DPPH with syringol were 0.059 in toluene and 0.063 in acetonitrile, which were enhanced by about 9-fold and 8-fold, respectively, on going to the protic solvent methanol. Also, it was found that the time required to reach the steady state was increased by 2-fold in toluene and acetonitrile, indicating that the reaction rates of DPPH• with syringol, gallic acid and Trolox in aprotic solvent were reduced.

The syringol showed the highest radical scavenging activity in methanol followed by in acetonitrile and the lowest in toluene. These results seem to be consistent with other research that found that for some phenolic compounds the rate constants in methanol and ethanol were higher than those in other solvents tested, followed by non-alcoholic but polar solvents, such as acetonitrile, tetrahydrofuran, and dimethyl sulfoxide, which were also greater than the rate constants in other solvents (Litwinienko and Ingold, 2007). This result may be explained by the kinetic solvent effect (KSE) mechanism proposed earlier by Litwinienko and Ingold. The mechanism deals with the KSE for H-atom abstractions (HAT) from an HB donor (HBD) substrate, ArOH, to a radical, DPPH• as shown in Scheme 5.9. In this mechanism, each ArOH molecule can form hydrogen bond with only one molecule of hydrogen bond accepting (HBA) solvent, S. However, the hydrogen bonded substrate (ArOH) is essentially unreactive for steric reasons and only the free non-hydrogen bonded fraction reacts with the DPPH radical as shown in Scheme 5.9 (Litwinienko and Ingold, 2003, 2005, 2007).



Scheme 5.9: H-atom abstraction and kinetic solvent effect (KSE) (Litwinienko and Ingold, 2007).

In Scheme 5.9, the stronger the hydrogen bond, ArOH - -S, the smaller k_1 becomes. The strength of ArOH - -S hydrogen bonds obviously depends on the HBA ability of S and the HBD ability of PhOH. Therefore, the ability of phenols to act as radical traps declines as the reaction medium becomes a stronger hydrogen bond acceptor (HBA) (MacFaul *et al.*, 1996). According to Valgimigli *et al.* (Valgimigli *et al.*, 1996) the reactivity of DPPH• in hydrogen atom abstractions was enhanced in tert-butyl alcohol by a factor of about 5 relatives to its reactivity in many other solvents.

It was also reported that the H-atom donation mechanisms of antioxidant (lignin related-monomers compounds and standards in our study) with DPPH• could occur through three pathways (i) one step H-atom transfer (HAT) (equation (1)); (ii) stepwise electron transfer–proton-transfer (ET–PT) (equation (2));(iii) sequential proton-loss–electron-transfer (SPLET) (equation (3)), provided ROH can deprotonate (Zhang and Ji, 2006).

HAT (1) $DPPH^{\bullet} + ROH \longrightarrow DPPH\text{-}H + RO^{\bullet}$

ETPT (2) $DPPH^{\bullet} + ROH \longrightarrow DPPH^{-} + ROH^{\bullet+} \longrightarrow DPPH\text{-}H + RO^{\bullet}$

SPLET (3) $ROH \longrightarrow RO^{-} + H^{+}; RO^{-} + DPPH^{\bullet} \longrightarrow RO^{\bullet} + DPPH^{-}; DPPH^{-} + H^{+} \longrightarrow DPPH\text{-}H$

Although the same final products are formed in the three pathways, they behave quite noticeably different in different solvents. Generally, the non-polar solvents facilitate the first pathway as no charge separation is needed, whereas the second and the third are preferred in polar media, due to the charge separation processes. As such, these mechanisms may be expected to be favoured in ILs. In addition to the solvent effect, the radical-scavenging mechanisms also depend on the characteristics of the radical. For radicals with high electron affinity, ETPT and SPLET are favoured, while for radicals with high H-atom affinity, HAT is preferred. Therefore, the same antioxidant may exhibit different behaviours in scavenging different radicals and/or under different environmental conditions. (Zhang and Ji, 2006, Litwinienko and Ingold, 2007, Salamone and Bietti, 2015). Accordingly, the HAT pathway is preferred in toluene, while ETPT and SPLET are the main pathways in acetonitrile and methanol.

The results of the present study show that not only the intrinsic reactivity with radicals, such as DPPH•, is important, but that also other factors, like the solvent, play an

important role in the antioxidant capacity of lignin-related compounds and standards, and that this can be potentially assessed using high-throughput analysis.

5.3.7 Absorption Spectra of DPPH• in Different Solvents

For a better understanding of the radical behaviours of lignin compounds in ionic liquids and to find out why the radical activity of lignin monomers using DPPH assay were high in organic solvents compare to that in ILs, the decay of the DPPH• in different solvents (methanol, [DMEA][HCOO] and [C_2mim][C_2SO_4]) was monitored at different wavelengths between 300 nm and 1000 nm, including the DPPH• band maximum at 520 nm.

Absorption spectra of DPPH• in methanol at the initial time, after 5 h stored at -20 °C, and after 5 h kept under the light and at room temperature are presented in Figure 5.15. The absorbance of DPPH• in methanol at 520 nm did not change significantly under light for 5 h, indicating stability under these conditions. Similar spectra were found for DPPH• in acetonitrile and toluene (Appendix A.22). However, the findings of the current study do not support the previous research. Ozcelik *et al*. found that the absorbance of DPPH at 520 nm in methanol decreased significantly under light exposure after 120 min (Ozcelik *et al.*, 2003).

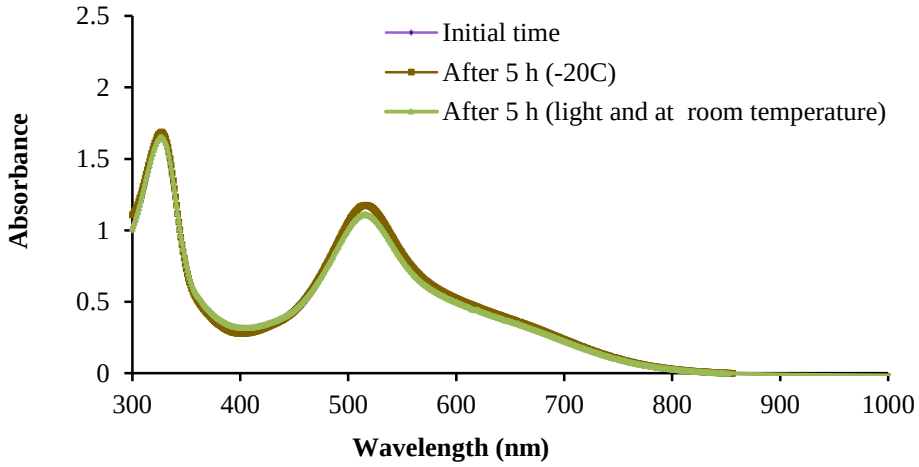


Figure 5.15: UV spectra of DPPH radical (60.86 μM) in methanol at different times and storage conditions.

The spectra of DPPH• in [C_2mim][C_2SO_4] at different times are shown in Figure 5.16. Commercial [C_2mim][C_2SO_4] has a light yellow colour and shows an absorption maximum in the range 210–260 nm. The absorption due to the presence of DPPH• was

intensely purple and shifted to 330 nm for the first peak and to 520 nm for the second peak immediately after the mixing. Then, after 1.0 h the small new peak at 440 nm appeared and after 3 h the 520 nm-peak shifted to 440 nm. This shift may be due to either intermediate formation or adducts formed between DPPH and the ionic liquid, and indicates increased reactivity of DPPH• in this solvent.

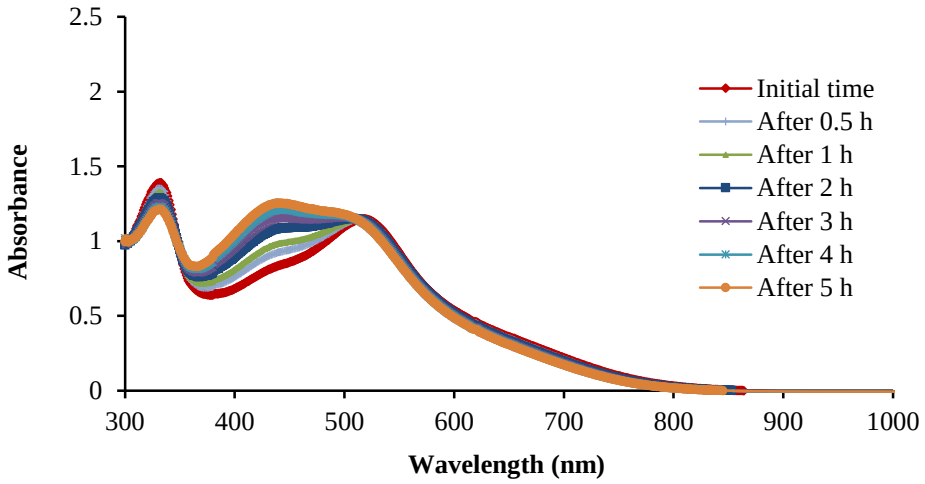


Figure 5.16**:** Time dependence of DPPH• (60.86 μM) absorption spectra in $[C_2mim][C_2SO_4]$ at 25 °C.

As shown in Figure 5.17, the 520 nm peak of DPPH• shifted to shorter wavelengths (440 nm) after 5 h under light exposure at room temperature and this shift happened even if the sample was stored at a low temperature of 4 °C. The spectra of DPPH• in [DMEA][HCOO] are illustrated in Figure 5.18 over different times. The intensely purple DPPH• has maxima at 440 nm in this solvent, either indicating an extremely fast reaction to form adducts or a different chemical environment. There was no change in spectra with time under light exposure at room temperature. However, the absolute value of the absorbance of DPPH• in [DMEA][HCOO] was slightly altered after 5 h and 24 h.

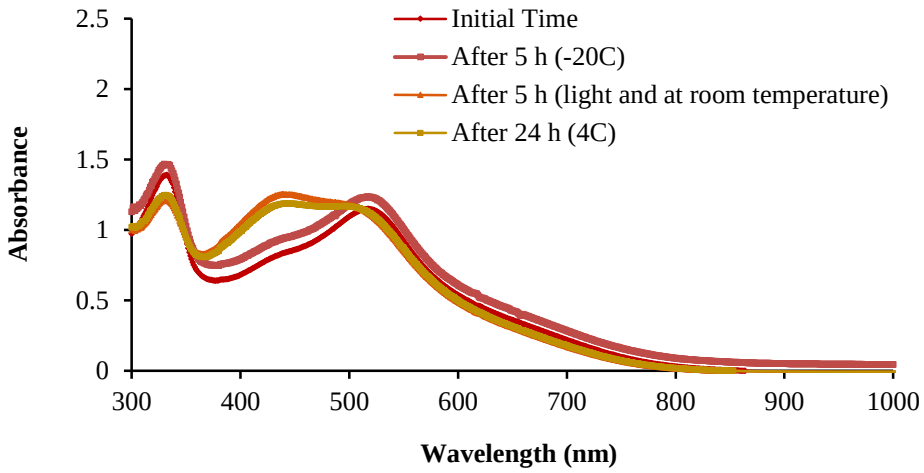


Figure 5.17: UV spectra of DPPH (60.86 μM) in $[C_2mim][C_2SO_4]$ at a different time and different storage conditions.

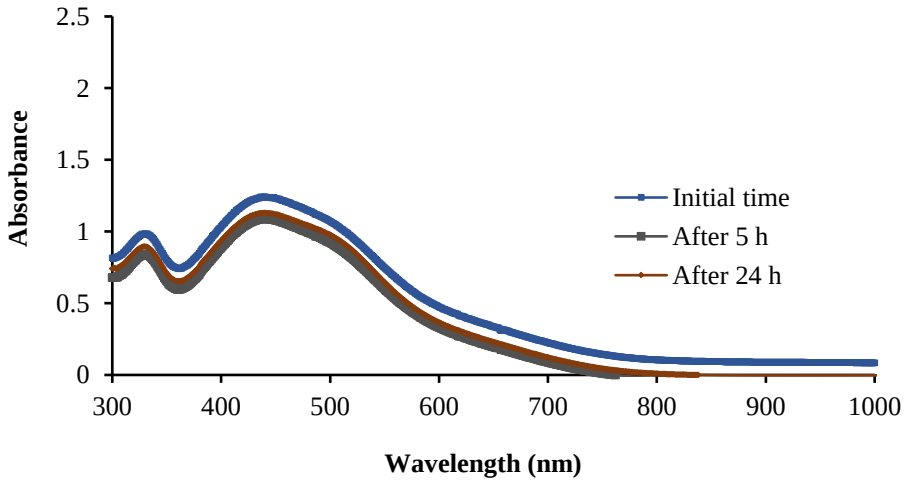


Figure 5.18: Time dependence of DPPH• (60.86 μM) absorption spectra in [DMEA][HCOO] at 25 °C.

Considerable differences in DPPH• spectra were observed as a function of the dissolving media. The absorbance of the DPPH• measured at 330 nm was different for the solvents investigated at the same concentration of DPPH• (Figure 5.19). The lowest absorbance was observed for DPPH• in [DMEA][HCOO] and the highest was in methanol, although the absorbance at 520 nm was similar in $[C_2mim][C_2SO_4]$ and methanol. This implies differences in DPPH• behaviour in combination in these solvents. Furthermore, the maximum absorbance of DPPH• in [DMEA][HCOO] was at 440 nm instead of 520 nm as shown in methanol and $[C_2mim][C_2SO_4]$. A possible explanation for this might be that adduct was formed with DPPH•. However, after 5 hours the maximum peak of DPPH• was measured at 440 nm in both ionic liquids

([DMEA][HCOO] and [C_2mim][C_2SO_4]) (Figure 5.20). Similar spectra were recorded at the initial time and after 5 h for methanol (520 nm) and [DMEA][HCOO] (440 nm). However, the peak of DPPH in [C_2mim][C_2SO_4] was shifted from 520 nm to 440 nm after 3 hours. A possible explanation for this might be that adduct the rate of adduct-DPPH• formation in [DMEA][HCOO] was faster than in [C_2mim][C_2SO_4]. Furthermore, the interactions between DPPH and the ionic liquid may be governed by ionic or hydrogen bonding. These examples have shown that the behaviour of DPPH• is a complex process that is influenced by the solvent types and by solvent viscosity.

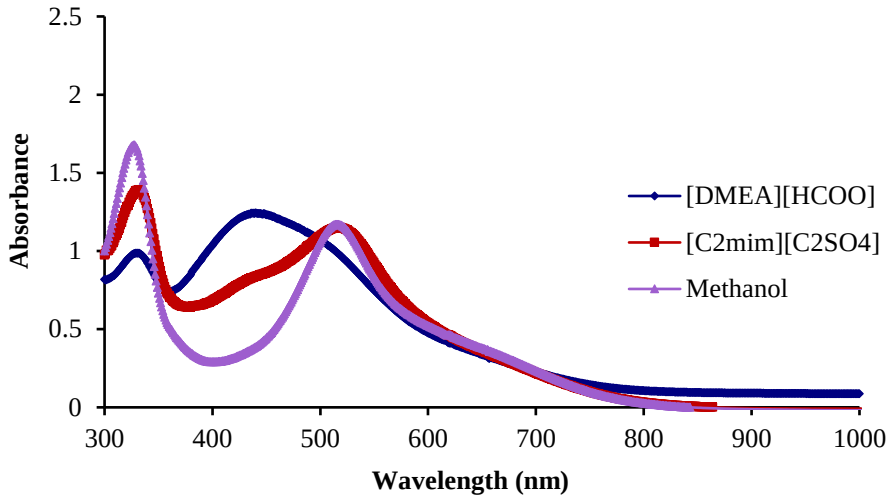


Figure 5.19: Absorption spectra of DPPH (60.86 µM) in selected solvents ([DMEA][HCOO], [C_2mim][C_2SO_4] and methanol) at the initial time.

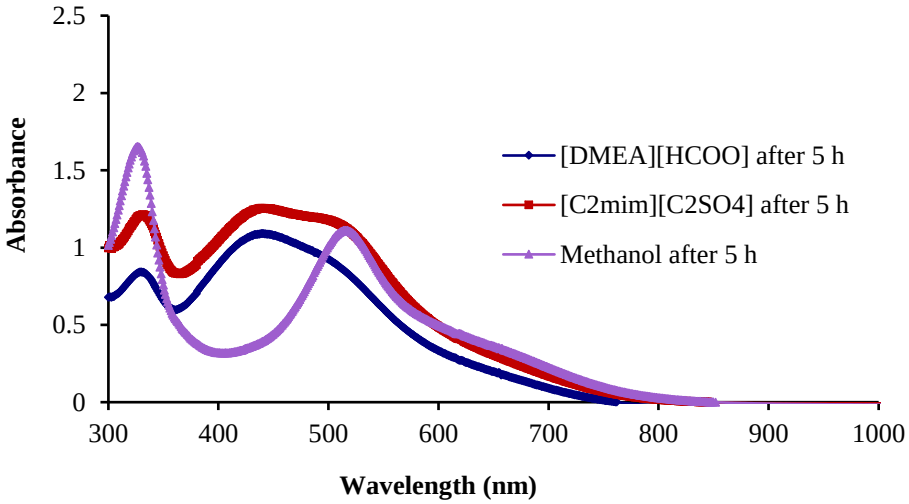


Figure 5.20: Absorption spectra of DPPH (60.86 µM) in selected solvents ([DMEA][HCOO], [C_2mim][C_2SO_4] and methanol) after 5 h under light exposure at room temperature.

This study has shown that the colourimeric interaction with DPPH is different in ILs compared to that in organic solvents. Thus the radical behaviour may also be different. In order to understand more about the interaction between lignin monomers in DPPH solution in different solvents especially ionic liquids, the scavenging of DPPH free radical by Trolox in [C_2mim][C_2SO_4] and [DMEA][HCOO] as well as in methanol was monitored at different wavelengths including the DPPH• band maximum at 520 nm for 24 h.

As shown in Figure 5.21, there were no significant differences found between the absorbance associated with the addition of 10 mM of Trolox to DPPH solution in [C_2mim][C_2SO_4] at the initial time and after 24 h of reaction. However, the position of the DPPH peak was shifted from 522 nm at the initial time to 498 nm after 24 h. In contrast to [C_2mim][C_2SO_4] there was no shift observed in the DPPH peak dissolved in [DMEA][HCOO] even after 24 h. Moreover, the DPPH peak position and height was not altered by the addition of Trolox to DPPH solution over 24 h of reaction as shown in Figure 5.22.

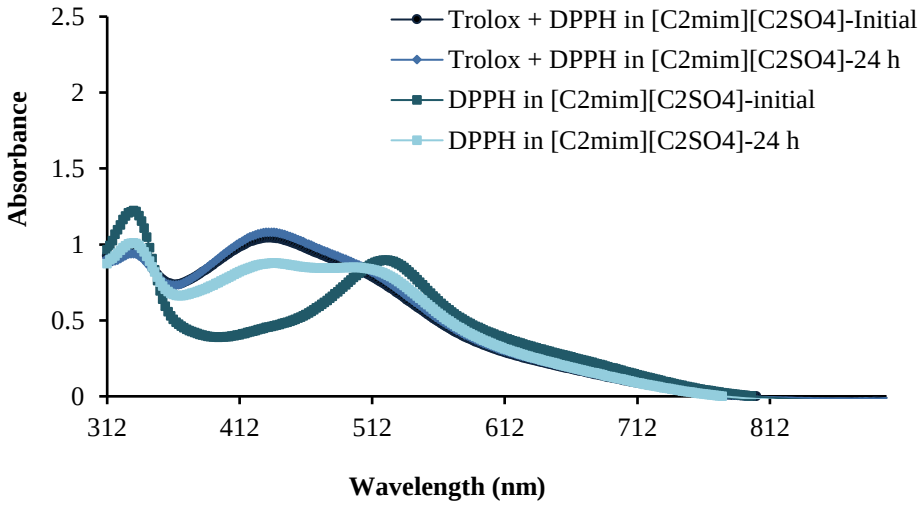


Figure 5.21: Absorption spectra of DPPH (60.86 μM) in [C_2mim][C_2SO_4] with and without Trolox (10 mM) at the initial time and after 24 h of reaction recorded at 25 °C.

It is interesting to note that the absorbance of DPPH• in [DMEA][HCOO] with Trolox and without the addition of Trolox were identical until 320 nm whereas a new peak at 296 nm associated with the presence of Trolox appeared (Figure 5.22).

As expected, the intensity of the DPPH peak in methanol was significantly reduced immediately after addition of Trolox indicating high radical scavenging activity of DPPH free radical by Trolox as mention previously (Figure 5.23).

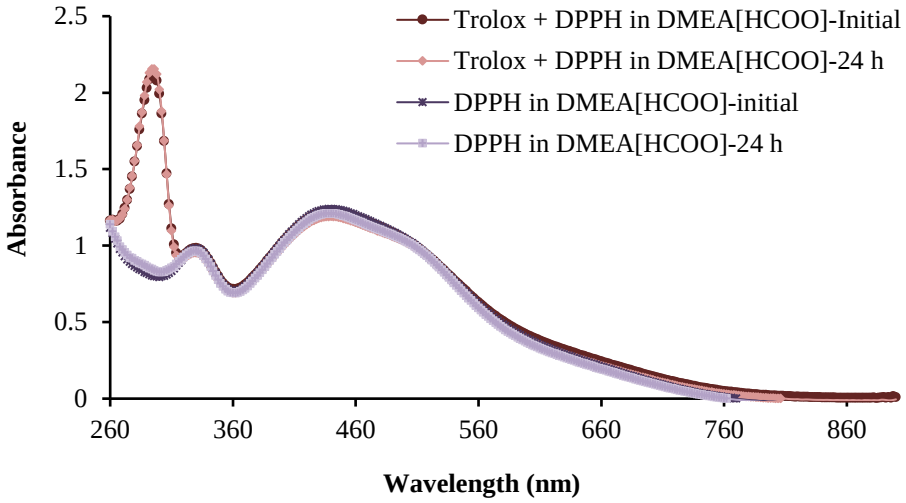


Figure 5.22: Absorption spectra of DPPH (60.86 μM) in [DMEA][HCOO] with and without Trolox (10 mM) at the initial time and after 24 h of reaction recorded at 25 °C.

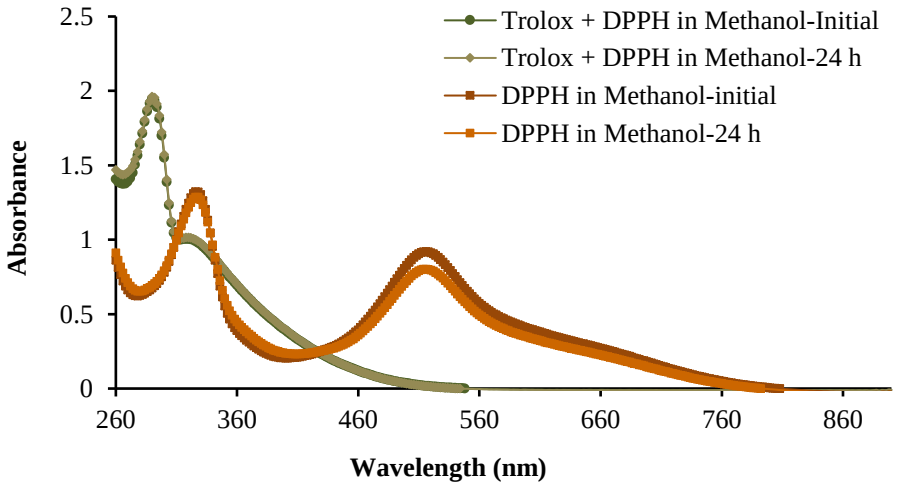


Figure 5.23: Absorption spectra of DPPH (60.86 μM) in methanol with and without Trolox (10 mM) at the initial time and after 24 h of reaction recorded at 25 °C.

In summary, the DPPH peak height at 520 nm in the presence of Trolox was significantly reduced in methanol (Figure 5.24) while there was no significant change in DPPH peak intensity at 520 nm was found after addition of Trolox in both types of ILs as illustrated in Figure 5.21 and Figure 5.22. However, the DPPH peak at 520 nm was shifted in [C_2mim][C_2SO_4] to 446 nm after addition of Trolox. No change was

observed in DPPH intensity and position in [DMEA][HCOO] with the presence of Trolox compares with DPPH solution without Trolox. A possible explanation for this might be that complex formation between Trolox and DPPH occurred in ILs, as the quenching of DPPH by Trolox is regulated by electron transfer. For other systems, the photoinduced electron transfer rate in [DMEA][HCOO] was decreased by an order of magnitude compared to that in acetonitrile, and it also found that a complex between the Coumarin dyes and dimethyl aniline molecules was formed in [DMEA][HCOO] (Sarkar *et al.*, 2009).

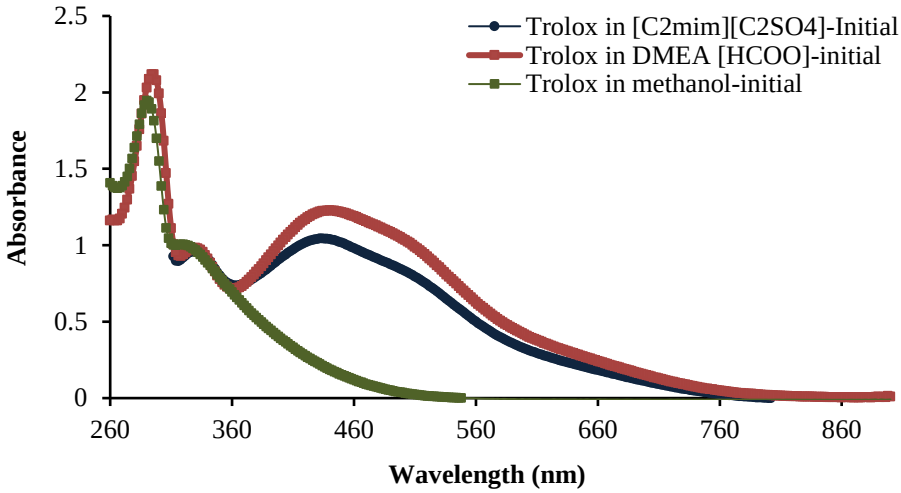


Figure 5. 24: Absorption spectra of Trolox (10 mM) in DPPH solution dissolved in selected solvents ([DMEA][HCOO], $[C_2mim][C_2SO_4]$ and methanol) at the initial time recorded at 25 °C.

5.3.8 ABTS Radical Scavenging Activity of Lignin-Related Compounds and Standards

To further investigate the free radical behaviour of lignin-related monomer compounds, the ABTS radical cation assay was employed. $ABTS^{\bullet+}$ is a relatively stable radical and its characteristic colour blue-green at 734 nm disappears when it is quenched. As such, the decrease of this radical can be easily monitored spectroscopically during the reaction (Tai *et al.*, 2011). Syringol was used in this study as an example of a lignin monomer, with vitamin C and Trolox as standards to compare the antioxidant potential toward the ABTS radical cation. The results expressed as vitamin C equivalent antioxidant capacity (VCEAC) values, are presented in Figure 5.26.

AAPH was selected as an initiator for generation of ABTS radical cation. This compound is water-soluble and oxidises ABTS to the ABTS radical cation. It is a thermolabile azo compound and the rate of free radical production as a result of AAPH thermal decomposition increases with increasing temperature (Kim *et al.*, 2002). The generation of the ABTS radical cation before the addition of test compounds has been recommended to prevent the interference of compounds with radical production (van den Berg *et al.*, 1999).

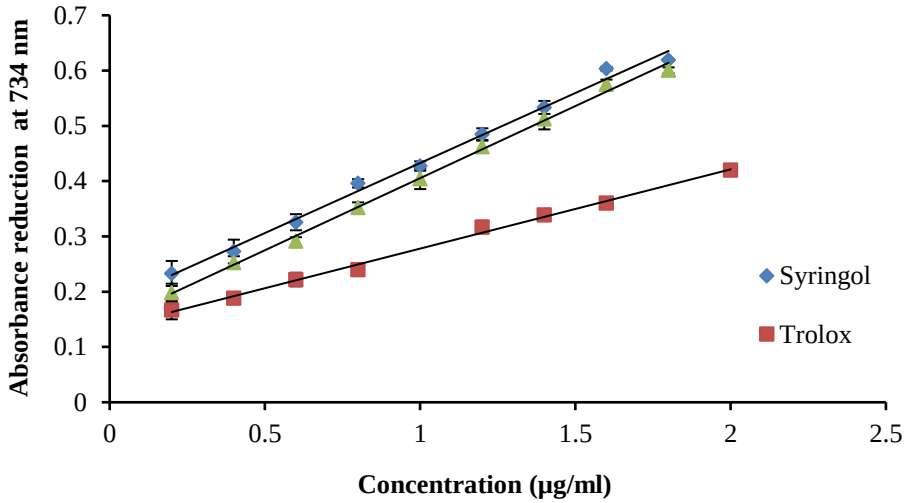


Figure 5.25: The effect of syringol, vitamin C and Trolox concentration on the absorbance reduction of the $ABTS^{\bullet+}$ in phosphate buffer solution (pH 7.4) at 10 min and 37 °C. Values are means ± standard deviations (n=3), the absence of standard deviations (SD) bar means that the SD bar is within the symbol.

The standard curve showed a linear relationship between vitamin C concentration and $ABTS^{\bullet+}$ absorbance reduction at 734 nm in aqueous solution (Figure 5.25). A first order regression model in relation to absorbance reduction versus different concentrations of syringol and Trolox was obtained. The standard curve that relates the concentration of vitamin C and the amount of $ABTS^{\bullet+}$ absorbance reduction caused by vitamin C was used to calculate VCEACs based on the absorbance reduction of syringol and Trolox. The antioxidant capacity of syringol and Trolox also showed a first-order relationship with VCEAC (Figure 5.26). The VCEAC values were obtained from the capacity of syringol and Trolox to inhibit the $ABTS^{\bullet+}$ relative to vitamin C. The antioxidant capacity of Trolox was lower than that of vitamin C (Figure 5.26). These results are in good agreement with those obtained by Kim *et al*. (Kim *et al.*, 2002).

Syringol showed stronger antioxidant activity than vitamin C and Trolox in the $ABTS^{\bullet+}$ scavenging assay on weight basis, whereas, in the DPPH radical assay, syringol had lower ARP than Trolox and vitamin C. The different trend of antioxidant activity in DPPH and ABTS observed in the present work was also reported by Badanai *et al.* (Badanai *et al.*, 2015). A possible explanation for this might be that the phenolic compounds on the free radicals react differently in either aqueous phase ($ABTS^{\bullet+}$ solution) or organic phase (DPPH• solution) (Kim *et al.*, 2002). Alternatively, specific reactions between the different assay reagents and the compounds and unrelated reactions of phenols (dimerisation, polymerisation) may occur during the assays (Kristinova *et al.*, 2009). According to Arts *et al.* (Arts *et al.*, 2004), the product resulting from the oxidation of flavonoids with $ABTS^{\bullet+}$ also itself reacts with $ABTS^{\bullet+}$. The product had a higher antioxidant capacity and reacted faster with $ABTS^{\bullet+}$ than the parent compound. On the other hand, the reaction product of Trolox formed during scavenging of $ABTS^{\bullet+}$, i.e. Trolox quinone, does not react with $ABTS^{\bullet+}$ (Arts *et al.*, 2004). As such, there is no correlation of activities between the DPPH and ABTS assays and caution must be taken when interpreting antioxidant capacities from different assays.

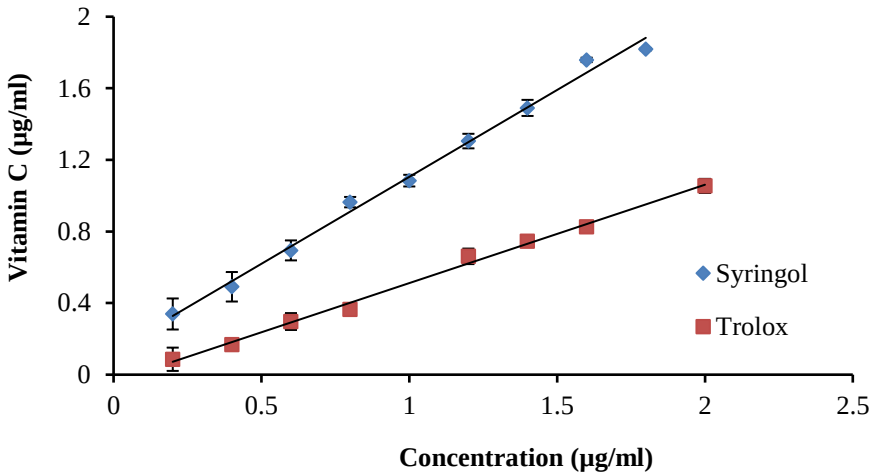


Figure 5.26: Syringol and Trolox antioxidant potential as a vitamin C equivalent capacity (VCEAC) by ABTS assay. Values are means ± standard deviations (n=3).

The high activity found for syringol does not seem to follow the classical structure-antioxidant activity relationship principles, where an increase in the number of hydroxyl groups attached to the aromatic ring is favourable for the antioxidant activity. However, despite the extensive use of the ABTS assay, very little is known about the reaction mechanism of the antioxidants with the ABTS radical cation.

5.3.8.1 *ABTS Radical Scavenging Activity of Lignin Related Compounds and Standards in Organic Solvents and Ionic Liquids*

To find the behaviour and formation of ABTS radical cation in organic solvents and ionic liquids, several solvents, such as acetonitrile, ethanol, methanol, $[C_2mim][C_2SO_4]$ and [DMEA][HCOO] were tested.

A previous study found that the antioxidant capacity using ABTS, FRAP and DPPH assays depend strongly on the sample solvents used (Perez-Jimenez and Saura-Calixto, 2006). However, the authors only studied the effect of sample solvents on the antioxidant capacity and not the solvent of the assay. This is not the case in this study where the solvent was used both to dissolve the sample and in the assay as well.

As can be seen from Table 5.6, no ABTS radical cation was detected in organic solvents (ethanol and acetonitrile) and ionic liquids ($[C_2mim][C_2SO_4]$, [DMEA][HCOO]) under assay conditions. However, $ABTS^{\bullet+}$ was formed in methanol for a short time only. Surprisingly, ABTS radical cation generation was not detected in ethanol and $[C_2mim][C_2SO_4]$ despite the fact that both ABTS and AAPH apparently dissolved well in these solvents under the assay conditions. It seems possible that these results are due to the transformation of ABTS radicals cation ($ABTS^{\bullet+}$) to its reductive form (ABTS) in organic solvents. These results seem to be consistent with other research that found that the organic solvents such as acetone, ethanol and methanol (80% v/v) could transform ABTS radicals cation into its reductive form or a new form, and the scavenging rate of $ABTS^{\bullet+}$ was lower in methanol compare with the other solvents (Liu *et al.*, 2015). On the other hand, Cantarella *et al.* (Cantarella *et al.*, 2003) found that the decreased $ABTS^{\bullet+}$ stability in organic solvents resulted from the decomposition of the radical cation into other species, rather than from a return of $ABTS^{\bullet+}$ to ABTS. Furthermore, it was found that the alternative radical initiator potassium persulfate ($K_2S_2O_8$) did not dissolve in any of organic solvents and ionic liquids used in this study, thus eliminating this as an alternative.

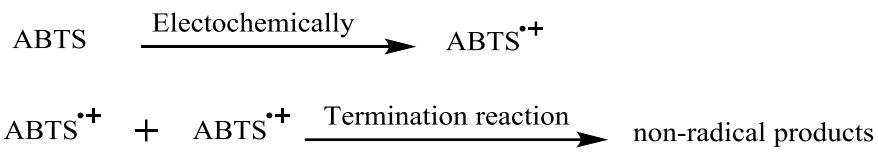
Table 5.6**:** Solubility of ABTS and AAPH in solvents tested.

Solvent	ABTS Solubility	AAPH Solubility	ABTS + AAPH
Acetonitrile	Not soluble (white colour)	Not soluble	White colour (precipitate)
Methanol	Soluble	Soluble	$ABTS^{\bullet+}$ solution (light green) the absorbance is low (0.260) and the colour disappeared very quickly
Ethanol	Soluble	Soluble	White colour (precipitate)
$[C_2mim][C_2SO_4]$	Soluble	Soluble	$ABTS^{\bullet+}$ solution not forming as a blue-green colour not formed
[DMEA][HCOO]	Soluble	Non-soluble	

5.3.8.2 Generation of ABTS Radical Cation in Ionic Liquid

Several methods can be used for generation of reactive radicals in ionic liquids, such as thermal processes using initiators or precursors, by photoprocesses, or electrochemically (Strehmel, 2012). However, in reviewing the literature, no data were found on the specific generation of ABTS radical cation in ionic liquids.

An electrochemical process with a three-electrode cell was used for ABTS radical cation formation in $[C_2mim][C_2SO_4]$. Nevertheless, the lifetime of this radical was very short in compared with aqueous systems, indicating that the termination reaction was very fast. The intensive blue-green colour obtained from electrochemical oxidation of ABTS in $[C_2mim][C_2SO_4]$ disappeared after only a few minutes (see Scheme 5.10 and Figure 5.27). These results are in agreement with Strehmel *et al.* (Strehmel *et al.*, 2009) findings, which showed that photolytically generated lophyl radicals species formed in the ionic liquid solutions have shorter lifetimes when compared to those formed in other organic solvents tested.



Scheme 5.10: ABTS radical cation formation and termination reactions

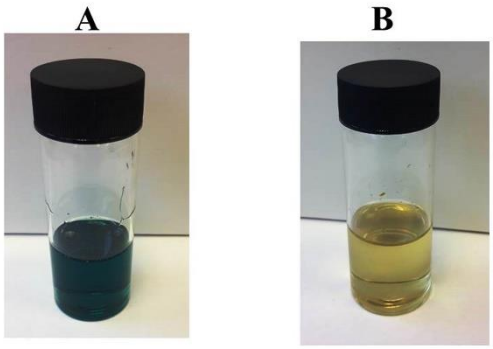


Figure 5.27: Electrochemically formation of ABTS radical cation in $[C_2mim][C_2SO_4]$ (A): Figure shows the blue-green colour intensity of ABTS radical formation after 24 h of reaction (B) disappeared of the blue-green colour after few minutes from removing from the electrochemical cell (24 h of reaction).

A possible explanation for these results may be that the transformation of ABTS radical cation into its reductive form could occur in ionic liquids as well as in organic solvents, as discussed previously. Another possible explanation for this is that after formation of the ABTS radical cation, this species can recombine with another ABTS radical cation either within the solvent cage or through escaping out of the solvent cage and diffusing through the matrix, resulting in formation of a dimer (Strehmel *et al.*, 2009, Berdzinski *et al.*, 2013). It is also possible that the radical cation may be decomposed into other species (Cantarella *et al.*, 2003).

More research on the mechanism of ABTS radical cation formation in ionic liquids and termination reaction is clearly required, especially if the ABTS assay is to become a viable proposition for the assessment of radical stability within ionic liquids. This would include a clear assessment of the rates of reaction. However, the behaviour noted here has implications also for the use of ABTS in attempting to depolymerise lignin in the presence of ionic liquids, especially relating to the possible changes in rates and radical stabilities.

5.4 Conclusions

The following conclusions can be drawn from the present study; the apparent reactivity of DPPH• is solvent dependent; it was larger in methanol than in any other solvent. Another important practical implication is that the methods of measuring antioxidant

activity did not always provide the same results due to differing reaction conditions and the substrates or products monitored. The majority of lignin-related monomer compounds tested reacted slowly with DPPH• in organic solvents and the mechanisms of reaction for these compounds with DPPH• seem to be complex.

Although various solvents and methods (chemical initiator and electrochemical) have been applied for ABTS radical cation generation. No ABTS radical cation was detected in organic solvents (ethanol and acetonitrile) and ionic liquids ($[C_2mim][C_2SO_4]$, [DMEA][HCOO]) using chemical methods under assay conditions. However, the formation of the ABTS radical cation can be identified when using an electrochemical generation process in $[C_2mim][C_2SO_4]$, but the lifetime of this radical was very short in this ionic liquid, compared with aqueous systems.

The main goal of this chapter was to understand the free radical behaviour of lignin monomers in ionic liquids using simple and inexpensive methods. It is somewhat surprising that low antiradical activities of lignin monomers and standards in ionic liquids were found in ABTS and DPPH methods. Generally, the viscosity of the ionic liquid strongly affects the mobility of radicals and therefore potentially the activity measurements. However, this research will serve as a base for future study that is investigating the molecular interactions between the radicals and ionic liquids that would help to clarify why ionic liquids appear to prevent radical reactions under the assay conditions tested here.

Further investigation and experimentation using different types of ionic liquids are strongly recommended. DPPH shows the dependence of its absorption on the IL in which it is dissolved. However, it is extremely stable in organic solvent media and no shift in the maximum absorption wavelength occurred in organic solvents. Thus, it is strongly recommended to study the absorption spectra of DPPH in ionic liquids or any solvent first before finding radical scavenging activity.

This study has shown that the 96-well microplate was successfully applied for DPPH assay and proved to be as robust, reproducible, rapid, and efficient and also offers significant time-saving compared with the conventional UV-Vis spectrophotometer methods. However, further research should be carried out to establish the correlation

between 96-well microplate DPPH method and a conventional method using UV-Vis spectrophotometer and the sample preparation procedure. The calibration process for microplate DPPH assay by finding molar absorptivity for pathlength correction would be very interesting to confirm the utility of this assay.

CHAPTER SIX

GENERAL DISCUSSION, CONCLUSIONS AND SUGGESTIONS FOR FUTURE WORK

6.1 Summary and Conclusions

This chapter summarises the main findings and principal issues of the work presented in this thesis and suggests recommendations for future work.

Lignin is potentially a major renewable feedstock, a non-fossil source of aromatic compounds. Currently, most lignin is burned as a source of energy in the pulping industry. However, depolymerisation of lignin is often limited by mass transfer because of its limited solubility in water and traditional solvents. This thesis has provided additional evidence that lignin solubility is both enhanced in ionic liquids, and that this can improve yields of aromatic small molecules *via* enzymatic and electrochemical treatments.

In the first method, a detailed study on potential transformation conditions for organosolv lignin in $[C_2mim][C_2SO_4]$ was presented, where the effect of temperature (30 °C & 160 °C), the concentration of IL in sodium acetate buffer solution pH 5.0 (0% v/v, 30% v/v and 100% v/v), and enzymatic process using commercial enzyme laccase from *Trametes versicolor* (LTV) was explored. The highest amount of product that was obtained when dissolving organosolv lignin in 100% (v/v) IL at 30 °C, followed by treatment of lignin with the assistance of commercial laccase (LTV) in 30% (v/v) IL at 30 °C. The enzymatic conversions were higher in IL/buffer mixtures compared to aqueous media. Syringaldehyde and vanillin were found to be the major products through all experiments performed (Chapter 3). The implications here are that low temperatures are most effective in maximising yields of small aromatics. This can improve future processing in this area by minimising energy inputs. However in the enzymatic process, a significant volume of water is required for maximal activity, meaning issues such as water treatment and how amenable the IL will be for recycling will need to be addressed as potential process challenges.

Since the product concentrations obtained from organosolv lignin treatment with ABTS assistance in 30% (v/v) IL/buffer mixtures was apparently the highest, further research was performed to explore the mechanism and to know more about the role of free radicals resulting from oxidation of ABTS in the lignin transformation process. This was initially achieved by using electrochemical oxidation techniques (CV and bulk electrolysis). First, electrochemical oxidation using CV has been investigated for enhancing the oxidation of the non-phenolic lignin model compound veratryl alcohol and three types of lignin (organosolv, Kraft and lignosulfonate) using ABTS in $[C_2mim][C_2SO_4]$. The oxidation currents on the CVs for the formation of either or both of the ABTS radical cation and the ABTS dication were observed to increase after addition of all types of lignin and veratryl alcohol under select conditions, proving ABTS to be an effective mediator for electrochemical oxidation of lignin. However, the use of ABTS was found to affect more significantly the oxidation of organosolv lignin, which is consistent with the greater solubility of this lignin in this IL over the other types of lignin examined in this study. Similarly, the solubility of this lignin decreased dramatically at around 10% (v/v) buffer concentration and resulted in a concomitant reduction in the oxidation peak current. This does, however, provide scope for developing recyclable processes for organosolv lignin.

The solubility of lignin and viscosity of the solvent or solution are likely to play a vital role in the electrochemical oxidation reaction of lignin. Overall, the rates of heterogeneous and homogeneous electron-transfer reactions are lower in $[C_2mim][C_2SO_4]$ compared to those measured in the buffer solution. Furthermore, CV was applied as a quick and efficient way to explore the impact of water in the ABTS mediated oxidation of both organosolv and lignosulfonate lignin. The CV studies of ABTS mediator with lignin demonstrated a high level of catalytic efficiency toward lignosulfonate in buffer (ABTS dication 17.6-fold) and 15% (v/v) $[C_2mim][C_2SO_4]$/buffer (ABTS radical cation 5.9-fold and ABTS dication 6.7-fold) but there was no increase in catalytic efficiency associated with the presence of the $[C_2mim][C_2SO_4]$ relative to ABTS alone. In contrast, organosolv showed an initial increase in oxidation, followed by a significant decrease on increasing the water content of a $[C_2mim][C_2SO_4]$ solution.

On the basis of lignin electrochemistry using bulk electrolysis, an electrochemical oxidation process was performed using organosolv lignin in $[C_2mim][C_2SO_4]$ with the presence of ABTS. Syringaldehyde and some other aromatic compounds such as vanillin, syringol, 2,5-dimethoxybenzyl acetate, guaiacylacetone and DHCD were identified by GC-MS after ethyl acetate extraction. On the other hand, 2-furoic acid, vanillic acid, homovanillyl alcohol, homovanillic acid and levulinic acid were identified as the major products obtained from the electrochemical oxidation of lignosulfonate in sodium acetate buffer solution (pH 4.5) with the presence of ABTS. However, the treatment of both types of lignin did not exhibit a significant enhancement with the electrolytic process compared to the control reactions. The pattern of the product formed during the electrochemical oxidation of organosolv lignin was significantly different from those obtained from electrochemical oxidation of lignosulfonate. This result may be explained by the fact that the lignosulfonate from softwood was used as the substrate in this study so most of the lignosulfonate products detected were guaiacyl derivatives as expected. However, organosolv lignin in this study was produced from mixed hardwoods which consist of both guaiacyl and syringyl units and produced more syringaldehyde and vanillin **(**Chapter 4).

As can be seen from Table 6.1, the products obtained from the lignin dissolution process depend on the method used, solvent, lignin type and process conditions performed. The total amount and selectivity of the products that were obtained when dissolving organosolv lignin in 100% (v/v) IL were higher compared to the treatment of lignin with or without the assistance of LTV in 30% (v/v) IL (Table 6.1, entry 1-3). However, the total amount of DMBQ obtained from organosolv lignin dissolution process in the presence of LTV was higher when compared to dissolving organosolv lignin without LTV (Table 6.1, entry 1-2). DHCD was only obtained from organosolv lignin dissolution in IL, which affords an advantage for ILs with their unique properties as a sustainable solvent that can dissolve lignin at low temperature and pressure. However, the quantity of products obtained after initial ethyl acetate extraction of organosolv lignin without bulk electrolysis was higher than the treatment with and without bulk electrolysis (Table 6.1, entry 1-6). DMBQ and 3,4-dimethoxythiophenol were only obtained from electrochemical oxidation of lignosulfonate in buffer solution (Table 6.1, entry 7), while syringaldehyde was formed from electrochemical oxidation

of lignosulfonate in buffer solution in presence of ABTS (Table 6.1, entry 7 and entry 9).

In order to have a full picture of lignin treatment in ionic liquids and since some depolymerisation approaches are often thought to proceed *via* free-radical mediated mechanisms, three different methods were carried out to evaluate the antiradical capacity of lignin-related monomer compounds including; FRAP assay, DPPH radical scavenging and an ABTS-based assay. In this work, six lignin monomers; syringaldehyde, vanillin, vanillic acid, guaiacol, syringol and homovanillyl alcohol were chosen, based on the most common components identified from the lignin dissolution processe in the ionic liquid that have been discussed in Chapter 3 and Chapter 4. Three well-known antioxidant standard compounds; vitamin C, gallic acid and Trolox were used to compare the antioxidant potential. Whilst these assays are successful in aqueous and organic solvent systems, there appears to be little measurable activity in ionic liquids (Chapter 5).

Although various solvents and methods (chemical initiator and electrochemical) have been applied for ABTS radical cation generation, no ABTS radical cation was detected in organic solvents (ethanol and acetonitrile) and ionic liquids ($[C_2mim][C_2SO_4]$, [DMEA][HCOO]) using chemical methods under assay conditions. However, the formation of the ABTS radical cation could be detected when using an electrochemical generation process in $[C_2mim][C_2SO_4]$, but the lifetime of this radical was very short in this ionic liquid, compared with aqueous systems.

Table 6. 1: Summary of types of solvent used and the major products obtained from different lignin process covered in this thesis

Entry	Method Used	Lignin type/ Solvent	Experimental Conditions	Products
1	Dissolution process with LTV	Organosolv lignin 30% v/v IL	30 °C for 6 h	Furfural, vanillin, DMBQ and syringaldehyde
2	Dissolution process without LTV	Organosolv lignin 30% v/v IL	30 °C for 6 h	Furfural, vanillin, DMBQ, DHCD and syringaldehyde
3	Dissolution process without LTV	Organosolv lignin 100% v/v IL	30 °C for 6 h	Furfural, syringol, vanillin, DMBQ, HMCD, DHCD, DHPAA and syringaldehyde
4	Bulk electrolysis	Organosolv lignin 100% v/v IL	RT for 6 h	Phenol, syringol, vanillin, guaiacylacetone, 3,4-dimethoxythiophenol, 2,5-dimethoxybenzyl acetate, DHCD and syringaldehyde
5	Without bulk electrolysis	Organosolv lignin 100% v/v IL	RT for 6 h	Furfural, 5-methyl-, phenol, vanillin, 2,5-dimethoxybenzyl, DHCD, syringol, guaiacylacetone acetate, 3,4-dimethoxythiophenol and syringaldehyde
6	Without bulkelectrolysis Initial extraction using ethyl acetate	Organosolv lignin Ethyl acetate	RT at initial time	Furfural, 5-methyl-, phenol, vanillin, 2,5-dimethoxybenzyl, syringol, guaiacol, guaiacylacetone acetate, 3,4-dimethoxythiophenol and syringaldehyde
7	Bulk electrolysis	Lignosulfonate Sodium acetate buffer pH 4.5	RT for 8 h	1H-Pyrrole-2-carboxaldehyde, levulinic acid, 2-furoic acid, guaiacol, vanillin, acetovanillone, guaiacylacetone, homovanillyl alcohol, methyl-(2-hydoxy-3-ethoxy-benzyl)ether, vanillic acid, DMBQ, homovanillic acid, 3,4-dimethoxythiophenol and syringaldehyde
8	Without bulk electrolysis Initial extraction using ethyl acetate	Lignosulfonate Ethyl acetate	RT at initial time	1H-Pyrrole-2-carboxaldehyde, levulinic acid, 2-furoic acid, guaiacol, syringol, vanillin, acetovanillone, homovanillyl alcohol, methyl-(2-hydoxy-3-ethoxy-benzyl)ether, vanillic acid and homovanillic acid
9	Without bulk electrolysis	Lignosulfonate Sodium acetate buffer pH 4.5	RT for 8 h	1H-Pyrrole-2-carboxaldehyde, levulinic acid, 2-furoic acid, guaiacol, syringol, vanillin, acetovanillone, homovanillyl alcohol, methyl-(2-hydoxy-3-ethoxy-benzyl) ether, vanillic acid, homovanillic acid, and syringaldehyde
10	Without bulk electrolysis and without ABTS	Lignosulfonate Sodium acetate buffer pH 4.5	RT for 8 h	1H-Pyrrole-2-carboxaldehyde, levulinic acid, 2-furoic acid, syringol, vanillin, acetovanillone, guaiacylacetone, homovanillyl alcohol, methyl-(2-hydoxy-3-ethoxy-benzyl)ether, vanillic acid and homovanillic acid

RT: Room Temperature

6.2 Suggestions for Future Work

One of the greatest challenges in this study is the complete identification and quantification of the low-molecular weight compounds produced from the complex mixtures of lignin formed after bulk electrolysis reaction, especially in IL. Only the products from solvent extraction were characterised using GC-MS. However, it was found that the IL causes a problem in the GC-MS system (incompatibility of the IL with the MS detector) so it was not utilised further. Further investigation would be needed to identify the compounds in aqueous and solid fractions or to find a direct method to identify and detect the products obtained from the reaction mixtures without doing an extraction process prior to the analysis.

The complex structure of lignin means it is difficult to elucidate the polymeric structures and composition of lignin by analytical methods. However, molecular weight analysis using gel permeation chromatography (GPC) can be employed as an effective analytical method to monitor molecular weight changes during lignin treatment, providing insights into the changes that might occur in the depolymerisation experiments. It is also worth noting that the matrix-assisted laser desorption/ionization time-of-flight mass spectrometry (MALDI-TOF) experiments were attempted in this present research to measure the molecular weight of lignin in ionic liquids. Due to its low efficiency of ionisation, only low molecular mass regions between m/z 400 and 800 were observed.

1D NMR spectroscopy (^{1}H NMR and ^{13}C NMR) has been also used to attempt the identification and quantification of the products obtained from lignin depolymerisation process in IL. However, 1D NMR spectra do not allow detailed assignment and quantification of individual signals due to broad and overlapping NMR signals resulting in low-resolution spectra, especially in IL. Sensitivity is also an issue due to the low quantities of material typically identified.

A 2D NMR spectroscopic technique such as heteronuclear single quantum coherence (HSQC) and heteronuclear multiple quantum coherence (HMQC) experiments, which combines the sensitivity of ^{1}H NMR with the higher resolution of ^{13}C NMR may provide a valid analytical technique in the analysis of complex samples and a great

platform for lignin characterisation (Sette *et al.*, 2011, Yuan *et al.*, 2013). Thus, further research on the limitations of 2D NMR in the context of lignin analysis would be of great help in the further understanding of the products formed after lignin treatment with IL.

Gas chromatography-flame ionization detector (GC-FID) (Agilent technologies) with two different types of column; HP-INNOWAX and HP-5MS fused silica capillary column (30 m x 25 mm ID, 0.25 µm film thickness) were also used to analyse the complex mixtures obtained from electrochemical oxidation of organosolv lignin in $[C_2mim][C_2SO_4]$ with standards such as syringaldehyde and vanillin. In this method, the sample was injected directly into the column without any solvent extraction or pretreatment. However, only the peak corresponding to impurities in the IL was observed on both columns. In general, therefore, new analytical methods are needed that are capable of solving problems associated with lignin analysis.

This research provides a framework for the exploration of depolymerisation of lignin using electrochemical oxidation processes in the presence of an ionic liquid. Further investigation and experimentation using different types of ionic liquids (i.e. [DMEA][HCOO]) is strongly recommended. The influence of different electrode materials on the depolymerisation process would be a fruitful area for further work. Thin-layer electrochemical cells could also be examined.

Investigating the molecular interactions between ABTS/ionic liquid/lignin and lignin/ionic liquid would help to clarify the specific influence of ionic liquids, both in terms of their solubilisation of lignin components, specific solute-solvent interactions, and viscosity, and delineate their impact on reactivity.

This study has shown that 96-well microplate was successfully applied for the DPPH assay and proved to be robust, reproducible, rapid, and efficient. The use of a high-throughput approach also offers significant time-savings compared with the conventional UV spectrophotometer methods. However, further research should be carried out to establish the correlation between the 96-well microplate DPPH method results and the conventional method using UV-spectrophotometer, especially with respect to the sample preparation procedure. The calibration process for the microplate

DPPH assay by calculating molar absorptivity for path-length correction would be useful.

DPPH shows a dependence of its absorption on the IL in which it is dissolved. However, it is extremely stable in organic solvent media and no shift in the maximum absorption wavelength occurred in organic solvents. Thus, it is strongly recommended to study the absorption spectra of DPPH in ionic liquids or any type of solvent first before calculating the radical scavenging activity.

Overall, ionic liquids show good potential for the treatment of lignins to obtain small molecules because of their ability to help solubilise this polymeric material. This thesis demonstrated that the reactions with lignin can be catalysed, especially with mediator under electrolytic conditions and that there are mass-transfer advantages. Challenges in using radical chemistries to depolymerise lignin include repolymerisation, which limit the small molecules that can be readily obtained. As such, high throughput methods to understand which ionic liquids promote the right sort of radical chemistry, as developed here, show promise, but have opened up a number of questions on how radical behaviour in ionic liquid media differs from that known in molecular solvents and how this might impact on the lignin chemistries described here. Tackling these issues can lead to efficient methods to transform a hugely abundant waste material to fill a key gap in the much needed non-fossil fuel derived chemicals required for the next generation.

REFERENCES

Achyuthan, K. E., Achyuthan, A. M., Adams, P. D., Dirk, S. M., Harper, J. C., Simmons, B. A. & Singh, A. K. 2010. Supramolecular self-assembled chaos: polyphenolic lignin's barrier to cost-effective lignocellulosic biofuels. *Molecules,* 15**,** 8641-8688.

Alcalde, M., Bulter, T. & Arnold, F. H. 2002. Colorimetric assays for biodegradation of polycyclic aromatic hydrocarbons by fungal laccases. *Journal of Biomolecular Screening,* 7**,** 547-553.

Antolovich, M., Prenzler, P. D., Patsalides, E., Mcdonald, S. & Robards, K. 2002. Methods for testing antioxidant activity. *Analyst (Cambridge, U. K.),* 127**,** 183-198.

Aracri, E., Tzanov, T. & Vidal, T. 2013. Use of Cyclic Voltammetry as an Effective Tool for Selecting Efficient Enhancers for Oxidative Bioprocesses: Importance of pH. *Industrial & Engineering Chemistry Research,* 52**,** 1455-1463.

Ardalan, P., Ardalan, T. & Momen Heravi, M. 2014. A DFT Study on Antioxidant Activity of Trolox and Substituted Trolox and Their Radicals. *Journal of Applied Chemistry,* 8**,** 45-50.

Arts, M. J. T. J., Haenen, G. R. M. M., Voss, H.-P. & Bast, A. 2004. Antioxidant capacity of reaction products limits the applicability of the Trolox Equivalent Antioxidant Capacity (TEAC) assay. *Food and Chemical Toxicology,* 42**,** 45-49.

Azadi, P., Inderwildi, O. R., Farnood, R. & King, D. A. 2013. Liquid fuels, hydrogen and chemicals from lignin: A critical review. *Renewable & Sustainable Energy Reviews,* 21**,** 506-523.

Badanai, J., Silva, C., Martins, D., Antunes, D. & Miguel, M. G. 2015. Ability of scavenging free radicals and preventing lipid peroxidation of some phenols and ascorbic acid. *Journal of Applied Pharmaceutical Science,* 5**,** 034-041.

Badhani, B., Sharma, N. & Kakkar, R. 2015. Gallic acid: a versatile antioxidant with promising therapeutic and industrial applications. *RSC Advances,* 5**,** 27540-27557.

Baldrian, P. 2004. Purification and characterization of laccase from the white-rot fungus Daedalea quercina and decolorization of synthetic dyes by the enzyme. *Applied Microbiology and Biotechnology,* 63**,** 560-563.

Baldrian, P. 2006. Fungal laccases - occurrence and properties. *FEMS Microbiol Rev,* 30**,** 215-42.

Barreca, A. M., Sjogren, B., Fabbrini, M., Galli, C. & Gentili, P. 2004. Catalytic efficiency of some mediators in laccase-catalyzed alcohol oxidation. *Biocatalysis and Biotransformation,* 22**,** 105-112.

Barta, K., Warner, G. R., Beach, E. S. & Anastas, P. T. 2014. Depolymerization of organosolv lignin to aromatic compounds over Cu-doped porous metal oxides. *Green Chemistry,* 16**,** 191-196.

Benzie, I. F. F. & Strain, J. J. 1996. The ferric reducing ability of plasma (FRAP) as a measure of "antioxidant power": The FRAP assay. *Analytical Biochemistry,* 239**,** 70-76.

Benzie, I. F. F. & Strain, J. J. 1999. Ferric reducing/antioxidant power assay: direct measure of total antioxidant activity of biological fluids and modified version for simultaneous measurement of total antioxidant power and ascorbic acid concentration. *Methods in Enzymology,* 299**,** 15-27.

Berdzinski, S., Horst, J., Strassburg, P. & Strehmel, V. 2013. Recombination of Lophyl Radicals in Pyrrolidinium-Based Ionic Liquids. *ChemPhysChem,* 14**,** 1899-1908.

Berdzinski, S., Strehmel, B. & Strehmel, V. 2015. Photogenerated lophyl radicals in 1-alkyl-3-vinylimidazolium bis(trifluoromethylsulfonyl)imides. *Photochemical & Photobiological Sciences,* 14**,** 714-725.

Binder, J. B., Gray, M. J., White, J. F., Zhang, Z. C. & Holladay, J. E. 2009. Reactions of lignin model compounds in ionic liquids. *Biomass & Bioenergy,* 33**,** 1122-1130.

Blois, M. S. 1958. Antioxidant determinations by the use of a stable free radical. *Nature (London, U. K.),* 181**,** 1199-200.

Bortolomeazzi, R., Sebastianutto, N., Toniolo, R. & Pizzariello, A. 2007. Comparative evaluation of the antioxidant capacity of smoke flavouring phenols by crocin bleaching inhibition, DPPH radical scavenging and oxidation potential. *Food Chemistry,* 100**,** 1481-1489.

Bountagkidou, O. G., Ordoudi, S. A. & Tsimidou, M. Z. 2010. Structure–antioxidant activity relationship study of natural hydroxybenzaldehydes using in vitro assays. *Food Research International,* 43**,** 2014-2019.

Bourbonnais, R. & Paice, M. G. 1990. Oxidation of non-phenolic substrates. An expanded role for laccase in lignin biodegradation. *FEBS Letters,* 267**,** 99-102.

Bourbonnais, R., Paice, M. G., Reid, I. D., Lanthier, P. & Yaguchi, M. 1995. Lignin oxidation by laccase isoenzymes from Trametes versicolor and role of the mediator 2,2'-azinobis(3-ethylbenzthiazoline-6-sulfonate) in kraft lignin depolymerization. *Applied and Environmental Microbiology,* 61**,** 1876-80.

Bourbonnais, R., Paice, M. G., Freiermuth, B., Bodie, E. & Borneman, S. 1997. Reactivities of various mediators and laccases with kraft pulp and lignin model compounds. *Applied and Environmental Microbiology,* 63**,** 4627-32.

Bourbonnais, R., Leech, D. & Paice, M. G. 1998. Electrochemical analysis of the interactions of laccase mediators with lignin model compounds. *Biochimica et Biophysica Acta (BBA) - General Subjects,* 1379**,** 381-390.

Bourbonnais, R. & Paice, M. 2004. Voltammetric measurement of lignin in pulp and paper samples - An electron transfer catalytic approach with mediators. *Journal of The Electrochemical Society,* 151**,** E246-E249.

Brand-Williams, W., Cuvelier, M. E. & Berset, C. 1995. Use of a free radical method to evaluate antioxidant activity. *LWT - Food Science and Technology,* 28**,** 25-30.

Brandt, A., Ray, M. J., To, T. Q., Leak, D. J., Murphy, R. J. & Welton, T. 2011. Ionic liquid pretreatment of lignocellulosic biomass with ionic liquid-water mixtures. *Green Chemistry,* 13**,** 2489-2499.

Brebu, M., Tamminen, T. & Spiridon, I. 2013. Thermal degradation of various lignins by TG-MS/FTIR and Py-GC-MS. *Journal of Analytical and Applied Pyrolysis,* 104**,** 531-539.

Bugg, T. D. H., Ahmad, M., Hardiman, E. M. & Rahmanpour, R. 2011. Pathways for degradation of lignin in bacteria and fungi. *Natural Product Reports,* 28**,** 1883-1896.

Campos, A. M. & Lissi, E. A. 1997. Kinetics of the reaction between 2,2?-azinobis (3-ethylbenzothiazoline-6-sulfonic acid (ABTS) derived radical cations and phenols. *International Journal of Chemical Kinetics,* 29**,** 219-224.

Cantarella, G., D'acunzo, F. & Galli, C. 2003. Determination of laccase activity in mixed solvents: Comparison between two chromogens in a spectrophotometric assay. *Biotechnology and Bioengineering,* 82**,** 395-398.

Chakraborty, D. & Barton, S. C. 2011. Influence of Mediator Redox Potential on Fuel Sensitivity of Mediated Laccase Oxygen Reduction Electrodes. *Journal of The Electrochemical Society,* 158**,** B440-B447.

Chatel, G. & Rogers, R. D. 2014. Review: Oxidation of Lignin Using Ionic Liquids-An Innovative Strategy To Produce Renewable Chemicals. *ACS Sustainable Chemistry & Engineering,* 2**,** 322-339.

Chen, A., Rogers, E. I. & Compton, R. G. 2010. Abrasive Stripping Voltammetric Studies of Lignin and Lignin Model Compounds. *Electroanalysis,* 22**,** 1037-1044.

Chen, Y., Xiao, H., Zheng, J. & Liang, G. 2015. Structure-Thermodynamics-Antioxidant Activity Relationships of Selected Natural Phenolic Acids and Derivatives: An Experimental and Theoretical Evaluation. *PLoS ONE,* 10**,** e0121276.

Cheng, G., Kent, M. S., He, L., Varanasi, P., Dibble, D., Arora, R., Deng, K., Hong, K., Melnichenko, Y. B., Simmons, B. A. & Singh, S. 2012. Effect of Ionic Liquid Treatment on the Structures of Lignins in Solutions: Molecular Subunits Released from Lignin. *Langmuir,* 28**,** 11850-11857.

Childs, R. E. & Bardsley, W. G. 1975. The steady-state kinetics of peroxidase with 2,2′-azino-di-(3-ethyl-benzthiazoline-6-sulphonic acid) as chromogen. *Biochemical Journal,* 145**,** 93-103.

Christopher, L. P., Yao, B. & Ji, Y. 2014. Lignin biodegradation with laccase-mediator systems. *Frontiers in Energy Research,* 2**,** 1-13.

Cirillo, G., Iemman, F. & Editors 2012. *Antioxidant Polymers: Synthesis, Properties, and Applications,* Scrivener Publishing LLC.

Cox, B. J. & Ekerdt, J. G. 2012. Depolymerization of oak wood lignin under mild conditions using the acidic ionic liquid 1-H-3-methylimidazolium chloride as both solvent and catalyst. *Bioresource Technology,* 118**,** 584-588.

Cui, C., Sadeghifar, H., Sen, S. & Argyropoulos, D. S. 2013. Toward thermoplastic lignin polymers; part II: thermal & polymer characteristics of kraft lignin & derivatives. *BioResources,* 8**,** 864-886, 23 pp.

Cybulska, I., Brudecki, G., Rosentrater, K., Julson, J. L. & Lei, H. 2012. Comparative study of organosolv lignin extracted from prairie cordgrass, switchgrass and corn stover. *Bioresource Technology,* 118**,** 30-36.

Dhumal, N. R., Kim, H. J. & Kiefer, J. 2011. Electronic Structure and Normal Vibrations of the 1-Ethyl-3-methylimidazolium Ethyl Sulfate Ion Pair. *The Journal of Physical Chemistry A,* 115**,** 3551-3558.

Díaz-González, M., Vidal, T. & Tzanov, T. 2009. Electrochemical Study of Phenolic Compounds as Enhancers in Laccase-Catalyzed Oxidative Reactions. *Electroanalysis,* 21**,** 2249-2257.

Díaz-González, M., Vidal, T. & Tzanov, T. 2011. Phenolic compounds as enhancers in enzymatic and electrochemical oxidation of veratryl alcohol and lignins. *Applied Microbiology and Biotechnology,* 89**,** 1693-1700.

Dizhbite, T., Telysheva, G., Jurkjane, V. & Viesturs, U. 2004. Characterization of the radical scavenging activity of lignins--natural antioxidants. *Bioresource Technology,* 95**,** 309-317.

Domínguez, A., Rodríguez, O., Tavares, A. P. M., Macedo, E. A., Asunción Longo, M. & Ángeles Sanromán, M. 2011. Studies of laccase from Trametes versicolor

in aqueous solutions of several methylimidazolium ionic liquids. *Bioresource Technology,* 102**,** 7494-7499.

Dominguez, V. C., Mcdonald, C. R., Johnson, M., Schunk, D., Kreuter, R., Sykes, D., Wigton, B. T. & Chohan, B. S. 2010. The Characterization of a Custom-Built Coulometric Karl Fischer Titration Apparatus. *Journal of Chemical Education,* 87**,** 987-991.

Dupont, J., De Souza, R. F. & Suarez, P. a. Z. 2002. Ionic Liquid (Molten Salt) Phase Organometallic Catalysis. *Chemical Reviews (Washington, DC, U. S.),* 102**,** 3667-3691.

Dziedzic, S. Z. & Hudson, B. J. F. 1983. Hydroxy isoflavones as antioxidants for edible oils. *Food Chemistry,* 11**,** 161-166.

Eshtaya, M., Ejigu, A., Stephens, G., Walsh, D. A., Chen, G. Z. & Croft, A. K. 2016. Developing energy efficient lignin biomass processing - towards understanding mediator behaviour in ionic liquids. *Faraday Discussions,* 190**,** 127-45.

Fabbrini, M., Galli, C. & Gentili, P. 2002. Comparing the catalytic efficiency of some mediators of laccase. *Journal of Molecular Catalysis B-Enzymatic,* 16**,** 231-240.

Faure, D., Bouillant, M. L., Jacoud, C. & Bally, R. 1996. Phenolic derivatives related to lignin metabolism as substrates for Azospirillum laccase activity. *Phytochemistry,* 42**,** 357-359.

Floegel, A., Kim, D. O., Chung, S. J., Koo, S. I. & Chun, O. K. 2011. Comparison of ABTS/DPPH assays to measure antioxidant capacity in popular antioxidant-rich US foods. *Journal of Food Composition and Analysis,* 24**,** 1043-1048.

Foti, M. C., Daquino, C., Mackie, I. D., Dilabio, G. A. & Ingold, K. U. 2008. Reaction of Phenols with the 2,2-Diphenyl-1-picrylhydrazyl Radical. Kinetics and DFT Calculations Applied To Determine ArO-H Bond Dissociation Enthalpies and Reaction Mechanism. *The Journal of Organic Chemistry,* 73**,** 9270-9282.

Franzoi, A. C., Dupont, J., Spinelli, A. & Vieira, I. C. 2009a. Biosensor based on laccase and an ionic liquid for determination of rosmarinic acid in plant extracts. *Talanta,* 77**,** 1322-1327.

Franzoi, A. C., Vieira, I. C., Dupont, J., Scheeren, C. W. & De Oliveira, L. F. 2009b. Biosensor for luteolin based on silver or gold nanoparticles in ionic liquid and laccase immobilized in chitosan modified with cyanuric chloride. *Analyst,* 134**,** 2320-2328.

Friaa, O. & Brault, D. 2006. Kinetics of the reaction between the antioxidant Trolox and the free radical DPPH• in semi-aqueous solution. *Organic & Biomolecular Chemistry,* 4**,** 2417-2423.

Fu, D., Mazza, G. & Tamaki, Y. 2010. Lignin Extraction from Straw by Ionic Liquids and Enzymatic Hydrolysis of the Cellulosic Residues. *Journal of Agricultural and Food Chemistry,* 58**,** 2915-2922.

Gaikwad, P., Barik, A., Priyadarsini, K. I. & Rao, B. S. M. 2010. Antioxidant activities of phenols in different solvents using DPPH assay. *Research on Chemical Intermediates,* 36**,** 1065-1072.

Galiński, M., Lewandowski, A. & Stępniak, I. 2006. Ionic liquids as electrolytes. *Electrochimica Acta,* 51**,** 5567-5580.

George, A., Tran, K., Morgan, T. J., Benke, P. I., Berrueco, C., Lorente, E., Wu, B. C., Keasling, J. D., Simmons, B. A. & Holmes, B. M. 2011. The effect of ionic liquid cation and anion combinations on the macromolecular structure of lignins. *Green Chemistry,* 13**,** 3375-3385.

Gómez, E., González, B., Calvar, N., Tojo, E. & Domínguez, Á. 2006. Physical Properties of Pure 1-Ethyl-3-methylimidazolium Ethylsulfate and Its Binary Mixtures with Ethanol and Water at Several Temperatures. *Journal of Chemical & Engineering Data,* 51**,** 2096-2102.

Gong, Y.-H., Shen, C., Lu, Y.-Z., Meng, H. & Li, C.-X. 2012. Viscosity and Density Measurements for Six Binary Mixtures of Water (Methanol or Ethanol) with an Ionic Liquid ([BMIM][DMP] or [EMIM][DMP]) at Atmospheric Pressure in the Temperature Range of (293.15 to 333.15) K. *Journal of Chemical & Engineering Data,* 57**,** 33-39.

González Arzola, K., Arévalo, M. C. & Falcón, M. A. 2009. Catalytic efficiency of natural and synthetic compounds used as laccase-mediators in oxidising veratryl alcohol and a kraft lignin, estimated by electrochemical analysis. *Electrochimica Acta,* 54**,** 2621-2629.

Guan, D., Kurra, Y., Liu, W. & Chen, Z. 2015. A click chemistry approach to site-specific immobilization of a small laccase enables efficient direct electron transfer in a biocathode. *Chemical Communications*.

Hallett, J. P. & Welton, T. 2011. Room-Temperature Ionic Liquids: Solvents for Synthesis and Catalysis. 2. *Chemical Reviews,* 111**,** 3508-3576.

Halliwell, B. & Gutteridge, J. M. C. 1995. The definition and measurement of antioxidants in biological systems. *Free Radical Biology and Medicine,* 18**,** 125-126.

Hamidi, N. H. 2013. *Enzymatic depolymerization of lignin by laccases.* PhD, University of Nottingham.

Han, D. & Row, K. H. 2010. Recent applications of ionic liquids in separation technology. *Molecules,* 15**,** 2405-2426.

Harwardt, N., Stripling, N., Roth, S., Liu, H. F., Schwaneberg, U. & Spiess, A. C. 2014. Effects of ionic liquids on the reaction kinetics of a laccase-mediator system. *RSC Advances,* 4**,** 17097-17104.

Hatakka, A. 2005. Biodegradation of Lignin. *Biopolymers Online.* Wiley-VCH Verlag GmbH & Co. KGaA.

Heinzkill, M., Bech, L., Halkier, T., Schneider, P. & Anke, T. 1998. Characterization of laccases and peroxidases from wood-rotting fungi (family Coprinaceae). *Applied and Environmental Microbiology,* 64**,** 1601-1606.

Higuchi, T. 2004. Microbial degradation of lignin: Role of lignin peroxidase, manganese peroxidase, and laccase. *Proceedings of the Japan Academy, Series B,* 80**,** 204-214.

Hinckley, G., Mozhaev, V., Budde, C. & Khmelnitsky, Y. 2002. Oxidative enzymes possess catalytic activity in systems with ionic liquids. *Biotechnology Letters,* 24**,** 2083-2087.

Ho, T. D., Zhang, C., Hantao, L. W. & Anderson, J. L. 2014. Ionic Liquids in Analytical Chemistry: Fundamentals, Advances, and Perspectives. *Analytical Chemistry (Washington, DC, U. S.),* 86**,** 262-285.

Hossain, M. M. & Aldous, L. 2012. Ionic Liquids for Lignin Processing: Dissolution, Isolation, and Conversion. *Australian Journal of Chemistry,* 65**,** 1465-1477.

Hou, X.-D., Smith, T. J., Li, N. & Zong, M.-H. 2012. Novel renewable ionic liquids as highly effective solvents for pretreatment of rice straw biomass by selective removal of lignin. *Biotechnology and Bioengineering,* 109**,** 2484-2493.

Hou, Y., Ren, Y., Peng, W., Ren, S. & Wu, W. 2013. Separation of Phenols from Oil Using Imidazolium-Based Ionic Liquids. *Industrial & Engineering Chemistry Research,* 52**,** 18071-18075.

Hu, L., Pan, H., Zhou, Y. & Zhang, M. 2011. Methods to improve lignin's reactivity as a phenol substitute and as replacement for other phenolic compounds: a brief review. *BioResources,* 6**,** 3515-3525.

Huang, D., Ou, B. & Prior, R. L. 2005. The Chemistry behind Antioxidant Capacity Assays. *Journal of Agricultural and Food Chemistry,* 53**,** 1841-1856.

Huber, G. W., Iborra, S. & Corma, A. 2006. Synthesis of Transportation Fuels from Biomass: Chemistry, Catalysts, and Engineering. *Chemical Reviews (Washington, DC, U. S.),* 106**,** 4044-4098.

Ibrahim, V., Volkova, N., Pyo, S.-H., Mamo, G. & Hatti-Kaul, R. 2013. Laccase catalysed modification of lignin subunits and coupling to p-aminobenzoic acid. *Journal of Molecular Catalysis B: Enzymatic,* 97**,** 45-53.

Idris, A., Vijayaraghavan, R., Patti, A. F. & Macfarlane, D. R. 2014. Distillable Protic Ionic Liquids for Keratin Dissolution and Recovery. *ACS Sustainable Chemistry & Engineering,* 2**,** 1888-1894.

Jacquemin, J., Husson, P., Padua, A. a. H. & Majer, V. 2006. Density and viscosity of several pure and water-saturated ionic liquids. *Green Chemistry,* 8**,** 172-180.

Ji, W., Ding, Z., Liu, J., Song, Q., Xia, X., Gao, H., Wang, H. & Gu, W. 2012. Mechanism of Lignin Dissolution and Regeneration in Ionic Liquid. *Energy & Fuels,* 26**,** 6393-6403.

Johnson, K. A. & Goody, R. S. 2011. The Original Michaelis Constant: Translation of the 1913 Michaelis–Menten Paper. *Biochemistry,* 50**,** 8264-8269.

Karamac, M., Kosinska, A. & Pegg, R. B. 2005. Comparison of radical-scavenging activities for selected phenolic acids. *Polish Journal of Food and Nutrition Sciences* 14**,** 165-170.

Keaveney, S. T., Haines, R. S. & Harper, J. B. 2015a. Developing principles for predicting ionic liquid effects on reaction outcome. The importance of the anion in controlling microscopic interactions. *Organic & Biomolecular Chemistry,* 13**,** 3771-3780.

Keaveney, S. T., Haines, R. S. & Harper, J. B. 2015b. Ionic liquid effects on a multistep process. Increased product formation due to enhancement of all steps. *Organic & Biomolecular Chemistry,* 13**,** 8925-8936.

Kedare, S. B. & Singh, R. P. 2011. Genesis and development of DPPH method of antioxidant assay. *Journal of Food Science and Technology,* 48**,** 412-422.

Kilpeläinen, I., Xie, H., King, A., Granstrom, M., Heikkinen, S. & Argyropoulos, D. S. 2007. Dissolution of Wood in Ionic Liquids. *Journal of Agricultural and Food Chemistry,* 55**,** 9142-9148.

Kim, D.-O., Lee, K. W., Lee, H. J. & Lee, C. Y. 2002. Vitamin C Equivalent Antioxidant Capacity (VCEAC) of Phenolic Phytochemicals. *Journal of Agricultural and Food Chemistry,* 50**,** 3713-3717.

Kristinova, V., Mozuraityte, R., Storro, I. & Rustad, T. 2009. Antioxidant Activity of Phenolic Acids in Lipid Oxidation Catalyzed by Different Prooxidants. *Journal of Agricultural and Food Chemistry,* 57**,** 10377-10385.

Kunamneni, A., Ghazi, I., Camarero, S., Ballesteros, A., Plou, F. J. & Alcalde, M. 2008a. Decolorization of synthetic dyes by laccase immobilized on epoxy-activated carriers. *Process Biochemistry (Amsterdam, Neth.),* 43**,** 169-178.

Kunamneni, A., Plou, F., Ballesteros, A. & Alcalde, M. 2008b. Laccases and Their Applications: A Patent Review. *Recent Patents on Biotechnology,* 2**,** 10-24.

Lahtinen, M., Viikari, L., Karhunen, P., Asikkala, J., Kruus, K. & Kilpeläinen, I. 2013. On the reactivity of the Melanocarpus albomyces laccase and formation of coniferyl alcohol dehydropolymer (DHP) in the presence of ionic liquid 1-allyl-

3-methylimidazolium chloride. *Journal of Molecular Catalysis B: Enzymatic,* 85–86**,** 169-177.

Lai, C., Zeng, G.-M., Huang, D.-L., Zhao, M.-H., Huang, H.-L., Huang, C., Wei, Z., Li, N.-J., Xu, P., Zhang, C. & Xie, G.-X. 2013. Effect of ABTS on the adsorption of Trametes versicolor laccase on alkali lignin. *International Biodeterioration & Biodegradation,* 82**,** 180-186.

Lange, H., Decina, S. & Crestini, C. 2013. Oxidative upgrade of lignin – Recent routes reviewed. *European Polymer Journal,* 49**,** 1151-1173.

Lateef, H., Grimes, S., Kewcharoenwong, P. & Feinberg, B. 2009. Separation and recovery of cellulose and lignin using ionic liquids: a process for recovery from paper-based waste. *Journal of Chemical Technology & Biotechnology,* 84**,** 1818-1827.

Lee, S. H., Doherty, T. V., Linhardt, R. J. & Dordick, J. S. 2009. Ionic liquid-mediated selective extraction of lignin from wood leading to enhanced enzymatic cellulose hydrolysis. *Biotechnology and Bioengineering,* 102**,** 1368-1376.

Leopoldini, M., Marino, T., Russo, N. & Toscano, M. 2004. Antioxidant Properties of Phenolic Compounds: H-Atom versus Electron Transfer Mechanism. *The Journal of Physical Chemistry A,* 108**,** 4916-4922.

Litwinienko, G. & Ingold, K. U. 2003. Abnormal solvent effects on hydrogen atom abstractions. 1. The reactions of phenols with 2,2-diphenyl-1-picrylhydrazyl (dpph•) in alcohols. *Journal of Organic Chemistry,* 68**,** 3433-3438.

Litwinienko, G. & Ingold, K. U. 2005. Abnormal Solvent Effects on Hydrogen Atom Abstraction. 3. Novel Kinetics in Sequential Proton Loss Electron Transfer Chemistry. *Journal of Organic Chemistry,* 70**,** 8982-8990.

Litwinienko, G. & Ingold, K. U. 2007. Solvent Effects on the Rates and Mechanisms of Reaction of Phenols with Free Radicals. *Accounts of Chemical Research,* 40**,** 222-230.

Liu, H., Zhu, L., Bocola, M., Chen, N., Spiess, A. C. & Schwaneberg, U. 2013a. Directed laccase evolution for improved ionic liquid resistance. *Green Chemistry,* 15**,** 1348-1355.

Liu, H., Zhou, P., Wu, X., Sun, J. & Chen, S. 2015. Radical scavenging by acetone: a new perspective to understand Laccase/ABTS inactivation and to recover redox mediator. *Molecules,* 20**,** 19907-19913.

Liu, Q.-P., Hou, X.-D., Li, N. & Zong, M.-H. 2012. Ionic liquids from renewable biomaterials: synthesis, characterization and application in the pretreatment of biomass. *Green Chemistry,* 14**,** 304-307.

Liu, S., Shi, Z., Li, L., Yu, S., Xie, C. & Song, Z. 2013b. Process of lignin oxidation in an ionic liquid coupled with separation. *RSC Advances,* 3**,** 5789-5793.

Liu, S., Zhang, C., Li, L., Yu, S., Xie, C., Liu, F. & Song, Z. 2014. Application of Dissociation Extraction in Oxidation Degradation Reaction of Lignin. *Ind. Eng. Chem. Res.,* 53**,** 19370-19374.

Lobo, V., Patil, A., Phatak, A. & Chandra, N. 2010. Free radicals, antioxidants and functional foods: Impact on human health. *Pharmacognosy Reviews,* 4**,** 118-26.

Lorenzo, M., Moldes, D., RodríGuez Couto, S. & Sanromán, M. 2005. Inhibition of laccase activity from Trametes versicolor by heavy metals and organic compounds. *Chemosphere,* 60**,** 1124-1128.

Lovelock, K. R. J., Ejigu, A., Loh, S. F., Men, S., Licence, P. & Walsh, D. A. 2011. On the diffusion of ferrocenemethanol in room-temperature ionic liquids: an electrochemical study. *Physical Chemistry Chemical Physics* 13**,** 10155-10164.

Lucarini, M. & Pedulli, G. F. 2010. Free radical intermediates in the inhibition of the autoxidation reaction. *Chemical Society Reviews,* 39**,** 2106-2119.

Macfaul, P. A., Ingold, K. U. & Lusztyk, J. 1996. Kinetic solvent effects on hydrogen atom abstraction from phenol, aniline, and diphenylamine. The importance of hydrogen bonding on their radical-trapping (antioxidant) activities. *Journal of Organic Chemistry,* 61**,** 1316-1321.

Mäki-Arvela, P., Anugwom, I., Virtanen, P., Sjöholm, R. & Mikkola, J. P. 2010. Dissolution of lignocellulosic materials and its constituents using ionic liquids—A review. *Industrial Crops and Products,* 32**,** 175-201.

Matsumura, E., Yamamoto, E., Numata, A., Kawano, T., Shin, T. & Murao, S. 1986. Structures of the laccase-catalyzed oxidation products of hydroxybenzoic acids in the presence of ABTS (2,2'-azino-di-(3-ethylbenzothiazoline-6-sulfonic acid)). *Agricultural and Biological Chemistry,* 50**,** 1355-1357.

Medina, F., Aguila, S., Baratto, M. C., Martorana, A., Basosi, R., Alderete, J. B. & Vazquez-Duhalt, R. 2013. Prediction model based on decision tree analysis for laccase mediators. *Enzyme and Microbial Technology,* 52**,** 68-76.

Miller, N. J., Rice-Evans, C., Davies, M. J., Gopinathan, V. & Milner, A. 1993. A novel method for measuring antioxidant capacity and its application to monitoring the antioxidant status in premature neonates. *Clinical science (London),* 84**,** 407-12.

Mohan, D., Pittman, C. U., Jr. & Steele, P. H. 2006. Pyrolysis of Wood/Biomass for Bio-oil: A Critical Review. *Energy Fuels,* 20**,** 848-889.

Molyneux, P. 2004. The use of the stable free radical diphenylpicrylhydrazyl (DPPH) for estimating antioxidant activity. *Songklanakarin Journal of Science and Technology,* 26**,** 211-219.

Moniruzzaman, M., Kamiya, N. & Goto, M. 2010a. Activation and stabilization of enzymes in ionic liquids. *Organic & Biomolecular Chemistry,* 8**,** 2887-2899.

Moniruzzaman, M., Nakashima, K., Kamiya, N. & Goto, M. 2010b. Recent advances of enzymatic reactions in ionic liquids. *Biochemical Engineering Journal,* 48**,** 295-314.

Moniruzzaman, M. & Ono, T. 2012. Ionic liquid assisted enzymatic delignification of wood biomass: A new 'green' and efficient approach for isolating of cellulose fibers. *Biochemical Engineering Journal,* 60**,** 156-160.

Morozova, O. V., Shumakovich, G. P., Shleev, S. V. & Yaropolov, Y. I. 2007. Laccase-mediator systems and their applications: A review. *Applied Biochemistry and Microbiology,* 43**,** 523-535.

Muhammad, N., Man, Z., Bustam, M. A., Mutalib, M. I. A. & Rafiq, S. 2013. Investigations of novel nitrile-based ionic liquids as pre-treatment solvent for extraction of lignin from bamboo biomass. *Journal of Industrial and Engineering Chemistry,* 19**,** 207-214.

Nanayakkara, S., Patti, A. F. & Saito, K. 2014. Chemical depolymerization of lignin involving the redistribution mechanism with phenols and repolymerization of depolymerized products. *Green Chemistry,* 16**,** 1897-1903.

O'toole, S., Pentlavalli, S. & Doherty, A. P. 2007. Behavior of Electrogenerated Bases in Room-Temperature Ionic Liquids. *Journal of Physical Chemistry B,* 111**,** 9281-9287.

O'mahony, A. M., Silvester, D. S., Aldous, L., Hardacre, C. & Compton, R. G. 2008. Effect of Water on the Electrochemical Window and Potential Limits of Room-Temperature Ionic Liquids. *Journal of Chemical & Engineering Data,* 53**,** 2884-2891.

Ohno, H. 2006. Functional Design of Ionic Liquids. *Bulletin of the Chemical Society of Japan,* 79**,** 1665-1680.

Oliveira, S. D., Souza, G. a. D., Eckert, C. R., Silva, T. A., Sobral, E. S., Fávero, O. A., Ferreira, M. J. P., Romoff, P. & Baader, W. J. 2014. Evaluation of antiradical assays used in determining the antioxidant capacity of pure compounds and plant extracts. *Química Nova,* 37**,** 497-503.

Osma, J. F., Toca-Herrera, J. L. & Rodriguez-Couto, S. 2010. Uses of laccases in the food industry. *Enzyme Research***,** No pp. given.

Ou, B., Huang, D., Hampsch-Woodill, M., Flanagan, J. A. & Deemer, E. K. 2002. Analysis of Antioxidant Activities of Common Vegetables Employing Oxygen Radical Absorbance Capacity (ORAC) and Ferric Reducing Antioxidant Power (FRAP) Assays: A Comparative Study. *Journal of Agricultural and Food Chemistry,* 50**,** 3122-3128.

Ozcelik, B., Lee, J. H. & Min, D. B. 2003. Effects of Light, Oxygen, and pH on the Absorbance of 2,2-Diphenyl-1-picrylhydrazyl. *Journal of Food Science,* 68**,** 487-490.

Palafox-Carlos, H., Gil-Chavez, J., Sotelo-Mundo, R. R., Namiesnik, J., Gorinstein, S. & Gonzalez-Aguilar, G. A. 2012. Antioxidant interactions between major phenolic compounds found in 'Ataulfo' mango pulp: chlorogenic, gallic, protocatechuic and vanillic acids. *Molecules,* 17**,** 12657-12664.

Pardini, V. L., Smith, C. Z., Utley, J. H. P., Vargas, R. R. & Viertler, H. 1991. Electroorganic reactions. 38. Mechanism of electrooxidative cleavage of lignin model dimers. *J. Org. Chem.,* 56**,** 7305-13.

Perez-Jimenez, J. & Saura-Calixto, F. 2006. Effect of solvent and certain food constituents on different antioxidant capacity assays. *Food Research International,* 39**,** 791-800.

Piontek, K., Antorini, M. & Choinowski, T. 2002. Crystal Structure of a Laccase from the FungusTrametes versicolor at 1.90-Å Resolution Containing a Full Complement of Coppers. *Journal of Biological Chemistry,* 277**,** 37663-37669.

Plechkova, N. V. & Seddon, K. R. 2008. Applications of ionic liquids in the chemical industry. *Chemical Society reviews,* 37**,** 123-150.

Prior, R. L., Wu, X. & Schaich, K. 2005. Standardized Methods for the Determination of Antioxidant Capacity and Phenolics in Foods and Dietary Supplements. *Journal of Agricultural and Food Chemistry,* 53**,** 4290-4302.

Pulido, R., Bravo, L. & Saura-Calixto, F. 2000. Antioxidant activity of dietary polyphenols as determined by a modified ferric reducing/antioxidant power assay. *Journal of Agricultural and Food Chemistry,* 48**,** 3396-3402.

Rahimi, A., Ulbrich, A., Coon, J. J. & Stahl, S. S. 2014. Formic-acid-induced depolymerization of oxidized lignin to aromatics. *Nature (London, U. K.),* 515**,** 249-252.

Rancaño, G., Lorenzo, M., Molares, N., RodríGuez Couto, S. & Sanromán, M. Á. 2003. Production of laccase by Trametes versicolor in an airlift fermentor. *Process Biochemistry,* 39**,** 467-473.

Re, R., Pellegrini, N., Proteggente, A., Pannala, A., Yang, M. & Rice-Evans, C. 1999. Antioxidant activity applying an improved ABTS radical cation decolorization assay. *Free Radical Biology & Medicine,* 26**,** 1231-1237.

Rehmann, L., Ivanova, E., Ferguson, J. L., Gunaratne, H. Q. N., Seddon, K. R. & Stephens, G. M. 2012. Measuring the effect of ionic liquids on laccase activity using a simple, parallel method. *Green Chemistry,* 14**,** 725-733.

Reichert, E., Wintringer, R., Volmer, D. A. & Hempelmann, R. 2012. Electro-catalytic oxidative cleavage of lignin in a protic ionic liquid. *Physical Chemistry Chemical Physics,* 14**,** 5214-5221.

Rice-Evans, C., Miller, N. J. & Paganga, G. 1996. Structure-antioxidant activity relationships of flavonoids and phenolic acids. *Free Radical Biology & Medicine,* 20**,** 933-956.

Riva, S. 2006. Laccases: blue enzymes for green chemistry. *Trends in Biotechnology,* 24**,** 219-226.

Rochefort, D., Bourbonnais, R., Leech, D. & Paice, M. G. 2002. Oxidation of lignin model compounds by organic and transition metal-based electron transfer mediators. *Chemical Communications (Cambridge, United Kingdom)***,** 1182-1183.

Rochefort, D., Leech, D. & Bourbonnais, R. 2004. Electron transfer mediator systems for bleaching of paper pulp. *Green Chemistry,* 6**,** 14-24.

Rodriguez, H. & Brennecke, J. F. 2006. Temperature and composition dependence of the density and viscosity of binary mixtures of water plus ionic liquid. *Journal of Chemical and Engineering Data,* 51**,** 2145-2155.

Rodriguez, O., Tavares, A. P. M., Cristovao, R. & Macedo, E. A. Ionic liquids: alternative reactive media for oxidative enzymes. 2011. InTech, 499-516.

Rodríguez, O., Cristóvão, R., Tavares, A. M. & Macedo, E. 2011. Study of the Alkyl Chain Length on Laccase Stability and Enzymatic Kinetic with Imidazolium Ionic Liquids. *Applied Biochemistry and Biotechnology,* 164**,** 524-533.

Rubim, J. C., Trindade, F. A., Gelesky, M. A., Aroca, R. F. & Dupont, J. 2008. Surface-Enhanced Vibrational Spectroscopy of Tetrafluoroborate 1-n-Butyl-3-methylimidazolium (BMIBF4) Ionic Liquid on Silver Surfaces. *The Journal of Physical Chemistry C,* 112**,** 19670-19675.

Ruiz-Duenas, F. J. & Martinez, A. T. 2009. Microbial degradation of lignin: how a bulky recalcitrant polymer is efficiently recycled in nature and how we can take advantage of this. *Microbial Biotechnology,* 2**,** 164-177.

Saito, T., Perkins, J. H., Vautard, F., Meyer, H. M., Messman, J. M., Tolnai, B. & Naskar, A. K. 2014. Methanol Fractionation of Softwood Kraft Lignin: Impact on the Lignin Properties. *ChemSusChem,* 7**,** 221-228.

Salamone, M. & Bietti, M. 2015. Tuning Reactivity and Selectivity in Hydrogen Atom Transfer from Aliphatic C-H Bonds to Alkoxyl Radicals: Role of Structural and Medium Effects. *Accounts of Chemical Research,* 48**,** 2895-2903.

Sanchez-Moreno, C., Larrauri, J. A. & Saura-Calixto, F. 1998. A procedure to measure the antiradical efficiency of polyphenols. *Journal of the Science of Food and Agriculture,* 76**,** 270-276.

Sarkar, S., Pramanik, R., Seth, D., Setua, P. & Sarkar, N. 2009. Photoinduced electron transfer (PET) from N,N-dimethylaniline to 7-amino Coumarin dyes in a room temperature ionic liquid (RTIL): Slowing down of electron transfer rate compared to conventional solvent. *Chemical Physics Letters,* 477**,** 102-108.

Schlesier, K., Harwat, M., Bohm, V. & Bitsch, R. 2002. Assessment of antioxidant activity by using different in vitro methods. *Free Radical Research,* 36**,** 177-187.

Schmidt-Naake, G., Schmalfuß, A. & Woecht, I. 2008. Free radical polymerization in ionic liquids—Influence of the IL-concentration and temperature. *Chemical Engineering Research and Design,* 86**,** 765-774.

Schroder, I., Steckhan, E. & Liese, A. 2003. In situ NAD(+) regeneration using 2,2 '-azinobis(3-ethylbenzothiazoline-6-sulfonate) as an electron transfer mediator. *Journal of Electroanalytical Chemistry,* 541**,** 109-115.

Sette, M., Wechselberger, R. & Crestini, C. 2011. Elucidation of Lignin Structure by Quantitative 2D NMR. *Chem. - Eur. J.,* 17**,** 9529-9535, S9529/1-S9529/2.

Sharma, O. P. & Bhat, T. K. 2009. DPPH antioxidant assay revisited. *Food Chemistry,* 113**,** 1202-1205.

Shin, K.-S. & Lee, Y.-J. 1999. Depolymerisation of lignosulfonate by peroxidase of the white-rot basidiomycete, Pleurotus ostreatus. *Biotechnology Letters,* 21**,** 585-588.

Shipovskov, S., Gunaratne, H. Q. N., Seddon, K. R. & Stephens, G. 2008. Catalytic activity of laccases in aqueous solutions of ionic liquids. *Green Chemistry,* 10**,** 806-810.

Shiraishi, T., Sannami, Y., Kamitakahara, H. & Takano, T. 2013. Comparison of a series of laccase mediators in the electro-oxidation reactions of non-phenolic lignin model compounds. *Electrochimica Acta,* 106**,** 440-446.

Shumakovich, G. P., Shleev, S. V., Morozova, O. V., Khohlov, P. S., Gazaryan, I. G. & Yaropolov, A. I. 2006. Electrochemistry and kinetics of fungal laccase mediators. *Bioelectrochemistry,* 69**,** 16-24.

Snook, G. A., Best, A. S., Pandolfo, A. G. & Hollenkamp, A. F. 2006. Evaluation of a Ag|Ag+ reference electrode for use in room temperature ionic liquids. *Electrochemistry Communications,* 8**,** 1405-1411.

Stärk, K., Taccardi, N., Bösmann, A. & Wasserscheid, P. 2010. Oxidative Depolymerization of Lignin in Ionic Liquids. *ChemSusChem,* 3**,** 719-723.

Stiefel, S., Schmitz, A., Peters, J., Di Marino, D. & Wessling, M. 2016. An integrated electrochemical process to convert lignin to value-added products at mild conditions. *Green Chemistry*.

Strehmel, V., Rexhausen, H., Strauch, P., Goernitz, E. & Strehmel, B. 2008. Temperature dependence of interactions between stable piperidine-1-yloxyl derivatives and an ionic liquid. *ChemPhysChem,* 9**,** 1294-1302.

Strehmel, V., Wishart, J. F., Polyansky, D. E. & Strehmel, B. 2009. Recombination of photogenerated lophyl radicals in imidazolium-based ionic liquids. *ChemPhysChem,* 10**,** 3112-3118.

Strehmel, V., Rexhausen, H., Strauch, P. & Strehmel, B. 2010. Temperature Dependence of Interactions Between Stable Piperidine-1-yloxyl Derivatives and a Semicrystalline Ionic Liquid. *ChemPhysChem,* 11**,** 2182-2190.

Strehmel, V. 2012. Radicals in Ionic Liquids. *ChemPhysChem,* 13**,** 1649-1663.

Strehmel, V., Berdzinski, S. & Rexhausen, H. 2014a. Interactions between ionic liquids and radicals. *Journal of Molecular Liquids,* 192**,** 153-170.

Strehmel, V., Wetzel, H. & Laschewsky, A. 2014b. Ionic Liquids as Advantageous Reaction Media for Free Radical Polymerization. *Macromolecular Symposia,* 342**,** 78-85.

Sun, N., Rahman, M., Qin, Y., Maxim, M. L., Rodriguez, H. & Rogers, R. D. 2009. Complete dissolution and partial delignification of wood in the ionic liquid 1-ethyl-3-methylimidazolium acetate. *Green Chemistry,* 11**,** 646-655.

Sun, Y.-C., Xu, J.-K., Xu, F. & Sun, R.-C. 2013. Efficient separation and physico-chemical characterization of lignin from eucalyptus using ionic liquid–organic solvent and alkaline ethanol solvent. *Industrial Crops and Products,* 47**,** 277-285.

Tai, A., Sawano, T., Yazama, F. & Ito, H. 2011. Evaluation of antioxidant activity of vanillin by using multiple antioxidant assays. *Biochimica et Biophysica Acta,* 1810**,** 170-177.

Tan, S. S. Y., Macfarlane, D. R., Upfal, J., Edye, L. A., Doherty, W. O. S., Patti, A. F., Pringle, J. M. & Scott, J. L. 2009. Extraction of lignin from lignocellulose at atmospheric pressure using alkylbenzenesulfonate ionic liquid. *Green Chemistry,* 11**,** 339-345.

Tang, S., Baker, G. A. & Zhao, H. 2012. Ether- and Alcohol-Functionalized Task-Specific Ionic Liquids: Attractive Properties and Applications. *Chemical Society reviews,* 41**,** 4030-4066.

Tanner, E. E. L., Yau, H. M., Hawker, R. R., Croft, A. K. & Harper, J. B. 2013. Does the cation really matter? The effect of modifying an ionic liquid cation on an SN2 process. *Organic & Biomolecular Chemistry,* 11**,** 6170-6175.

Tavares, A. P. M., Rodriguez, O. & Macedo, E. A. 2008. Ionic liquids as alternative co-solvents for laccase: Study of enzyme activity and stability. *Biotechnology and Bioengineering,* 101**,** 201-207.

Tavares, A. P. M., Pereira, J. a. N. & Xavier, A. M. R. B. 2012. Effect of ionic liquids activation on laccase from Trametes versicolor: Enzymatic stability and activity. *Engineering in Life Sciences,* 12**,** 648-655.

Tavares, A. P. M., Rodríguez, O., Fernández-Fernández, M., Domínguez, A., Moldes, D., Sanromán, M. A. & Macedo, E. A. 2013. Immobilization of laccase on modified silica: Stabilization, thermal inactivation and kinetic behaviour in 1-ethyl-3-methylimidazolium ethylsulfate ionic liquid. *Bioresource Technology,* 131**,** 405-412.

Taylor, A. W., Puttick, S. & Licence, P. 2012. Probing Solvation in Ionic Liquids via the Electrochemistry of the DPPH Radical. *Journal of the American Chemical Society,* 134**,** 15636-15639.

Tejado, A., Peña, C., Labidi, J., Echeverria, J. M. & Mondragon, I. 2007. Physico-chemical characterization of lignins from different sources for use in phenol–formaldehyde resin synthesis. *Bioresource Technology,* 98**,** 1655-1663.

Thielemans, W., Can, E., Morye, S. S. & Wool, R. P. 2002. Novel applications of lignin in composite materials. *Journal of Applied Polymer Science,* 83**,** 323-331.

Tolba, R., Tian, M., Wen, J., Jiang, Z.-H. & Chen, A. 2010. Electrochemical oxidation of lignin at IrO2-based oxide electrodes. *Journal of Electroanalytical Chemistry,* 649**,** 9-15.

Toledano, A., Serrano, L. & Labidi, J. 2012. Organosolv lignin depolymerization with different base catalysts. *Journal of Chemical Technology and Biotechnology,* 87**,** 1593-1599.

Valgimigli, L., Ingold, K. U. & Lusztyk, J. 1996. Solvent Effects on the Reactivity and Free Spin Distribution of 2,2-Diphenyl-1-picrylhydrazyl Radicals1. *The Journal of Organic Chemistry,* 61**,** 7947-7950.

Valgimigli, L., Banks, J. T., Lusztyk, J. & Ingold, K. U. 1999. Solvent Effects on the Antioxidant Activity of Vitamin E. *Journal of Organic Chemistry,* 64**,** 3381-3383.

Van Den Berg, R., Haenen, G. R. M. M., Van Den Berg, H. & Bast, A. 1999. Applicability of an improved Trolox equivalent antioxidant capacity (TEAC) assay for evaluation of antioxidant capacity measurements of mixtures. *Food Chemistry,* 66**,** 511-517.

Van Rantwijk, F. & Sheldon, R. A. 2007. Biocatalysis in Ionic Liquids. *Chemical Reviews,* 107**,** 2757-2785.

Varanasi, P., Singh, P., Auer, M., Adams, P., Simmons, B. & Singh, S. 2013. Survey of renewable chemicals produced from lignocellulosic biomass during ionic liquid pretreatment. *Biotechnology for Biofuels,* 6**,** 14.

Vishtal, A. G. & Kraslawski, A. 2011. CHALLENGES IN INDUSTRIAL APPLICATIONS OF TECHNICAL LIGNINS. *BioResources; Vol 6, No 3 (2011),* 6**,** 3547-3568.

Wang, H., Tucker, M. & Ji, Y. 2013. Recent Development in Chemical Depolymerization of Lignin: A Review. *Journal of Applied Chemistry,* 2013**,** 1-9.

Wang, J., Zheng, Y. & Zhang, S. 2010. The application of ionic liquids in dissolution and separation of lignocellulose. *In:* EGUCHI, K. (ed.) *Clean Energy Systems and Experiences.* Sciyo.

Wang, Y.-N., Lau, K.-C., Lam, W. W. Y., Man, W.-L., Leung, C.-F. & Lau, T.-C. 2009. Kinetics and Mechanism of the Oxidation of Ascorbic Acid in Aqueous Solutions by a trans-Dioxoruthenium(VI) Complex. *Inorganic Chemistry,* 48**,** 400-406.

Wen, J.-L., Yuan, T.-Q., Sun, S.-L., Xu, F. & Sun, R.-C. 2014. Understanding the chemical transformations of lignin during ionic liquid pretreatment. *Green Chemistry,* 16**,** 181-190.

Werner, S., Haumann, M. & Wasserscheid, P. 2010. Ionic Liquids in Chemical Engineering. *Annual Review of Chemical and Biomolecular Engineering,* 1**,** 203-230.

Wolfenden, B. S. & Willson, R. L. 1982. Radical-cations as reference chromogens in kinetic studies of one-electron-transfer reactions: pulse-radiolysis studies of 2,2'-azinobis(3-ethylbenzothiazoline-6-sulfonate). *Journal of the Chemical Society, Perkin Transactions 2***,** 805-12.

Wong, D. W. S. 2009. Structure and action mechanism of ligninolytic enzymes. *Appl. Biochem. Biotechnol.,* 157**,** 174-209.

Wright, J. S., Johnson, E. R. & Dilabio, G. A. 2001. Predicting the Activity of Phenolic Antioxidants: Theoretical Method, Analysis of Substituent Effects, and Application to Major Families of Antioxidants. *Journal of the American Chemical Society,* 123**,** 1173-1183.

Wu, G., Heitz, M. & Chornet, E. 1994. Improved Alkaline Oxidation Process for the Production of Aldehydes (Vanillin and Syringaldehyde) from Steam-Explosion Hardwood Lignin. *Industrial & Engineering Chemistry Research,* 33**,** 718-723.

Yang, Y., Fan, H., Song, J., Meng, Q., Zhou, H., Wu, L., Yang, G. & Han, B. 2015. Free radical reaction promoted by ionic liquid: a route for metal-free oxidation depolymerization of lignin model compound and lignin. *Chem. Commun. (Cambridge, U. K.),* 51**,** 4028-4031.

Yau, H. M., Barnes, S. A., Hook, J. M., Youngs, T. G. A., Croft, A. K. & Harper, J. B. 2008. The importance of solvent reorganisation in the effect of an ionic liquid on a unimolecular substitution process. *Chemical Communications (Cambridge, U. K.)***,** 3576-3578.

Yau, H. M., Chan, S. J., George, S. R. D., Hook, J. M., Croft, A. K. & Harper, J. B. 2009. Ionic liquids: just molten salts after all? *Molecules,* 14**,** 2521-2534.

Yau, H. M., Keaveney, S. T., Butler, B. J., Tanner, E. E. L., Guerry, M. S., George, S. R. D., Dunn, M. H., Croft, A. K. & Harper, J. B. 2013. Towards solvent-controlled reactivity in ionic liquids. *Pure and Applied Chemistry,* 85**,** 1979-1990.

Yoshida, T., Mori, K., Hatano, T., Okumura, T., Uehara, I., Komagoe, K., Fujita, Y. & Okuda, T. 1989. Studies on inhibition mechanism of autoxidation by tannins and flavonoids. V. Radical-scavenging effects of tannins and related polyphenols on 1,1-diphenyl-2-picrylhydrazyl radical. *CHEMICAL & PHARMACEUTICAL BULLETIN,* 37**,** 1919-1921.

Yu, X., Zou, F., Li, Y., Lu, L., Huang, X. & Qu, Y. 2013. Effect of three trifluoromethanesulfonate ionic liquids on the activity, stability and conformation of laccase. *International Journal of Biological Macromolecules,* 56**,** 62-68.

Yuan, T.-Q., Xu, F. & Sun, R.-C. 2013. Role of lignin in a biorefinery: separation characterization and valorization. *J. Chem. Technol. Biotechnol.,* 88**,** 346-352.

Zakzeski, J., Bruijnincx, P. C. A., Jongerius, A. L. & Weckhuysen, B. M. 2010a. The Catalytic Valorization of Lignin for the Production of Renewable Chemicals. *Chemical Reviews (Washington, DC, U. S.),* 110**,** 3552-3599.

Zakzeski, J., Jongerius, A. L. & Weckhuysen, B. M. 2010b. Transition metal catalyzed oxidation of Alcell lignin, soda lignin, and lignin model compounds in ionic liquids. *Green Chemistry,* 12**,** 1225-1236.

Zakzeski, J., Bruijnincx, P. C. A. & Weckhuysen, B. M. 2011. In situ spectroscopic investigation of the cobalt-catalyzed oxidation of lignin model compounds in ionic liquids. *Green Chemistry,* 13**,** 671-680.

Zhang, H. Y. & Ji, H. F. 2006. How vitamin E scavenges DPPH radicals in polar protic media. *New Journal of Chemistry,* 30**,** 503-504.

Zhang, Q.-G., Wang, N.-N. & Yu, Z.-W. 2010. The Hydrogen Bonding Interactions between the Ionic Liquid 1-Ethyl-3-Methylimidazolium Ethyl Sulfate and Water. *The Journal of Physical Chemistry B,* 114**,** 4747-4754.

Zhang, Y. L., Zhang, H. B., Zhu, Y. S. & Huang, F. 2011. The effect of laccase on cellulase-treated lignin in 1-n-butyl-3-methylimidazolium chloride/H2O homogeneous and H2O heterogeneous solutions. *African Journal of Biotechnology,* 10**,** 15647-15655.

Zhang, Y. M., Peng, Y., Yin, X. L., Liu, Z. H. & Li, G. 2014. Degradation of lignin to BHT by electrochemical catalysis on Pb/PbO2 anode in alkaline solution. *Journal of Chemical Technology and Biotechnology,* 89**,** 1954-1960.

Zhao, H. 2010. Methods for stabilizing and activating enzymes in ionic liquids - a review. *Journal of Chemical Technology and Biotechnology,* 85**,** 891-907.

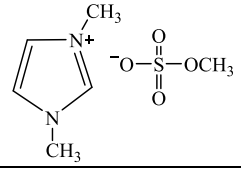
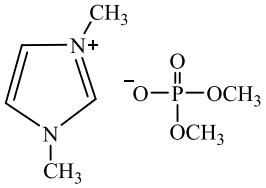
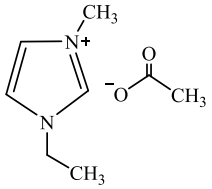
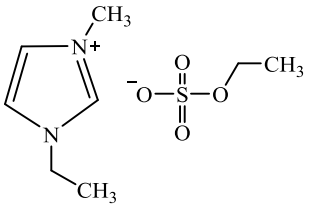
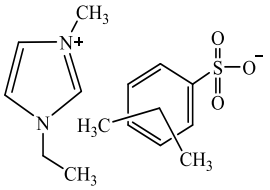
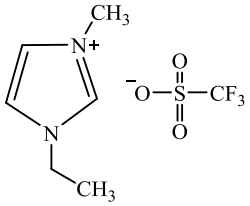
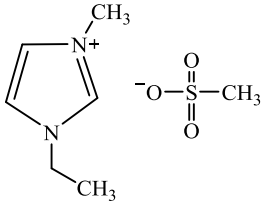
Zhao, X., Cheng, K. & Liu, D. 2009. Organosolv pretreatment of lignocellulosic biomass for enzymatic hydrolysis. *Applied Microbiology and Biotechnology,* 82**,** 815-827.

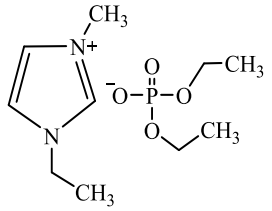
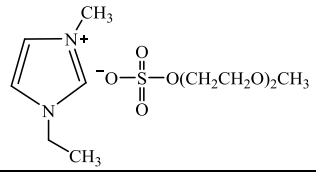
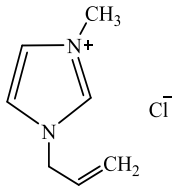
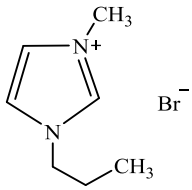
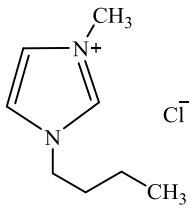
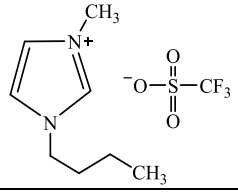
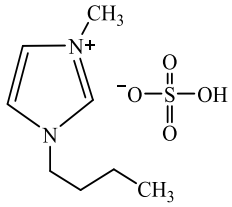
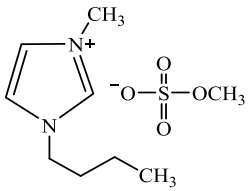
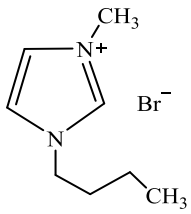
Zhu, H. B., Wang, L., Chen, Y. M., Li, G. Y., Li, H., Tang, Y. & Wan, P. Y. 2014. Electrochemical depolymerization of lignin into renewable aromatic compounds in a non-diaphragm electrolytic cell. *RSC Advances,* 4**,** 29917-29924.

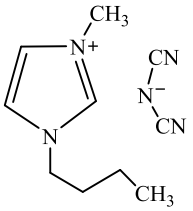
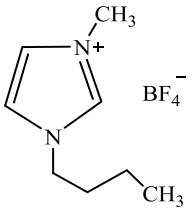
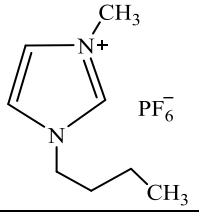
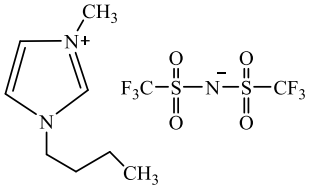
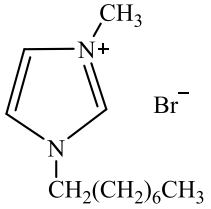
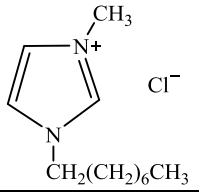
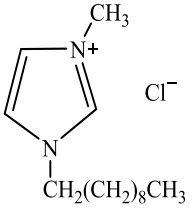
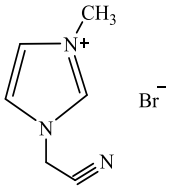
Zhu, Y., Karen Tang, Y. & Narayan, S. H. 2013. Applications of Ionic Liquids in Lignin Chemistry.

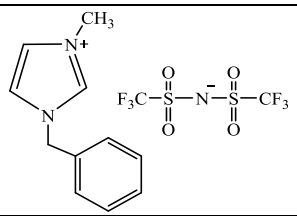
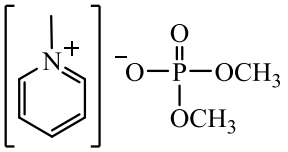
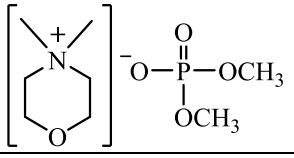
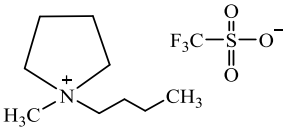
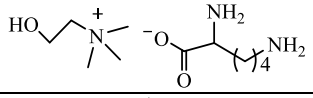
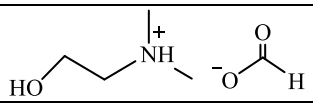
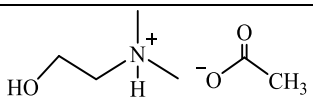
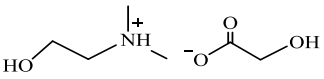
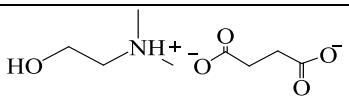
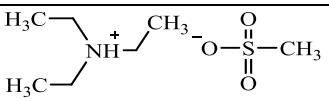
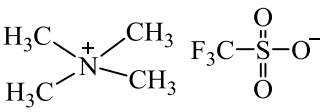
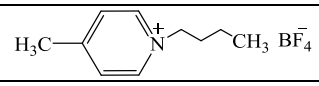
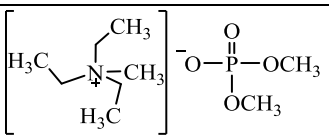
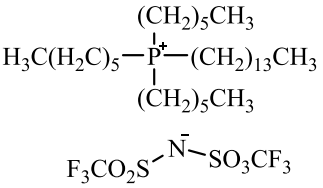
APPENDICES

Appendix A.1: Names, abbreviation and chemical structure of Ionic liquids mention in this study

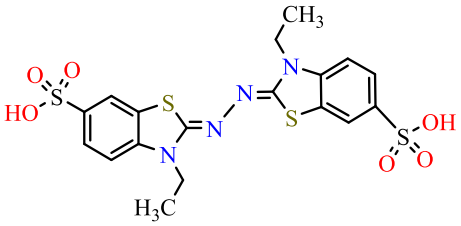
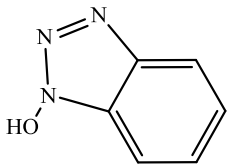
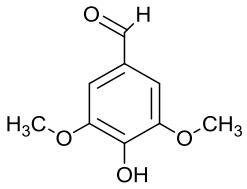
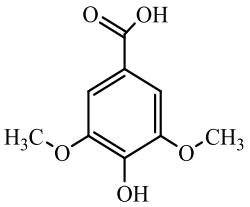
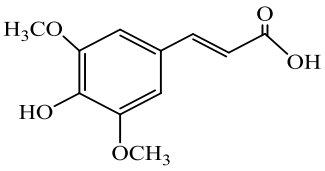
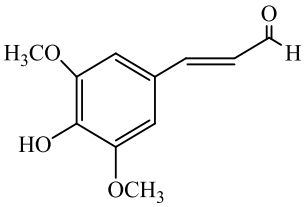
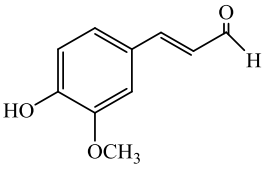
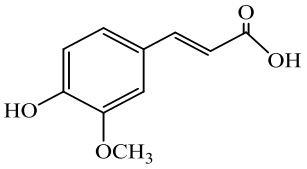
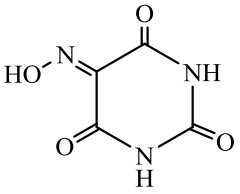
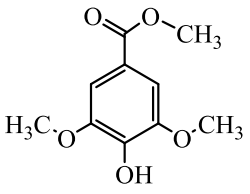
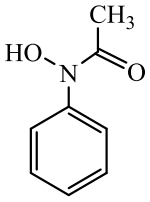
Abbreviation	Name	Structure
$[C_1mim][C_1SO_4]$ ($[Mmim][MeSO_4]$)	1,3-dimethylimidazolium methyl sulfate	
$[C_1mim][C_1C_1PO_4]$ $[C_1mim][Me_2PO_4]$	1,3-dimethylimidazolium dimethyl phosphate	
$[C_2mim][C_1CO_2]$ ($[Emim][OAc]$, ($[C_2mim][OAc]$)	1-ethyl-3-methylimidazolium acetate	
$[C_2mim][C_2SO_4]$ ($[Emim]$ $[EtSO_4]$	1-ethyl-3-methylimidazolium ethyl sulfate	
$[C_2mim][ABS]$ ($[Emim][ABS]$)	1-ethyl-3-methylimidazolium xylenesulfonate	
$[C_2mim][CF_3SO_3]$ ($[Emim][OTf]$, $[C_2mim][OTf]$)	1-ethyl-3-methylimidazolium trifluoro methane sulfonate	
$[C_2mim][C_1SO_3]$ ($[Emim][MeSO_3]$)	1-ethyl-3-methylimidazolium methane sulfonate	

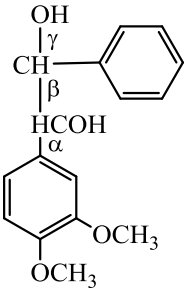
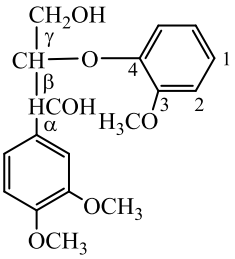
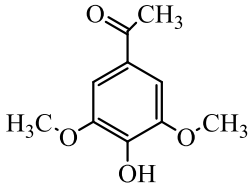
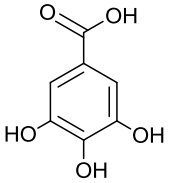
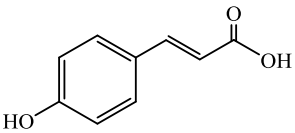
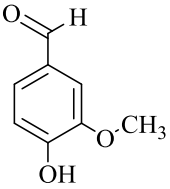
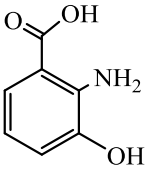
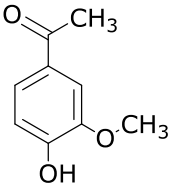
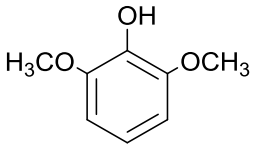
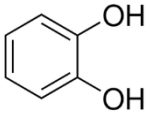
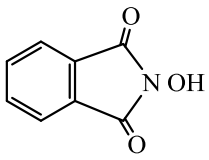
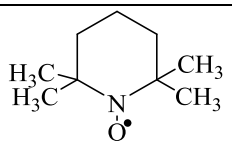
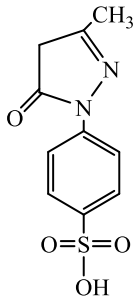
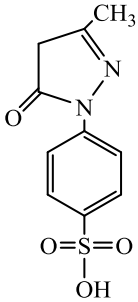
$[C_2mim][C_2C_2PO_4]$ ($[C_2mim][Et_2PO_4]$, EMIM DEP)	1-ethyl-3-methylimidazolium diethylphosphate	
$[C_2mim][MDEGSO_4]$	1-ethyl 3-methylimidazolium 2-(2-methoxyethoxy) ethyl sulfate	
$[C=C_2mim]Cl$ ([Amim][Cl])	1-allyl-3-methylimidazolium chloride	
$[C_3mim]Br$ ([PrlMIM][Br])	1-propyl-3-methylimidazolium bromide	
$[C_4mim]Cl$ ([Bmim][Cl])	1-butyl-3-methylimidazolium chloride	
$[C_4mim][OTf]$ ($[Bmim][CF_3SO_3]$)	1-butyl-3-methylimidazolium trifluoro methane sulfonate	
$[C_4mim][HSO_4]$ ($[C_4C_1im][HSO_4]$)	1-butyl-3-methylimidazolium hydrogen sulfate	
$[C_4mim][C_1SO_4]$ ($[Bmim][MeSO_4]$)	1-butyl-3-methylimidazolium methyl sulfate	
$[C_4mim]Br$ [Bmim]Br	1-butyl-3-methylimidazolium bromide	

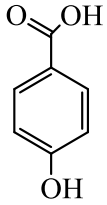
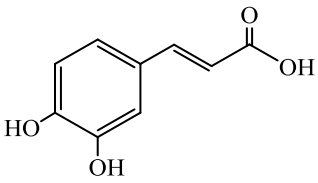
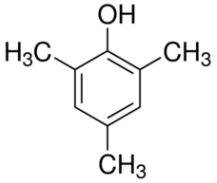
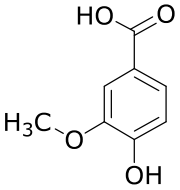
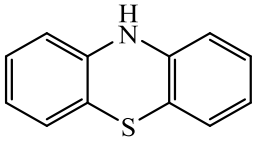
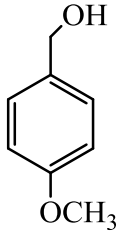
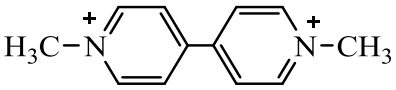
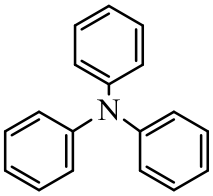
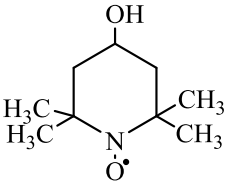
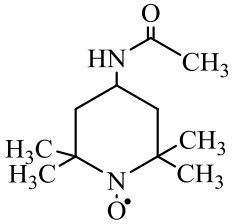
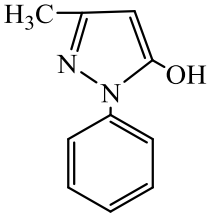
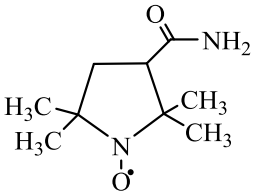
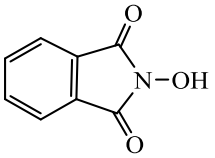
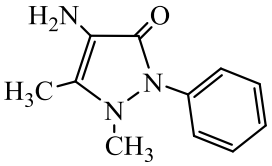
$[C_4mim][N(CN_2)]$	1-butyl-3-methylimidazolium dicyanamide	
$[C_4mim][BF_4]$ ([Bmim][BF_4])	1-butyl-3-methylimidazolium tetrafluoroborate	
$[C_4mim][PF_6]$ [Bmim][PF_6]	1-butyl-3-methylimidazolium hexafluoro phosphate	
$[C_4mim][NTf_2]$ [Bmim][NTf_2]	1-butyl-3-methylimidazolium bis(trifluoromethylsulfonyl)-imide	
$[C_6mim]Br$	1-octyl-3- methylimidazolium bromide	
$[C_8mim]Cl$	1-octyl-3- methylimidazolium chloride	
$[C_{10}mim]Cl$	1-decyl-3-methylimidazolium chloride	
[Cyanomim]Br	1-(2-cyanoethyl)-3-methylimidazolium bromide (1-cyano-3-methylimidazolium bromide)	

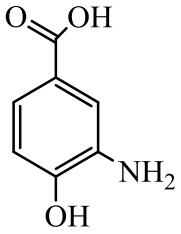
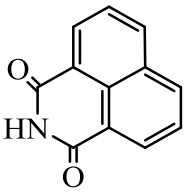
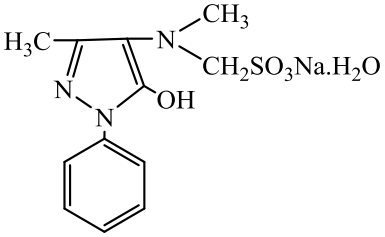
[Bnmim][NTf_2]	1-benzyl-3-methylimidazolium bis(trifluoromethylsulfonyl)-imide	
[C_1py][$C_1C_1PO_4$] ([mPy][Me_2PO_4])	methyl pyridinium dimethyl phosphate	
[C_1mmo][$C_1C_1PO_4$] ([mmo][Me_2PO_4])	4,4-dimethylmorpholin-4-ium dimethyl phosphate	
[C_4mpyr][TfO]	1-butyl 1-methylpyrrolidinium trifluoro methane sulfonate	
[Ch][Lys]	Cholinium lysine	
[DMEA][HCOO] (DMEAF)	N,N-dimethyl ethanol ammonium formate	
[DMEA][C_1CO_2] (DMEAA)	N,N-dimethyl ethanol ammonium acetate	
[DMEA][glycolate] [DMEA][C_1OHCO_2] (DMEAG)	N,N-dimethyl ethanol ammonium glycolate	
[DMEA][succinate] DMEAS	N,N-dimethyl ethanol ammonium succinate	
[HN_{222}][C_1SO_3] ([$HNEt_3$][$MeSO_3$])	Triethyl ammonium methane sulfonate	
[TMA][TfO]	Tetra-methylammonium trifluoro methane sulfonate	
[4-BMP][BF_4]	4-methyl-N-butyl-pyridinium tetrafluoroborate	
[N_{1222}][$C_1C_1PO_4$] ([mtetn][Me_2PO_4])	N, N-diethyl-N-methylethanaminium dimethyl phosphate	
[$P_{6,6,6,14}$][Tf_2N]	Tetradecyl(trihexyl) phosphonium bis[(trifluoromethane) sulfonyl] imide	

Appendix A.2: Names, abbreviation and chemical structure of the mediators mention in this study

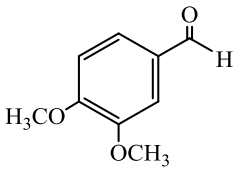
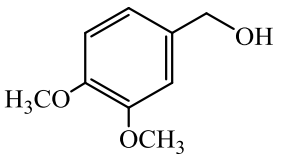
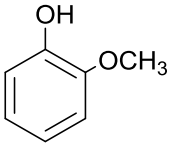
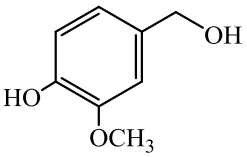
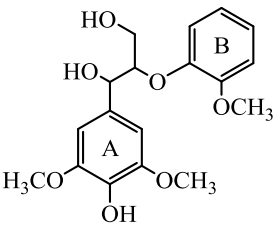
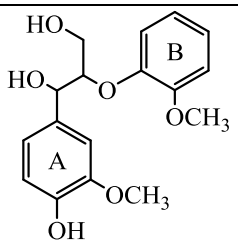
Mediator (Structure)	Mediator (Structure)
 2,2'-azino-bis(3-ethylbenthiazoline-6-sulfonic acid) diammonium salt **(ABTS)**	 1-Hydroxybenzotriazole **(HBT)**
 Syringaldehyde	 Syringic acid
 Sinapic acid	 Sinapyl aldehyde
 Coniferyl aldehyde	 Ferulic acid
 Violuric Acid (VLA)	 Methyl syringate
Potassium octacyanomolybdate (IV) (MoCN) $K_4Mo(CN)_8$	 *N*-hydroxyacetanilide (NHA)

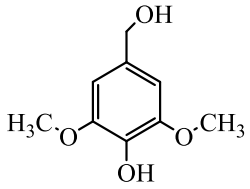
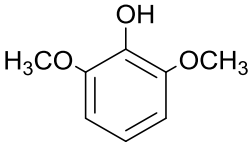
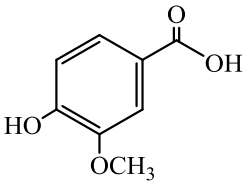
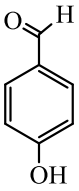
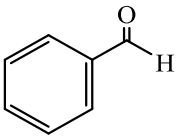
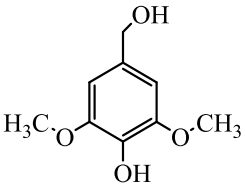
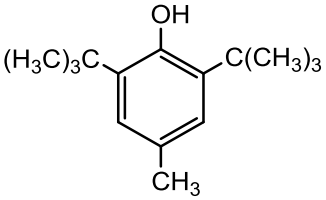
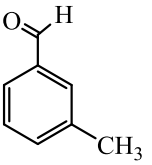
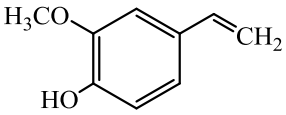
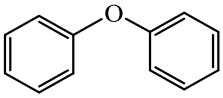
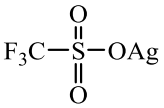
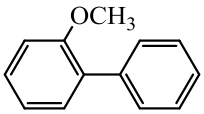
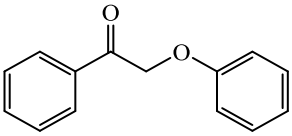
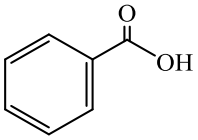
 1-(3,4-dimethoxyphenyl)- 2-phenylethanediol	 1-(3,4-dimethoxyphenyl)-2-(2-methoxyphenoxy) propane-1,3-diol
 Acetosyringone	 Gallic acid (GA)
 *p*-Coumaric acid	 Vanillin
 3-Hydroxyanthranilic acid (HAA)	 Acetovanillone
 2,6-dimethoxyphenol (syringol) (DMP)	 Catechol
 N-hydroxyphthalimide (NHPI)	 2,2′,6,6′-tetramethylpiperidine-N-oxyl (TEMPO)
 1-(4′-sulphophenyl)-3 methyl-pyrazolone-5 (SPP-p)	 1-(3′-sulphophenyl)-3 methyl-5-pyrazolone (SPP-m)

 4-hydroxybenzoic acid (HBA)	 Caffeic acid (CA)
 Mesitol (2,4,6-trimethylphenol)	 Vanillic acid (VaA)
 Phenothiazine (PT)	 4-methoxybenzyl alcohol
 Methyl viologen (MV)	 Triphenylamine (TPA)
 4-hydroxy-TEMPO	 4-acetamido-TEMPO
 1-phenyl-3methyl-5-pyrazolone (PP)	 3-carbamoyl-PROXYL-ene
 N hydroxyphthalimide N-(OH) PhI	 1-phenyl-2,3- dimethyl-4-amino-5-pyrazolone (PPA)

 3-amino-(6-hydroxy)-benzoic acid (HABA)	 1,8 N-hydroxynaphthalimide N-(OH) NaPhI
 1-phenyl-3-methyl--4-methylamino--pyrazolone-5-N(4)-methanesulfonate (PPA-Na)	

Appendix A.3: Names, abbreviation and chemical structure of the compounds mention in this study

Compound (Structure)	Compound (Structure)
 Veratryl aldehyde	 Veratryl alcohol (VA)
 Guaiacol	 Vanillyl alcohol
 Syringylglycol β-guaiacyl ether	 Guaiacylglycerol β-guaiacyl ether
Guaiacylglycol β-guaiacyl ether	Syringylglycerol β-guaiacyl ether
Dehydrodivanillyl alcohol	

 Syringyl alcohol	 Syringol
 Vanillic acid	 *P*-hydroxybenzaldehyde
 Benzaldehyde	 Syringol aldehyde
 2,6-Di-tert-butyl-4-methylphenol	 *m*-Tolualdehyde
 2-Methoxy-4-vinylphenol	 Diphenyl ether
 Silver trifluoromethanesulfonate (silver triflate)	 2-Methoxybiphenyl
 2-Phenoxyacetophenone	 Benzoic acid

Appendix A.4: Laccase (EC 1.10.3.2) Enzyme Assay with ABTS as a Substrate

Sodium Acetate buffer preparation

- 0.82 g of sodium acetate (CH_3COONa, Molar Mass = 82.0343 g/mol) was weighted into a 100 ml volumetric flask and made up the volume with distilled water to make 0.1 M solution.

- 0.60 g of Acetic acid ($C_2H_4O_2$, Molar Mass = 60.05 g/mol) was weighted into a 100 ml volumetric flask and made up volume with distilled water to make 0.1 M solution.

- 70 ml of sodium acetate solution (0.1 M) was mixed with 30 ml of acetic acid solution (0.1 M) at 30 °C to make pH = 5 buffer.

- Acetate buffer was stored at room temperature at the end of the experiment to be warmed to 30 °C again for future use.

Laccase stock solution

- 10 mg (0.001 g) laccase was weighted into a 10 ml volumetric flask and made up to volume with acetate buffer to make a solution with the nominal concentration of 1.0 mg/ml.

- 400 µL aliquots of the laccase stock solution (1mg/ml) were transferred to Eppendorf tubes and frozen for future use (These are in 0.1 M acetate buffer, pH 5 at 30°C).

Laccase and ABTS solutions

- Laccase stock solution (1.0 mg/ml) was diluted to 0.1 mg/ml in buffer (100 µL (1.0 mg/ml) laccase in 900 µL acetate buffer).

- 10.9736 mg (0.019736 g) of ABTS, Molar mass = 548.68 g/mol, $C_{18}H_{24}N_6O_6S_4$) was weighted into a 5 ml volumetric flask and made up to volume with distilled water to make 4 mM nominal solution and stored on ice.

Assay

- 895 µL acetate buffer and 5 µL laccase were added to a cuvette. A blank was taken.

- 100 µL ABTS was added to start the reaction and mixed well. Absorbance at 420 nm was measured and recorded for 900 s on Agilent 8453 UV-vis spectrometer with chemstation software.

Appendix A.5: DC Protein assay (20 µL sample scale)

1. Prepare a stock solution of Bovine serum albumin **(BSA)** 5 mg/mL and then standards for calibration. A standard curve should be prepared each time the assay is performed. For best results, the standards should always be prepared in the same buffer as the sample.

[BSA] (mg/mL)	**Stock solution (5 mg/mL BSA) (µL)**	**Buffer (sodium acetate, pH =5) (µL)**
0.05	4	396
0.1	8	392
0.2	16	384
0.5	40	360
0.8	64	336
1	80	320

2. Prepare samples (laccase from stock, 1.0 mg/ml) to analyse in 2-3 replicates.
3. Into Eppendorf, add 20 µL samples (standards and samples) and add 100 µL **Solution A (**an alkaline copper tartrate solution), 800 µL **Solution B** (a dilute Folin Reagent, sodium 1,2-naphthoquinone-4-sulfonate)**. Blank:** (20 µL buffer + 100 µL Solution A + 800 µL Solution B)
4. Mix well (vortex) and let the reaction go for 15 min.
5. Transfer the liquid into a cuvette and read absorbance at 750nm (Standard, cell 8, blank then sample 1, then blank, sample 2. etc).
6. Draw calibration curve and calculate sample [protein]

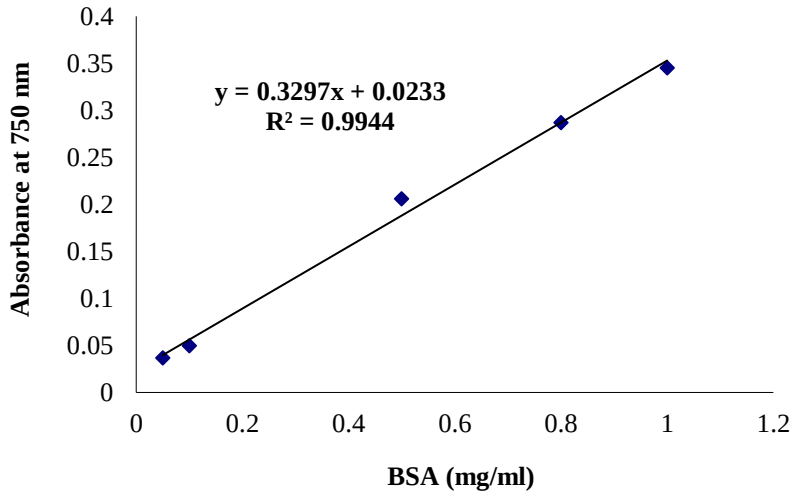


Figure A.5: Standard curve for the Bio-Rad protein assay

Appendix A.6: GC-MS Syringaldehyde Standard Calibration Curve

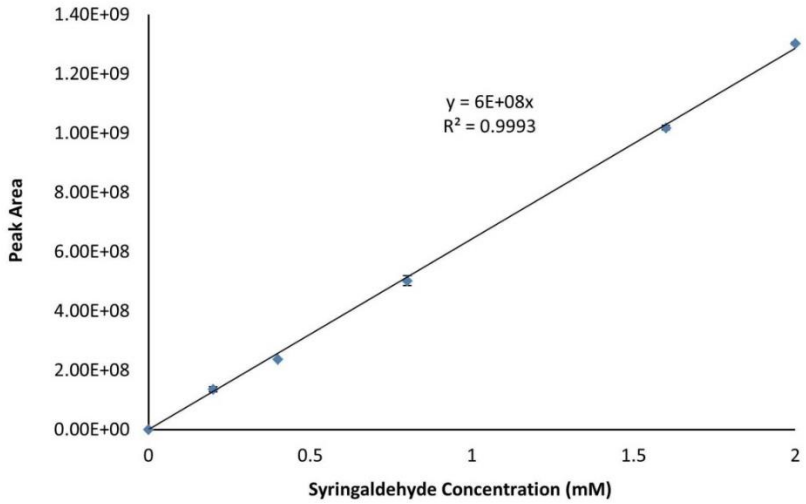


Figure A.6: GC-MS syringaldehyde standard calibration curve

Appendix A.7: Enzyme kinetics by Eadie-Hofstee plot

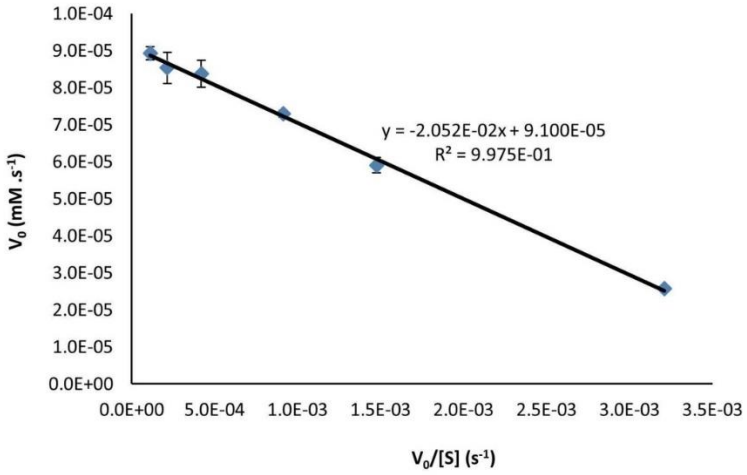


Figure A.7: Determination of Michaelis-Menten parameters by Eadie-Hofstee plot. Values are means ± standard deviations (n=3)

By plotting $v_0/[S]$ versus v_0, a Eadie-Hofstee plot is obtained as the y-intercept is V_{max} and the slope is-K_m.

$\boldsymbol{K_m}$= 0.0205 mM

$\boldsymbol{V_m}$ = 9.100 X 10^{-5} mM/s

Appendix A.8: GC-MS Analysis of Organosolv Lignin Treatment Products after dissolution with 30% (v/v) IL/buffer at 30 °C for 6 h.

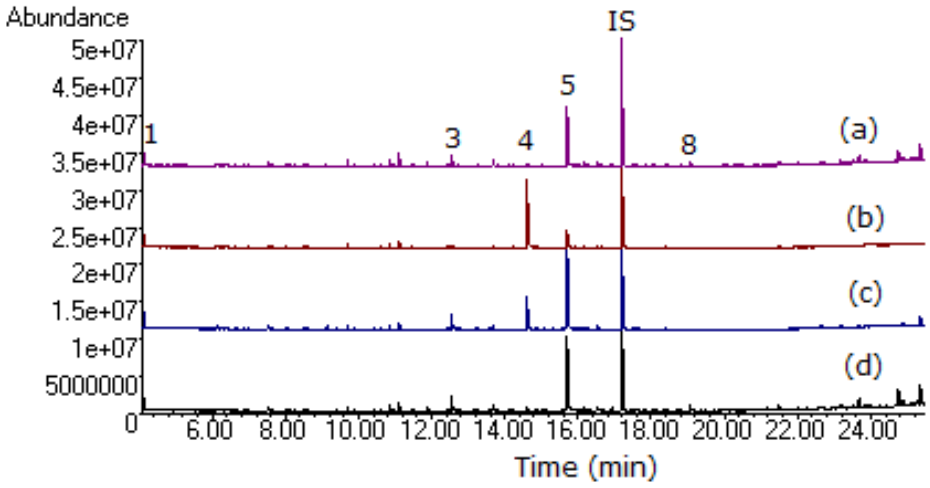
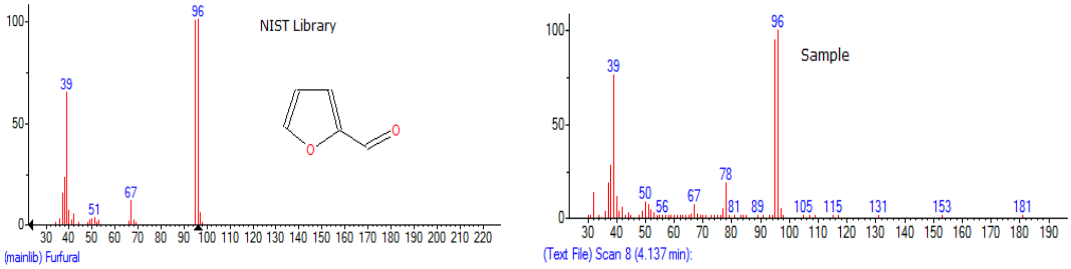


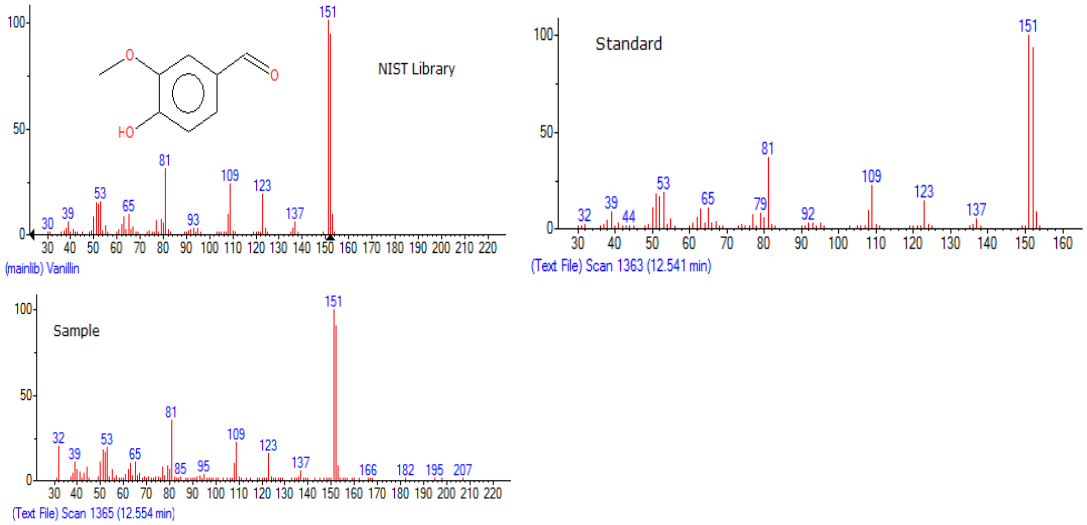
Figure A.8: GC-MS chromatogram of lignin breakdown products from organosolv lignin after dissolution with 30% (v/v) of $[C_2mim][C_2SO_4]$ with LTV and without LTV at 30 °C for 6 h. Identification of products was based on the NIST library data. Benzene extract fraction of organosolv lignin after treatment with (a) LTV and ABTS (b) LTV only (c) ABTS only and (D) benzene extract fraction of organosolv lignin only. The other peaks without a label were contamination peaks.

Mass Spectrum of Furfural (1) NIST library



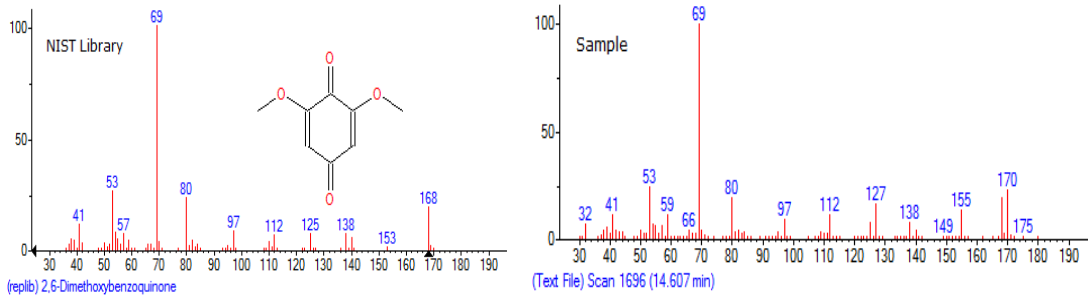
NIST#: 118785, MF: $C_5H_4O_2$, MW:96 and CAS#: 98-01-1, the retention time (RT) 4.137 min

Mass Spectrum of Vanillin (3) NIST library



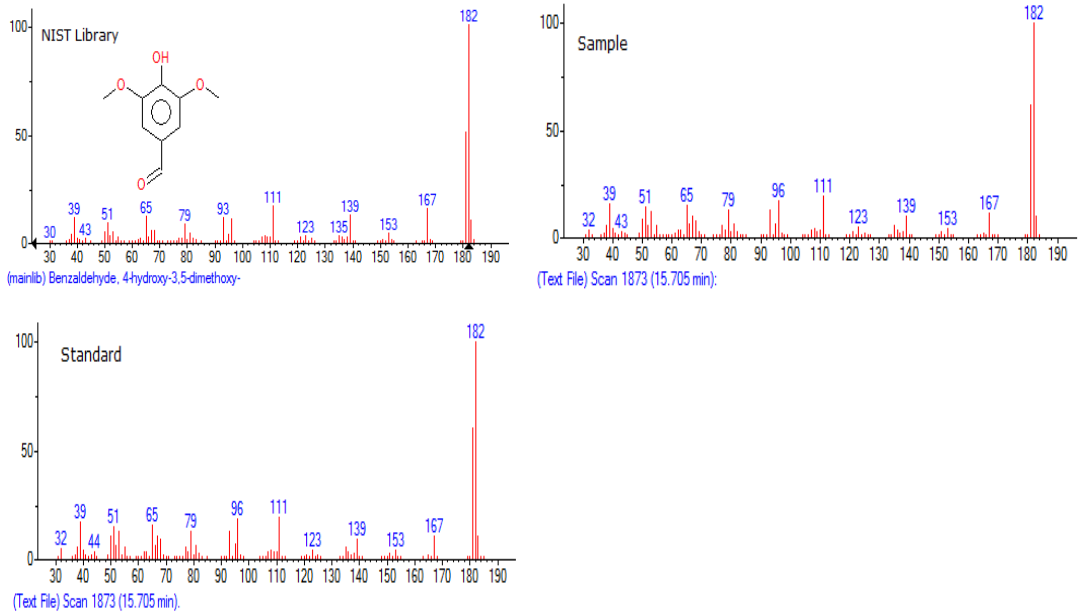
Name: Vanillin
NIST#: 290719, MF: $C_8H_8O_3$, MW: 152 CAS#: 121-33-5, RT: 12.554 min

Mass Spectrum of 2,6-Dimethoxybenzoquinone (DMBQ) (4) NIST library



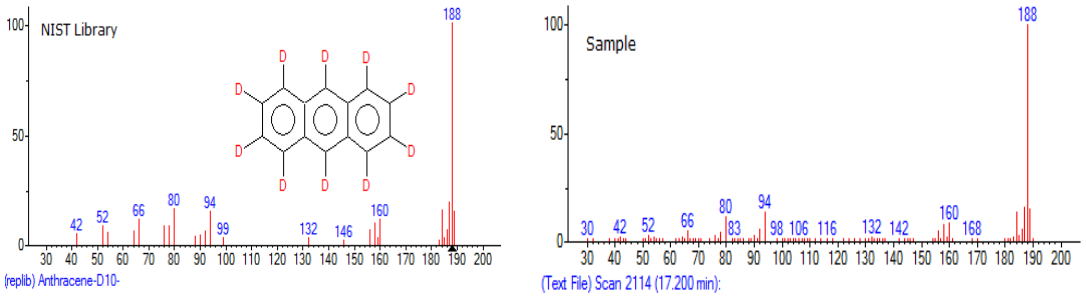
Name: 2,6-Dimethoxybenzoquinone (DMBQ)
NIST#: 136693, MF: $C_8H_8O_4$, MW: 168 CAS#: 530-55-2, RT: 14.607 min

Mass Spectrum of Syringaldehyde (5) NIST library



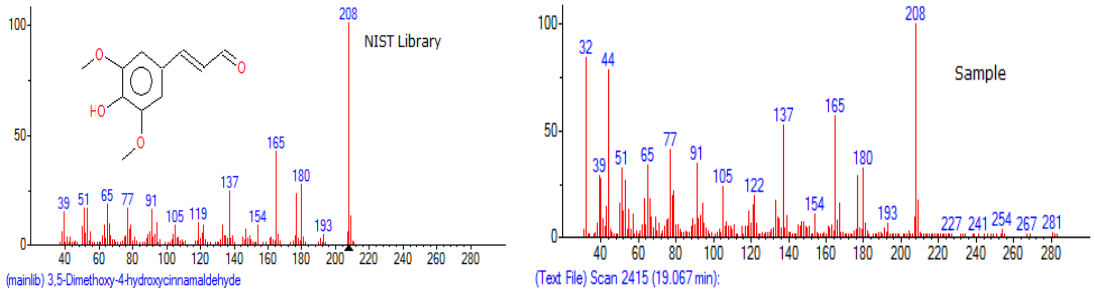
Name: Benzaldehyde, 4-hydroxy-3,5-dimethoxy- (Syringaldehyde)
NIST#: 231017, MF: $C_9H_{10}O_4$, MW: 168 CAS#: 134-96-3, RT: 15.705 min

Mass Spectrum of Internal standard (IS) Anthracene-D_{10} NIST library



Name: Anthracene-D10
NIST#: 134852, MF: $C_{14}D_{10}$, MW: 188 CAS#: 1719-06-8, RT: 16.200 min

Mass Spectrum of 3,5-Dimethoxy-4-hydroxycinnamaldehyde (DHCD) (8) NIST library



Name: 3,5-Dimethoxy-4-hydroxycinnamaldehyde
NIST#: 250264, MF: $C_{11}H_{12}O4$, MW: 208 CAS#: 87345-53-7, RT: 19.067 min

Appendix A.9: GC-MS Analysis of Organosolv Lignin Treatment Products in [C2mim][C2SO4]

Appendix A.9.1: GC-MS Analysis of Organosolv Lignin Treatment Products in [C2mim][C2SO4] at 30 °C for 6 h

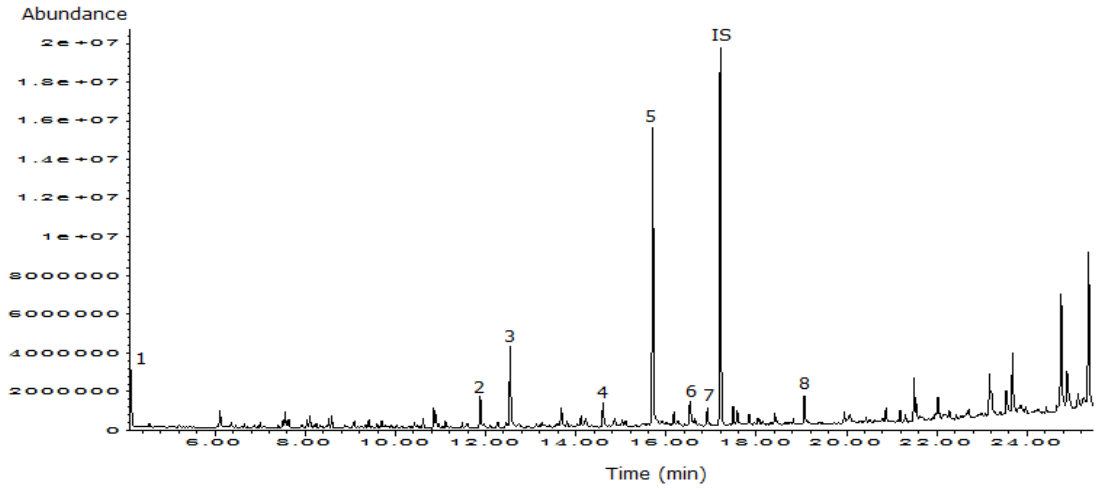
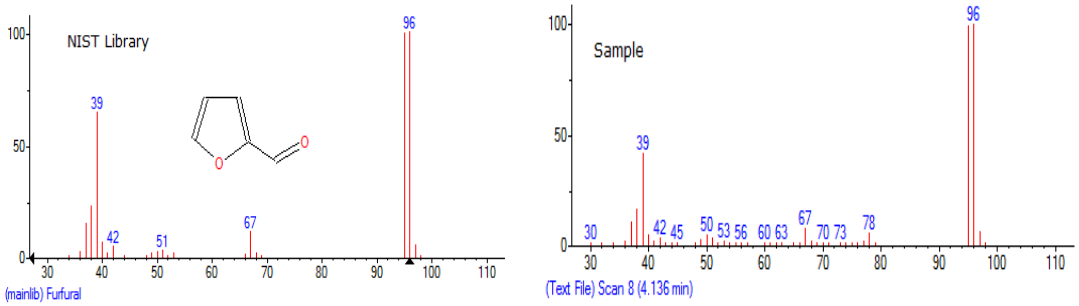


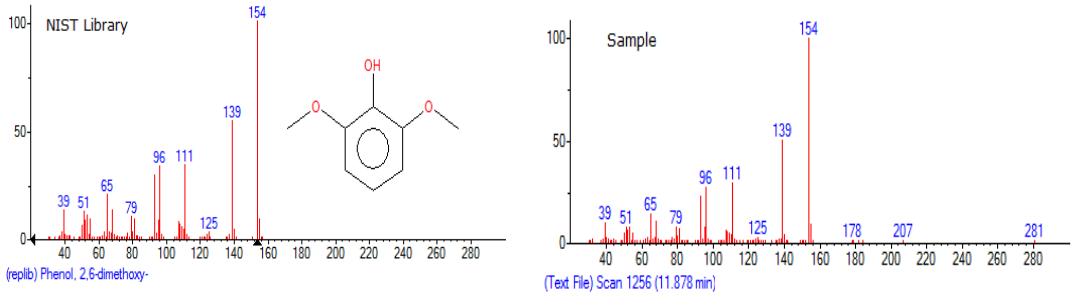
Figure A.9.1: GC-MS chromatogram of aqueous benzene extract fraction after organosolv lignin dissolution with [C_2mim][C_2SO_4] at 30 °C for 6 h. Identification of the compounds was based on the NIST library. Identification of vanillin and syringaldehyde were based on single-point internal standard method and NIST library data. The other peaks without a label were contamination peaks.

Mass Spectrum of Furfural (1) NIST library



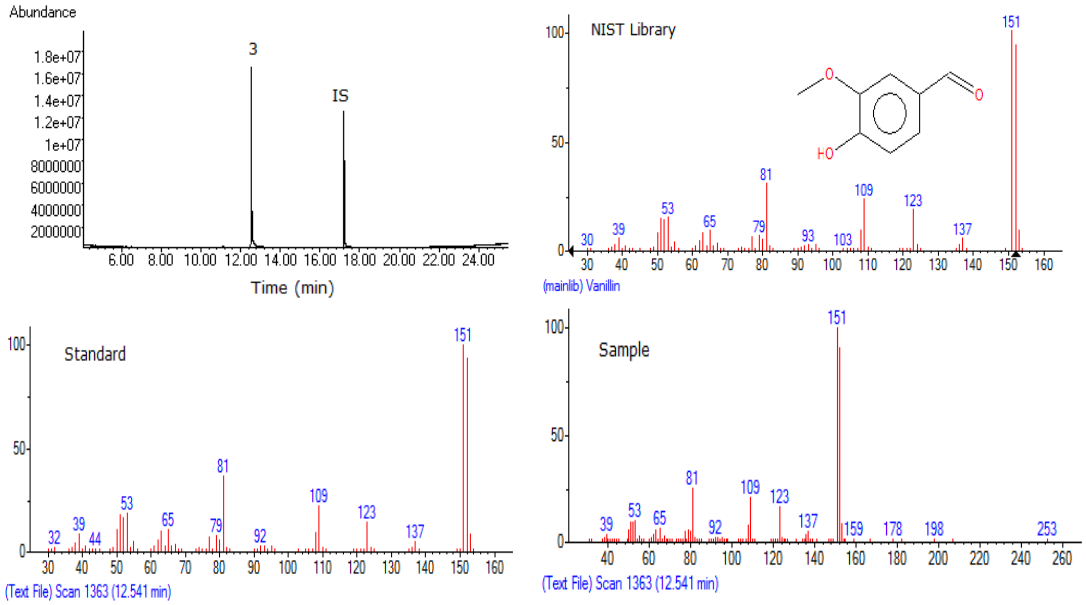
NIST#: 118785, MF: $C_5H_4O_2$, MW:96 and CAS#: 98-01-1, the retention time (RT) 4.136 min

Mass Spectrum of Syringol (2) NIST library



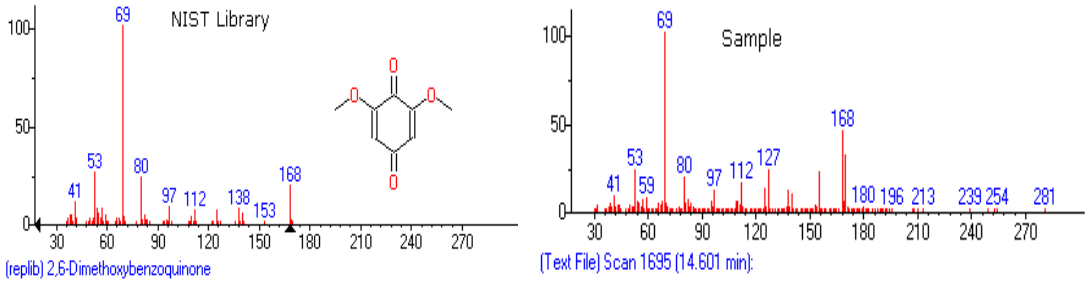
Name: Phenol, 2,6-dimethoxy- (Syringol)
NIST#: 333381, MF: $C_8H_{10}O_3$, MW: 154 and CAS#: 91-10-1

Mass Spectrum of Vanillin (3) NIST library



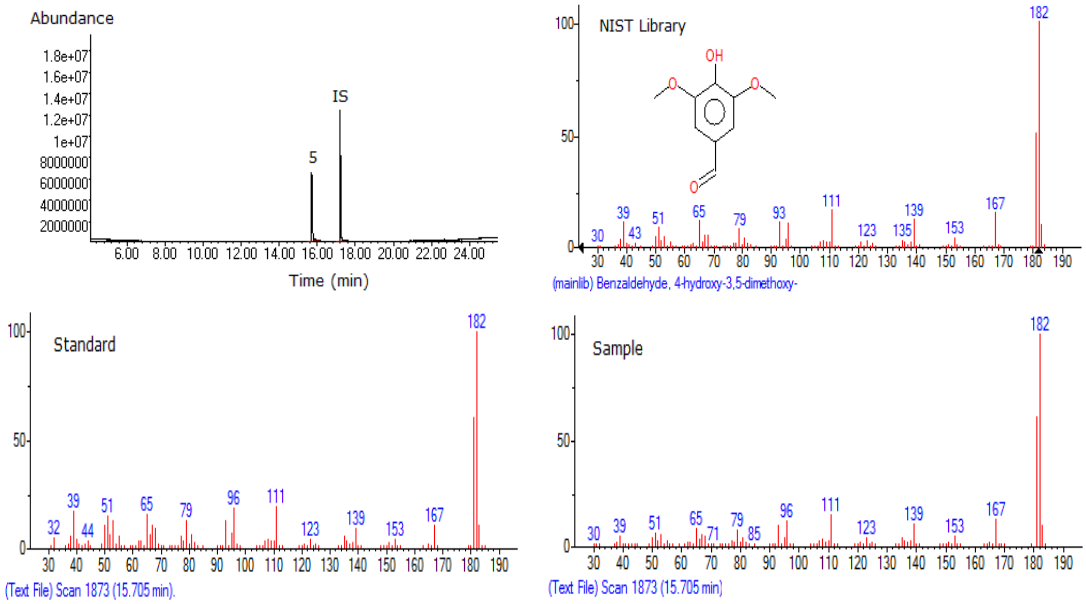
Name: Vanillin
NIST#: 290719, MF: $C_8H_8O_3$, MW: 152 CAS#: 121-33-5, RT: 12.541 min

Mass Spectrum of 2,6-Dimethoxybenzoquinone (DMBQ) (4) NIST library



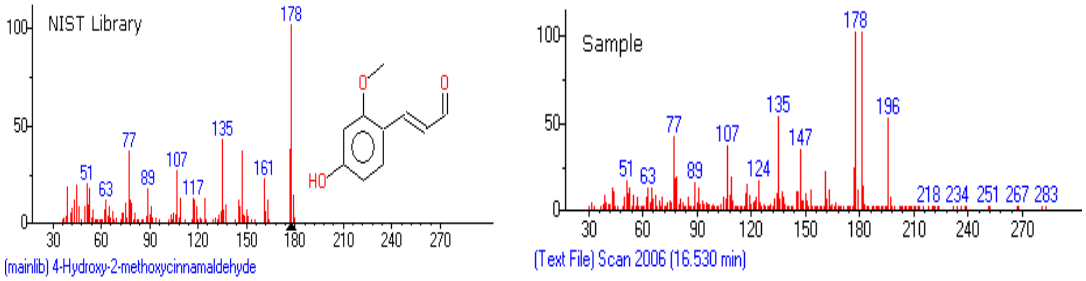
Name: 2,6-Dimethoxybenzoquinone (DMBQ)
NIST#: 136693, MF: $C_8H_8O_4$, MW: 168 CAS#: 530-55-2, RT: 14.601 min

Mass Spectrum of Syringaldehyde (5) NIST library



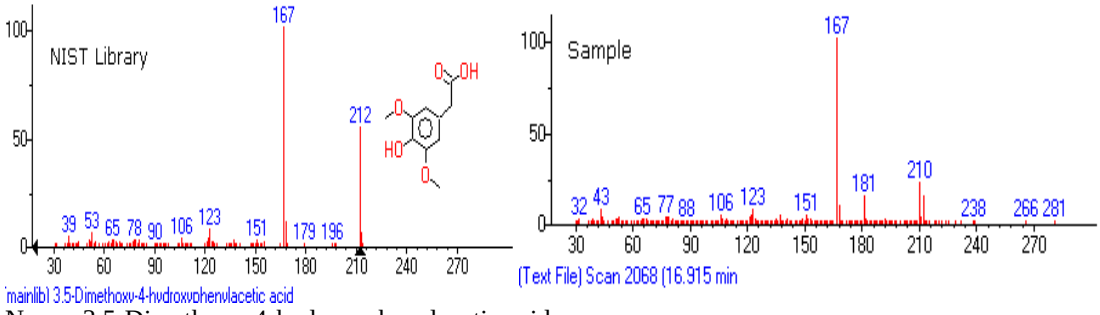
Name: Benzaldehyde, 4-hydroxy-3,5-dimethoxy- (Syringaldehyde)
NIST#: 231017, MF: $C_9H_{10}O_4$, MW: 168 CAS#: 134-96-3, RT: 15.705 min

Mass Spectrum of 4-Hydroxy-2-methoxycinnamaldehyde (HMCD) (6) NIST library



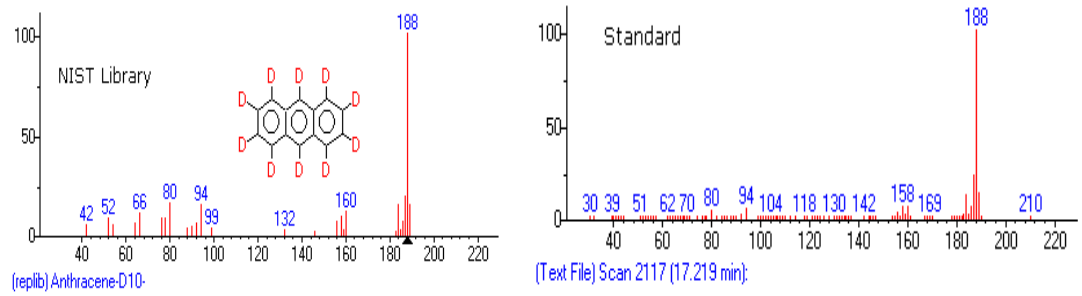
Name: 4-Hydroxy-2-methoxycinnamaldehyde
NIST#: 250265, MF: $C_{10}H_{10}O_3$, MW: 178 CAS#: 127321-19-1, RT: 16.530 min

Mass Spectrum of 3,5-Dimethoxy-4-hydroxyphenylacetic acid (DHPAA) (7) NIST library



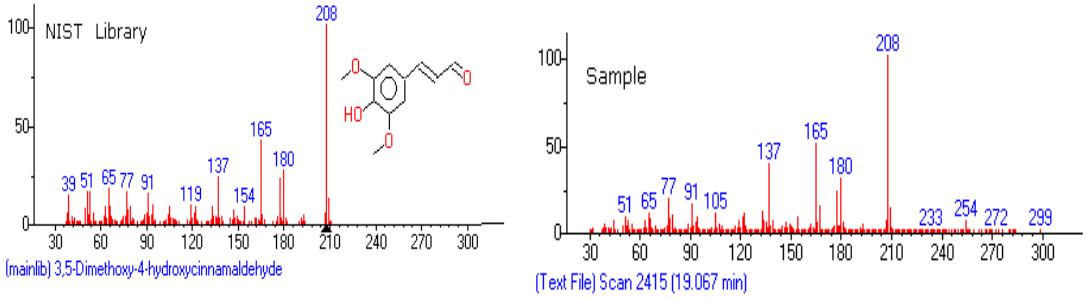
Name: 3,5-Dimethoxy-4-hydroxyphenylacetic acid
NIST#: 134852, MF: $C_{10}H_{12}O5$, MW: 212 CAS#: 4385-56-2, RT: 16.915 min

Mass Spectrum of Internal standard (IS) anthracene-D_{10} NIST library



Name: Anthracene-D10-
NIST#: 134852, MF: $C_{14}D_{10}$, MW: 188 CAS#: 1719-06-8, RT: 16.219 min

Mass Spectrum of 3,5-Dimethoxy-4-hydroxycinnamaldehyde (DHCD) (8) NIST library



Name: 3,5-Dimethoxy-4-hydroxycinnamaldehyde
NIST#: 250264, MF: $C_{11}H_{12}O4$, MW: 208 CAS#: 87345-53-7, RT: 19.067 min

Appendix A.9.2: GC-MS Analysis of Organosolv Lignin Treatment Products in $[C_2mim][C_2SO_4]$ at 160 °C for 6 h

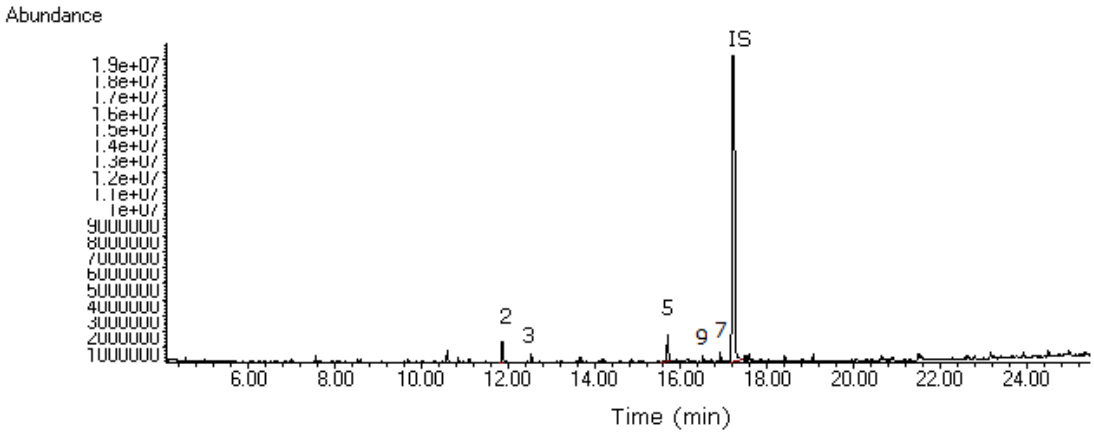
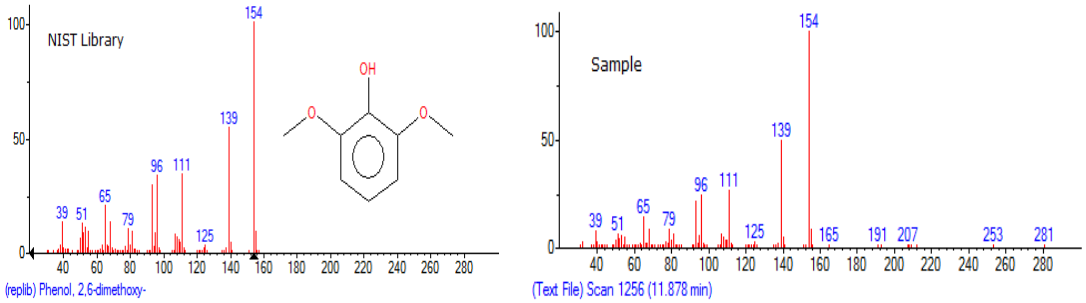


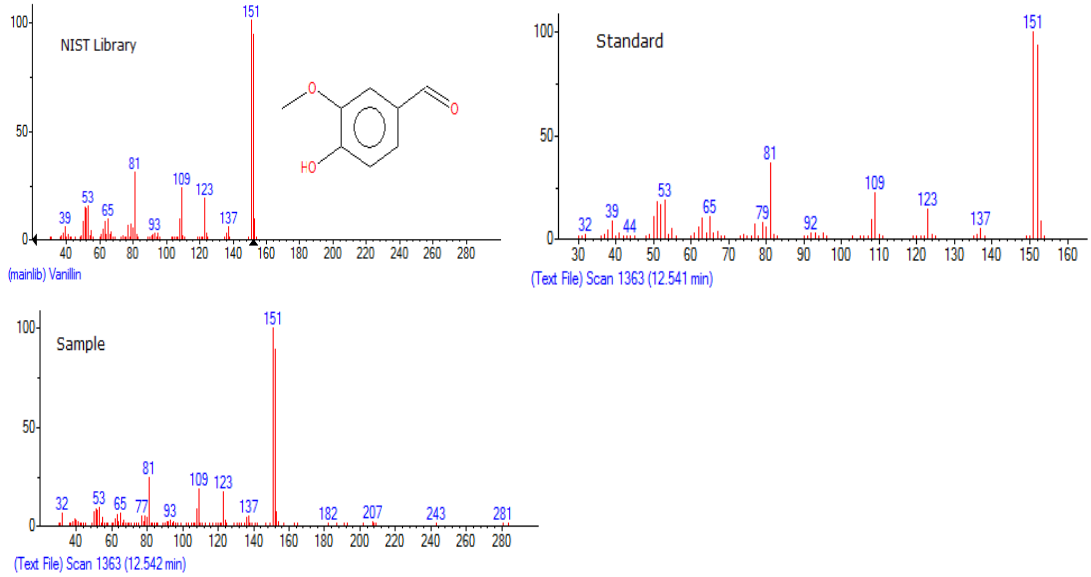
Figure A.9.2: GC-MS chromatogram of aqueous benzene extract fraction after organosolv lignin dissolution with $[C_2mim][C_2SO_4]$ at 160 °C for 6 h. Identification of the compounds was based on the NIST library. Identification of vanillin and syringaldehyde were based on single-point internal standard method and NIST library data. The other peaks without a label were contamination peaks.

Mass Spectrum of Syringol (2) NIST library



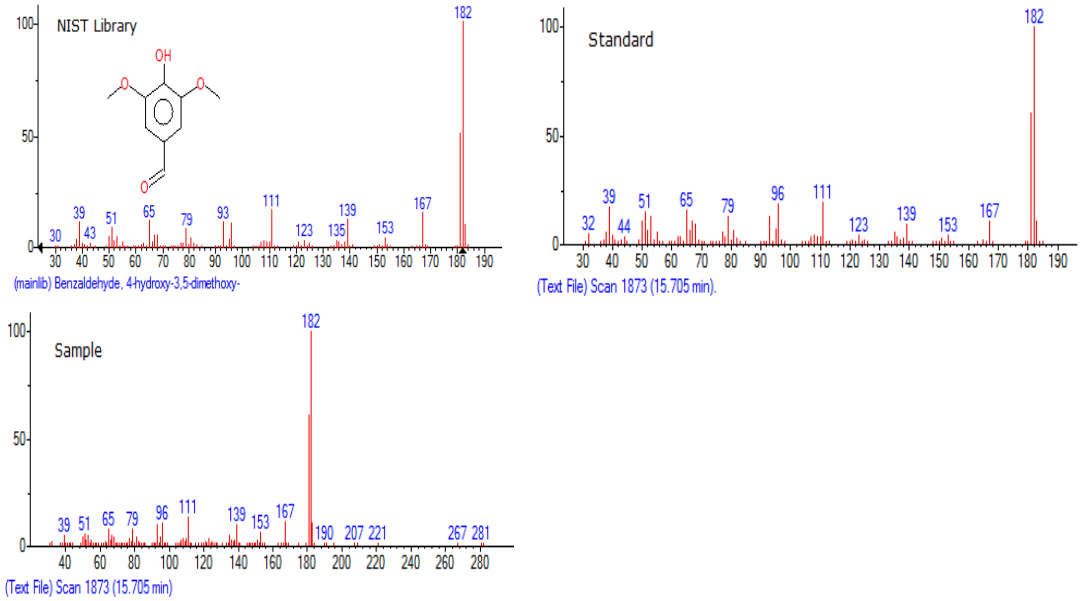
Name: Phenol, 2,6-dimethoxy- (Syringol)
NIST#: 333381, MF: $C_8H_{10}O_3$, MW: 154 and CAS#: 91-10-1

Mass Spectrum of Vanillin (3) NIST library



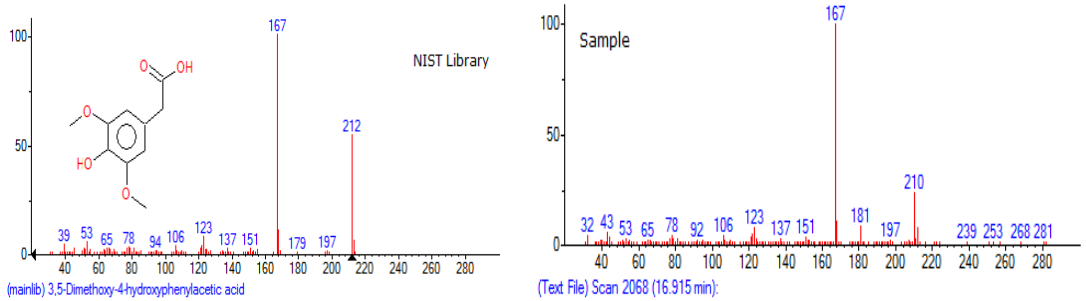
Name: Vanillin
NIST#: 290719, MF: $C_8H_8O_3$, MW: 152 CAS#: 121-33-5, RT: 12.541 min

Mass Spectrum of Syringaldehyde (5) NIST library



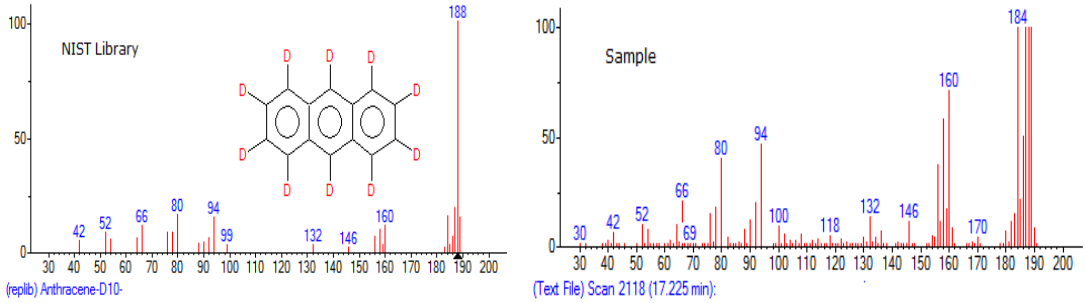
Name: Benzaldehyde, 4-hydroxy-3,5-dimethoxy- (Syringaldehyde)
NIST#: 231017, MF: $C_9H_{10}O_4$, MW: 168 CAS#: 134-96-3, RT: 15.705 min

Mass Spectrum of 3,5-Dimethoxy-4-hydroxyphenylacetic acid (DHPAA) (7) NIST library



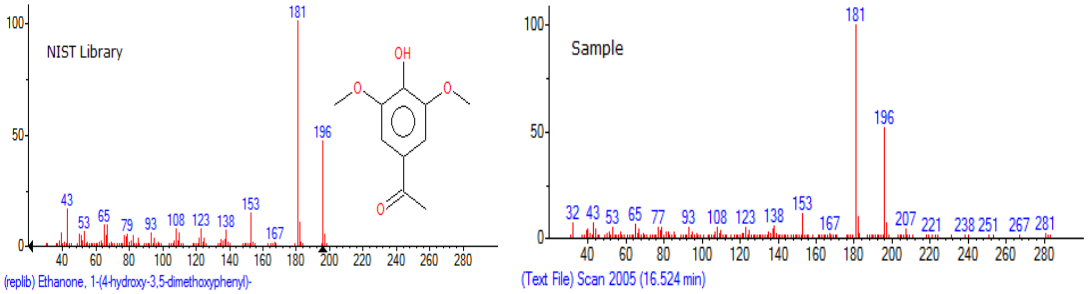
Name: 3,5-Dimethoxy-4-hydroxyphenylacetic acid
NIST#: 134852, MF: $C_{10}H_{12}O5$, MW: 212 CAS#: 4385-56-2, RT: 16.915 min

Mass Spectrum of Internal standard (IS) anthracene-D_{10} NIST library



Name: Anthracene-d10
NIST#: 134852, MF: $C_{14}D_{10}$, MW: 188 CAS#: 1719-06-8, RT: 16.219 min

Mass Spectrum of 3,5-Dimethoxy-4-hydroxyacetophenone (DHAP) (9) NIST library



Name: Ethanone, 1-(4-hydroxy-3,5-dimethoxyphenyl)- (3,5-Dimethoxy-4-hydroxyacetophenone)
NIST#: 291615, MF: $C_{10}H_{12}O4$, MW: 196 CAS#: 2478-38-8, RT: 16.524 min

Appendix A.10: GC-MS Analysis of products obtained by extraction with different solvents after organosolv dissolution in [C2mim][C2SO4] at 30 °C for 6 h.

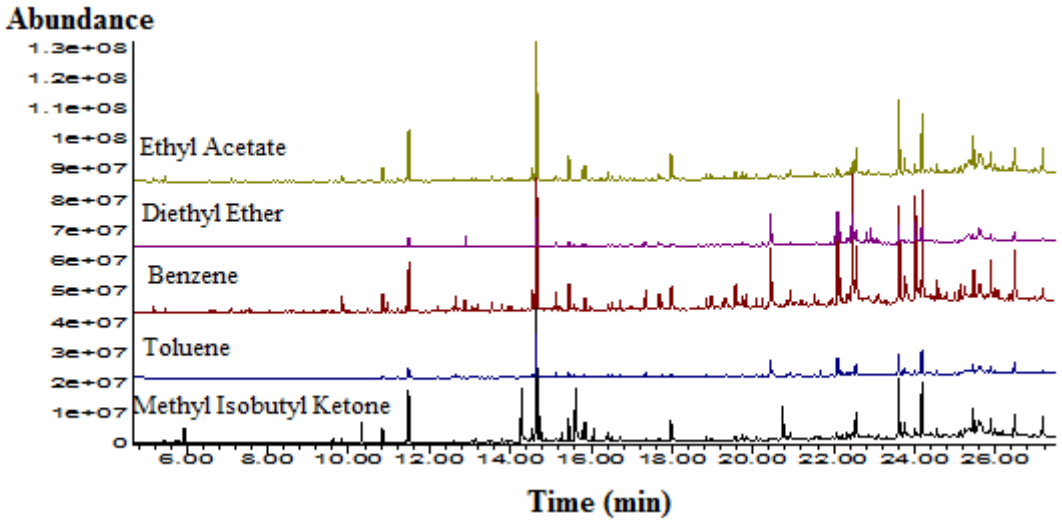


Figure A.10: Major and minor lignin products obtained from organosolv lignin after dissolution in [C_2mim][C_2SO_4] extraction with different solvents. Identification of the compounds was based on the NIST library.

Appendix A.11: GC-MS Syringaldehyde Standard Calibration Curve

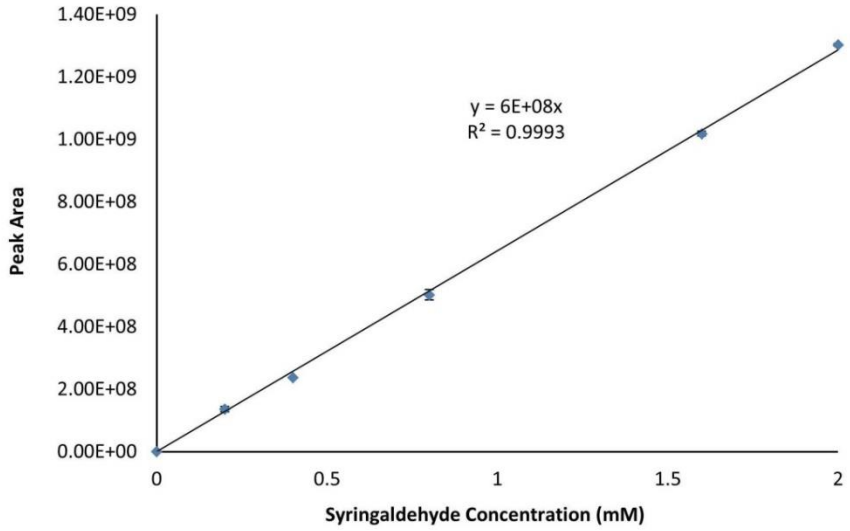
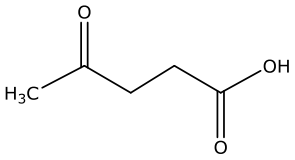
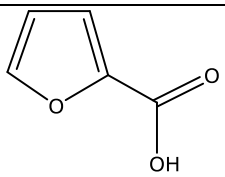
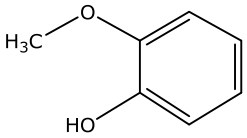
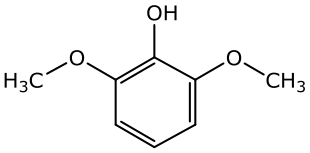
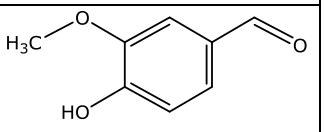
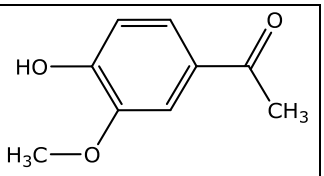
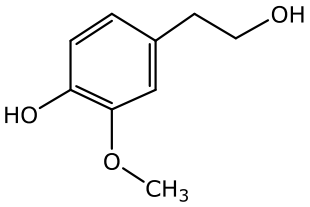
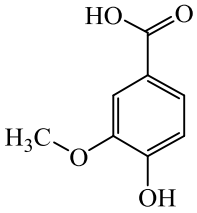
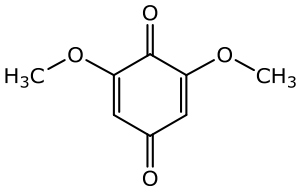
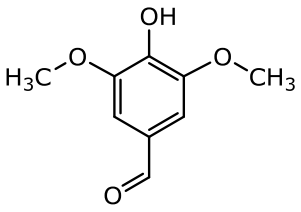


Figure A.11: GC-MS syringaldehyde standard calibration curve in $[C_2mim][C_2SO_4]$.

Appendix A.12: Standards for Lignosulfonates-Bulk Electrolysis Experiment

Table A.12: GC-MS retention times of reference standards and structure

Compound	MW (g/mol)	RT (min)	Probability (%)	Structure
Levulinic acid (4-oxopentanoic acid)	116.11	7.937	95.6	
2-Furancarboxylic acid (2-Furoic acid)	112.08	8.179	87.7	
Guaiacol	124.14	8.291	84.6	
Syringol (2,6-Dimethoxyphenol)	154.16	12.037	88.9	
Vanillin	152.15	12.738	70.1	

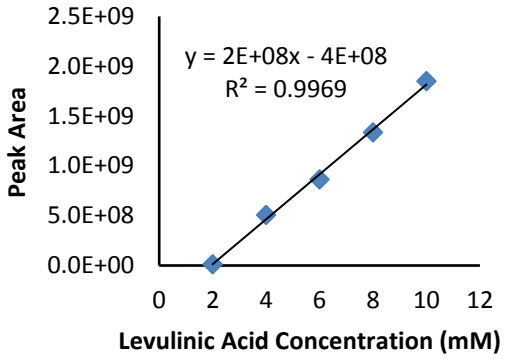
Acetoguaiacone (Acetovanillone)	166.17	13.836	75	
Homovanillyl alcohol	168.19	14.432	93.8	
Homovanillic acid (4-Hydroxy-3 methoxyphenylacetic acid, HVA)	182.17	15.648		
Vanillic acid	168.14	14.949	70.8	
2,6-Dimethoxybenzoquinone (2,6-Dimethoxy-1,4-benzoquinone, DMBQ)	168.15	14.767	88.9	
Syringaldehyde	182.17	15.902	81.7	

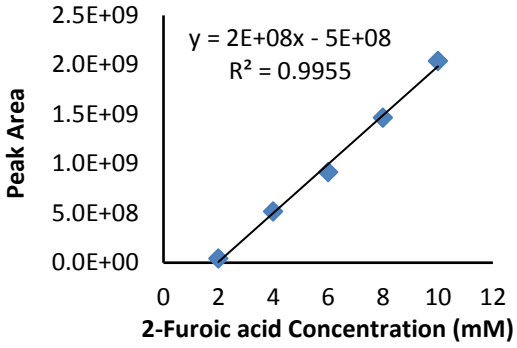
GC-MS standard calibration curve

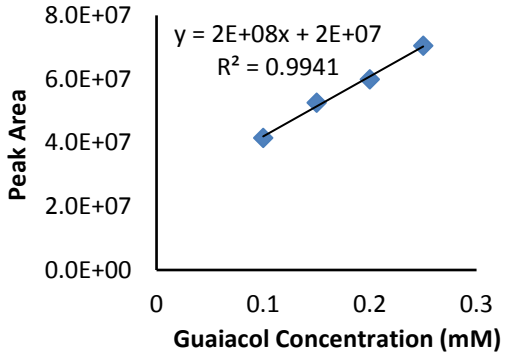
All the compounds were soluble in dichloromethane except vanillic acid so it dissolved in ethyl acetate.

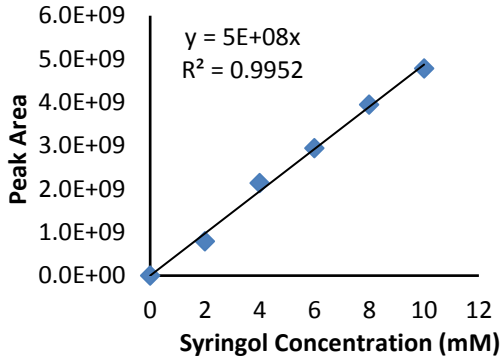
The concentration range for all compounds 2 mM-10 mM except guaiacol 0.1- 0.3 mM

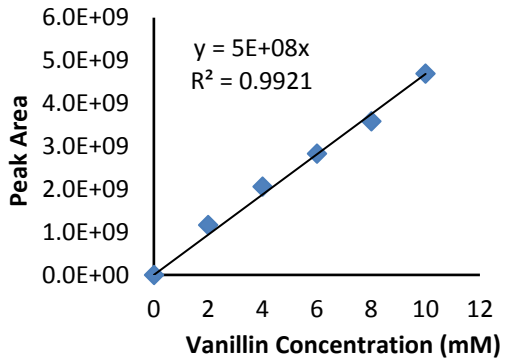
GC-MS Standard Calibration Curve

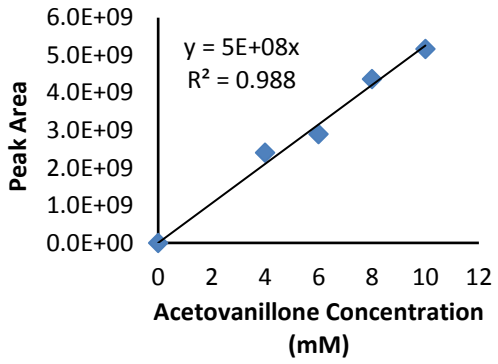


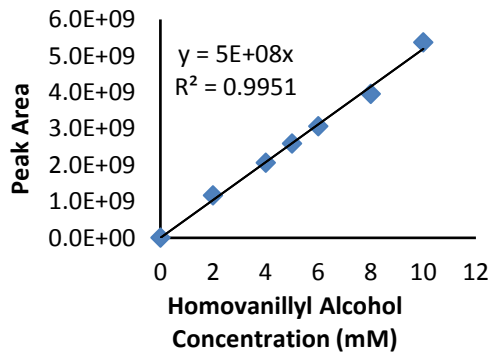


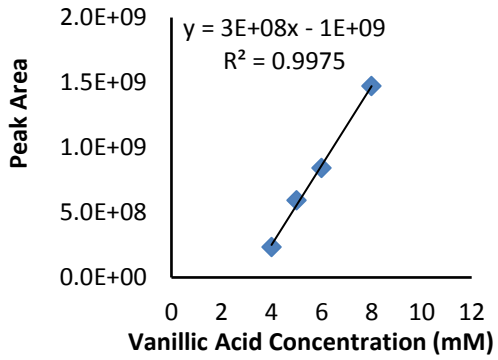


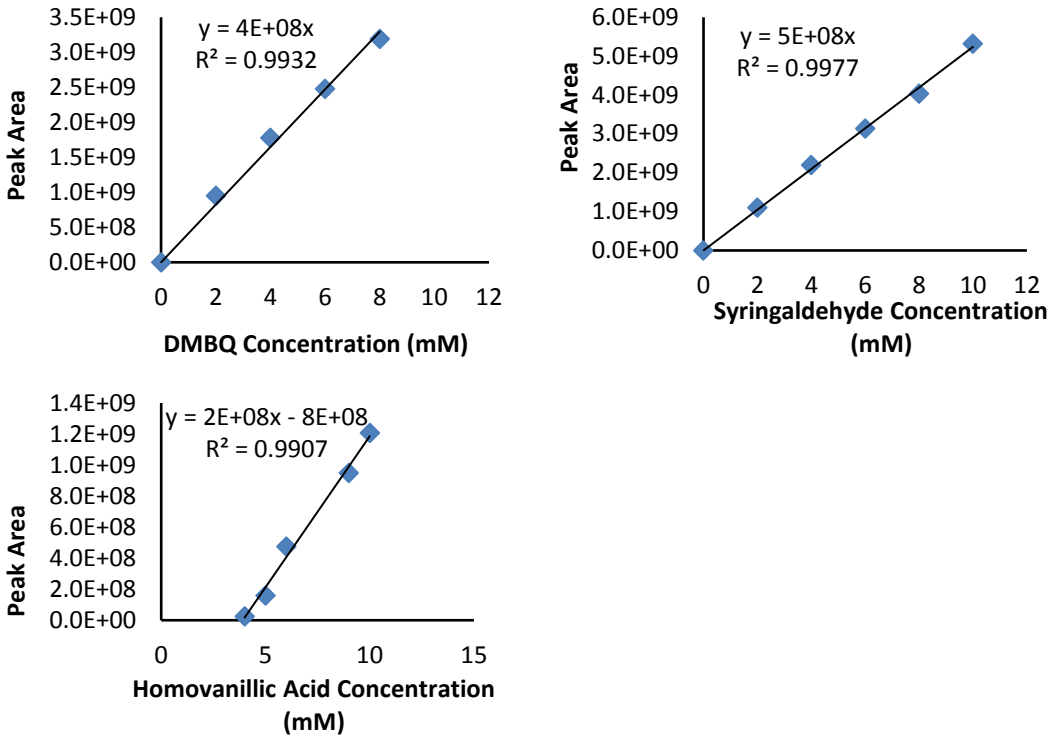












Appendix A.13: Cyclic voltammograms of 1 mM ABTS in 0.1 M sodium acetate buffer (pH 4.5) recorded at a scan rate of 400 mV/s

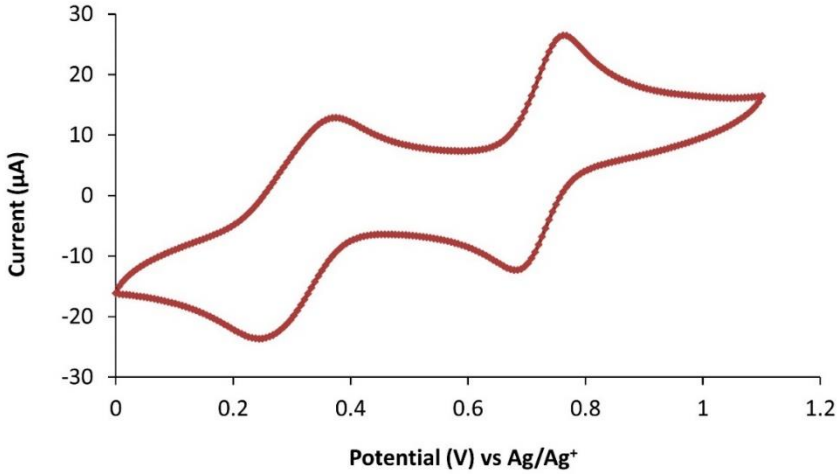


Figure A.13: Cyclic voltammograms of 1 mM ABTS in 0.1 M sodium acetate buffer (pH 4.5) recorded at a scan rate of 400 mV/s

Appendix A.14: GC-MS analysis of products obtained from electrochemical oxidation of organosolv Lignin after 6 h in [C_2mim][C_2SO_4].

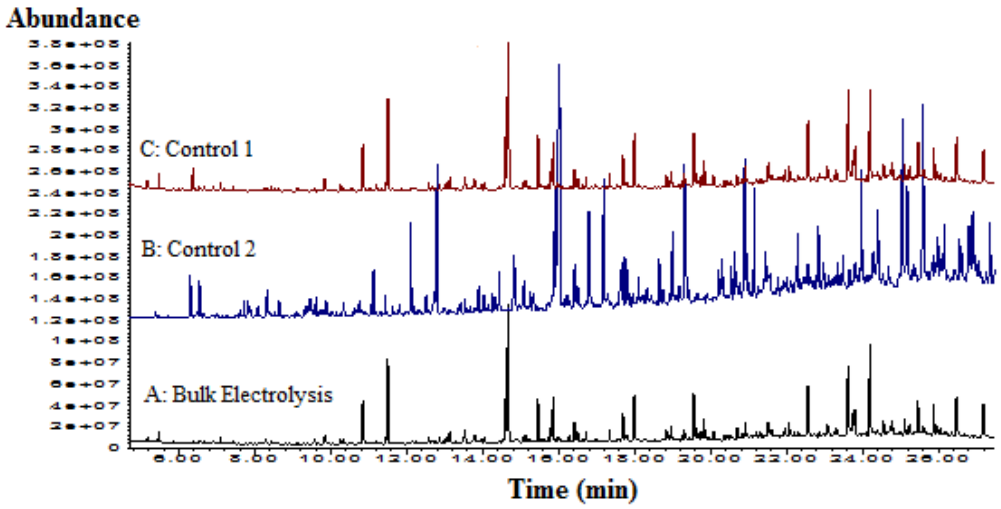


Figure A.14: The GC-MS chromatograms of lignosulfonate products that have been extracted in ethyl acetate. Ethyl acetate extract fraction of organosolv lignin after treatment with (A) electrochemical oxidation in the IL for 6 h at 1.0 V (B) without electrochemical oxidation in the IL after 6 h (C) without electrochemical oxidation and without the IL at initial time.

Appendix A.15: GC-MS analysis of products obtained from electrochemical oxidation of as-received lignosulfonate after 8 h in sodium acetate buffer.

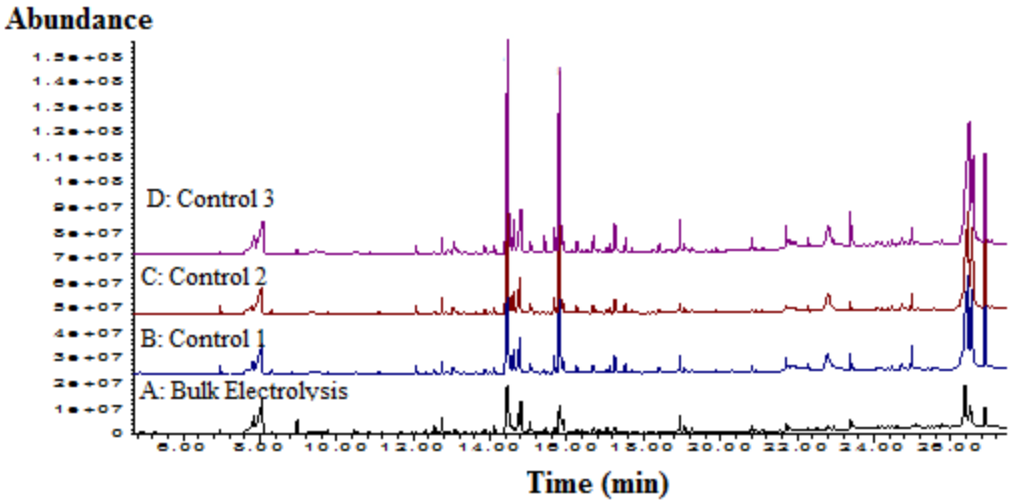


Figure A.15: The GC-MS chromatograms of as-received lignosulfonate products that have been extracted in ethyl acetate. Ethyl acetate extract fraction of lignosulfonate after treatment with (A) electrochemical oxidation for 8 h at 1.0 V (B) without electrochemical oxidation at initial time (C) without electrochemical oxidation after 8 h (D) without electrochemical oxidation and without ABTS after 8 h.

Appendix A.16: GC-MS analysis of products obtained from electrochemical oxidation of lignosulfonate after MeOH washing after 8 h in sodium acetate buffer.

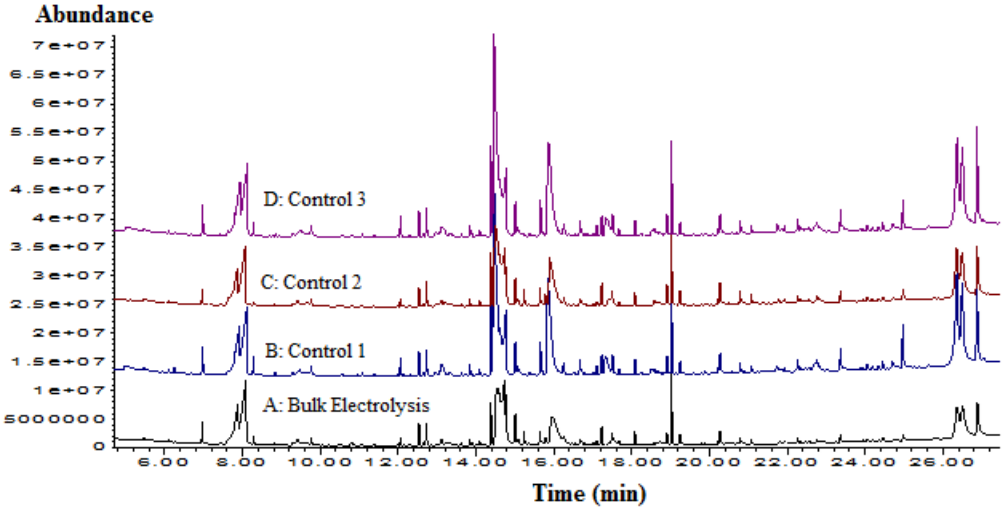


Figure A.16: The GC-MS chromatograms of lignosulfonate after MeOH washing products that have been extracted in ethyl acetate. Ethyl acetate extract fraction of lignosulfonate after treatment with (A) electrochemical oxidation for 8 h at 1.0 V (B) without electrochemical oxidation at initial time (C) without electrochemical oxidation after 8 h (D) without electrochemical oxidation and without ABTS after 8 h.

Appendix A.17: ^{1}H NMR and ^{13}C NMR spectra of the [DMEA][HCOO]

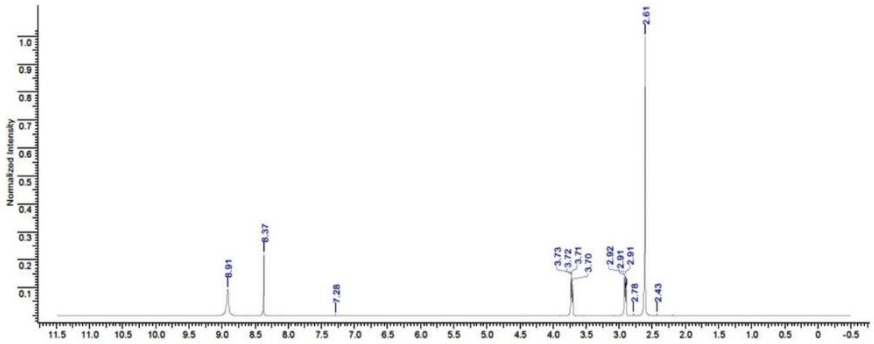


Figure A.17.1: ^{1}H NMR spectrum of the [DMEA][HCOO].

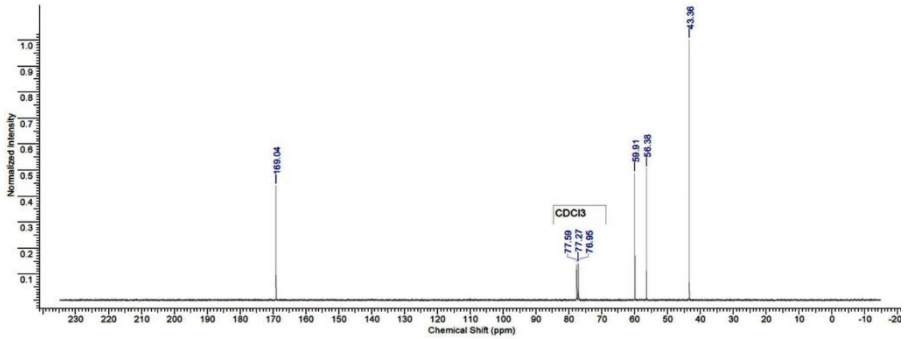


Figure A.17.2: ^{13}C NMR spectrum of the [DMEA][HCOO].

Appendix A.18: FRAP assay

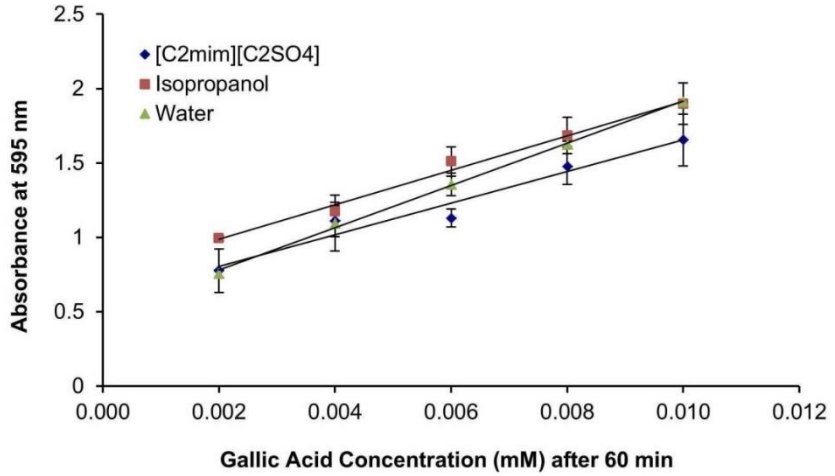


Figure A.18.1: The effect of gallic acid concentration dissolved in different solvent on the absorbance of the FRAP solution after 60 min of reaction. Values are means ± standard deviations (n=3).

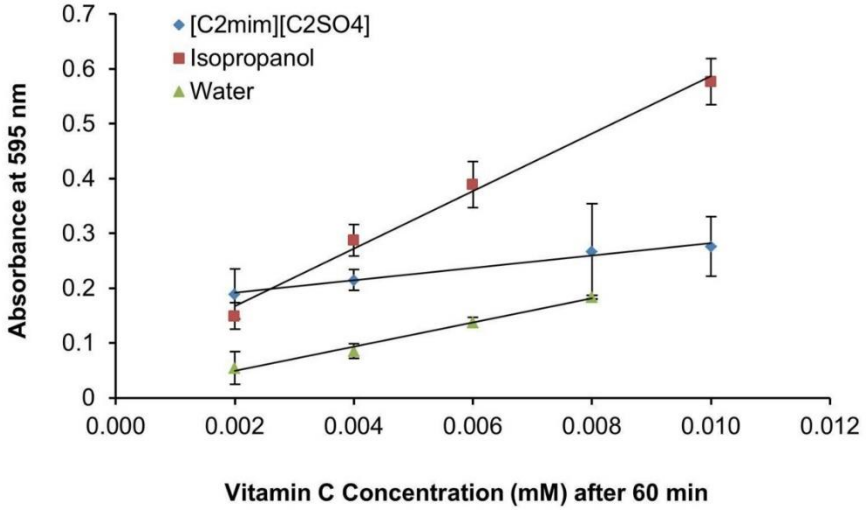


Figure A.18.2: The effect of vitamin C concentration dissolved in different solvent on the absorbance of the FRAP solution after 60 min of reaction. Values are means ± standard deviations (n=3).

Appendix A.19: Rate of increase in absorbance at 593 nm of vitamin C and gallic acid in [C_2mim][C_2SO_4], water and isopropanol.

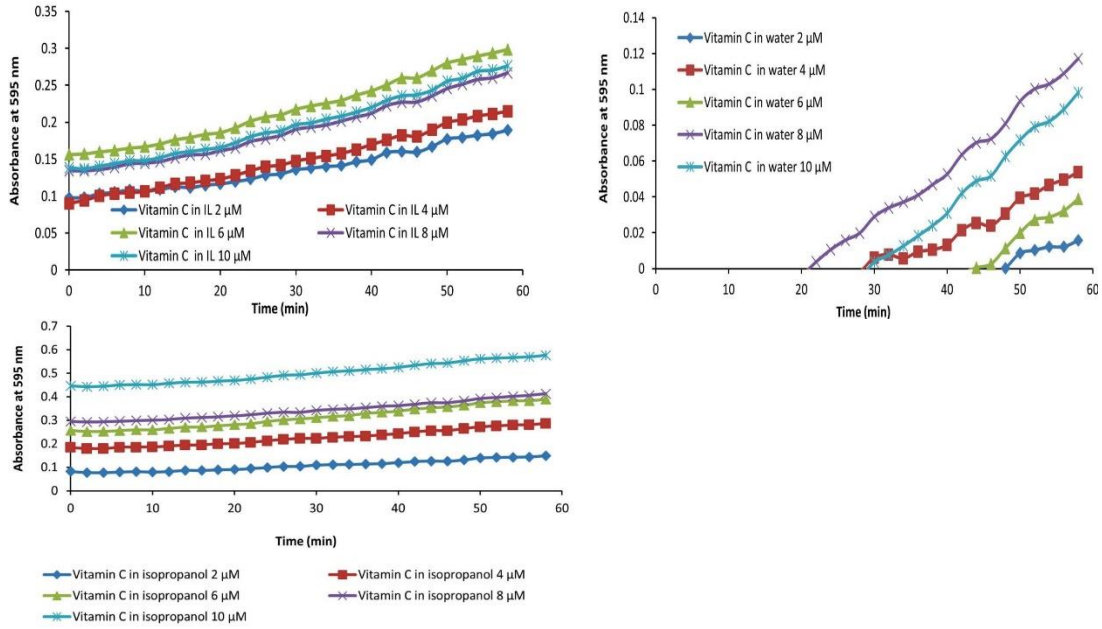


Figure A.19.1: Rate of increase in absorbance at 593 nm of vitamin C in [C_2mim][C_2SO_4], water and isopropanol.

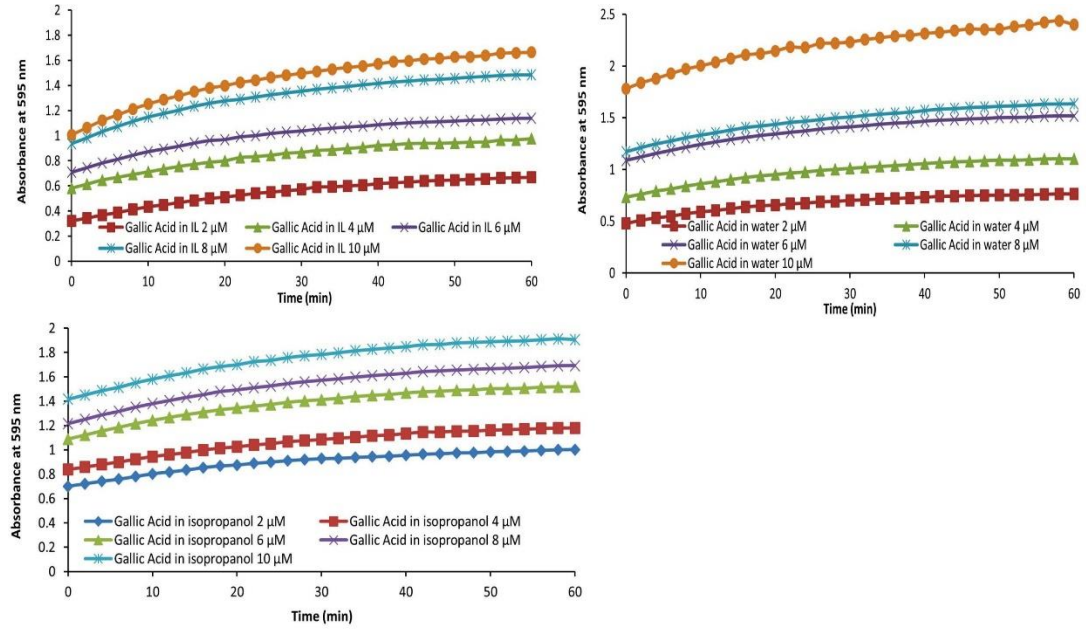


Figure A.19.2: Rate of increase in absorbance at 593 nm of Gallic Acid in [C_2mim][C_2SO_4], water and isopropanol.

Appendix A.20: Reaction kinetics behaviour and DPPH radical scavenging activities by standards and lignin monomers.

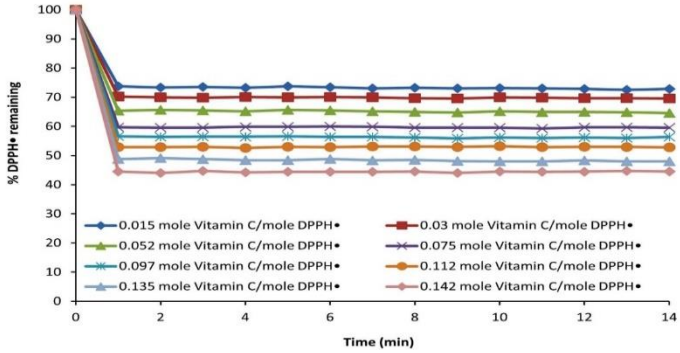


Figure A.20.1: Reaction kinetics behaviour of vitamin C in methanol.

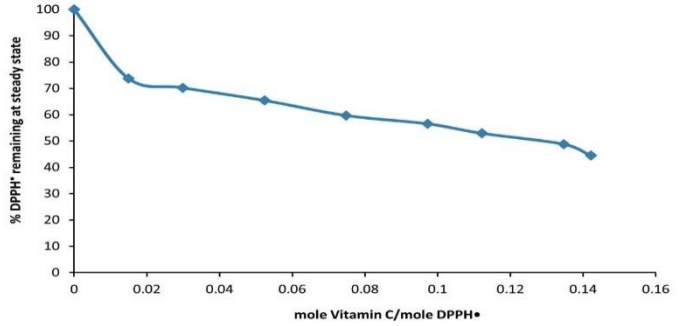


Figure A.20.2: DPPH radical scavenging activities by vitamin C as a function of the number of moles of vitamin C/mole DPPH•.

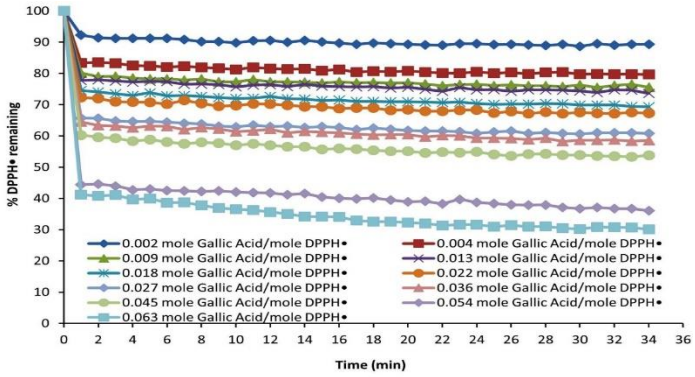


Figure A.20.3: Reaction kinetics behaviour gallic acid in methanol.

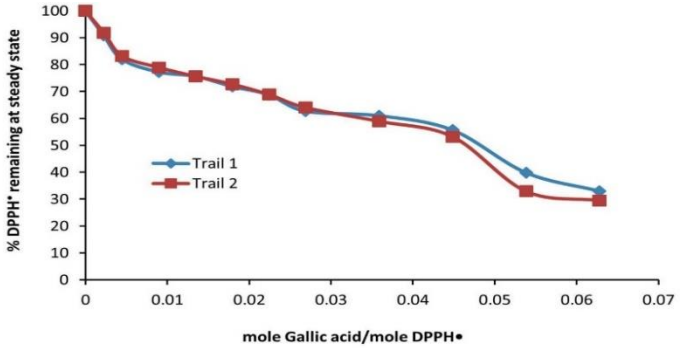


Figure A.20.4: DPPH radical scavenging activities by gallic acid as a function of the number of moles of gallic acid/mole DPPH•.

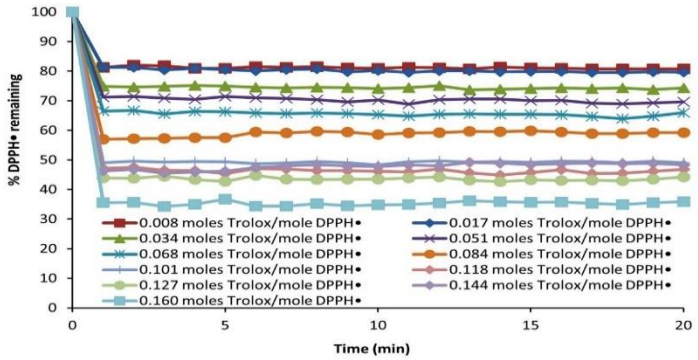


Figure A.20.5: Reaction kinetics behaviour of Trolox in methanol.

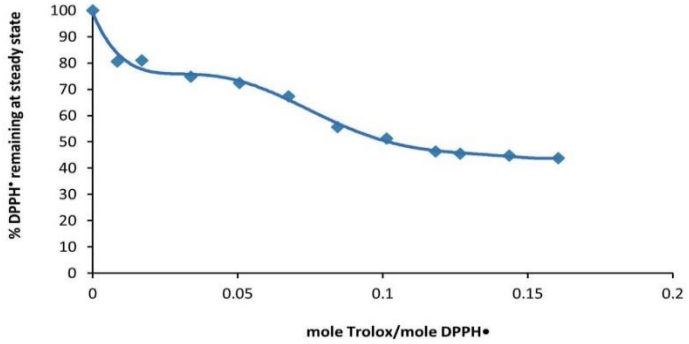


Figure A.20.6: DPPH radical scavenging activities by Trolox as a function of the number of moles of Trolox/mole DPPH•.

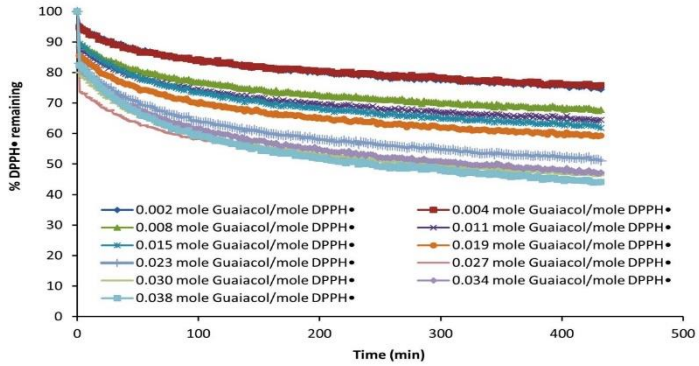


Figure A.20.13: Reaction kinetics behaviour of Guaiacol in methanol

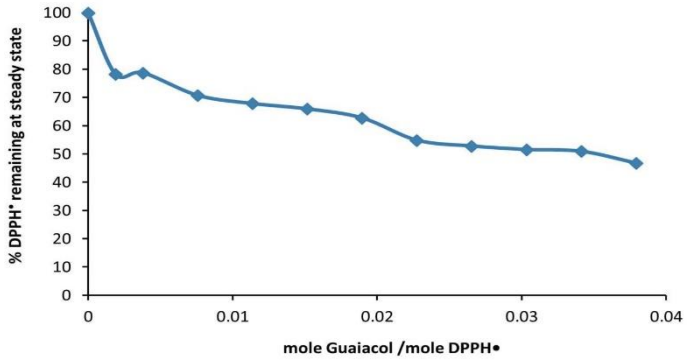


Figure A.20.14: DPPH radical scavenging activities by Guaiacol as a function of the number of moles of Guaiacol /mole DPPH•.

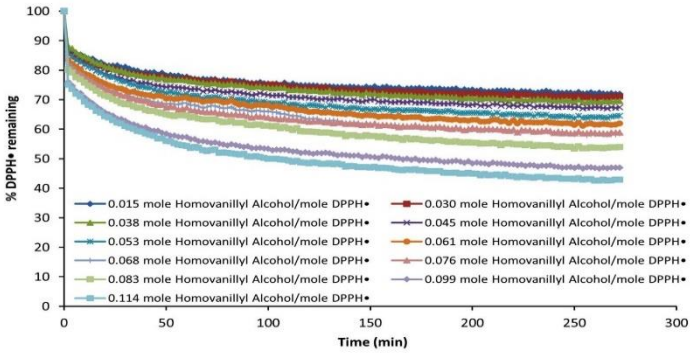


Figure A.20.15: Reaction kinetics behaviour of Homovanilly alcohol in methanol

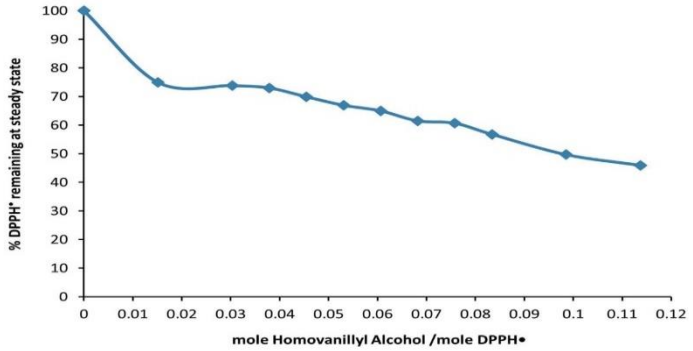


Figure A.20.16: DPPH radical scavenging activities by Homovanilly alcohol as a function of the number of moles of Homovanilly alcohol /mole DPPH•.

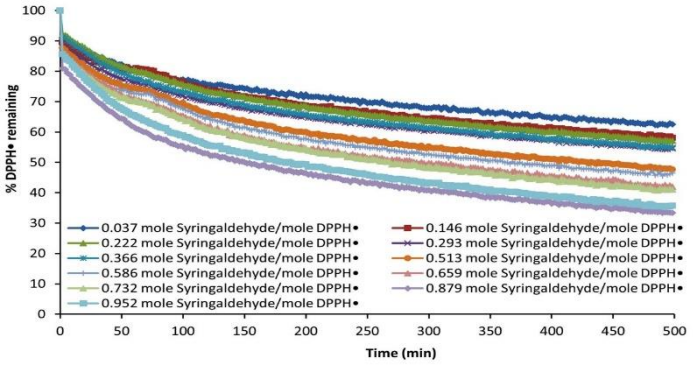


Figure A.20.17: Reaction kinetics behaviour of Syringaldehyde in methanol.

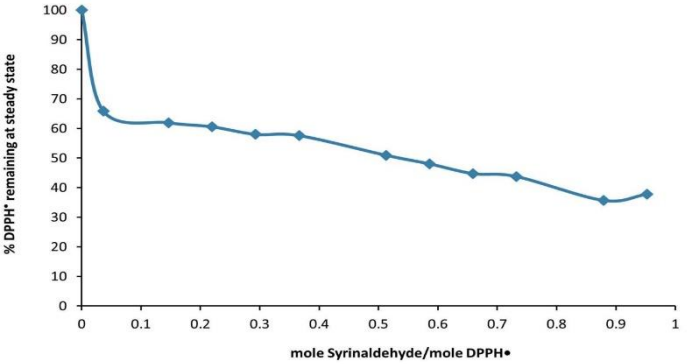


Figure A.20.18: DPPH radical scavenging activities by Syringaldehyde as a function of the number of moles of Syringaldehyde /mole DPPH•.

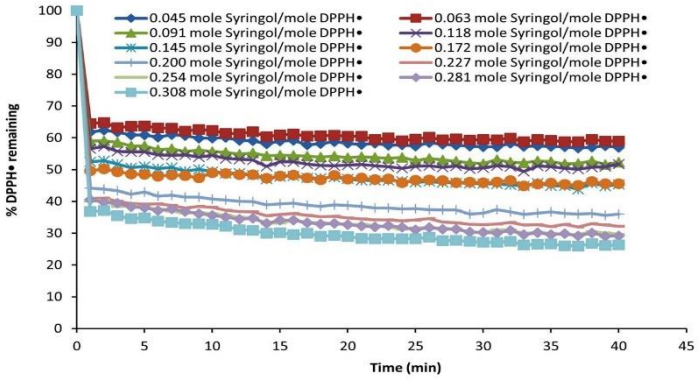


Figure A.20.19: Reaction kinetics behaviour of Syringol in methanol.

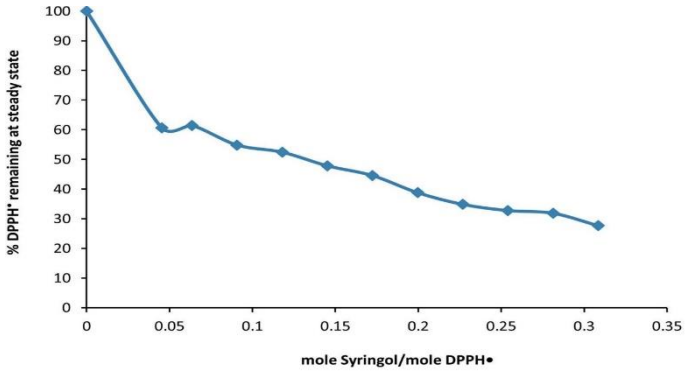


Figure A.20.20: DPPH radical scavenging activities by Syringol as a function of the number of moles of Syringol /mole DPPH•.

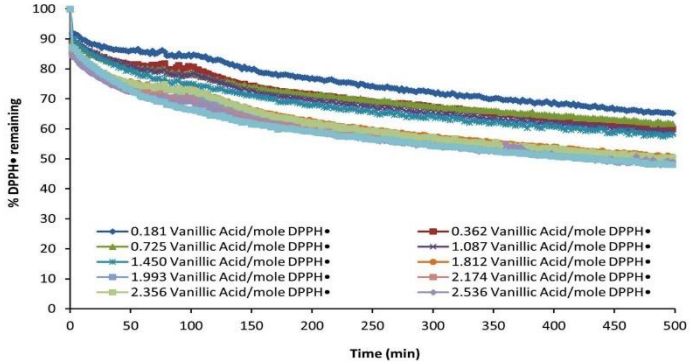


Figure A.20.21: Reaction kinetics behaviour of Vanillic Acid in methanol.

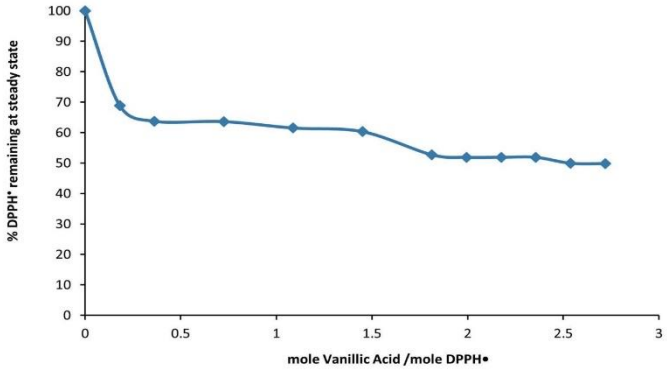


Figure A.20.22: DPPH radical scavenging activities by Vanillic Acid as a function of the number of moles of Vanillic Acid /mole DPPH•.

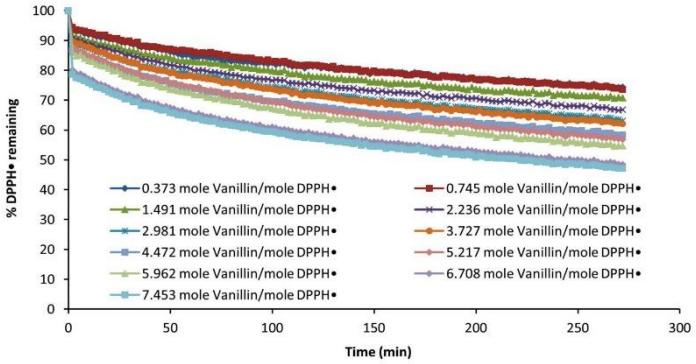


Figure A.20.23: Reaction kinetics behaviour of Vanillin in methanol.

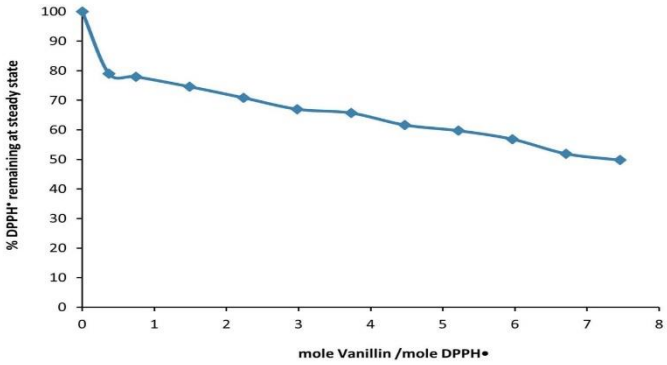


Figure A.20.24: DPPH radical scavenging activities by Vanillin as a function of the number of moles of Vanillin /mole DPPH•.

Appendix A.21: Time course (8 h) of scavenging of DPPH free radical by lignin monomers dissolved in ILs ([C_2mim][C_2SO_4] and [DMEA][HCOO])

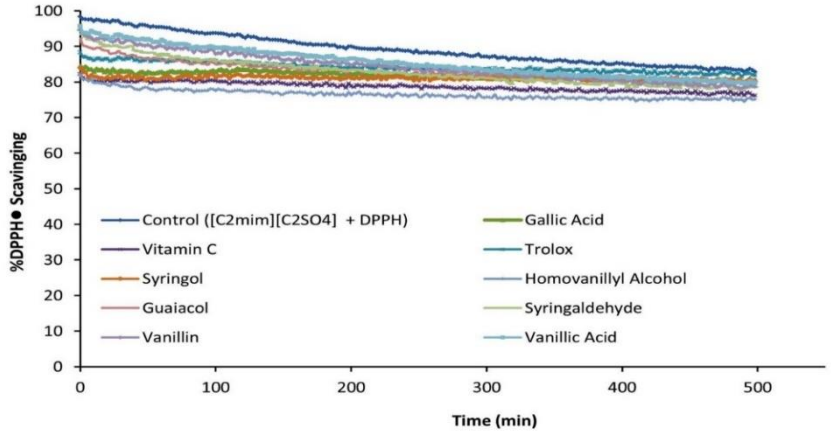


Figure A.21.1: Time course (8 h) of scavenging of DPPH free radical by lignin monomers (10 mM) dissolved in [C_2mim][C_2SO_4].

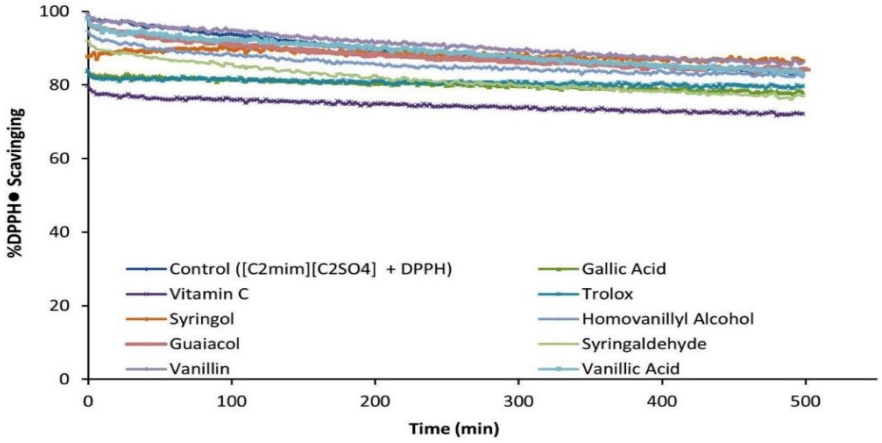


Figure A.21.2: Time course (8 h) of scavenging of DPPH free radical by lignin monomers (1.5 mM) dissolved in [C_2mim][C_2SO_4].

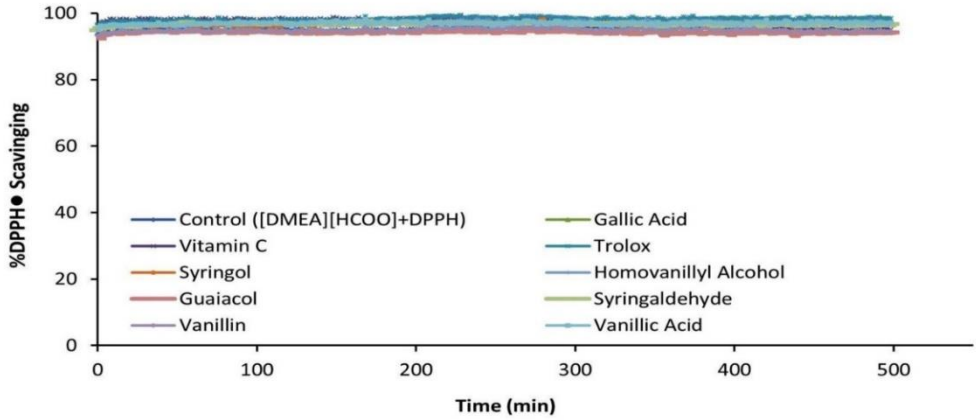


Figure A.21.3: Time course (8 h) of scavenging of DPPH free radical by lignin monomers (10 mM) dissolved in [[DMEA][HCOO].

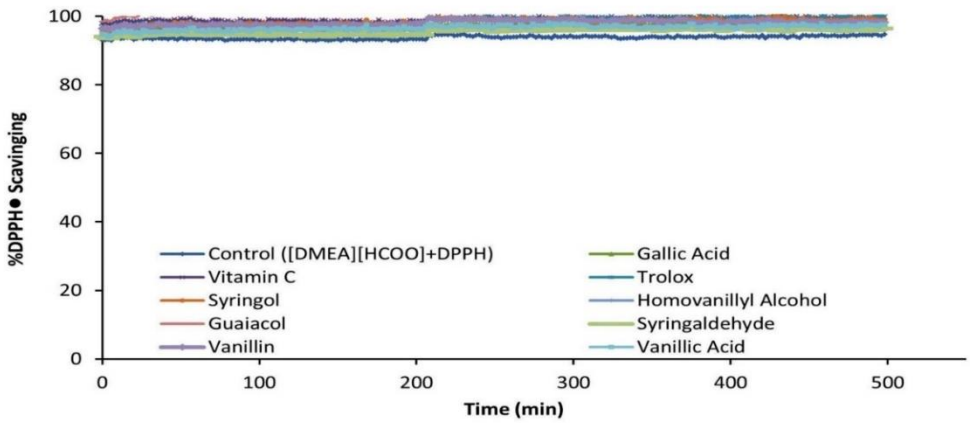


Figure A.21.4: Time course (8 h) of scavenging of DPPH free radical by lignin monomers (1.5 mM) dissolved in [DMEA][HCOO].

Appendix A.22: UV spectra of DPPH (60.86 μM) in acetonitrile and toluene at different time and different storage conditions.

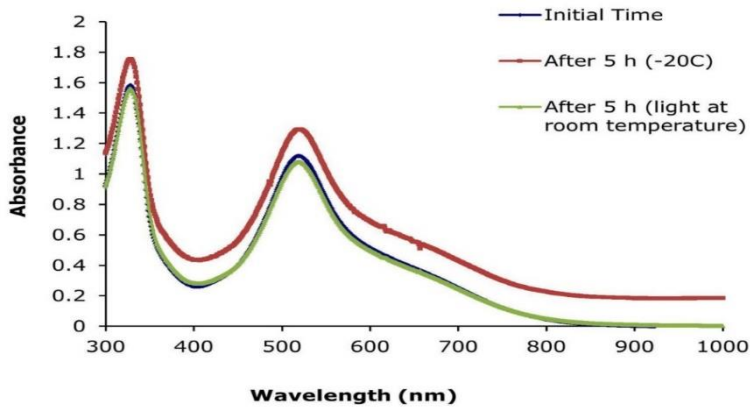


Figure A.22.1: UV spectra of DPPH (60.86 μM) in acetonitrile at different time and different storage conditions.

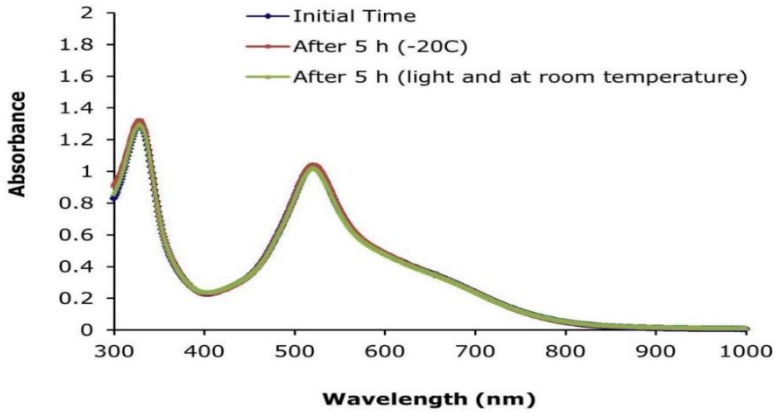


Figure A.22.2: UV spectra of DPPH (60.86 μM) in toluene at different time and different storage conditions.

Appendix A.23: Published Paper